

**Targeted local combination therapy  
with checkpoint inhibitors and CAR-NK cells in glioblastoma  
using DARPIn-linked AAV vectors**

Dissertation

zur Erlangung des Doktorgrades

der Naturwissenschaften

vorgelegt beim Fachbereich 15 – Biowissenschaften

der Johann Wolfgang Goethe - Universität

in Frankfurt am Main

von

Maja Isabelle Strecker

aus Marburg

Frankfurt (2022)

(D 30)

vom Fachbereich 15 - Biowissenschaften der Johann Wolfgang Goethe - Universität als  
Dissertation angenommen.

Dekan:

Prof. Dr. Sven Klimpel

Gutachter:

Prof. Dr. Amparo Acker-Palmer, Fachbereich 15 - Biowissenschaften

PD Dr. Michael Burger, Fachbereich 16 - Medizin

Datum der Disputation: 05.05.2022

**Vorbemerkung:**

Teile dieser Arbeit wurden bereits in einem Manuskript zusammengefasst (in Revision):

Strecker M. I., Wlotzka K., Strassheimer F., Röder J., Opitz C., Alekseeva T., Reul J., Sevenich L., Tonn T., Wels W.S., Steinbach J.P., Buchholz C.J., Burger M.C. *AAV-mediated gene transfer of a checkpoint inhibitor in combination with HER2-targeted CAR-NK cells as experimental therapy for glioblastoma.*

## Zusammenfassung

Mit 5-10 neu diagnostizierten Patienten pro 100.000 Einwohner pro Jahr ist das Glioblastom der häufigste bösartige primäre Hirntumor. Trotz intensiver Forschungsaktivitäten in den letzten Jahrzehnten ist die klinische Wirksamkeit des derzeit verfügbaren Therapiestandards in Bereichen der Chirurgie, Radiochemotherapie und Tumor Treating Fields (TTFields)-Technologie noch begrenzt. Die mittlere Überlebensrate in unselektierten Kollektiven beträgt nur etwa ein Jahr. Folglich besteht ein dringender Bedarf an der Erforschung weiterer therapeutischer Optionen. Der aktuelle Therapiestandard umfasst eine Operation mit anschließender Strahlentherapie in Kombination mit dem alkylierenden Chemotherapeutikum Temozolomid. Das Auftreten eines Tumorrezidivs ist auch bei erfolgreicher Erstlinientherapie unausweichlich, und in der Rezidivsituation gibt es derzeit noch keine definierte Standardtherapie. Nur bei 20-30% der Patienten ist eine Rezidivresektion möglich. Neben der Möglichkeit einer Rezidivbestrahlung kann eine erneute Chemotherapie mit Temozolomid, CCNU (Lomustin) oder Regorafenib durchgeführt werden. In den letzten Jahren stand insbesondere die Entwicklung von Immuntherapien für das Glioblastom im Mittelpunkt intensiver präklinischer und klinischer Bemühungen. Geringe Mutationsraten und eine stark immunsuppressive Tumormikroumgebung führen jedoch dazu, dass das Glioblastom als immunologisch „kalter“ Tumor angesehen wird. Erfolgreich etablierte Strategien bei mutagen-induzierten Tumoren mit Antikörpern gegen die Immuncheckpoints PD-1, PD-L1 oder CTLA-A4 sind daher beim Glioblastom gescheitert.

Zelluläre Immuntherapien auf Basis der chimären Antigenrezeptor (CAR)-Technologie haben sich als alternative, wirksame Option zur Bekämpfung immunologisch „kalter“ Tumore herausgestellt. Es wurden mehrere CAR-T Zellprodukte entwickelt, welche gegen Gliom-Antigene gerichtet sind und einige Hinweise auf klinische Aktivität mit sich brachten. Natürliche Killer (NK)-Zellen als Träger von CAR-Konstrukten haben gegenüber T-Zellen eine Reihe von Vorteilen, darunter ein viel geringeres Risiko für Neurotoxizität und eine effizientere Interaktion mit Immunzellen in der Mikroumgebung. Basierend auf der humanen NK-Zelllinie NK-92 wurde eine Zelltherapie entwickelt, die sich als gebrauchsfertiges Therapeutikum eignet. Der Klon NK-92/5.28.z (CAR-NK) exprimiert neben signalverstärkenden CD28- und CD3 $\zeta$ -Domänen ein CAR basierend auf dem HER2-spezifischen Antikörper FRP5.



Ähnlich wie bei mehreren anderen Tumorentitäten findet sich bei Glioblastom-Patienten häufig eine Überexpression des Wachstumsfaktor-Rezeptors HER2. Aufgrund der substanziellen Rolle bei der Regulation von Zellproliferation, Überleben, Differenzierung, Angiogenese und Invasion wird dieser Rezeptor als Onkogen klassifiziert. Die Überexpression von HER2 spielt eine entscheidende Rolle bei der malignen Transformation von Zellen, was insbesondere bei Brustkrebs detailliert charakterisiert wurde. Allerdings konnte eine HER2-Expression auch in bis zu 80% der Glioblastome nachgewiesen werden, was mit einer beeinträchtigten Überlebenswahrscheinlichkeit einhergeht. Unter physiologischen Bedingungen wird HER2 im zentralen Nervensystem von Erwachsenen nicht exprimiert, weshalb es ein vielversprechendes Ziel-Antigen für die Glioblastom-Immuntherapie darstellt.

In früheren Projekten konnte bereits gezeigt werden, dass diese CAR-NK Zellen eine hohe und spezifische lytische Aktivität gegenüber HER2<sup>+</sup> Glioblastomzellen aufweisen. Wiederholte intratumorale Injektionen von CAR-NK Zellen verlängerten das symptomfreie Überleben in orthotopen Xenotransplantatmodellen der Maus bereits signifikant. Darüber hinaus förderte die CAR-NK Zelltherapie bei immunkompetenten Mäusen mit Tumoren im Frühstadium eine endogene anti-Tumor Immunantwort, welche einerseits zur Tumorbekämpfung und andererseits zu anhaltender anti-Tumor Immunität führte. In Stadien fortgeschrittenen Tumorwachstums ist die Wirksamkeit jedoch begrenzt. In diesem Zusammenhang wurde die Expression des Checkpoint-Moleküls PD-L1 als Reaktion auf die CAR-NK Zelltherapie als Schlüsselmechanismus der Therapieresistenz identifiziert.

Die Immuntherapie durch intravenöse Gabe von Checkpoint-Inhibitoren hat bereits die Behandlung verschiedener maligner Erkrankungen wie z.B. des Melanoms oder des Lungenkarzinoms revolutioniert. Der Ansatz der Krebsimmuntherapie verfolgt bisher insbesondere die systemische Gabe von Antikörpern, die gegen Immuncheckpoints wie PD-1, PD-L1 und CTLA-4 gerichtet sind. Im Glioblastom exprimieren sowohl Tumorzellen als auch Mikroglia, die hirneigenen Makrophagen, hauptsächlich PD-L1, was die Aktivierung von CD8<sup>+</sup> und CD4<sup>+</sup> T-Zellen behindert. Daher ist eine Immuntherapie, welche sich gegen die PD-1/PD-L1-Achse richtet, ein vielversprechender Ansatz für die Behandlung des Glioblastoms. Problematisch ist jedoch die starke Toxizität, die durch die systemische Wirkung der Checkpoint-Inhibitoren verursacht wird, denn die Immunantwort wird nicht nur im Tumorgewebe, sondern auch in gesunden Organen stimuliert. So wurde beispielsweise über

schwerwiegende Nebenwirkungen wie Kolitis, Hepatitis, Pankreatitis oder Hypophysitis, unter anderem mit zahlreichen Todesfällen, berichtet.

Das Ziel dieser Arbeit war es daher, die Wirksamkeit der CAR-NK Zelltherapie zu verbessern, indem sie mit dem adeno-assoziierten Virus (AAV)-vermittelten Transfer von anti-PD-1-Antikörpern kombiniert wird, um dadurch eine lokale Kombinationstherapie zur Bekämpfung intrakranieller Tumore zu ermöglichen. Hierzu wurden AAVs eingesetzt, welche für ein anti-PD-1-Immunadhäsion (aPD-1) kodieren. Die genetische Fusion von sogenannten Designed-Ankyrin-Repeat-Proteinen (DARPs) mit einem viralen Hüllprotein ermöglicht die Generierung von AAVs mit einer Spezifität für HER2<sup>+</sup> Zellen. Durch die Verwendung von HER2-AAVs kann die Checkpoint-Inhibitor-Therapie auf die Tumorkläsion beschränkt werden, was hohe intratumorale und niedrige systemische Wirkstoffkonzentrationen zur Folge hat. Durch die Transduktion von HER2<sup>+</sup> Zellen induzieren die HER2-AAVs die Sezernierung eines scFv-Fc-Fusionsproteins. Zwei scFv-Fc-Moleküle dimerisieren dann über ihre Fc-Domänen zu einem Y-förmigen Antikörperähnlichen Molekül, einem sogenannten aPD-1-Immunadhäsion.

Im ersten Teil der Arbeit wurden die einzelnen Komponenten der Kombinationstherapie, bestehend aus adoptiver HER2-zielgerichteter CAR-NK Zelltherapie und lokalem Gentransfer von aPD-1 über HER2-spezifische AAV-Vektoren, *in vitro* charakterisiert. Die HER2-spezifischen CAR-NK Zellen zeigten eine hohe spezifische lytische Aktivität gegen HER2<sup>+</sup> Gliomzellen, während Zellen ohne Zielantigenexpression von CAR-NK Zellen kaum angegriffen wurden. CAR-NK Zellen lysierten effizient Gliomzellen murinen und menschlichen Ursprungs, einschließlich primärer und von Patienten stammender Gliomzellen. Wichtig ist, dass keine direkte Antigen-Herunterregulierung als Reaktion auf die CAR-NK Zelltherapie beobachtet wurde, was für einen nachhaltigen Therapieerfolg von großer Bedeutung ist.

Darüber hinaus wurde gezeigt, dass die CAR-NK Zelltherapie das Zytokinmilieu moduliert, indem die Sezernierung von inflammatorischen Zytokinen wie IFN- $\gamma$ , TNF- $\alpha$ , MCP-1, IL-8 und IL-6 ausgelöst wird. Auch Mikroglia tragen in hohem Maße zum Tumormikromilieu von Glioblastomen bei, da sie bis zu 40% der gesamten Tumormasse ausmachen. Interessanterweise wurden Mikroglia in Bezug auf Aktivierung und Phagozytose durch die

CAR-NK Zelltherapie beeinflusst, während die Anwesenheit von Mikroglia die CAR-NK Zellvermittelte Tumorzelllyse zu verstärken schien. Darüber hinaus zeigten Mikroglia ein hohes Maß an Toleranz gegenüber zytotoxischen Mediatoren wie Perforin und Granzym B, welches nach Aktivierung und anschließender Degranulation von CAR-NK Zellen ausgeschüttet wird.

Da die PD-1/PD-L1-Achse eine entscheidende Determinante der immunsuppressiven Mikroumgebung ist, wurden PD-L1 Level und deren Regulation als Reaktion auf die CAR-NK Zelltherapie in unterschiedlichen Zelllinien untersucht. Das Abtöten von Glioblastomzellen durch CAR-NK Zellen induzierte eine IFN- $\gamma$ -vermittelte Hochregulation von PD-L1 nicht nur in nahegelegenen Glioblastomzellen, sondern auch in hirneigenen Zelltypen wie Mikroglia und Astrozyten. Die Hochregulierung von PD-L1 als Reaktion auf CAR-NK Zelltherapie ist ein bedeutendes Ergebnis, da erhöhte PD-L1-Level die Immunsuppression innerhalb der Tumormikroumgebung weiter verstärken und somit einen potentiellen Resistenzmechanismus gegenüber CAR-NK Zellen darstellen könnten. In diesem Zusammenhang erscheint die Blockade der PD-1/PD-L1-Interaktion durch selektive lokale Verabreichung eines Checkpoint-Inhibitors durch die HER2-gerichteten AAV-Vektoren umso vielversprechender.

In der Tat konnten HER2<sup>+</sup> Glioblastomzellen mittels HER2-AAV<sup>aPD-1</sup> effizient und mit hoher Spezifität transduziert werden, was die Produktion und Sezernierung von aPD-1 zur Folge hatte. Darüber hinaus korrelierte die Transduktionseffizienz die mit den Expressionsniveaus von humanem HER2 auf den Zielzellen. Hinsichtlich der Funktionalität konnte gezeigt werden, dass HER2-AAV-kodiertes aPD-1 in der Lage ist, seinen Zielrezeptor PD-1 zu erkennen und T-Zellen nach PD-1/PD-L1-Blockade *in vitro* zu reaktivieren. Die konstitutive Expression und Präsentation von HER2 auf der Zelloberfläche ist für den in diesem Projekt untersuchten therapeutischen Ansatz von großer Bedeutung. Die AAV-Transduktion führte jedoch nicht zu einer Herunterregulierung von HER2. Darüber hinaus hatte die virale Transduktion einen lediglich geringen Einfluss auf die Viabilität der Tumorzellen. Auch die Abtötungseffizienz von CAR-NK Zellen gegenüber AAV-transduzierten Glioblastomzellen blieb unverändert. Erhöhte Konzentrationen von inflammatorischen Zytokinen wie MCP-1, IL-23 und IL-27 wurden nicht nur in Glioblastom-Zielzellen nachgewiesen, sondern auch in Zelltypen, die, wie Mikroglia und Astrozyten, einen relevanten Teil der zellulären Mikroumgebung des Gehirns ausmachen.

Im zweiten Teil der Arbeit wurde die Transduktionseffizienz von HER2-AAVs *in vivo* untersucht. Zunächst wurde die kontinuierliche Expression des Zielantigens auf murinen Gliomzellen 8 Wochen nach der ersten subkutanen Tumorzellinjektion in immunkompetente Mäuse bestätigt. Die Analyse der explantierten Tumore zeigte auch eine Hochregulierung von PD-L1 auf den Tumorzellen *in vivo*, was die Relevanz der Checkpoint-Blockade für anti-Tumor-Immunantworten zusätzlich betont. Auch *in vivo* vermittelten die Vektoren eine spezifische aPD-1-Genexpression spezifisch im Tumorgewebe, was hohe intratumorale Wirkstoffkonzentrationen und vergleichsweise niedrige aPD-1-Spiegel in peripheren Organen zur Folge hatte. In diesem Zusammenhang ist es wichtig zu erwähnen, dass sich ebenfalls das *in vivo* sezernierte aPD-1 als funktionell erwies, wie durch die Analyse von Tumorinterstitieller Flüssigkeit aus HER2-AAV<sup>aPD-1</sup>-behandelten Tumoren bestätigt wurde. Darüber hinaus gaben die Untersuchungen Aufschluss über das Vorhandensein von bereits bestehenden neutralisierenden Antikörpern gegen HER2-AAVs in den Versuchstieren. Diese Antikörperspiegel stiegen im Laufe der Zeit nach der Vektorverabreichung weiter an, unabhängig vom Verabreichungsweg der HER2-AAVs (intratumorale Gabe vs. intravenöse Gabe).

In einer Überlebensstudie zeigten Tiere, die die Kombinationstherapie (HER2-AAV<sup>aPD-1</sup> + CAR-NK Zellen) erhielten, ein verlangsamtes Tumorwachstum. Zudem waren die Überlebensraten im Vergleich zu allen anderen Kontrollkohorten signifikant erhöht, was auf eine synergistische Wirkung von CAR-NK Zellen mit intratumoral bzw. intravenös injizierten HER2-AAV<sup>aPD-1</sup> hindeutet. Sowohl die intratumorale als auch die intravenöse Verabreichung von HER2-AAVs erwies sich als wirksam. Allerdings wurde eine komplette Tumorabstoßung im subkutanen Mausmodell häufiger nach intratumoraler Injektion beobachtet. Während der Studie wurden in keiner der Behandlungsgruppen Gewichtsverlust oder andere Anzeichen beobachtet, die auf behandlungsbedingte Toxizitäten hinweisen. Auch im orthotopen intrakraniellen Mausmodell war das Überleben bei Mäusen, die die intratumorale Kombinationstherapie (HER2-AAV<sup>aPD-1</sup> + CAR-NK Zellen) erhielten, signifikant verlängert. Während Kontrolltiere innerhalb von 42 Tagen nach der anfänglichen Tumorzellimplantation der Tumorbelastung erlagen, war die Mehrheit der Tiere nach Gabe der Kombinationstherapie nach 63 Tagen noch immer am Leben. Außerdem wurde in dieser Kohorte bei 3 Tieren eine vollständige Tumorabstoßung beobachtet. Zusammengenommen bestätigen diese Daten die

anti-Tumor-Wirkung des adoptiven CAR-NK Zelltransfers in Kombination mit einer HER2-AAV<sup>aPD-1</sup>-Gentherapie.

Zusammenfassend stellt die HER2-AAV-Therapie in Kombination mit dem CAR-NK Zelltransfer eine neue Strategie für die Glioblastom-Immuntherapie dar, welche das Potenzial mit sich bringt, die Wirksamkeit zu verbessern und Nebenwirkungen zu reduzieren. Aufgrund der hohen Flexibilität bei der Auswahl der AAV- und CAR-NK Zielzellen sowie der von den AAVs kodierten Moleküle ermöglicht dieses System die Anpassung der Immuntherapie an die Eigenschaften von Tumorzellen und deren Mikroumgebung. Diese Strategie ist für die klinische Translation geeignet und stellt einen interessanten neuen Ansatz für die lokale Kombinationsimmuntherapie dar.

## Summary

With 5-10 newly diagnosed patients per 100,000 people every year, glioblastoma is the most common malignant primary brain tumor. Despite extensive research activity in the last decades, clinical effectiveness of the currently available therapy standard of surgery, radiochemotherapy and tumor-treating fields is still limited and mean survival rates in unselected collectives are only about one year. Accordingly, there is an urgent need to explore new therapeutic options. The current standard of care includes surgery followed by radiation therapy in combination with the alkylating chemotherapeutic agent Temozolomide. Even with successful initial therapy, tumor recurrence is still inevitable. Currently, there are no defined recommendations for clinical management of the disease in the event of tumor recurrence. Only 20-30% of patients qualify for a second surgical resection, while other options include retreatment with Temozolomide, CCNU (Lomustine) or Regorafenib and enrollment in a clinical trial.

The development of immunotherapies for glioblastoma, in particular, has been the focus of intense preclinical and clinical efforts. However, low numbers of mutations and a highly immunosuppressive tumor microenvironment result in glioblastoma being considered an immunologically “cold” tumor. Strategies successfully established in mutagen-induced tumors with antibodies directed against the PD-1, PD-L1 or CTLA-A4 immune checkpoints have therefore failed in glioblastoma.

Cellular immunotherapies based on chimeric antigen receptor (CAR)-technology have emerged as an alternative powerful option to tackle immunologically “cold” tumors. Several CAR-T cell products targeting glioma antigens have been developed and some evidence of clinical activity has been demonstrated. Natural killer (NK) cells as carriers of CAR constructs have several advantages over T cells, including a much lower risk of neurotoxicity and better interaction with immune cells in the microenvironment. Based on the human NK cell line NK-92, a clinical-grade product, suitable as an off-the-shelf therapeutic, has been developed. The NK-92/5.28.z clone (CAR-NK) expresses a CAR based on the HER2-specific antibody FRP5 in addition to signal-enhancing CD28 and CD3 $\zeta$  domains. Similar to several other tumor entities, overexpression of the growth factor receptor HER2 is often found in glioblastoma patients. Because of its substantial role in the regulation of cell proliferation, survival, differentiation, angiogenesis and invasion, this receptor is classified as an oncogene. HER2 overexpression

plays a major role in the malignant transformation of cells and its oncogenic potential has been studied in detail in breast cancer. However, HER2 expression was also found in up to 80% of glioblastomas, which correlates with an impaired probability of survival. Under physiological conditions, HER2 is not expressed in the adult central nervous system, making it a promising target antigen for glioblastoma immunotherapy.

In previous projects, it has already been shown that these CAR-NK cells exhibit a high and specific lytic activity towards HER2<sup>+</sup> glioblastoma cells. While repetitive intratumoral injections of CAR-NK cells already significantly extended symptom-free survival in murine orthotopic xenograft models, CAR-NK cell therapy in immunocompetent mice promotes an endogenous anti-tumor immune response which improves tumor control and provides persisting anti-tumor immunity after therapy of early-stage tumors. However, in more advanced tumor models, efficacy is limited and induction of the checkpoint-molecule PD-L1 in response to CAR-NK-cell therapy was identified as a key mechanism of therapy resistance.

Immunotherapy employing the intravenous administration of checkpoint inhibitors has already revolutionized the treatment of various malignant diseases such as melanoma or lung cancer. In particular, the approach of cancer immunotherapy has focused on the systemic administration of antibodies directed against immune checkpoints such as PD-1, PD-L1 and CTLA-4. In glioblastoma, both tumor cells and microglia, the brain-resident macrophages, express PD-L1, which hinders the activation of CD8<sup>+</sup> and CD4<sup>+</sup> T cells. Therefore, immunotherapy directed against the PD-1/PD-L1 axis represents a promising approach for the treatment of glioblastoma. One problem, however, is the severe toxicity caused by the systemic effects of checkpoint inhibitors, since the immune response is stimulated not only in tumor tissue but also in healthy organs. Serious side effects such as colitis, hepatitis, pancreatitis or hypophysitis, including numerous deaths, have been reported.

This study aimed to improve the efficacy of CAR-NK cell therapy by combining it with adeno-associated virus (AAV)-mediated transfer of anti-PD-1 antibodies as a strategy to enable local combination therapy to control intracranial tumors.

AAVs carrying a payload coding for an anti-PD-1 immunoadhesin (aPD-1) retargeted to HER2-expressing cells by fusion of so-called Designed Ankyrin Repeat Proteins (DARPs) with a viral capsid protein were employed for this to focus checkpoint inhibitor therapy to the

tumor area, resulting in high intratumoral and low systemic drug concentrations. With this strategy, after the transduction of target cells, an scFv-Fc fusion protein is produced. Two scFv-Fc molecules then dimerize via their Fc domains to form a Y-shaped antibody-like molecule, a so-called aPD-1 immunoadhesin.

In the first part of the work, the individual components of the combination therapy, comprising adoptive HER2-targeted CAR-NK cell therapy and local gene delivery of aPD-1 via HER2-specific AAV vectors, were characterized *in vitro*. The HER2-specific CAR-NK cells exhibited high specific lytic activity against HER2<sup>+</sup> glioma cells, while cells without target antigen expression were hardly attacked by CAR-NK cells. CAR-NK cells efficiently lysed murine and human glioma cells, including primary and patient-derived glioma cells. No direct antigen downregulation was observed as a reaction to CAR-NK cell therapy, which is of great importance for sustained therapeutic success. In addition, CAR-NK cell therapy was shown to modulate the cytokine profile by triggering the secretion of inflammatory cytokines such as IFN- $\gamma$ , TNF- $\alpha$ , MCP-1, IL-8 and IL-6. Microglia also contribute to the tumor microenvironment of glioblastomas to a large extent, as they make up to 40% of the total tumor mass. Interestingly, microglia were affected by CAR-NK cell therapy in terms of activation and increased phagocytosis, while the presence of microglia appeared to enhance CAR-NK cell-mediated tumor cell lysis. In addition, microglia showed a high degree of tolerance to cytotoxic mediators such as perforin and granzyme B, which are released by CAR-NK cells after activation and subsequent degranulation.

Since the PD-1/PD-L1 axis is a decisive determinant of the immunosuppressive microenvironment, PD-L1 regulation in response to CAR-NK cell therapy was investigated in different cell lines. The killing of glioblastoma cells by CAR-NK cells induced an IFN- $\gamma$ -mediated upregulation of PD-L1 not only in nearby glioblastoma cells but also in brain-resident cell types such as microglia and astrocytes. The upregulation of PD-L1 in response to CAR-NK cell therapy represents a key finding, providing a mechanistic rationale for the disruption of the PD-1/PD-L1 interaction. These findings further reinforced the need to induce the blockade of the PD-1/PD-L1 axis by the selective local administration of a checkpoint inhibitor.



*In vitro*, HER2<sup>+</sup> glioblastoma cells were transduced efficiently and with high specificity using HER2-AAV<sup>aPD-1</sup>, which resulted in the production and secretion of aPD-1. In addition, transduction efficiency correlated with expression levels of human HER2 on target cells. In terms of functionality, HER2-AAV-encoded aPD-1 was able to recognize its target receptor PD-1 and to reactivate T cells after PD-1/PD-L1 blockade *in vitro*. The constitutive expression and presentation of HER2 on the cell surface is of great importance for the therapeutic approach investigated in this project, and AAV transduction did not result in downregulation of HER2. Furthermore, viral transduction had little impact on tumor cell viability. In addition, the killing efficiency of CAR-NK cells towards AAV-transduced glioma cells was unaltered. Some induction of inflammatory cytokines such as MCP-1, IL-23 and IL-27 by AAV-infection was detected both in glioblastoma target cells and in resident brain cell types which are a relevant part of the cellular microenvironment of the brain, such as microglia and astrocytes.

In the second part of the thesis, the transduction efficacy of HER2-AAVs was investigated *in vivo*. First, the continuous expression of the HER2 target antigen on murine glioma cells was confirmed 8 weeks after subcutaneous tumor cell injection into immunocompetent mice. The analysis of the explanted tumors also showed an upregulation of PD-L1 on the tumor cells *in vivo*, which further emphasizes the relevance of checkpoint blockade for anti-tumor immune responses.

Further, the AAV-vectors mediated aPD-1 gene expression specifically in tumor tissue, which resulted in high intratumoral drug concentrations and comparatively low aPD-1 levels in peripheral organs. In this context, it is important to mention that the aPD-1 that was secreted *in vivo* was also shown to be functional, as confirmed by the analysis of tumor-interstitial fluid from HER2-AAV<sup>aPD-1</sup>-treated tumors. In addition, the analyses revealed the presence of pre-existing neutralizing antibodies against HER2-AAV in experimental animals. These antibody levels continued to increase over time after vector administration, regardless of the route of HER2 AAVs administration (intratumoral vs. intravenous).

In a survival study, animals with subcutaneous tumors that received combination therapy (HER2-AAV<sup>aPD-1</sup> + CAR-NK) showed slower tumor growth as well as significantly prolonged survival rates compared to control cohorts, which indicates a synergistic effect of CAR-NK cells with intratumorally or intravenously injected HER2-AAV<sup>aPD-1</sup>. While both intratumoral

as well as intravenous administration of HER2-AAVs was found to be effective, complete tumor rejection in the subcutaneous mouse model was more frequently observed after intratumoral injection. No weight loss or other signs indicating treatment-related toxicities were seen in any of the treatment groups during the study.

Also in the orthotopic intracranial mouse model, survival in mice receiving the combination therapy (HER2-AAV<sup>aPD-1</sup> + CAR-NK) was significantly prolonged. While control animals succumbed to tumor burden within 42 days after initial tumor cell implantation, the majority of animals that received the combination therapy were still alive after 63 days. In addition, in this cohort, complete tumor rejection was observed in 3 animals.

These data confirm the anti-tumor effects of adoptive CAR-NK cell transfer in combination with HER2-AAV<sup>aPD-1</sup> gene therapy.

In summary, HER2-AAV therapy in combination with CAR-NK cell transfer is a new strategy for glioma immunotherapy, with the potential to improve efficacy and reduce side effects. Due to the high flexibility in the selection of the AAV and CAR-NK target cells, as well as in the molecules encoded by AAV vectors, this system enables the adaptation of immunotherapy to the characteristics of tumor cells and their microenvironment. This strategy is suitable for clinical translation and represents an interesting novel approach towards local combination immunotherapy.

---

**List of tables**

<b>Table 1:</b> Reagents, chemicals, recombinant proteins and cytokines .....	26
<b>Table 2:</b> Kits .....	28
<b>Table 3:</b> Enzymes .....	29
<b>Table 4:</b> Buffer and media composition.....	29
<b>Table 5:</b> Antibodies .....	30
<b>Table 6:</b> Primer sequences .....	32
<b>Table 7:</b> Plasmids .....	32
<b>Table 8:</b> Eukaryotic cells.....	32
<b>Table 9:</b> Viral vectors.....	35
<b>Table 10:</b> Animals.....	35
<b>Table 11:</b> Materials for experimental mouse work.....	35
<b>Table 12:</b> Equipment.....	36
<b>Table 13:</b> Software.....	37

---

**List of figures**

<b>Figure 1:</b> Schematic overview of glioma subtypes .....	2
<b>Figure 2:</b> Clinical management of glioblastoma. ....	4
<b>Figure 3:</b> The glioblastoma microenvironment.....	7
<b>Figure 4:</b> Challenges of glioblastoma management. ....	11
<b>Figure 5:</b> NK cell functions in tumor control.....	14
<b>Figure 6:</b> Generation of HER2-specific CAR-NK cells. ....	16
<b>Figure 7:</b> The principle of immunotherapy. ....	17
<b>Figure 8:</b> Adeno-associated virus (AAV) structure and genome organization.....	19
<b>Figure 9:</b> Schematic representation of a DARPIn and a DARPIn-linked AAV vector. ....	22
<b>Figure 10:</b> Schematic representation of HER2-AAV encoding murine aPD-1. ....	23
<b>Figure 11:</b> Synergy between CAR-NK cells and aPD-1 encoding HER2-AAV. ....	25
<b>Figure 12:</b> HER2-targeted CAR-NK cell therapy.....	50
<b>Figure 13:</b> CAR-NK cells efficiently lyse HER2 <sup>+</sup> glioma cells. ....	51
<b>Figure 14:</b> Cytotoxic activity of NK-92/R1.28.z cells against glioma cells.....	52
<b>Figure 15:</b> Cytotoxic activity of CAR-NK cells against GL261-HER2-low cells.. ....	53
<b>Figure 16:</b> CAR-NK cells efficiently lyse primary and patient-derived glioma cells.. ....	54
<b>Figure 17:</b> HER2 expression on target cells in response to CAR-NK cell activity.....	55
<b>Figure 18:</b> Adjacent CAR-NK cell-mediated tumor cell killing leads to cytokine secretion by surrounding immune cells. ....	56
<b>Figure 19:</b> CAR-NK cell-mediated tumor cell killing results in PD-L1 regulation. ....	58
<b>Figure 20:</b> Cytokine release of activated CAR-NK cells and the effect on PD-L1 regulation on surrounding cell types. ....	59
<b>Figure 21:</b> IFN- $\gamma$ is the major driver for PD-L1 upregulation in surrounding cell types.....	60
<b>Figure 22:</b> Regulation of microglia markers in response to adjacent CAR-NK cell-mediated tumor cell lysis.....	62
<b>Figure 23:</b> Synergy between CAR-NK cells and murine microglia.....	63
<b>Figure 24:</b> Killing efficiency of CAR-NK cells towards murine microglia.....	63
<b>Figure 25:</b> Brain-resident immune cells are not susceptible to lysis by CAR-NK cells.....	65
<b>Figure 26:</b> Expression of HLA-E on the surface of target cells and degranulation of CAR-NK cells in response to various target cell types.....	66

---

<b>Figure 27:</b> Microglial phagocytosis activity is increased upon adjacent CAR-NK cell-mediated tumor cell lysis. ....	67
<b>Figure 28:</b> Expression of HER2-AAV-encoded aPD-1 on the RNA level.....	68
<b>Figure 29:</b> Expression of HER2-AAV-encoded aPD-1 on the protein level. ....	69
<b>Figure 30:</b> Secretion of HER2-AAV-encoded aPD-1 in a time-dependent manner. ....	70
<b>Figure 31:</b> Production and purification of recombinant aPD-1 for the establishment of a sandwich ELISA. ....	71
<b>Figure 32:</b> Quantification of <i>in vitro</i> produced aPD-1 via sandwich ELISA. ....	72
<b>Figure 33:</b> Target binding of HER2-AAV-encoded aPD-1. ....	74
<b>Figure 34:</b> PD-1/PD-L1 axis disruption of HER2-AAV-encoded aPD-1. ....	75
<b>Figure 35:</b> The Effect of HER2-AAV transduction on proliferation and viability of glioma cells. ....	76
<b>Figure 36:</b> The Effect of HER2-AAV transduction on HER2 and PD-L1 expression on glioma cells. ....	77
<b>Figure 37:</b> The Effect of HER2-AAV transduction on cytokine secretion of target cells. ....	78
<b>Figure 38:</b> The Effect of HER2-AAV on cytokine secretion of target cells. ....	79
<b>Figure 39:</b> The Effect of HER2-AAV transduction on killing capacity of CAR-NK cells.....	80
<b>Figure 40:</b> HER2- and PD-L1 expression of glioma cells <i>in vivo</i> . ....	81
<b>Figure 41:</b> Distribution kinetics of HER2-AAV-encoded aPD-1 <i>in vivo</i> and generation of neutralizing antibodies. ....	83
<b>Figure 42:</b> Functionality of <i>in vivo</i> secreted aPD-1.....	85
<b>Figure 43:</b> Cytokine levels in the serum of HER2-AAV <sup>aPD-1</sup> -treated animals bearing an intracranial tumor.....	86
<b>Figure 44:</b> Generation of neutralizing antibodies against HER2-AAV <i>in vivo</i> . ....	87
<b>Figure 45:</b> Combination therapy conveys a survival benefit upon intratumoral HER2-AAV administration in the subcutaneous GL261-HER2 model. ....	89
<b>Figure 46:</b> Survival benefit in mice receiving HER2-AAV in the subcutaneous GL261-HER2 model.....	90
<b>Figure 47:</b> Survival benefit in mice receiving HER2-AAV in the orthotopic intracranial GL261-HER2 model. ....	92
<b>Figure 48:</b> Volumetries of orthotopic intracranial tumors of mice of different treatment cohorts.....	92

**List of abbreviations**

°C	Degree celsius	DC	Dendritic cell
μ	Micro	DMEM	Dulbecco's Modified Eagle Medium
μg	Microgram	DMSO	Dimethyl sulfoxide
μl	Microliter	DNA	Desoxyribonucleic acid
μm	Micrometer	dNTP	Desoxyribonucleotide triphosphate
AAV	Adeno-associated virus	ECM	Extracellular matrix
AC	Astrocyte	EDTA	Ethylenediaminetetraacetic acid
AKT	Protein kinase B	ELISA	Enzyme-linked immunosorbent assay
APC	Antigen-presenting cell	et al.	and others
APS	Ammonium persulfate	Fc	Fragment crystallizable
ATCC	American Type Culture Collection	FC	Flow cytometry
BBB	Blood-brain barrier	FCS	Fetal calf serum
BMDM	Bone-marrow derived macrophage	FDA	Food and Drug Administration
bp	Base pair	FITC	Fluorescein isothiocyanate
BSA	Bovine serum albumine	FOXP3	Forkhead box P3
CAR	Chimeric antigen receptor	GAM	Glioma-associated macrophages/microglia
CD	Cluster of differentiation	GB	Glioblastoma
cDNA	Complementary DNA	GM-CSF	granulocyte macrophage colony-stimulating factor
CNS	Central nervous system	GrB	Granzyme B
CTLA-4	Cytotoxic T-Lymphocyte-Associated Protein 4	GvHD	graft-versus-host disease
CV	Calcein violet	h	hour
DAMP	Danger-associated molecular pattern	HA	hemagglutinin

DARPin	Designed ankyrin repeat protein	HBSS	Hanks' Balanced Salt Solution
HEK	Human embryonic kidney	MHC	Major histocompatibility complex
Her2/neu	Human epidermal growth factor 2	min	Minutes
HRP	Horseradish peroxidase	ml	Milliliter
HSPG	Heparan sulfate proteoglycan	mM	Millimolar
ICI	Immune checkpoint inhibitor	MRI	Magnetic resonance imaging
IDH1	Isocytate dehydrogenase 1	mRNA	messenger RNA
IDO	Indoleamine 2,3-dioxygenase	mTOR	Mammalian target of rapamycin
IFN	Interferon	n.s.	not significant
IgG	Immunoglobulin	nAb	Neutralizing antibody
IL	Interleukin	ng	Nanogram
irAE	Immune-related adverse events	NK cell	Natural killer cell
ITR	Inverted terminal repeat	PBS	Phosphate buffered saline
kb	Kilobase	PCR	Polymerase chain reaction
kDa	Kilo Dalton	PD-1	Programmed death protein 1
KPS	Karnofsky Performance Status	PDGFD	Platelet Derived Growth Factor D
l	Liter	PD-L1	Programmed death ligand 1
LAG-3	Lymphocyte-activation gene 3	PE	Phycoerythrin
LOH	Loss of heterozygosity	PI	Propidium iodide
LV	Lentiviral vector	PIP3	Phosphatidylinositol (3,4,5)-trisphosphate
M	Molar	PTEN	Phosphatase and tensin homolog
mAb	Monoclonal antibody	qPCR	Quantitative PCR
MCP-1	Monocyte chemotactic protein 1	qPCR	Quantitative real time PCR
MDSC	Myeloid-derived suppressor cell	RNA	Ribonucleic acid
MG	Microglia	ROS	Reactive oxygen species

MGMT	O6-methylguanine-DNA methyltransferase	rpm	Rounds per minute
RPMI	Roswell Park Memorial Institute	TMB	3,3',5,5'-Tetramethylbenzidine
scAAV	Self-complementary AAV	TME	Tumor microenvironment
scFv	Single chain Fragment variable	TMZ	Temozolomide
SD	Standard deviation	TNF- $\alpha$	Tumor necrosis factor $\alpha$
SDS	Sodium dodecyl sulfate	T <sub>reg</sub> cells	Regulatory T cells
SDS-PAGE	SDS-polyacrylamide gel electrophoresis	Tris	Tris(hydroxymethyl)aminomethane
SFFV	Spleen focus forming virus	TTFs	Tumor-treating fields
STAT3	Signal Transducer And Activator Of Transcription 3	U	Unit
TCR	T cell receptor	V	Volt
TEMED	Tetramethylethylenediamine	v/v	Volume per volume
TGF- $\beta$	Transforming growth factor $\beta$	VH	Variable region of heavy chain
TILs	Tumor infiltrating lymphocytes	VL	Variable region of light chain
STAT3	Signal Transducer And Activator Of Transcription 3	VP	Viral protein
TCR	T cell receptor	VP-SFM	Virus production serum-free medium
TEMED	Tetramethylethylenediamine	WB	Western blot
TGF- $\beta$	Transforming growth factor $\beta$	$\alpha$	Alpha or anti
TILs	Tumor infiltrating lymphocytes	$\beta$	Beta
TIM-3	T cell immunoglobulin and mucin-domain containing-3	$\gamma$	Gamma



---

**Table of content**

<b>Zusammenfassung</b> .....	VII
<b>Summary</b> .....	VII
<b>List of tables</b> .....	XII
<b>List of figures</b> .....	XIII
<b>List of abbreviations</b> .....	XXV
<b>Table of content</b> .....	XVIII
<b>1 Introduction</b> .....	1
<b>1.1 Glioblastoma</b> .....	1
<b>1.1.1</b> Epidemiology and clinical presentation .....	1
<b>1.1.2</b> Classification and genetic alterations .....	1
<b>1.1.3</b> Therapy .....	3
<b>1.1.4</b> The tumor microenvironment of glioblastoma .....	5
<b>1.1.5</b> Clinical challenges .....	10
<b>1.2 Natural killer cells</b> .....	12
<b>1.2.1</b> Genetically engineered chimeric antigen receptor NK cells .....	15
<b>1.3 Cancer immunotherapy</b> .....	16
<b>1.3.1</b> Immunotherapy in glioblastoma .....	18
<b>1.4 Gene therapy using adeno-associated viruses</b> .....	19
<b>1.4.1</b> Generation of HER2-specific adeno-associated viral vectors .....	21
<b>1.5 Aim of the thesis</b> .....	24
<b>2 Material and Methods</b> .....	26
<b>2.1 Material</b> .....	26
<b>2.1.1</b> Reagents .....	26
<b>2.1.2</b> Kits .....	28

---

2.1.3	Enzymes .....	29
2.1.4	Buffers and media .....	29
2.1.5	Antibodies .....	30
2.1.6	Oligonucleotides.....	32
2.1.7	Plasmids .....	32
2.1.8	Eukaryotic cells.....	32
2.1.9	Viral vectors.....	35
2.1.10	Animals .....	35
2.1.11	Materials for experimental mouse work .....	35
2.1.12	Equipment .....	36
2.1.13	Software.....	37
<b>2.2</b>	<b>Molecular biology .....</b>	<b>37</b>
2.2.1	Quantitative real time PCR.....	37
<b>2.3</b>	<b>Protein biochemical methods.....</b>	<b>37</b>
2.3.1	Preparation of cell lysates .....	37
2.3.2	Determination of protein concentration .....	37
2.3.3	Sodium dodecyl sulfate polyacrylamide gel electrophoresis .....	38
2.3.4	Western blot analysis.....	38
2.3.5	Enzyme-linked immunosorbent assay (ELISA).....	39
2.3.6	Production of recombinant aPD-1 .....	39
2.3.7	Protein affinity tag purification from cell culture supernatant.....	39
<b>2.4</b>	<b>Immunological methods .....</b>	<b>40</b>
2.4.1	Flow cytometry.....	40
2.4.2	Transwell assay .....	40
2.4.3	Target binding assay .....	41
2.4.4	Blockade assay.....	41

---

2.4.5	Cytokine measurements .....	41
<b>2.5</b>	<b>Cell Culture .....</b>	<b>42</b>
2.5.1	Cultivation of cells.....	42
2.5.2	Isolation and cultivation of primary cells.....	42
2.5.3	Freezing and thawing of cells.....	43
2.5.4	Generation of transgenic cell lines.....	43
2.5.5	Determination of cell density and cell viability .....	43
2.5.6	Cytotoxicity assays .....	43
2.5.7	Degranulation assays.....	43
<b>2.6</b>	<b>Virological methods .....</b>	<b>44</b>
2.6.1	AAV vector production.....	44
2.6.2	Viral transduction of cells.....	44
<b>2.7</b>	<b><i>In vivo</i> analyses .....</b>	<b>44</b>
2.7.1	Glioblastoma mouse models .....	44
2.7.2	Injection of vector particles and CAR-NK cells .....	45
2.7.3	MR imaging.....	45
2.7.4	Blood sampling and serum isolation.....	46
2.7.5	Isolation of tumor and organ tissue.....	46
2.7.6	Preparation of single-cell suspensions .....	46
2.7.7	Preparation of tumor and organ lysates .....	46
2.7.8	Isolation and cultivation of splenocytes from mice .....	47
2.7.9	Neutralization assay .....	47
<b>2.8</b>	<b>Schematics .....</b>	<b>47</b>
<b>2.9</b>	<b>Statistical analysis .....</b>	<b>48</b>
<b>3</b>	<b>Results .....</b>	<b>49</b>
3.1	Selective cytotoxic activity of CAR-NK cells against HER2 <sup>+</sup> cells.....	49

---

<b>3.2</b>	<b>The effect of CAR-NK cell-mediated tumor cell lysis on target and bystander cells</b> .....	54
3.2.1	Target antigen expression and cytokine secretion.....	54
3.2.2	Regulation of PD-L1 expression .....	56
<b>3.3</b>	<b>The effect of CAR-NK cells on brain-resident immune cells</b> .....	61
3.3.1	The effect of activated CAR-NK cells on murine microglia .....	61
3.3.2	The effect of activated CAR-NK cells on human microglia.....	64
<b>3.4</b>	<b>aPD-1 encoding HER2-AAV vectors</b> .....	67
3.4.1	<i>In vitro</i> transduction efficacy of HER2-AAV .....	68
3.4.2	Establishment of a ELISA approach for the detection of HER2-AAV-encoded aPD-1..	71
3.4.3	Functionality of HER2-AAV-encoded aPD-1 .....	73
3.4.4	The effect of HER2-AAV transduction on target cells.....	75
3.4.5	Interaction of HER2-AAV and CAR-NK cells .....	80
<b>3.5</b>	<b><i>In vivo</i> analyses</b> .....	81
3.5.1	Expression of HER2 and PD-L1 on glioma cells <i>in vivo</i> .....	81
3.5.2	Distribution kinetics and functionality of HER2-AAV-encoded aPD-1 <i>in vivo</i> .....	82
3.5.3	Cytokine responses after HER2-AAV transduction <i>in vivo</i> .....	86
3.5.4	Generation of neutralizing antibodies against HER2-AAV.....	86
3.5.5	The effect of CAR-NK cell / HER2-AAV combination therapy on survival .....	88
<b>4</b>	<b>Discussion</b> .....	95
4.1	<b>CAR-NK cell therapy</b> .....	95
4.2	<b>Cytokine release upon CAR-NK cell therapy</b> .....	98
4.3	<b>Regulation of surface molecules in response to CAR-NK cell therapy</b> .....	99
4.4	<b>Possible mechanisms to augment CAR-NK cell function in the TME</b> .....	102
4.5	<b>Tolerance of microglia and astrocytes towards CAR-NK cell lysis</b> .....	103
4.6	<b>Refinement of targeted CAR-NK cell therapies for the treatment of glioblastoma</b> .....	105
4.7	<b>Intratumoral delivery of immune checkpoint inhibitors</b> .....	106

---

4.8	Local expression of aPD-1 via HER2-AAV-mediated transgene delivery.....	107
4.9	Distribution kinetics of HER2-AAV-encoded aPD-1 <i>in vivo</i> .....	109
4.10	The effect of combined HER2-AAV/CAR-NK cell therapy on survival .....	112
4.11	Conclusions and outlook .....	114
5	References .....	117
6	Appendix.....	153
7	Curriculum vitae.....	153
8	Publications .....	154
9	Danksagung.....	156
10	Ehrenwörtliche Erklärung .....	157

## **1 Introduction**

### **1.1 Glioblastoma**

#### **1.1.1 Epidemiology and clinical presentation**

Glioblastoma (GB) is the most common malignant primary intracranial malignancy. Annually, 5-10 per 100,000 people are diagnosed with GB [1], [2]. The prognosis is still very poor with a median survival of only 14.6 months and a 5-year survival rate of < 5% in current clinical trial collectives [1], [2]. Population-wide, median survival is still below 12 months [5]. Established baseline prognostic factors include age and clinical performance status (Karnofsky Performance Scale (KPS)). Depending on the initial location of tumor growth and its size, a variety of brain structures can be compromised, leading to a wide range of clinical symptoms at presentation. Those include seizures, headaches and nausea due to an increase in intracranial pressure, but also focal neurological symptoms such as impaired vision, cognitive deficits, confusion, motor deficits, dyspnea, personality changes, dysphasia, hemiparesis and paraesthesia [6]–[8]. Although the spread of GB cells to tissues outside the brain occurs in less than 2% of cases [9], [10], their invasive growth within healthy brain tissue results in infiltration of the adjacent brain parenchyma and distant lobes, including the spread via the corpus callosum to the other hemisphere [4], [11]. The impairment of neural structures in affected regions due to infiltrative and destructive growth and the mass effect is ultimately fatal.

#### **1.1.2 Classification and genetic alterations**

Despite immense research efforts, broad molecular characterization of tumors and the optimization of therapy modalities, relapse of GB is inevitable, and the lack of successful treatment options upon recurrence results in invariable lethality. More promising therapeutic interventions heavily depend on the development of novel treatment modalities such as gene therapy or immunotherapy. GB as a particularly heterogeneous tumor harbors necrotic areas, as well as sites of angiogenesis, leaky vessel growth and endothelial hyperplasia. Diagnosis, prognosis and treatment are hampered by the beforementioned severe heterogeneity of tumor cells.

Molecular characterization including whole-exome and whole-genome sequencing, transcriptomic analyses and epigenetic profiling have resulted in the current understanding and classification of GB [4], [12], [13].

Glial stem and precursor cells are viewed as the cells of glioma origin [14], [15]. Glioblastomas, astrocytomas and oligodendrogliomas are all referred to as gliomas [16]. As major glioma types in adults, the World Health Organization (WHO) distinguishes between isocitrate dehydrogenase (IDH) mutant grade 2, 3 and 4 astrocytomas, IDH mutant grade 2 and 4 oligodendrogliomas, and IDH wild-type grade 4 glioblastoma [16], which represents the deadliest and most aggressive glioma [17]–[22].

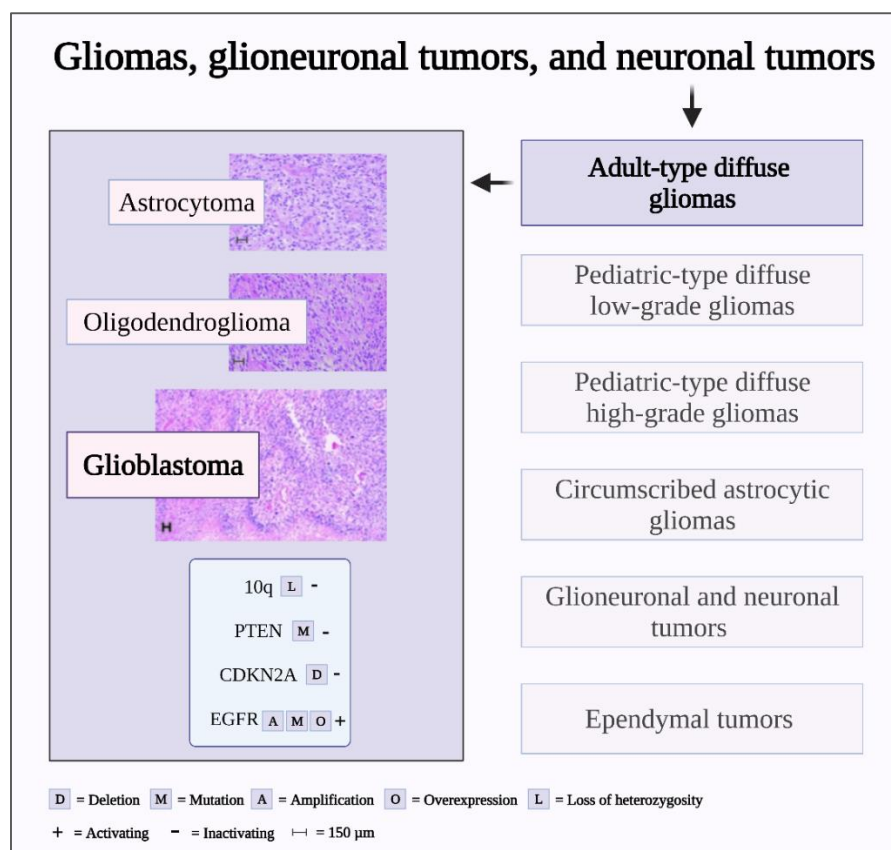


**Figure 1: Schematic overview of glioma subtypes** (adapted from [23], [24]).

Molecular hallmarks of GB include telomerase reverse transcriptase (TERT) promotor mutation, loss of heterozygosity (LOH) of chromosome 10q, resulting in deletion of phosphatase and tensin homolog (PTEN), amplification of chromosome 7 including the EGFR locus and homozygous deletion of cyclin-dependent kinase inhibitor 2A (CDKN2A). This results in immortalization, frequent activation of oncogenic signaling via the phosphatidylinositol (3,4,5)- trisphosphate/mammalian target of rapamycin/protein kinase B

(PIP3/mTor/AKT) pathway and loss of cell cycle control, respectively [3], [23]. Additionally, isolated amplifications and mutations of EGFR are commonly observed, resulting in expression of the EGFRvIII variant and the subsequent constitutive cell proliferation combined with apoptosis inhibition caused by permanent activation of the PIP3/mTor/AKT pathway [25], [26].

Also, HER2 expression is seen in up to 80% of GB patients [27], [28] and GB cells often also show elevated HER2 mRNA levels [29]. HER2 (alternative name: Her-2/neu) is a 185 kDa transmembrane protein belonging to the family of epidermal growth factor receptors. On the cell surface, HER2 exists as a monomeric receptor that dimerizes in response to ligand binding, resulting in signal transduction via transphosphorylation of intracellular domains. Due to its prominent role in the regulation of cell proliferation, survival, differentiation, angiogenesis, and invasion it is also classified as an oncogene [30] [31]. Its overexpression has been reported to play an important role in the malignant transformation of cells and its oncogenic potential has mostly been studied in breast cancer [32], [33]. Under physiological conditions, HER2 has been reported to be absent in the adult central nervous system [34]. The interest in HER2 as a therapeutic target has led to the initiation of clinical phase 1/2 trials (NCT02442297, NCT01109095) and is also under investigation for CAR-T cell therapy in GB [35].

In 2010, Verhaak et al. proposed four transcriptional subtypes of GB, namely the Proneural, Neural, Classical and Mesenchymal subtype [4]. Patients of younger age mainly show the proneural subtype, which is associated with a more favorable prognosis. The gene expression profile of the neural subtype mainly resembles normal brain tissue and like the classical subtype, it responds better to chemotherapy and radiotherapy. Although the mesenchymal subtype is also responsive to therapy, it is characterized by extensive necrosis and inflammation and accounts for the worst survival prognosis of all subtypes [4], [36].

### **1.1.3 Therapy**

The standard therapy for GBs comprises surgical resection followed by radiotherapy and alkylating chemotherapy with Temozolomide (TMZ) in patients in sufficient clinical condition [37]. Additionally, alternating electrical fields for patients stable after radiochemotherapy can be used as a therapeutic intervention [38]. If the location of tumor growth does not allow for surgical resection, the performance of a stereotactic biopsy is recommended [39]. In general,



gross total resection of the tumor mass should be performed whenever practicable, because it has a substantial impact on survival [40], although GB's infiltrative growth impedes complete surgical resection in many cases [6], [41]. However, advanced surgical tools such as intraoperative magnetic resonance imaging (MRI), ultrasonography, functional monitoring and visualization of GB cells with 5-aminolevulinic acid aid realization of maximum resection while minimizing the risk of neurological damage [39], [42]. 3-5 weeks after surgery, it is recommended to start radiotherapy regimens, usually consisting of 60 Gy administered in 1.8–2 Gy daily fractions. In elderly patients, hypofractionated protocols have been established [39], [43].

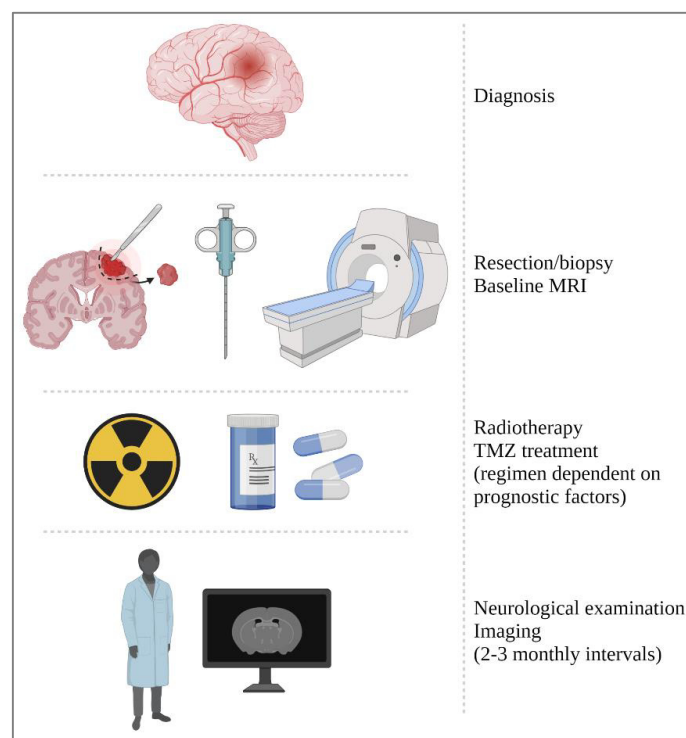


**Figure 2: Clinical management of glioblastoma.**

TMZ is the standard chemotherapeutic compound for GB therapy as it can be administered orally and is able to penetrate the blood-brain barrier (BBB), which otherwise often reflects a major hurdle in systemic brain tumor chemotherapy [37], [44]. During DNA replication, TMZ introduces thymine mismatches into the DNA, which ultimately leads to cell cycle arrest and subsequent autophagy. An important predictive factor for TMZ is O6-methylguanine-DNA methyltransferase (MGMT) promoter methylation status [39], since inactivation of the enzymatic activity of MGMT by methylation of CpG islands in the MGMT promoter, which is

observed in 30-40% of GB patients, is associated with substantially improved efficacy of TMZ therapy [45], [46].

In 2005, the EORTC 26981/NCIC CE.3 trial revealed that median patient survival was significantly prolonged when TMZ was combined with radiotherapy [37], [47]. Therefore, the current standard of care comprises surgery followed by radiotherapy combined with systemic TMZ therapy plus six cycles of maintenance TMZ for adults < 70 years who are in good general and neurological condition [37], [48].

As mentioned above, due to highly infiltrative growth surgical resection is incomplete in the majority of cases, which together with tumor cell heterogeneity and the persistence of glioma stem cells invariably results in GB relapse. Of note, molecular aberrations frequently vary between initial tumor growth and its relapse [49]–[52]. Upon recurrence, there are no uniform recommendations on clinical management of the disease. Only 20-30% of patients qualify for a second surgical resection, while other options comprise a re-challenge with TMZ chemotherapy or with CCNU (Lomustine), individual therapies with not yet licensed agents such as Regorafenib [53] or the inclusion into a clinical trial.

Other than TMZ and Lomustine, no agent has demonstrated efficacy against GB in a phase III trial. Noteworthy, while treatment with the vascular endothelial growth factor (VEGF) antibody Bevacizumab resulted in prolonged progression-free survival [39] it did not improve overall survival [54], [55]. Furthermore, immunotherapies have been unsuccessful so far. In particular, monotherapy with the PD-1 antibody Nivolumab did not improve survival [56], [57]. Consequently, there is an urgent need for the exploration of more advanced therapeutic options, e.g. targeted molecular and gene therapy, oncolytic virotherapy and immunotherapy.

#### **1.1.4 The tumor microenvironment of glioblastoma**

Interactions between GB cells and cells of the immune system play a pivotal role not only during the process of tumor formation but also in the maintenance of an immunosuppressive tumor microenvironment (TME). Apart from GB cells, the extracellular matrix (ECM), several cytokines and chemokines as well as numerous non-cancerous cell types such as fibroblasts, stromal and endothelial cells and cell types of the innate and adaptive immune system constitute the TME [58]–[60]. Among those are granulocytes, dendritic cells (DCs), monocytic cells, macrophages, natural killer (NK) cells, B cells and T cells [58], [61]. On account of the

BBB, the brain has been considered an immune-privileged site for several decades; however, the discovery of an interplay between brain resident cells and the peripheral immune system via the meningeal lymphatic system has been reported [62], [63]. In this context, damage to the brain parenchyma caused by trauma, inflammation or tumor growth has been shown to entail the recruitment of peripheral cell types to the brain [58], [64]–[66]. Still, the TME of GB is characterized by severe immunosuppressive traits. In the course of cancer immune-editing, tumor cells themselves actively reprogram immune effector cells in the TME to sustain and promote tumor outgrowth [67]. GB-mediated secretion of immune-modulating cytokines has also been shown to influence the cell infiltrate and to further promote immune suppression [68].

#### **1.1.4.1 Neutrophils and dendritic cells**

Neutrophils frequently infiltrate GB and have been reported to be of prognostic value in the course of tumor growth [69]–[71], and preclinical studies hint towards neutrophil-mediated support of the glioma stem cell pool [71] (Fig. 3A). As antigen-presenting cells (APCs), dendritic cells (DCs) are outnumbered by microglia (MG) in the unique cellular environment of the brain and therefore play a less important role in this specific context [72]–[75]. However, intratumoral DCs are still triggered by tumor antigens, reactive oxygen species (ROS) or danger-associated molecular patterns (DAMPs) released by GB cells (Fig. 3B), which are then cross-presented to cytotoxic T lymphocytes. Nevertheless, the high degree of immunosuppression commonly interferes with those anti-tumor responses. In this regard, peripheral blood DCs have attracted interest for the development of DC vaccines which may be able to intensify the stimulation of T cells [76]–[78].

#### **1.1.4.2 Astrocytes**

Astrocytes are the most abundant glial cell type in the central nervous system (CNS) and are responsible for neuronal protection, BBB maintenance, synaptic transmission and general metabolism of the brain microenvironment [79]–[81]. They participate in immune surveillance along with MG, as they are able to present antigens and release immune-modulatory cytokines [82]. Upon activation, their pro- or anti-inflammatory gene expression resembles M1/M2-like characteristics [83].

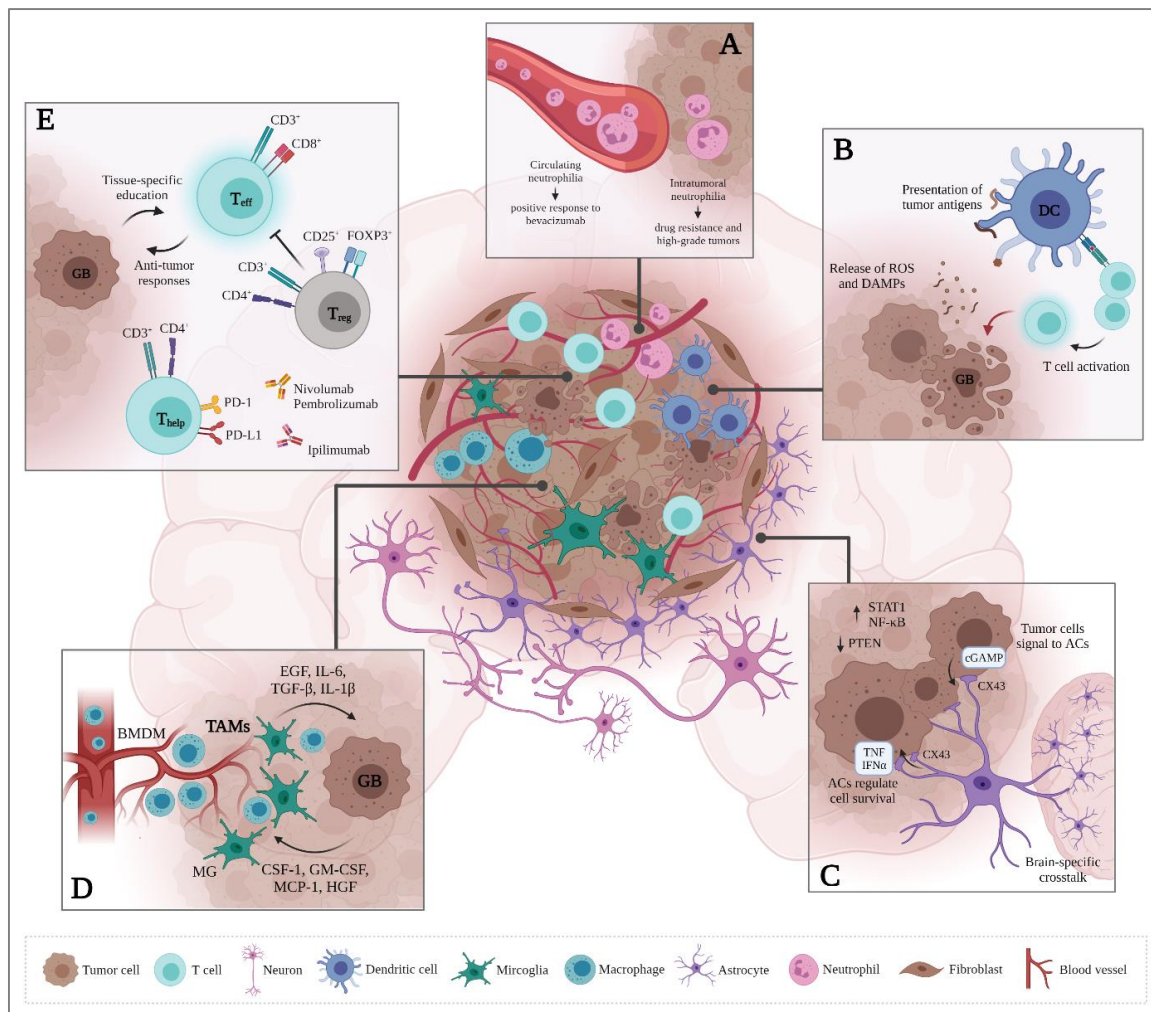


**Figure 3: The glioblastoma microenvironment (adapted from [58]).** Gliomas comprise distinct cell populations, including brain-resident cell types as well as immune cells infiltrating the tissue from the periphery, which contribute to the establishment and the modulation of the specialized TME. This microenvironment characteristically consists of glioma-associated macrophages and microglia (GAMs), astrocytes, DCs, neutrophils and T cells.

There is evidence for anti-tumor activity of astrocytes, since they mediate the tumor cell-damaging conversion of plasminogen to plasmin [84], [85]. However, their capacity of astrogliosis-formation in response to insults such as inflammation, ischemia or infection [79], [86], combined with growth factor and cytokine secretion promotes tumor growth and interferes with therapeutic interventions [87]–[89]. Not only does their secretion of a wide range of neurotrophic factors (e.g. transforming growth factor  $\beta$  (TGF- $\beta$ ), stromal cell-derived factor-1 (SDF-1), glial cell-derived neurotrophic factor (GDNF) and interleukin-6 (IL-6)) support tumor growth, astrocytes also mediate downregulation of major histocompatibility complex class II (MHC-II) and CD80 on tumor and microglial cells, which hampers T cell activation and further contributes to the immunosuppressive TME in GB [90], [91]. They have

even been shown to actively induce T cell apoptosis via Fas ligand (FasL)/CD95L interaction [91], [92] and mediate the downregulation of PTEN in tumor cells, which results in the secretion of CC-chemokine ligand 2 (CCL2) and ultimately attracts peripheral pro-tumorigenic myeloid cells [93]. Furthermore, Chen et al., reported a direct interaction of astrocytes and tumor cells via the gap junction protein connexin 43 (Cx43), aiding the maintenance of a pro-inflammatory and pro-tumorigenic state [94] (Fig. 3C).

#### **1.1.4.3 Microglia**

Although there are other macrophages in the CNS such as meningeal macrophages and choroid plexus macrophages, microglial cells as tissue-resident macrophages are the main immune effector cells of the brain. They account for 5-20% of all glial cells and represent a crosslink between the nervous and the immune system [95]. Whenever brain homeostasis is disturbed by insults such as inflammation, ischemia, trauma or neuronal dysfunction, they become activated and phagocytose pathogens or apoptotic cells and mediate both innate and adaptive immunity via the induction and expression of surface receptors and intracellular enzymes [96], [97]. They are able to modulate the immune response by the release of chemokines and cytokines [98], [99]. Although the concept of M1/M2-macrophage polarization is considered simplistic, MG, similar to peripheral macrophages, can still be characterized as 'classically' activated cells that secrete pro-inflammatory factors and eliminate microorganisms or tumor cells, whereas 'alternatively' polarized cells are associated with tissue repair and immune suppression [100]. For instance, the M1 phenotype induces the upregulation of MHC-I and II as well as further co-stimulatory receptors such as CD80, CD86 on their surface and thereby mediate immune activation via the presentation of antigens to T cells [89,92–94]. Additionally, M1 MG secrete pro-inflammatory cytokines such as IL-6, IL-12, IL-23, IL-1 $\beta$  and tumor necrosis factor  $\alpha$  (TNF- $\alpha$ ), thereby promoting the polarization of T cells to Th1 lymphocytes [101], [102]. On the other hand, MG have also been shown to increase expression of programmed death-ligand 1 (PD-L1), resulting in the suppression of the immune response via the PD-1/PD-L1 [103]. Those MG characterized as the M2 phenotype are poor antigen presenters, they express arginase 1 (Arg1) and suppress the immune response via the secretion of anti-inflammatory cytokines such as TGF- $\beta$  and IL-10 [104], [105].

MG contribute to the TME of GB to a great extent, as they account for up to 40% of the total tumor mass [106]–[109]. Glioma-associated microglia/macrophages (GAMs) comprise of

brain-resident MG and bone marrow-derived macrophages (BMDMs), which are recruited from the periphery [58], [108], [110]. To distinguish between MG and peripheral BMDMs, Bowman et al. recently presented CD49D/ITGA4 as a molecule for unequivocal discrimination in both mice and humans [110]. Tumor cells actively recruit GAMs via their secretion of cytokines and chemoattractants such as monocyte chemoattractant protein 1 (MCP-1) or granulocyte-macrophage colony-stimulating factor (GM-CSF) (Fig. 3D) [86, 89, 101]. Interactions between MG and GB cells have been shown to influence the severity of the disease as they have been shown to favor tumor progression [107], [111], [112]. Their ability to diminish the immune response is often exploited by tumor cells in terms of immune evasion and survival. For instance, Zeiner et al. reported that the M1:M2 ratio accounts for a favorable prognosis in IDH1 wild-type GB [113]. This finding was reinforced by several studies which generated evidence of a pro-tumorigenic TME maintenance by M2-like GAMs, which resulted in worse progression in high-grade gliomas [114]–[116]. M2 polarization is facilitated by GB metabolites like e.g. kynurenine [117]. Additionally, GAMs have been shown to secrete growth factors such as VEGF or endothelial growth factor (EGF) or cytokines like IL-6, ultimately promoting tumor growth, invasion and angiogenesis (Fig. 3D) [118]. In line with that, upregulation of the TGF- $\beta$  signaling pathway, as well as secretion of IL-10 and prostaglandin E2 (PGE2) into the TME, results in recruitment and stimulation of immune-suppressive regulatory T cells (Tregs) [119]. They further attenuate the immune response via expression of PD-L1, [111], [120] and mediate downregulation of co-stimulatory molecules such as CD86, CD80 and CD40, ultimately impeding T cell activation [121]. They also actively contribute to T cell apoptosis via the expression of FasL, fuel genetic instability and support cancer stem cell survival [96], [111], [122].

#### **1.1.4.4 T cells**

T cell-mediated inflammatory responses are mostly absent in the brain under physiological conditions; however, recruitment of T cells under pathological conditions has been reported [123], [124]. Especially cytotoxic CD8<sup>+</sup> T cells have been observed to mediate a potent anti-tumor response [125]. Nonetheless, their cytotoxic activity is commonly suppressed within the TME of brain tumors. Interaction of T cells and GB cells within the immunosuppressive environment drastically alters T cell effector function. T cell dysfunction mostly manifests in T cell senescence, tolerance, anergy or exhaustion. Although senescence in T cells is poorly

studied so far, there is evidence that immunosenescence of the CD4<sup>+</sup> compartment correlates with poor prognosis. For instance, GB patients with a high abundance of CD4<sup>+</sup>CD28<sup>-</sup>CD57<sup>+</sup> T cells in the TME showed significantly decreased overall survival [126]. Senescent T cells are mainly characterized by the expression of CD57, a marker of terminal differentiation and lack of co-stimulatory CD27 and CD28 [127], [128]. Tolerizing mechanisms are of crucial importance under physiological conditions; however, they are exploited by GB cells to evade immune attack. Not only FasL-mediated deletion has been described in GB [129]–[131], also the recruitment of Tregs, a CD4<sup>+</sup> T cells subset characterized by expression of the transcription factor forkhead box P3 (FOXP3), is commonly observed. The CD4<sup>+</sup> compartment of GB is highly infiltrated by Tregs, which contribute to immunosuppression within the TME to a great extent [132], [133] (Fig. 3E). For instance, they mediate decreased IL-2 and IFN- $\gamma$  production by T cells via their secretion of TGF- $\beta$  and IL-10 [134]–[136]. Treg expansion is also promoted by the STAT3 pathway, which is often overexpressed in GB cells, thereby stimulating proliferation and survival [137]–[139]. Another protective mechanism is posed by T cell exhaustion, which physiologically aims at limited collateral damage of an immune response. If T cells encounter an antigen several times under conditions that are not ideal, a specific transcriptional program renders them hyporesponsive, a mechanism that is misused by tumor cells as well (e.g. via the PD-1/PD-L1 interplay) [140]–[142]. In GB patients, the upregulation of several immune checkpoints such as programmed cell death protein 1 (PD-1), lymphocyte activation gene 3 (LAG-3), T cell immunoglobulin and mucin-domain containing-3 (TIM-3) or cytotoxic T-lymphocyte-associated protein 4 (CTLA-4) results in drastic T cell exhaustion [142], [143].

### 1.1.5 Clinical challenges

As mentioned above, the infiltrative nature of GB growth makes truly complete surgical resection of the tumor impossible. However, there are further aspects that represent major hurdles in implementing an effective treatment approach. Among the factors that render GB management highly challenging are the low mutational burden of the tumor, its heterogeneity, the prevailing immunosuppression as well as immune dysfunction within the TME, and the residency of GB cells in a microenvironment shielded by the BBB.

Although the concept of the brain being an inaccessible organ has been refuted [144], the BBB still preserves a specialized environment that is deprived of most external influences and lacks

surveillance by peripheral immune cells. The BBB is of crucial importance for the proper function of the brain [145], [146], but its highly selective permeability represents a grave obstacle in the context of chemotherapy in GB patients. The therapeutic effectiveness of chemotherapeutics is often compromised in brain tumors because drug concentrations within the tissue do not reach sufficient levels [147], [148]. Therapy resistance is also suspected to be connected to GB heterogeneity, albeit a complete understanding of the underlying genetic mechanisms is still poorly conceived [149], [150].

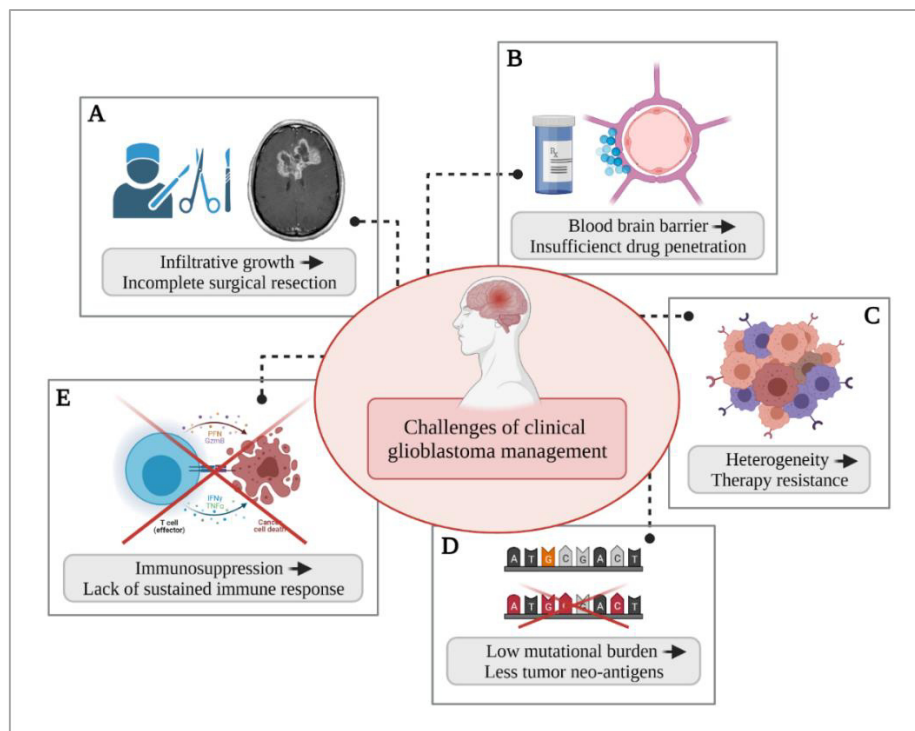


**Figure 4: Challenges of glioblastoma management.**

In this regard, the need for improved drug delivery strategies as well as for novel anti-GB treatments like selective inhibitors or immunotherapies that promote tumor cell death and enhance immunogenicity is enormous. However, despite the extensive research activity and the remarkable gain of knowledge concerning the genetic heterogeneity and characteristic traits of GB, the translation of many concepts into the clinical setting has failed. The establishment of a successful immune response is also impeded by the characteristically low mutational burden of GB [151]. In other malignancies, the accumulation of mutations throughout tumor progression results in the generation of tumor neo-antigens which are new to the immune system and thereby evoke an anti-tumor response [152]. For instance, when predicting the response to immunotherapies, a higher tumor mutational burden is associated



with improved treatment response in non-CNS tumor entities [153]. In GB, the low amount of neo-antigens might not be sufficient to mount an effective anti-tumor immune response.

Apart from the mutational burden, the composition of the immune infiltrate of GB is also relevant for treatment success. While a pro-inflammatory “hot” TME with comparatively high amounts of cytotoxic T cells combined with an immune-stimulatory cytokine milieu often implies a favorable prognosis [154], brain tumors like GB are mostly rated “cold” tumors characterized by severe and sustained immunosuppression. There is a variety of mechanisms employed by GB cells that prevent its TME from transitioning from “cold” to “hot”, such as the downregulation of MHC molecules, increased secretion of anti-inflammatory cytokines and chemokines as well as the recruitment of immunosuppressive cells like myeloid-derived suppressor cells (MDSC), M2-polarized GAMs, Tregs and regulatory B cells (Bregs) [67], [132], [155], [156]. The polarization of T cells and GAMs by GB cells has already been described in detail in sections 1.1.4.3 and 1.1.4.4. Treg proportions increase within 10 days of brain tumor implantation in mice [157], [158], and their recruitment and expansion seem to be TGF- $\beta$ - and enzyme indoleamine 2,3-dioxygenase (IDO)-induced [159]–[161]. This kind of local immune dysfunction is also reflected systemically via the GB-induced sequestration of T cells in the bone marrow [162].

To promote a rather “hot” TME that is less immunosuppressive and more susceptible to immune attack, an increase in immunogenicity via the release of tumor neo-antigens following GB cell death is desirable. Those therapy approaches also bear the potential to have synergistic effects when combined with immunotherapeutic interventions [163].

## **1.2 Natural killer cells**

NK cells are lymphocytes of the innate immune system and account for 5–20% of the circulating lymphocytes in humans [164]. Besides their dominant role in the clearance of bacterial and viral infections, NK cells are of crucial importance in tumor immunosurveillance due to their ability to recognize and lyse transformed cells [165]. They mediate their protective anti-tumor immunity via contact-dependent cytotoxicity, which is predominantly mediated by the release of perforin- and granzyme B (GrB)-containing granules [166]. Imai et al. found a positive correlation between decreased NK cell cytotoxic activity and an elevated risk for tumor development [167], and also other studies reported that high intratumoral NK cell

counts indicate a favorable prognosis in tumor entities like colorectal or gastric carcinoma [168], [169] and squamous cell lung cancer [170].

In humans, NK cells are mainly identified via the expression of CD56 as well as the activating Fc receptor CD16 [171], [172]. In mice, however, those markers are not expressed, which is why in murine studies NK1.1 and NCR1 are commonly used as NK cell markers [173]. Uniquely, antigen processing and presentation are not required for activation of cytotoxic activity of NK cells [174]. Since they do not express variable clonotypic receptors on their surface, their activation is mediated via the interaction of NK cell receptors and the respective target cell. They can be distinguished by the expression of several activating receptors such as NKG2D, NCR1, NCR2, NCR3, NKG2, Ly49D, or Ly49H. Within the cell, the activating signal is transmitted via receptor-associated adaptor molecules like Fc $\epsilon$ RI $\gamma$ , CD3 $\zeta$ , and the DAP12 [175]. Upon recognition of a target cell, NK cells can exert their cytolytic function through the release of perforin that is able to form pores in the target cell's membrane, through which granzymes have access to the cytoplasm [176], [177]. Inside the cell, they initiate apoptosis via the induction of BH3-interacting domain death agonist (Bid), caspase-3 or DNA-PKc [178]–[183]. Another mechanism of target cell lysis is the employment of death receptor ligation via the expression of CD95L or TNF-related apoptosis-inducing ligand (TRAIL), which activates the target cell's death receptors such as CD95/Fas and TRAIL-R1-R2 [182]–[186]. Additionally, NK cells produce and secrete large amounts of chemokines such as CCL3 (MIP-1 $\alpha$ ), CCL4 (MIP-1 $\beta$ ), CCL5 (RANTES), XCL1 (lymphotoxin), and CXCL8 (IL-8) [187] as well as pro-inflammatory Th1-type cytokines including IFN- $\gamma$ , GM-CSF, and TNF- $\alpha$  [188]–[193], inducing the recruitment and subsequent activation of T cells, macrophages, DCs and neutrophils [194], [195].

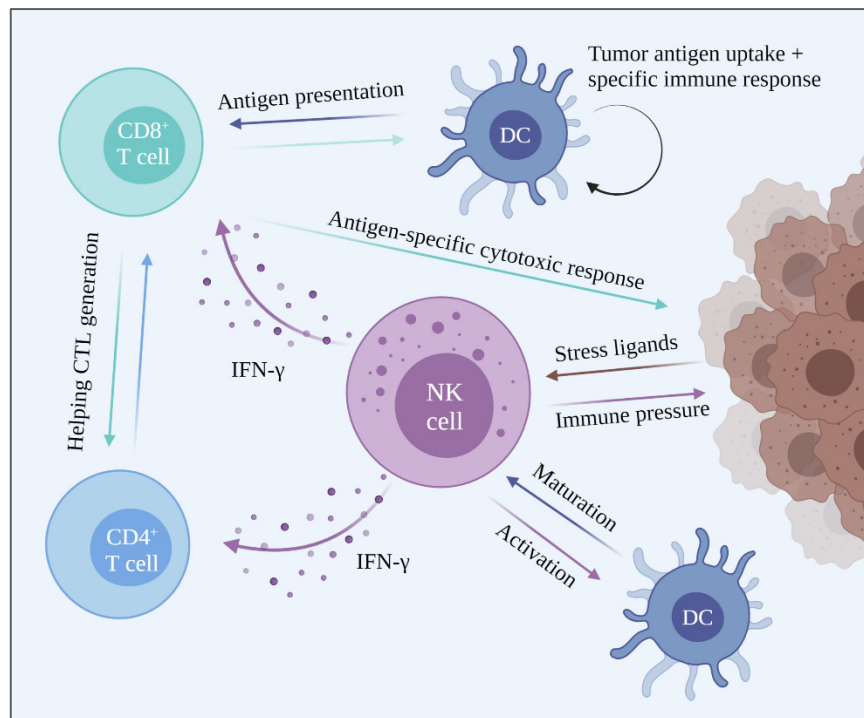


**Figure 5: NK cell functions in tumor control.**

Although the BBB mainly excludes NK cells from the brain microenvironment, increased BBB-permeability in response to neuropathological conditions enables access to the brain [191], [196]. NK cells have also been found in GB, although they infiltrate tumors at very low amounts, accounting for only 2% of immune cells in glioma [197]–[199]. Interestingly, radiotherapy and TMZ treatment have been shown to result in decreased NK cell numbers in patient blood samples [200]. GB cells further avoid NK cell-mediated lysis via the downregulation of NKG2D, an NK cell-activating receptor [201]. Despite their low abundance in the TME of GB, NK cells still have been shown to mediate anti-tumor activity in response to neuron-produced CX3CR1-mediated recruitment of NK cells to the brain [202]. Also, PDGFD, which is frequently upregulated in GB, has been shown to engage with the activating NK cell receptor Nkp44, which promoted the secretion of pro-inflammatory cytokines and subsequent anti-tumor response, resulting in prolonged patient survival [203]. In line with that, studies both in mice and humans revealed a correlation between activated NK cell transcriptional signatures and favorable prognosis [202]–[210]. Given their significant contribution to tumor control despite their low abundance, adoptive transfer of NK cells that have been activated and expanded *ex vivo* could contribute to the elicitation of a more enduring immune response in GB. Especially combination therapy approaches hold the potential to defeat GB immune escape and increase NK cell activity [211]. Given the low immunogenicity

within the brain tumor TME, immunotherapies represent a promising candidate for combination therapy with NK cells. By attenuating the dominant immunosuppression in GB, an NK cell-initiated immune response might become more persistent [212]. Recently, it has been shown that inhibition of the PD-1/PD-L1 checkpoint leads to increased NK cell activity, further reinforcing interest in the evaluation of combined immune strategies [213].

### **1.2.1 Genetically engineered chimeric antigen receptor NK cells**

To increase their anti-tumor activity and retarget it to tumor-specific antigens, NK cells have been genetically modified with chimeric antigen receptors (CARs). This has been accomplished with both primary NK cells and the clonal cell line NK-92. This cell line was derived from an NK cell lymphoma patient and has been genetically engineered to express a HER2-directed CAR construct [214]. Irradiated NK-92 cells for use in humans are not able to clonally expand and have not been reported to induce cytokine storms or graft-versus-host disease (GvHD), which contributes to their promising safety record that has also been validated in clinical trials [214]–[217].

Since HER2 has been reported to be expressed in up to 80% of GB patients [27], [28], [29], the ongoing CAR2BRAIN clinical trial employs these HER2-specific CAR-NK cells (named NK-92/5.28.z cells) for local GB therapy [216], [218], [219]. Those cells express a second-generation CAR based on the HER2-specific single-chain variable fragment (scFv) derived from the FRP5 monoclonal antibody, which has been fused to CD28 and CD3 $\zeta$  signaling domains.

CAR-NK cells are irradiated before being transferred into the patient, which suppresses their proliferation but does not impair their cytotoxic activity [29], making them eligible as a potential off-the-shelf contribution to cellular immunotherapy [191], [220]. In preclinical studies, NK-92/5.28.z cells exhibited potent specific lytic activity towards HER2<sup>+</sup> GB cells [29]. Symptom-free survival of experimental animals was significantly extended in murine orthotopic xenograft models upon repetitive intratumoral injection of NK-92/5.28.z cells. A key finding of the study by Zhang and Burger et al. was that in the GL261-HER2 mouse model, the efficacy of this therapy was largely driven by a CAR-NK-induced secondary immune response that was not exclusively HER2-dependent [29], [221].

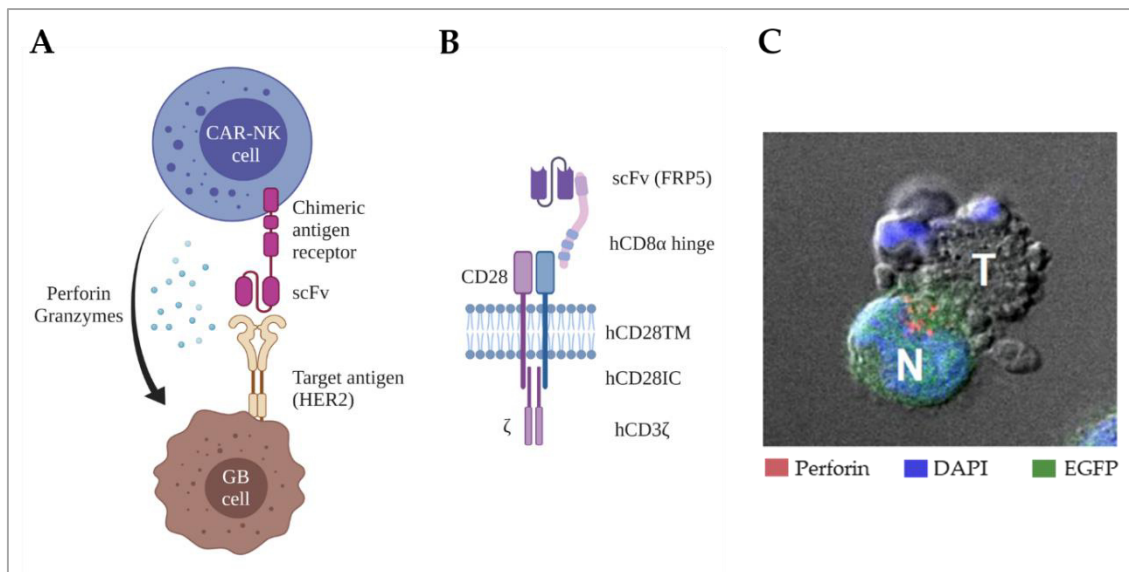


**Figure 6: Generation of HER2-specific CAR-NK cells. (A)** Schematic representation of targeted CAR-NK cell therapy. **(B)** Composition of the HER2-specific second-generation CAR. **(C)** Confocal microscopy image of CAR-NK cells lysing a human GB cell (adapted from [222]).

However, in the GL261-HER2 mouse model, the efficacy of treatment with NK-92/5.28.z was significantly limited in advanced larger tumors most likely due to the immunosuppressive microenvironment. Therefore, to further increase the anti-tumor potential of NK-92/5.28.z cells, combination therapy using systemically administered checkpoint inhibitors was implemented and revealed synergistic effects even at advanced tumor size up to complete remission in some animals [223].

### 1.3 Cancer immunotherapy

Recent advances in precision oncology have led to the development of novel immunoncology strategies such as checkpoint inhibitors and combination immunotherapies. Within the last decade, immunotherapy has revolutionized the clinical management of cancer and was awarded a Nobel Prize in medicine in 2018. Treatment with immune checkpoint inhibitors (ICIs) achieved promising clinical outcomes in a variety of tumor entities such as melanoma and non-small-cell lung cancer [224]–[226]. ICIs mediate the inhibition of certain T cell inhibitory receptors, such as immune checkpoints PD-1 and CTLA-4. Under physiological conditions, activation of those checkpoints results in restricted clonal T cell proliferation to ensure immune autoregulation. Tumor cells frequently hijack this mechanism by upregulating receptor ligands, thereby promoting T cell dysfunction and evasion of a sustained immune attack. Ipilimumab (Yervoy®, Bristol-Myers Squibb), a human monoclonal CTLA-4 antibody,

was the first ICI approved for the treatment of melanoma patients [226]–[228]. Other ICIs currently approved in Europe and the USA are e.g. the PD-1 antibodies Pembrolizumab (Keytruda®, Merck) and Nivolumab (Opdivo®, Bristol-Myers Squibb). Besides the “classical” checkpoints PD-1 and CTLA-4, there are several others, including TIM-3, TIGIT, LAG-3, BTLA, 2B4, CD160, and CD39, that also raise interest regarding the development of specific inhibitors [229]–[232].

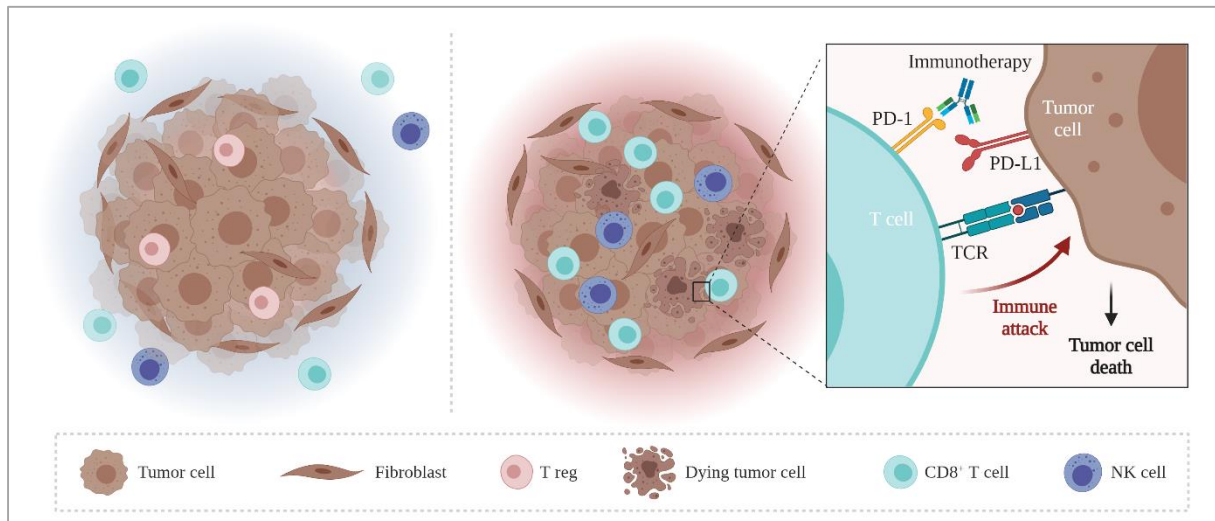


**Figure 7:** The principle of immunotherapy. An “immunologically cold” tumor lacking immune cell infiltration (left) opposed to an “immunologically hot” tumor. Anti-PD-1 antibody reduces PD-1/PD-L1-mediated intratumoral immune suppression inducing immune cell activation and tumor cell lysis.

Despite the tremendous benefits ICI therapy had on the outcomes of many cancer patients, not all tumor entities respond equally to treatment. A study showed that durable responses to anti-PD-1 and CTLA-4 therapy were only found in 20% to 40% of patients [233]. The therapeutic success of ICI therapies is strongly correlated to high mutational load and a subsequently elevated amount of neo-antigens [234]–[238], resulting in elevated response rates in T cell-inflamed, „hot“ tumors such as melanoma, bladder cancer, non-small-cell lung cancer (NSCLC) and head and neck squamous cell carcinoma (HNSCC) [235], [239]–[241]. In „cold“ tumors like several breast cancers, ovarian cancer, prostate cancer, pancreatic cancer, and GB, low T cells amounts obstruct the initiation of effective immune responses evoked by ICIs [58].

### 1.3.1 Immunotherapy in glioblastoma

The lack of effective treatment options upon GB recurrence and the consequent poor overall prognosis has prompted considerable efforts to explore more advanced therapeutic options, including immunotherapy. The most prominent challenge of immunotherapy in GB is the immunosuppressive TME, combined with a low mutational burden as well as low immunogenicity [242], [243]. Between 61% and 88% of patients' tumors express PD-L1, the ligand for the immune checkpoint PD-1, mainly on GB cells as well as tumor-associated monocytes/macrophages [120], [243]. Given the high amounts of myeloid cells within the GB immune infiltrate, immunotherapy using ICIs targeting the PD-1/PD-L1 axis represents a promising treatment approach [155], [244]. For instance, CTLA-4 inhibition in mice led to improved survival and increased CD4<sup>+</sup> T cell activity [245]. The induction of increased immunoreactivity of GB by the use of ICIs is also currently under clinical evaluation in humans, where it is often combined with standard of care therapy or after GB relapse [246], [247], e.g. the combination of Nivolumab (anti-PD-1) and radiotherapy (NCT02617589, phase III) or Nivolumab and/or Ipilimumab in recurrent GB (NCT02017717, phase III) [47]. However, due to severe T cell dysfunction and the prominent immunosuppressive TME, the majority of clinical trials evaluating ICI therapy for GB have been disappointing so far. Several randomized trials investigating the benefits of ICI monotherapies in adjuvant as well as recurrent settings have failed to meet their primary endpoint [56].

Similar to chemotherapeutics, ICI molecules as large molecules are commonly unable to cross the BBB, which entails insufficient ICI concentrations in the brain and in the tumor. An additional drawback of systemic administration of ICIs is the risk of severe immune-related side effects, while the use of several drugs further intensifies the risk and impedes the development of combination immunotherapies [248]. In the first major human clinical trial using anti-PD-1 (CheckMate143), patients receiving anti-PD-1 alone showed a tolerable safety profile, whereas severe adverse events in 8 of 10 patients who received anti-PD-1 plus anti-CTLA-4 led to discontinuation in 5 patients [249]. Another study reported the discontinuation of 20–30% of patients in the combination cohort, compared to 10% of patients who received the anti-PD-1 monotherapy [250].

A more efficient and tolerable strategy for immunotherapy approaches might be a more local administration of ICIs, allowing for high intratumoral and low systemic drug concentrations,

which could be achievable via the use of gene therapeutic approaches employing adeno-associated viral vectors (AAVs) [251].

#### 1.4 Gene therapy using adeno-associated viruses

Gene therapy is a gene delivery strategy that aims towards the treatment of various diseases arising from genetic errors that result in metabolic, cardiovascular, muscular, neurological, hematological or ophthalmological disorders, either via supply of a missing gene or knockdown of an overexpressed gene [252]–[255]. Among the vectors commonly used for gene therapy are retroviral, lentiviral or adenoviral vectors as well as adeno-associated virus (AAV) vectors [254], [255]. Over the last decades, mainly lentiviral viruses have been used for gene transfer [256], [257]; however, integration-competent viral vectors harbor the risk of insertional mutagenesis and transgene oncogenesis in response to vector integration, accounting for adverse events like the development of lymphoid leukemia in several cases [258]–[260]. More and more frequently, however, AAV vectors are the vectors of choice for gene transfer, as they combine several advantages over other delivery systems. The use of AAV vectors allows for highly efficient gene editing which is considered to be particularly safe. AAV is a parvovirus belonging to the genus of dependoviruses, therefore being unable to replicate without a helper-virus like an adenovirus or herpes virus. Therefore, they are non-pathogenic and rarely integrate into the host chromosome. Moreover, AAV shows a broad tropism, low immunogenicity and can be produced at very high titers [261]–[265]. Its ability to transduce post-mitotic cells enables long-term expression of the transgene.

It was first described by Bob Atchinson in 1965 and has been a versatile subject of research ever since [266].

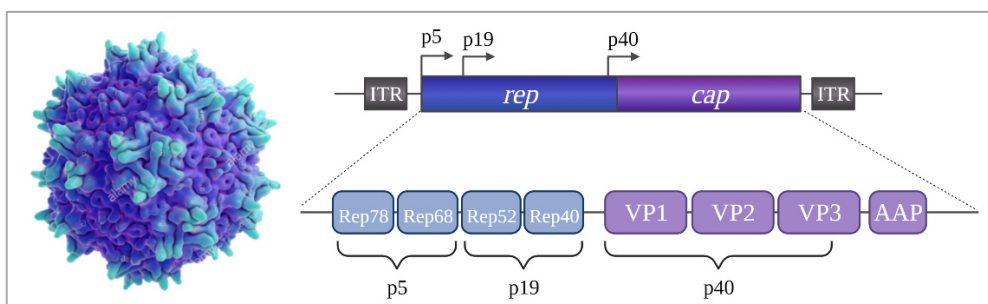


**Figure 8:** Adeno-associated virus (AAV) structure and genome organization (adapted from [252] and [253])



The virus is non-enveloped and has an icosahedral protein capsid. Enwrapped by the capsid is its linear single-strand DNA genome, which is approximately 4,7 kB in length and encodes replication as well as capsid genes. Since it does not encode its own polymerase, gene transcription is dependent on one of the host cell. Rep78, Rep68, Rep52 and Rep40 take on specific roles in genome replication as well as virus assembly and are encoded by the *rep* gene. The capsid comprises three distinct capsid proteins (virion protein (VP) 1, VP2 and VP3), whose genes are located in the *cap* ORF. Each AAV consists of 60 VPs at a 1:1:10 ratio of VP1:VP2:VP3. Furthermore, an in-frameshifted ORF encodes an assembly-activating protein (AAP), which is required for capsid assembly [263]–[265]. The first AAV vector-based gene delivery product, Glybera, was approved in Europe in 2012 and is now used for the treatment of patients suffering from lipoprotein lipase deficiency [269], [270]. It was followed by Luxturna, which delivers the human retinal pigment epithelium-specific protein (RPE65) for the treatment of patients with RPE65-associated Leber congenital amaurosis [271], delivering the human retinal pigment epithelium-specific protein (RPE65) (Smalley). Since 2019, spinal muscular atrophy is approved to be treated using the AAV-based gene therapy drug Zolgensma [272]. The high potential of virus-based gene therapies is also reflected by an FDA report in 2019, predicting that 10–20 new cell and gene therapy products per year will be approved by 2025 [273].

After binding to its primary receptor on target cells, AAV is internalized via a clathrin-coated pit into endosomes. Acidification of the endosome triggers a conformational change in capsid proteins and a subsequent endosomal escape. Following the entry into the nucleus, uncoating and release of the genome take place. Once the single-stranded genome has converted into a double-stranded DNA (dsDNA) template, the respective transgene is transcribed and subsequently translated in the cytosol [263], [264]. For the use in gene therapy, all the viral genes are replaced by the gene of interest, flanked by inverted terminal repeats. The size of the transgene should not exceed 5 kB [274]. AAV2 as the best studied and characterized AAV serotype is most commonly used for vector design. High gene expression of the transgene is ensured by the use of constitutively active, strong promoters such as the cytomegalovirus (CMV) promoter/enhancer, elongation factor 1a (EF1a) or simian virus 40 (SV40) [275]. Gene therapy recombinant AAVs (rAAVs) are generated via 3-plasmid co-transfection: generation requires a cassette containing the transgene, a plasmid encoding the *rep* and *cap* genes and a

plasmid containing the adenovirus helper genes. Human embryonic kidney (HEK) cells are commonly used as packaging cells.

#### **1.4.1 Generation of HER2-specific adeno-associated viral vectors**

As interest in gene therapies using recombinant AAVs (rAAVs) increases, the effort to enhance gene delivery efficiency does as well. Especially the efficacy of host cell transductions is addressed via refinement of cell entry targeting technologies. Vector engineering allows for the permanent modification of viral capsid or envelope proteins, optimizing the interaction of rAAVs with receptors on the target cell's surface [261], [276]. Re-directing rAAV vector tropism by capsid engineering represents a substantial advancement in gene therapy since targeting of specific cell types becomes feasible. The different wildtype AAV serotypes on which rAAVs are based exhibit a natural tropism for distinct tissues and cell types. For instance, AAV2 preferably transduces skeletal muscle, hepatocytes and vascular smooth muscle cells (VSMCs). Systemic administration of unmodified rAAV2 vectors resulted in the transduction of liver tissue and led to off-target effects, which limited the amount of transgene delivery to target tissues [277]–[280]. There have been attempts to re-direct tropism via the use of tissue-specific promoters; however, vector particles were still able to enter non-target cells and induce cytotoxicity [262], [276].

In the past, the strategy of specifically targeting tumor tissue using gene therapy has been extensively studied, using a variety of approaches including delivery of recombinant DNA, interfering RNA (iRNA), microRNAs (miRNAs), transcription activator-like effector nucleases (TALENs) or clustered regularly interspaced short palindromic repeats/CRISPR-associated protein 9 (CRISPR/Cas) [281]–[286]. Also, the employment of suicide genes has been extensively studied, including their implications for glioma therapy [287], [288].

However, none of the and non-viral gene delivery systems, including natural AAV serotypes are specific for malignant cells [289]–[293], which is problematic when envisaging them as vectors for targeted gene delivery to tumor cells. Most viral systems preferentially target liver tissue, which is of relevance for the targeting of hepatocellular carcinomas but impedes effective gene delivery to other organs [294], [295]. Although localized delivery techniques such as inhalation or intracranial, intratumoral and intravenous injection have been evaluated,

the broad expression of AAV's natural receptors still results in transduction of non-target cells [279], [296].

Therefore, to prevent gene transfer to non-relevant cell types and facilitate targeted transduction of tumor cells, Buchholz et al. designed rAAVs with specificity for HER2<sup>+</sup> cells (HER2-AAVs). To restrict gene transfer to HER2<sup>+</sup> cells only, they genetically fused designed ankyrin repeat proteins (DARPin), which act as targeting ligands, to VP2 [251], [290], [297], [298] [299]–[302].

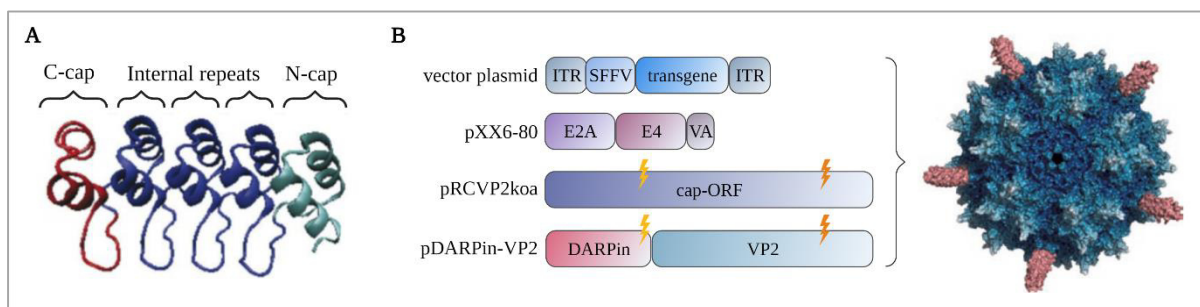


**Figure 9: Schematic representation of a DARPin and a DARPin-linked AAV vector (adapted from [236] and [288]) (A)** Ribbon model of a DARPin with three internal repeats [303]. **(B)** Plasmids for generation of AAV-targeting vectors designed by Münch et al. [236]. Expression of unmodified VP2 was excluded via mutation of the VP2-start codon (labeled by yellow flash). HSPG binding was prevented via the substitution of R585 and R588 by alanine (labeled by orange flash).

DARPin are highly specific genetically engineered proteins that can be selected by high-throughput screens from DARPin libraries. They consist of helical repeats with a concave protein interaction surface, which makes them high-affinity binding scaffolds. The artificial proteins are designed to mimic antibodies while being smaller (14–18 kDa) and more stable [251], [304]. Furthermore, they do not tend to aggregate and have been shown to be thermostable as well as resistant to proteases and denaturing agents [305]–[308]. Essentially any molecule can be selected as a target for such receptor-specific DARPin. In the case of HER2-AAVs, the coding sequence for DARPin 9.29 was chosen after the high-throughput selection of a DARPin library against the extracellular domains of HER2 [297], [309]. Neither the correct folding of the DARPin after its fusion to the N-terminus of VP2 nor capsid assembly or vector genome packaging was impaired [297], [305]. To unequivocally re-direct AAV tropism and ensure off-target free HER2-targeting specificity, natural tropism had to be eradicated. This was achieved by simultaneous ablation of natural receptor function via the introduction of two point mutations into the binding motif for AAV's primary receptor

heparan sulfate proteoglycan (HSPG). Site-directed mutagenesis did not hamper vector assembly and function [282], [299]–[302].

Taken together, the resulting viral vectors harbor cell type specificity that enables a restricted biodistribution in response to the systemic or local application without the risk of autoimmune-like side effects [236], [297]. The use of receptor-targeted AAVs facilitates the transduction of solid tumors which can be difficult to access. In previous studies, 75% of all tumor sites in experimental animals were tracked following a single intravenous administration of HER2-AAVs [251]. Concerning recent advances in immunotherapy and its investigation for the treatment of GB, HER2-AAV-mediated delivery of genes encoding ICIs represents a promising novel treatment approach. Using HER2-AAVs as a tool for gene delivery, the local expression and secretion of ICIs after the transduction of tumor cells *in vivo* becomes feasible [310]. Cargo gene expression limited to the tumor area allows for high intratumoral and low systemic drug concentrations.

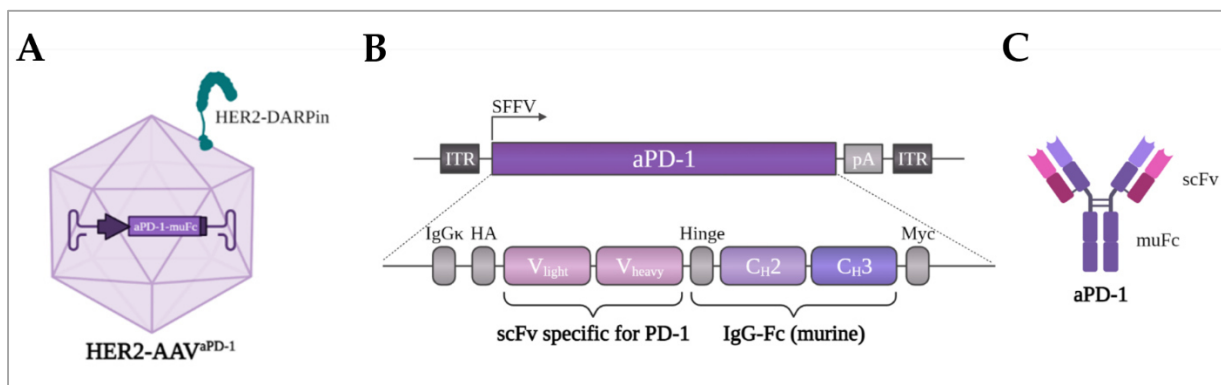


**Figure 10: Schematic representation of HER2-AAV encoding murine aPD-1 (adapted from [310]).**

In a study by Reul et al., the coding sequence of an scFv-Fc fusion protein directed against murine PD-1 was packaged into HER2-AAVs. The therapeutic protein is an antibody-like molecule that fuses the Fc region of an immunoglobulin and the ligand-binding region of a receptor or adhesion molecule. HER2<sup>+</sup> RENCA cells were efficiently transduced and secreted the HER2-AAV-encoded aPD-1 in large amounts [310], [311]. Conferring this approach to GB therapy, the modulation of the immunosuppressive TME by disruption of the PD-1/PD-L1 axis might be achieved, which in combination with tumor-specific CAR-NK cell therapy harbors the potential of mediating a sustained immune response against GB.

## 1.5 Aim of the thesis

GB, with its small number of mutations and its highly immunosuppressive microenvironment, is considered a prototypic immunologically “cold” tumor.

This project was set out to induce cell death and inflammation through the application of HER2-specific CAR-NK cells and to antagonize local PD-1-mediated immunosuppression with the use of aPD-1-encoding AAVs re-targeted to HER2 on tumor cells with the primary hypothesis that this strategy will result in potent local reversal of immunosuppression with little systemic side effects (Fig. 11).

Key aims regarding CAR-NK cell therapy include the analyses of inflammatory responses towards their application, in particular the cytokine release in tumor cells and cells of the microenvironment, as well as the regulation of PD-L1 expression in those cell types.

To establish HER2-AAV therapy, transduction efficacy, the functionality of the vector-encoded aPD1 as well as compatibility of both therapy approaches will be evaluated in specific *in vitro* models. Then, the production and secretion of PD-1-directed immunoadhesins will be investigated in the GL261-HER2 mouse model *in vivo*. Biodistribution studies will reveal whether or not transduction efficacy is dependent on the route of HER2-AAV application. The determination of the most effective route of administration in these pharmacokinetic studies will help define the application strategy in preclinical survival experiments.

The combination of HER2-AAVs and the resulting local secretion of anti-PD-1-directed immunoadhesins with CAR-NK cells is intended to exploit complementary mechanisms of action and thus achieve synergistic effects. Finally, the effect of HER2-AAV administration in combination with CAR-NK cells on tumor growth and symptom-free survival of the animals will be quantified in subcutaneous and orthotopic intracranial immune-competent mouse models. In the light of the highly innovational AAV / DARPIn-mediated gene transfer, the project would offer perspectives beyond brain tumor medicine.

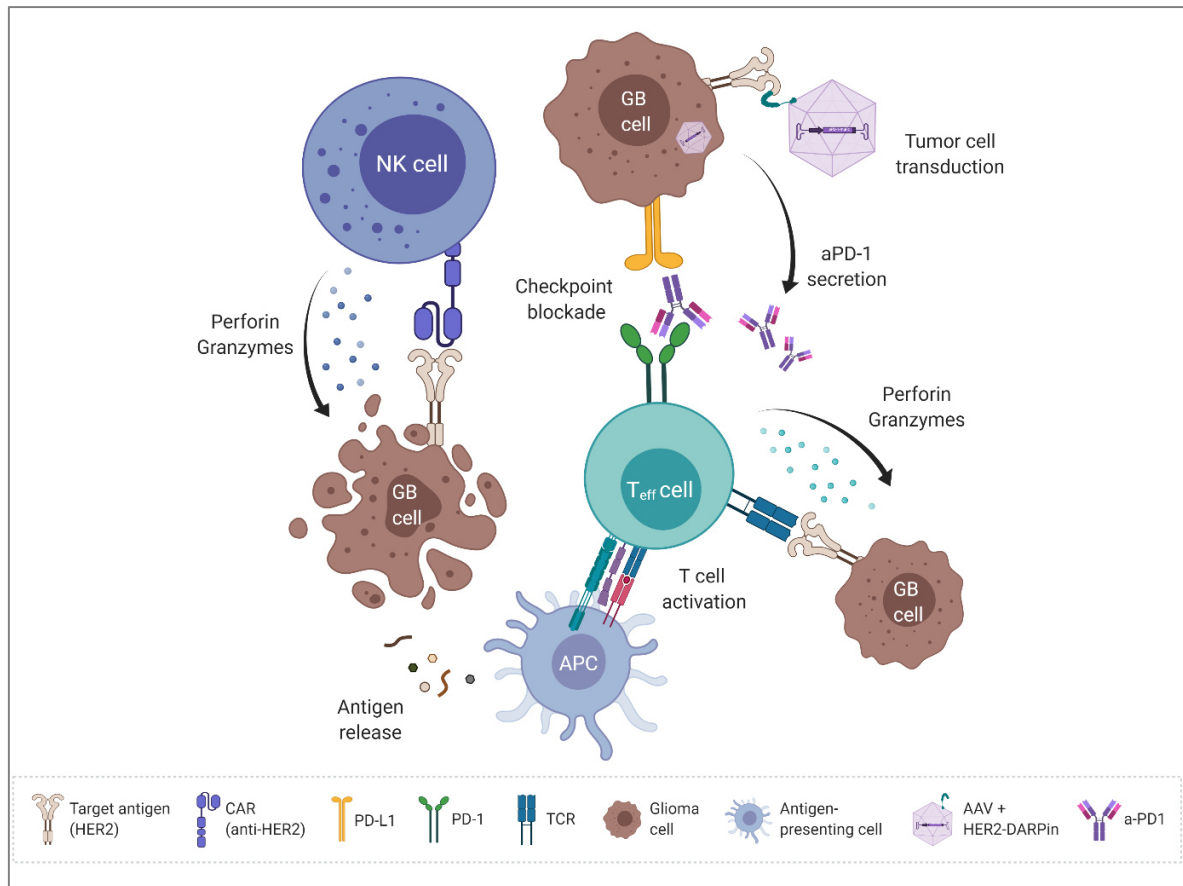


**Figure 11: Combination therapy with CAR-NK cells and aPD-1 encoding HER2-AAVs.** CAR-NK cell-mediated anti-tumor responses are inhibited by the immunosuppressive microenvironment. Upon selective transduction of HER2<sup>+</sup> tumor cells, HER2-AAV<sup>aPD-1</sup> induces local production of a PD-1 antibody enabling an anti-tumor immune response driven by endogenous immune cells.

## 2 Material and Methods

### 2.1 Material

Consumables and chemicals used for molecular biology and protein biochemical methods as well as for cell culture and animal work were obtained from Abcam, Applichem, Bayer, BD Bioscience, Beckman Coulter, Biolegend, Biotechne, Biozym, Carl Roth, Cell Signaling, Corning, Eppendorf, Fujifilm, GE Healthcare, Gibco, Greiner-Bio One, Lonza, Merck Millipore, Miltenyi Biotech, Novus Biologicals, PAN Biotech, Qiagen, R&D systems, Roche, Sarstedt, Sigma-Aldrich and Thermo Fisher Scientific. Commonly used reagents are listed in Table 1.

#### 2.1.1 Reagents

**Table 1:** Reagents, chemicals, recombinant proteins and cytokines

Name	Supplier
1-Step™ Ultra 3,3',5,5'-Tetramethylbenzidine (TMB) substrate	Thermo Fisher Scientific
2-Mercaptoethanol	Carl Roth
4% Paraformaldehyde	Carl Roth
ABsolute Blue qPCR SYBR Green Fluorescein Mix	Thermo Fisher Scientific
Acrylamide	Carl Roth
Ammonium persulfate (APS)	Sigma-Aldrich
Astrocyte medium	Innoprot
BD Pharm Lyse™ lysing buffer	BD
Basic fibroblast growth factor (bFGF)	ReliaTech
BIT medium	PeloBiotech
Bovine serum albumine (BSA)	Carl Roth
CD3 MicroBeads, human	Miltenyi Biotech
CellTrace™ Calcein Violet, AM (CV)	Thermo Fisher Scientific
cOmplete™ Mini Protease Inhibitor Cocktail Tablets	Roche
DMEM-F12	Gibco
DNase I	Thermo Fisher Scientific
Dulbecco's Modified Eagle Medium (DMEM)	Gibco
DYNAL™ Dynabeads™	Thermo Fisher Scientific

Epidermal growth factor (EGF)	ReliaTech
ELISA Stop Solution	Thermo Fisher Scientific
Fetal calf serum (FCS)	Gibco
G418 (Neomycin)	InVivo Gen
GolgiStop™ Protein Transport Inhibitor (containing Brefeldin A)	BD Biosciences
Halt™ Protease & Phosphatase Inhibitor Single-Use Cocktail (100x)	Thermo Fisher Scientific
Hanks' Balanced Salt Solution (HBSS)	Gibco
Recombinant IFN $\gamma$ (human/murine)	BioLegend
Interleukin-2 (IL-2)	Thermo Fisher Scientific
Laminin	Roche
Leibovitz-L15	Gibco
Lipofectamine™ 3000 Transfection reagent	Invitrogen
Myelin Removal Beads II	Miltenyi Biotech
Nuclease free water	Invitrogen
Penicillin/Streptomycin (PenStrep)	Pan Biotech
Pharmlyse RBC lysis buffer	BD BioSciences
Phosphate Buffered Saline (PBS)	Gibco
Pierce™ ECL Western Blotting substrate	Thermo Fisher Scientific
Pierce™ IgG Elution Buffer, pH 2.0	Thermo Fisher Scientific
Pierce™ Stop Solution for TMB	Thermo Fisher Scientific
Ponceau S	Carl Roth
Powdered milk	Carl Roth
Propidium Iodide (PI)	Sigma-Aldrich
Protein Assay Dye Reagent	Biorad
Puromycin	Sigma-Aldrich
Recombinant Human ErbB2/HER2 Fc Chimera Protein	R&D systems
Recombinant Protein A-Sepharose® 4B	Invitrogen
Roti® Quant Bradford Reagent	Carl Roth
Roswell Park Memorial Institute (RPMI) 1640 medium	Gibco



Spectra™ Multicolor Broad Range Protein Ladder	Thermo Fisher Scientific
SuperScript™ VILO™ Master Mix	Invitrogen
SYBR Green	Thermo Fisher Scientific
Tetramethylethylenediamine (TEMED)	Carl Roth
TRI Reagent®	Sigma-Aldrich
UltraPure™ 0.5M EDTA, pH 8.0	Invitrogen
Virus production serum-free medium (VP-SFM)	Gibco
X-Vivo™ 10	Lonza Bioscience

### 2.1.2 Kits

**Table 2:** Kits

<b>Name</b>	<b>Supplier</b>
Brain Tumor Dissociation Kit (P)	Miltenyi Biotech
Bright-Glo™ Luciferase Assay System	Promega
DNeasy® Blood & Tissue Kit	Qiagen
Extract Me Total RNA Kit	BLIRT
LEGENDplex™ Human Anti Virus Response Panel	BioLegend
LEGENDplex™ Human Inflammation Panel	BioLegend
LEGENDplex™ Mouse Anti Virus Response Panel	BioLegend
LEGENDplex™ Mouse Inflammation Panel	BioLegend
MicroBCA™ Protein Assay Kit	Thermo Fisher Scientific
PD-1/PD-L1 Blockade Assay	Promega
Spleen Dissociation Kit, mouse	Miltenyi Biotech
TGX Stain-Free™ FastCast™ Acrylamide Kit, 12%	Bio-Rad
Trans-Blot® Turbo™ RTA Mini Nitrocellulose Transfer Kit	Bio-Rad
Tumor Dissociation Kit, mouse	Miltenyi Biotech

### 2.1.3 Enzymes

Table 3: Enzymes

Name	Supplier
DNA Polymerase	Invitrogen
Papain	Worthington
Trypsin EDTA	Gibco

### 2.1.4 Buffers and media

Table 4: Buffer and media composition

Name	Composition
BIT medium	40 mL DMEM-F12 + P/S 100 $\mu$ L EGF 100 $\mu$ L bFGF 10 mL BIT
Collection buffer	1 M Tris in dH <sub>2</sub> O pH 9
ECL (Western blot)	10 % (v/v) solution B (1.1 mg/mL <i>p</i> -coumaric acid in DMSO) 0.03 % H <sub>2</sub> O <sub>2</sub> (30 %) in solution A (25 % (w/v) Luminol in 0.1 M Tris-HCl (pH 8.6))
ELISA blocking buffer	5 % (v/v) FCS 0.05 % (v/v) Tween 20 in PBS
ELISA wash buffer	0,05% (v/v) Tween 20 in PBS
FACS buffer	2% (v/v) FCS in PBS
Freeze medium	90% (v/v) FCS 10% (v/v) DMSO
Lysis Buffer	50 mM Tris/HCl (pH 8.0) 130 mM NaCl 0.5 % (v/v) NP-40 5 mM EDTA (pH 8.0) in dH <sub>2</sub> O

Laemmli-buffer (4x)	250 mM Tris/HCl (pH 6.8) 8 % (w/v) SDS 40 % (v/v) Glycerol 0.08 % (w/v) Bromphenol blue 20 % (v/v) 2-Mercaptoethanol in dH <sub>2</sub> O
NP-40 lysis buffer/ Lysis buffer P	50 mM Tris/HCl (pH 8.0) 130 mM NaCl 0.5 % (v/v) NP-40 5 mM EDTA (pH 8.0) in dH <sub>2</sub> O
Papain solution	5 mL Leibovitz-L15 55 µL Papain 0.5 µM EDTA
SDS running buffer (10x)	124 mM Tris 960 mM glycine 0.5 % (v/v) SDS in dH <sub>2</sub> O
TBS-T	50 mM Tris 150 mM NaCl 0.1 % (v/v) Tween in dH <sub>2</sub> O  pH 7.4
Western Blot 2nd antibody solution	5 % (w/v) BSA in TBS-T
Western Blot blocking buffer	5 % (w/v) powdered milk in TBS-T
Western Blot transfer buffer	250 mM Tris 1,92 M glycine 20 % (v/v) methanol  in dH <sub>2</sub> O

### 2.1.5 Antibodies

**Table 5:** Antibodies

Antibody	Species	Dilution	Supplier
$\alpha$ -mouse CD16/CD32 (Mouse BD Fc Block™)	Rat	FC <sup>1</sup> (1:1000)	BD Bioscience
$\alpha$ -HA-tag	Rabbit	WB <sup>2</sup> (1:5000) ELISA <sup>3</sup> (1:4000)	Abcam

$\alpha$ -mouse-PD-1	Rat	250 $\mu$ g	Bio X Cell
$\alpha$ -mouse-PD-1-FITC	Rat	FC (1:100)	Biolegend
$\alpha$ -mouse-PD-L1-PE	Rat	FC (1:100)	Biolegend
$\alpha$ -human-CD107a-APC	Mouse	FC (1:100)	Biolegend
$\alpha$ -human-HER2-Alexa647	Mouse	FC (1:100)	Biolegend
$\alpha$ -human-PD-L1-APC	Mouse	FC (1:100)	Biolegend
$\alpha$ -mouse-IgG-Fc-FITC	Goat	FC (1:100)	Abcam
$\alpha$ -mouse-IgG-HRP	Goat	ELISA (1:25.000)	Abcam
$\alpha$ -Actin	Goat	WB 1:5000	Santa Cruz Biotechnology
$\alpha$ -human-IgG-Fc-FITC	Goat	FC (1:100)	Abcam
Mouse IgG1, isotype control	-	FC (1:100)	Biolegend
$\alpha$ -rabbit-IgG-HRP	Goat	WB 1:8000	Invitrogen
$\alpha$ -goat-IgG-HRP	Mouse	WB 1:5000	Santa Cruz
$\alpha$ -human-HER2-Alexa647	Mouse	FC 1:100	BioLegend
$\alpha$ -human-EGFRvIII-Alexa488	Mouse	FC 1:100	Novus Biologicals
$\alpha$ -mouse-IgG-HRP	Goat	ELISA 1:30000	Abcam
$\alpha$ -mouse-IgG-Fc-FITC	Goat	FC 1:100	Abcam
$\alpha$ -mouse-PD-1-FITC	Rat	FC 1:100	BioLegend
$\alpha$ -mouse-PD-L1-BV421	Rat	FC 1:100	BioLegend
$\alpha$ -human-PD-L1-PE	Mouse	FC 1:100	BioLegend

FC<sup>1</sup>: Flow Cytometry, WB<sup>2</sup>: Western Blot, ELISA<sup>3</sup>: Enzyme-linked Immunosorbent Assay

### 2.1.6 Oligonucleotides

All oligonucleotides used in this thesis were synthesized by Sigma-Aldrich.

**Table 6:** Primer sequences

Name	Oligonucleotides (5' → 3')
18s_fwd	CTACCACATCCAAGGAAG
18s_rev	GGACTCATTCCAATTACAG
aPD1_fwd	CCAAGTCCTACAACATATG
aPD1_rev	GTCCTCAGATTGTTTCATC
SDHA_h_fwd	GTGCGGATTGATGAGTAC
SDHA_h_rev	CAACGTCCACATAGGACA
Sdha_m_fwd	CGACAAGACCTTGAATGA
Sdha_m_rev	GCTGTTGATCACAATCTATG

### 2.1.7 Plasmids

**Table 7:** Plasmids

Name	Description	Source
CMV HER2 WT	Plasmid encoding HER2	Mien-Chie Hung
psc $\alpha$ PD-1-SFFV	scAAV transfer vector encoding $\alpha$ PD-1 (SFFV promotor)	Johanna Reul, PEI <sup>1</sup> , Langen

<sup>1</sup>PEI: Paul-Ehrlich-Institut

### 2.1.8 Eukaryotic cells

Media used for the cultivation of cells are described in detail in chapter 2.5.1.

**Table 8:** Eukaryotic cells

Name	Source/Description
BV2	Murine microglia cell line (neonatal, from cerebral cortex, transformed via v-raf/v-myc oncogene) [312]
C20	Human microglia cell line [313]

EOC2	Murine microglial cell line (neonatal, M-CSF-dependent clones from whole-brain) [314]
G55T2	Human anaplastic astrocytoma cell line; provided by M. Westphal and K. Lamszus, University Clinic Hamburg Eppendorf
G55T2- HER2	G55T2 cells genetically engineered to express human HER2 (transfected with pcDNA3-HER2 WT [315], FACS sorted)
GL261	Murine glioma cell line, ATCC® HB-12317™
GL261-HER2	GL261 cells genetically engineered to express human HER2; provided by W. Wels, Georg Speyer Haus, Frankfurt
GL261-HER2-low	GL261 cells sorted to express HER2 at the level of endogenously HER2 <sup>+</sup> LN-319 cells; generated in this project
HEK-293-T/A	provided by D. Krause, Georg-Speyer Haus, Frankfurt
HMC3	Human microglia cell line [316]
HT1080	Human fibrosarcoma cell line; ATCC®, CCL-121™
HT1080-PD-1	Human fibrosarcoma cell line expressing mouse PD-1; generated by Johanna Reul, Paul-Ehrlich-Institut, Langen [310]
HuA	Human astrocyte cell line (Innoprot, Derio, Spain)
LN-319	Human astrocytoma cell line; provided by N. de Trebolet, Lausanne, Switzerland
LN-319- HER2	LN-319 cells genetically engineered to express human HER2 (transfected with pcDNA3-HER2 WT [315], FACS sorted)
LNT-229	Human glioblastoma cell line; provided by N. de Trebolet, Lausanne, Switzerland
LNT-229- HER2	LNT-229 cells genetically engineered to express human HER2 (transfected with pcDNA3-HER2 WT [315], FACS sorted)
LNT-229-EGFRvIII	LNT-229 cells genetically engineered to express human mutant EGFR (EGFRvIII, [317])
MDA-453-MB	Human breast cancer cell line (ATCC® HTB-131)
MDA-468-MB	Human breast cancer cell line (ATCC® HTB-132)
MuA	Murine astrocyte cell line (Innoprot, Derio, Spain)

NHA-E6/E7+hTERT	Human astrocyte cell line, abbreviated to “NHA” thereafter for brevity [318]
NK-92	NK cell line derived from peripheral blood mononuclear cells from a non-Hodgkin's lymphoma patient; ATCC® CRL-2407™
NK-92/5.28.z	NK.92 cell clone genetically engineered to express a second-generation CAR construct based on the HER2-specific antibody FRP5 and CD28 and CD3 $\zeta$ signaling domains; provided by W. Wels, Georg-Speyer Haus, Frankfurt [218]
NK-92/MR1-1.28.z	NK.92 cell clone genetically engineered to express an EGFRvIII-specific CAR, provided by W. Wels, Georg-Speyer Haus, Frankfurt [222]
Tu9648	Murine glioblastoma cell line derived from glial fibrillary acidic protein (GFAP)-v-src transgenic mice; provided by J. Weissenberger (Weissenberger et al., 1997)
Tu9648-HER2	Tu9648 cells genetically engineered to express human HER2 (transfected with pcDNA3-HER2 WT [315], FACS sorted)
U138MG	Human glioblastoma cell line; provided by N. de Trebolet, Lausanne, Switzerland
U138MG- HER2	U138MG cells genetically engineered to express human HER2 (transfected with pcDNA3-HER2 WT [315], FACS sorted)
U251MG	Human glioblastoma-astrocytoma grade III; provided by N. de Trebolet, Lausanne, Switzerland
U251MG- HER2	U251MG cells genetically engineered to express human HER2 (transfected with pcDNA3-HER2 WT [315], FACS sorted)
U87MG	Human glioblastoma cell line; provided by N. de Trebolet, Lausanne, Switzerland
U87MG- HER2	U87MG cells genetically engineered to express human HER2 (transfected with pcDNA3-HER2 WT [315], FACS sorted)

### 2.1.9 Viral vectors

Table 9: Viral vectors

Virus	Description	Source
HER2-AAV <sup>aPD-1</sup>	AAV2-based, HER2-DARPin-linked vector encoding an aPD-1 immunoadhesin	provided by Prof. C. Buchholz, Paul-Ehrlich-Institut Langen
HER2-AAV <sup>muFc</sup>	AAV2-based, HER2-DARPin-linked vector encoding a murine IgG-Fc portion	provided by Prof. C. Buchholz, Paul-Ehrlich-Institut Langen
HER2-AAV <sup>Luc</sup>	AAV2-based, HER2-DARPin-linked vector encoding a Firefly Luciferase	provided by Prof. C. Buchholz, Paul-Ehrlich-Institut Langen

### 2.1.10 Animals

Table 10: Animals

Mouse strain	Description	Supplier
C57Bl/6N	Inbred mouse strain	CharlesRiver Laboratories
CrI:NU(NCr)-Foxn1 <sup>nu</sup>	Immunodeficient due to a mutation of the Foxn1 <sup>nu</sup> locus, animals lack a thymus and are therefore unable to produce T cells	CharlesRiver Laboratories

### 2.1.11 Materials for experimental mouse work

Table 11: Materials for experimental mouse work

Name	Supplier
Gadovist® 1,0 mmol/ml	Bayer
Ketavet 100 mg/mL	Zoetis
Novaminsulfon Injekt 1000 mg	Zentiva
Rompun® 2%	Bayer
Surgibond Tissue Adhesive	SMI AG



### 2.1.12 Equipment

Table 12: Equipment

<b>Name</b>	<b>Manufacturer</b>
Amicon Ultra centrifugal filters	Merck Millipore
BioRad ChemiDoc XRS+ Imager	Bio-Rad
Bio-Rad Trans-Blot Turbo	Bio-Rad
CFX Connect™ Real-Time PCR Detection System	Bio-Rad
Centro LB 960 microplate luminometer	Berthold Technologies
C-tubes	Miltenyi Biotec
Econo-Pac chromatography column	Bio-Rad
FACSAria	BD Biosciences
FACSCanto II	BD Biosciences
gentleMACS™ Octo Dissociator	Miltenyi Biotec
Hamilton syringe	Hamilton Bonaduz AG
Heraeus™ Multifuge 3SR Plus™	Thermo Fisher Scientific
LS columns	Miltenyi Biotec
Mini-Protean 3 cell chamber	Bio-Rad
Mini-PROTEAN Tetra Vertical Electrophoresis Cells	Bio-Rad
Nunc MaxiSorp™ flat-bottom 96-well-plates	Thermo Fisher Scientific
Qiagen TissueLyser LT	Qiagen
Quintessential Stereotaxic Injector	Stoelting
Small Animal MR Scanner	Bruker
Stereotaxic fixation device	Stoelting
TecanSpark Microplate Reader	Tecan Group AG
ThinCert™ cell culture inserts	Greiner Bio-One
White 96-well-plates	Corning
Vortex-Genie 2	Scientific Industries

### 2.1.13 Software

Table 13: Software

Software	Company
DIVA	BD Biosciences
Excel	Microsoft
FlowJo (Version 10.0.7)	FlowJo LLC
GraphPadPrism 7 (Version 9.1.2.226)	GraphPad Software Inc.
Paravision 6.0.1 software	Bruker
PowerPoint	Microsoft

## 2.2 Molecular biology

### 2.2.1 Quantitative real-time PCR

Following viral transduction, total RNA of GL261, Tu9648 and LN-319 cells was extracted using TRI Reagent® and Extract Me Total RNA Kit, then cDNA was synthesized using the Vilo cDNA Synthesis Kit. Quantitative real-time PCR (qPCR) was performed using the Absolute Blue SYBR Green Fluorescein qPCR Mastermix. Corresponding primer pairs for the aPD1 transgene are listed in Table 1. Gene expression values were normalized to two house-keeping genes (18S and SDHA) and values were calculated using the  $\Delta$ CT method.

## 2.3 Protein biochemical methods

### 2.3.1 Preparation of cell lysates

To prepare cell lysates, cells were washed, detached using either trypsin or a plastic cell scraper and collected into a tube. Cells were pelleted at 1.300 rpm for 5 min, resuspended in 20-100  $\mu$ l (depending on the size of the pellet) lysis buffer completed with protease inhibitor cocktail and incubated on ice for 30 min. Afterward, the sample was centrifuged at 13.000 rpm at 4°C for 15 min and the supernatant was transferred to a fresh Eppendorf tube. The sample was either directly used for the determination of protein concentration (2.3.2) or stored at -20°C.

### 2.3.2 Determination of protein concentration

Protein concentrations of cell lysates were determined via Bradford assay using the ROTI®Quant Bradford Reagent according to the manufacturer's instructions. Briefly, 1  $\mu$ l of

sample or protein standard (1mg/ml BSA in H<sub>2</sub>O) was transferred to the wells of a flat bottom microplate. 150 µl Bradford Reagent were added to each well and incubated for 5 min at RT, then the absorbance was measured between 570–595 nm on TecanSpark Microplate Reader. After subtraction of a blank, concentrations of the unknown protein samples were calculated with the help of a standard curve. Protein concentrations of tumor and organ lysates were determined via MicroBCA using the MicroBCA™ Protein Assay Kit according to the manufacturer's instructions. Briefly, 1.0 ml of the working reagent was added to each tube containing either standard or the unknown sample. Tubes were covered and incubated at 60°C in a water bath for 1 hour. Afterward, tubes were cooled to RT and the absorbance of all samples was measured at 562 nm. Finally, a standard curve was prepared by plotting the average blank-corrected values.

### **2.3.3 Sodium dodecyl sulfate polyacrylamide gel electrophoresis (SDS PAGE)**

Using sodium dodecyl sulfate-polyacrylamide gel electrophoresis (SDS-PAGE), proteins are separated based on their molecular weight. Cell culture supernatants of transduced target cells or cell lysates were mixed with SDS-loading dye (4x) and boiled at 95°C for 10 min. Afterward, samples were loaded onto 12% SDS polyacrylamide gels (10 µg of cell lysate samples, 45 µl of denatured cell culture supernatants). Gels were prepared using the TGX Stain-Free™ FastCast™ Acrylamide Kit with 0.05% APS and 0.5% TEMED for the resolving gel and 0.1% APS and 0.5% TEMED for the stacking gel. For supernatants, 1.5 mm gels and for lysates 0.75 mm gels were used. 5 µl of Spectra™ Multicolor Broad Range Protein Ladder were used as a protein standard. Samples were separated using Mini-Protean 3 cell chamber filled with 1x SDS running buffer. Separation was carried out in Mini-PROTEAN Tetra Vertical Electrophoresis Cells at 300 V until the desired separation was achieved. Polyacrylamide gels were further subjected to Western blot analysis (2.3.4).

### **2.3.4 Western blot analysis**

For Western blot analyses, supernatants from target cell cultures were denatured at 95°C in Laemmli buffer containing SDS, β-mercaptoethanol and dithiothreitol (DTT). Proteins were separated via SDS-PAGE in a 12% polyacrylamide gel and transferred onto nitrocellulose membranes using a Trans-Blot Turbo system. AAV-encoded murine aPD-1 was detected using a primary antibody specific for the HA-tag included in the molecule. A secondary anti-rabbit

antibody was purchased from Santa Cruz. For chemiluminescence detection, membranes were treated with Pierce™ ECL Plus Western Blotting Substrate before exposure on X-ray films.

### **2.3.5 Enzyme-linked immunosorbent assay (ELISA)**

The concentration of HA-tagged AAV-encoded murine aPD-1 was measured by ELISA. 96-well immunoplates (Nunc MaxiSorp) were coated with an HA-tag antibody (50 µl, 1:4.000 in PBS) at 4°C overnight in a humidified chamber. After washing, wells were blocked at RT for 1h on a shaker, then 100 µl of prepared standard and sample (cell culture supernatant from transduced cells, mouse serum or organ lysate), respectively, were added to the wells. The plate was covered and incubated at RT for 2 h on a shaker. After washing 5x, bound aPD-1 was detected using a goat anti-mouse IgG HRP-conjugated detection antibody (1:30.000 in blocking buffer) and visualized using 1-Step™ Ultra TMB chromogenic substrate. Recombinant aPD-1 from transfected HEK293T/A cells was purified via Protein A affinity tag and subsequently concentrated before it was used as standard to generate reference values (2.3.7).

### **2.3.6 Production of recombinant aPD-1**

Production of recombinant aPD-1 was achieved via transfection of HEK-293T/A cells with an aPD-1 transfer plasmid (2.1.7., Table 7) using Lipofectamine 3000 according to the manufacturer's instructions. Briefly,  $2 \times 10^7$  cells were seeded in a T175 cell culture flask until they reached 80% confluency. On the day of transfection, 15 µl Lipofectamine 3000 Reagent was diluted in 250 µl DMEM (without supplements). 35 µg of DNA was diluted in 250 µl of DMEM, then 20 µl P3000 Reagent was added and everything was mixed well. Next, diluted DNA and Lipofectamine 3000 Reagent was mixed at a 1:1 ratio. After incubation for 5 minutes at RT, the DNA-lipid complex was added to the cells drop-wise. The transfection medium was replaced with DMEM (with supplements) 8 h after transfection. The next 4 days, cell culture supernatant of transfected HEK-293T/A cells was collected and pooled, filtered (0.45 µm pore size) and stored in the fridge. To prevent protein degradation, sodium acid was added as a preservative at a final concentration of 0.01 %.

### **2.3.7 Protein affinity tag purification from cell culture supernatant**

Recombinant aPD-1 proteins were purified utilizing Protein A affinity chromatography. Supernatants of transfected HEK-293T/A cells were sterile filtered and mixed with Protein A

beads (10  $\mu$ l beads/20 ml supernatant) in a falcon tube. The tube was incubated on a roller bottle shaker at 4°C overnight. All further purification steps were performed at 4°C. An Econo-Pac chromatography column was equilibrated with 10 column volumes (CV) of PBS and then loaded with the supernatant/bead mixture. The column was washed with 20 CV of PBS and proteins were eluted by the addition of 5 ml acidic elution buffer (pH 2.7). 1 ml of the eluate was transferred into vials containing 0.5 ml of collection buffer to neutralize the acidic pH. After purification, aPD-1 proteins were concentrated using Amicon Ultra centrifugal filters at 4,000xg at 4°C. To exchange the buffer, concentrated proteins were washed 3x with PBS. Proteins were stored at -80°C in 5% glycerol supplemented with protease inhibitor cocktail. The protein concentration was determined via MicroBCA (2.3.2).

## **2.4 Immunological methods**

### **2.4.1 Flow cytometry**

Expression of surface molecules on cells of interest was determined by flow cytometry using target-specific fluorochrome-conjugated antibodies. Detached cells were washed, counted and  $\sim 5 \times 10^5$  cells were pelleted in a polystyrene FACS tube. Antibodies were diluted in FACS buffer according to the manufacturer's recommendations. Cells were stained for 30 min – 1 h at 4°C in the dark. Following incubation, cells were washed 3x in FACS buffer and resuspended in 200  $\mu$ l FACS buffer for measurement. A FACSCanto II flow cytometer was used for flow cytometric analyses and a FACS Aria was used for cell, and data were analyzed using FlowJo™ software.

### **2.4.2 Transwell assay**

Cytokine release, as well as PD-L1 regulation in tumor and immune cells, was determined in transwell cytotoxicity assays using ThinCert™ cell culture inserts. Cells of interest were seeded into the wells of a 24 well plate at a density of  $5 \times 10^4$  cells per well. A cytotoxicity assay was performed in the insert for 24 h before the insert was removed and the culture medium in the base was replaced by serum-free DMEM. Human as well as murine recombinant IFN- $\gamma$  as a positive control for PD-L1 upregulation and cell stimulation was used at a concentration of 100 ng/ml. Stimulated cells in the base were cultivated for 24 h, then the conditioned medium was harvested, centrifuged, filtered and stored at -80°C until analysis.

### 2.4.3 Target binding assay

Specific target binding of AAV-encoded aPD-1 to PD-1 was assessed via flow cytometry using murine PD-1 expressing cells, either HT1080 cells that were transfected to express PD-1 (HT1080-PD-1) or freshly isolated murine splenocytes (2.7.8.). 400  $\mu$ l of cell culture supernatant from transduced GL261, Tu9648 or LN-319 cells were added to  $5 \times 10^4$  PD-1<sup>+</sup> cells followed by incubation at 4°C for 1 h. Binding was detected using a FITC-labeled antibody against the murine Fc part at 4°C for 15 min. PD-1<sup>-</sup> parental HT1080 cells were used as a negative control.

### 2.4.4 Blockade assay

The functionality of murine aPD-1 was determined using a PD-1/PD-L1 Blockade Bioassay according to the manufacturer's protocol. Briefly, PD-L1 expressing aAPC/CHO-K1 target cells that also harbor an engineered cell surface protein for activation of T cell receptors (TCRs) in an antigen-independent manner were incubated with PD-1 expressing effector T cells. The effector T cells express a luciferase reporter driven by an NFAT response element. Interruption of PD-1/PD-L1 signaling by the addition of cell culture supernatant containing aPD-1 re-activates TCR signaling. This results in NFAT-mediated luciferase expression, which was detected by the addition of Bio-Glo™ reagent. Luminescence was measured using a TecanSpark Luminescence Multi-Mode Microplate Reader.

### 2.4.5 Cytokine measurements

Cytokine concentrations in cell culture supernatant or serum samples were measured with the LEGENDplex™ Inflammation Panel and the LEGENDplex™ Anti-Virus Response Panel (Mouse & Human) Kits according to the manufacturer's protocol. Briefly, diluted samples were mixed with beads in a V-bottom plate. The plate was incubated at 800 rpm on a plate shaker for 2 h at RT. After washing, detection antibodies were added to each well. Samples were incubated at 800 rpm on a plate shaker for 1 h at RT and 25  $\mu$ L of Streptavidin R-phycoerythrin conjugate (SA-PE) were directly added to each well. After 30 min, the plate was washed again before samples were analyzed in 150  $\mu$ l of washing buffer on a flow cytometer.

## 2.5 Cell Culture

### 2.5.1 Cultivation of cells

Established human LN-319 glioblastoma cells as well as murine GL261 glioblastoma cells, immortalized murine microglia BV2, immortalized human microglia C20 and HMC3, human fibrosarcoma cells HT1080 and immortalized human astrocytes NHA-E6/E7+hTERT (abbreviated to "NHA" thereafter for brevity) were cultured in Dulbecco's modified Eagle's medium containing 10% fetal calf serum, 100 IU/ml penicillin and 100 µg/ml streptomycin in cell culture incubators at 37°C and 5% CO<sub>2</sub>. The immortalized murine microglial cell line EOC2 was cultured in DMEM with 2 mM L-glutamine supplemented with IL-34 (20 ng/ml) and TGF-β (5 ng/ml). NK-92/5.28.z (CAR-NK) cells were cultured in X-Vivo 10 medium supplemented with 5% heat-inactivated human plasma (German Red Cross Blood Donation Service Baden-Württemberg - Hessen, Frankfurt am Main, Germany) and 100 U/ml IL-2. Primary human glioblastoma cells MNOF-1300, MNOF-168 and MNOF-76 were grown in flasks pre-coated with 5 mg/ml laminin in DMEM/F12 medium containing 20 ng/ml each of recombinant epidermal growth factor (EGF) and human recombinant basic fibroblast growth factor 2 (bFGF2), and 20% BIT Admixture Supplement [29]. Human astrocytes (HuA) were cultured in Astrocyte medium according to the manufacturer's protocol. PD-1 expressing HT1080 cells (HT1080-PD-1) were cultured in DMEM supplemented with 10% FCS, 2 mM L-glutamine, and 10 µg/ml puromycin. Patient-derived glioma cells isolated from resected tumors were obtained and cultivated as described in section 2.5.2. All patient-derived material was obtained after written informed consent and all procedures were carried out according to guidelines from the Declaration of Helsinki (Ethics votum nr. 269/17).

### 2.5.2 Isolation and cultivation of primary cells

Resected human tumor tissue was minced with a scalpel, then a papain solution supplemented with 100 µl DNase was added and the tissue was incubated for 25 min at 37°C. The tissue was filtered through a 70 µm nylon mesh filter and washed with DMEM-12 twice (1.000 rpm, 4 min). Cells were transferred to cell culture flasks pre-coated with laminin and cultivated in BIT medium.

### **2.5.3 Freezing and thawing of cells**

For long-term storage, cells were cryopreserved and kept in liquid nitrogen at  $-196^{\circ}\text{C}$ . Cells were resuspended in 1 ml freezing medium (culture medium (90%), DMSO (10%)) and transferred to cryotubes. In a  $-80^{\circ}\text{C}$  freezer, cells were cooled down overnight and stored in a nitrogen tank for permanent storage the next day. To thaw frozen cells, they were placed in a water bath at  $37^{\circ}\text{C}$ , washed with culture medium and then transferred to a cell culture flask containing fresh culture medium.

### **2.5.4 Generation of transgenic cell lines**

HER2-overexpressing human tumor cell lines were generated by stably transfecting target cells with a pcDNA3-HER2 plasmid [29], [315]. HER2<sup>+</sup> murine glioma cell lines GL261-HER2 and Tu9648-HER2 were generated by lentiviral transduction with the human antigen.

### **2.5.5 Determination of cell density and cell viability**

Cell density was determined via crystal violet (CV) staining [319]. Cells were seeded in 96-well plates and were stained with crystal violet at a defined time point after treatment. Once the staining had dried it was dissolved using sodium citrate to enable even staining in the well. Absorption at 595 nm was measured using a TecanSpark Microplate Reader. Cell viability was determined via flow cytometric propidium iodide (PI) uptake assays as previously described [320].

### **2.5.6 Cytotoxicity assays**

Cytotoxic NK cell activity was determined using a fluorescence-activated cell scanning (FACS)-based assay as previously described [321]. Calcein violet AM-labelled target cells were washed and co-cultured with effector cells at different effector to target (E/T) ratios for 2 h at  $37^{\circ}\text{C}$ . Before flow cytometric analysis, cells were washed and resuspended in 200  $\mu\text{l}$  of a PI solution [1  $\mu\text{g}/\text{ml}$ ]. Calcein violet AM and PI double-positive cells represented dead target cells. Spontaneous target cell lysis in the absence of effector cells was subtracted from the values to determine specific lysis.

### **2.5.7 Degranulation assays**

CAR-NK cell activation was determined by measuring lysosomal-associated membrane protein LAMP-1 (CD107a) on the cell surface. Cells were incubated with target cells at an E/T



ratio of 1:1 for 1 h at 37°C in the presence of an APC-conjugated CD107a antibody. 1 µl of GolgiStop™ was added to each well, followed by incubation for 4 h at 37°C. After washing, CD107a expression was measured using a FACSCanto II flow cytometer.

## 2.6 Virological methods

### 2.6.1 AAV vector production

HER2-AAV<sup>aPD-1</sup> and HER2-AAV<sup>IgG-Fc</sup> have been described previously [310].

### 2.6.2 Viral transduction of cells

Transgene expression in HER2<sup>+</sup> target cells was assessed *in vitro* upon transduction with HER2-AAV<sup>aPD-1</sup> and HER2-AAV<sup>IgG-Fc</sup> vectors as described before [310]. Briefly, tumor cells were grown in 96-, 24- or 12-well plates at a cell density of 8×10<sup>3</sup>, 5×10<sup>4</sup> or 8×10<sup>4</sup> cells/well, respectively, before incubation with AAV particles (≥ 450,000 genome copies/cell). After 24 h, cells were washed in PBS and serum-free medium (virus production serum-free medium (VPSFM)) was added. Cells were cultured for 4 days before harvested media were centrifuged at 300xg for 5–7 min and stored at 4°C (or –80°C for long-term storage) before aPD-1 release was determined by Western blot and quantified by ELISA.

## 2.7 *In vivo* analyses

### 2.7.1 Glioblastoma mouse models

All *in vivo* experiments were carried out following the guidelines and regulations of the German animal protection law upon approval by the responsible government committee (Regierungspräsidium Darmstadt, Darmstadt, Germany, approval number FK-1088). For *in vivo* transduction and biodistribution analyses, 6-8 week old female C57BL/6N or Crl:NU(NCr)-Foxn1<sup>nu</sup> mice were used for syngeneic GL261-HER2 murine glioblastoma models and LN-319 human glioblastoma xenograft models, respectively. Crl:NU(NCr)-Foxn1<sup>nu</sup> mice were engrafted with 2×10<sup>6</sup> LN-319 tumor cells in 100 µl PBS, C57BL/6N mice were engrafted with 10<sup>6</sup> GL261-HER2 in 100 µl PBS cells at the right flank. For survival experiments, 6-8 week old female C57BL/6N mice were engrafted with 10<sup>6</sup> GL261-HER2 cells in 100 µl PBS (subcutaneous survival experiments) or 10<sup>5</sup> GL261-HER2 cells in 2 µL PBS (orthotopic intracranial survival experiments). Cells were detached, counted, washed with PBS and kept on ice until injection. Subcutaneous tumor growth was monitored 3x a week using a caliper. Tumor volume was determined using the following formula: Tumor volume

(mm<sup>3</sup>) = length (mm) x width (mm)<sup>2</sup> x 0.5. For orthotopic glioblastoma models, anesthetized mice were immobilized in a stereotaxic fixation device and injected with 5x10<sup>3</sup> GL261-HER2 tumor cells in 2 µL PBS using a 10 µL Hamilton syringe and a Quintessential Stereotaxic Injector through a burr hole in the skull. Tumor cells were injected into the right striatum with a depth of 3 mm to the skull, at a speed of 0.5 µL/min. After 2 min, the needle was withdrawn at a speed of 1 mm/min. Tumor growth, body weight and overall health status of all animals were monitored throughout the study. For the orthotopic model, tumor growth was monitored by magnetic resonance imaging (MRI) as described below.

### **2.7.2 Injection of vector particles and CAR-NK cells**

Mice bearing subcutaneous tumors at a volume of ~40 mm<sup>3</sup> or ~80 mm<sup>3</sup> were injected either intratumorally (i.t.) or intravenously (i.v.) into the tail vein with a single dose of 10<sup>11</sup> HER2-AAV gcs in 50 µl PBS. Control groups were injected with a single dose of 50 µl PBS. Mice bearing orthotopic intracranial tumors were injected with 3x10<sup>10</sup> HER2-AAV gcs in 3 µl PBS or 3 µl CAR-NK cell solution containing X-Vivo 10 over ~0.5 µl/min into the former tumor cell implantation site. Mice received intratumoral injections of 10<sup>7</sup> (subcutaneous model) and 2x10<sup>6</sup> (orthotopic intracranial model) CAR-NK cells. Tumor engraftment was confirmed using MRI measurements in cooperation with Georg-Speyer-Haus Frankfurt.

### **2.7.3 MR imaging**

Tumor engraftment was determined 7 days after tumor cell injection via a 7 Tesla Small Animal MR Scanner. Mice were injected intraperitoneally (i.p.) with 150 µl contrast agent and then anesthetized with isoflurane (1.5%). During scan acquisition, respiration rate was permanently monitored. Image acquisition was performed using Paravision 6.0.1 software in coronal planes (parameters: FOV=20x20 mm, 11 slices, 0.5 mm slice thickness, acquisition matrix = 256x256, flip angle 90°) [322].

#### **2.7.4 Blood sampling and serum isolation**

Whole blood was collected by cardiac puncture, allowed to clot for 30 min at RT. The clot was removed by centrifugation at 2.000xg for 10 min at 4°C. Serum was immediately apportioned into 0.5 ml aliquots and stored at -80°C if not directly processed.

#### **2.7.5 Isolation of tumor and organ tissue**

Mice were sacrificed by cervical dislocation and tumors and organs such as the brain, heart, lung, liver, spleen and kidney were isolated. Tissues were either snap-frozen in liquid nitrogen and stored at -80°C or processed directly for the preparation of single-cell suspensions (2.7.6), for homogenization (2.7.7) and subsequent ELISA (2.3.5), FACS analysis (2.4.1) or cell culture experiments.

#### **2.7.6 Preparation of single-cell suspensions**

Mice were sacrificed by cervical dislocation and the tissue of interest (tumor, organs) was isolated. Using scissors and a scalpel, tissues were minced and then transferred into C-tubes containing the corresponding enzymes of either the Tumor, Brain Tumor or Spleen Dissociation Kit according to the manufacturer's instructions and dissociated using the gentleMACS™ Dissociator. Afterward, the cell suspensions were passed through a 70 µm nylon mesh filter and washed with 10 ml RPMI medium before antibody staining. To remove excessive myelin from brain tumor samples, the Myelin Removal Kit was used. Cells were washed and resuspended in PBS, then the mixture was applied to LS columns (2 columns/brain). Columns were washed with 2 ml PBS (300xg, 10 mins, 4°C) and 5 ml of Pharmlyse RBC lysis buffer were added. After incubation for 15 min at RT in the dark, cells were washed twice in PBS, resuspended in 100 µl FACS buffer with FC block (1:1.000) and incubated in the dark for 15 min at RT. Afterward, staining antibodies were directly added to the cells and they were incubated for 15 min at RT or 4°C for 1 h. Finally, cells were washed with 200 µl PBS, pelleted at 400xg for 5 min, resuspended in 250 µl PBS and measured on a FACSCanto II flow cytometer.

#### **2.7.7 Preparation of tumor and organ lysates**

Isolated tumor or organ tissue was placed in 2 ml Eppendorf tubes, snap-frozen in liquid nitrogen and weighed on a precision scale. 5 µl lysis buffer (10 ml lysis buffer + 10 µl DNase, + protease inhibitor cocktail) per 1 mg of tissue were added. A stainless bead was transferred

to the tube, which was then placed in the TissueLyzer adaptor. Tissues were homogenized at a frequency of 50 kHz for 5 min. Afterward, samples were placed on ice for 15 min and spun down at 13.000 rpm at 4°C. The supernatant was transferred to a fresh tube and frozen at -80°C for storage if not directly used for determination of protein concentration by Bradford assay.

### **2.7.8 Isolation and cultivation of splenocytes from mice**

Mice were sacrificed by cervical dislocation, then spleens were isolated and dissociated using the gentleMACS Octo Dissociator according to the manufacturer's protocol. The resulting single-cell suspension was filtered through a 70 µm nylon mesh strainer and subsequently washed with RPMI medium, then cells were pelleted for 5 min at 1.600 rpm. Erythrocyte lysis was performed in 5 ml Pharmlyse RBC lysis buffer for 5 min at RT. Cells were washed 2x, resuspended in 5 ml RPMI and seeded in a round-bottom 96-well plate ( $5 \times 10^5$  cells/well). For binding assays, cells were cultivated in RPMI supplemented with 2 µl/well DYNAL™ Dynabeads™ for 48 h.

### **2.7.9 Neutralization assay**

For neutralization assays, Tu9648-HER2 cells were seeded in white 96-well-plates at a density of  $1 \times 10^4$  cells/well and cultured in a 37°C, 5% CO<sub>2</sub> incubator for 24 h. The next day, murine serum samples were heat-inactivated at 56°C for 30 min and diluted at 1:10 in FCS. Heat inactivated human plasma and FCS were used as controls. 20 µl of the sample were transferred to the wells of a 96-well U-bottom plate before HER2-AAV<sup>Luc</sup> was added ( $4 \times 10^7$  gc/µl in 20 µl serum-free DMEM) to each well. Plates were incubated at 37°C and 5% CO<sub>2</sub> for 1 h to allow neutralization. Next, 10 µl of the sample were added to the Tu9648-HER2 cells. Plates were incubated overnight before transduction was quantified with the Bright-Glo™ Luciferase Assay System according to the manufacturer's instructions. Luminescence was determined using a Centro LB 960 microplate luminometer.

## **2.8 Schematics**

Schematics were created using BioRender.com.

## 2.9 Statistical analysis

Quantitative data are expressed as mean and standard deviation (SD). Statistical significance was determined using a two-tailed student's t-test. If multiple sample groups were compared, significance was determined by ANOVA test.  $p < 0.05$  was regarded as significant. All analyses were performed using GraphPad Prism (Version 9.1.2.226; GraphPad Software, La Jolla, CA).

### 3 Results

In this thesis, targeted local combination immunotherapy as a novel therapeutic intervention of GB has been evaluated. Local intratumoral therapy with aPD-1 and CAR-NK cells aims towards the modulation of the immunosuppressive TME and the reactivation of anti-tumor immune responses. In the first part of the thesis, the individual components of the combination therapy, which comprises adoptive HER2-targeted CAR-NK cell therapy and local gene delivery of the immune checkpoint inhibitor aPD-1 via HER2-specific AAV vectors, have been characterized *in vitro*. In co-culture experiments, modification of tumor cells and bystander immune cells by target-activated CAR-NK cells was investigated concerning cytokine production and PD-L1 regulation. Tumor cell-specific delivery of aPD-1 was achieved by the selective transduction of HER2<sup>+</sup> cells. Production, secretion and functionality of the aPD-1 immunoadhesin were evaluated in various *in vitro* models. After demonstrating the functionality of both therapy components, the second part of this thesis describes the biodistribution kinetics of *in vivo* produced aPD-1 and the therapeutic efficacy of the CAR-NK/HER2-AAV combination therapy that was investigated in glioblastoma mouse models. In subcutaneous and orthotopic intracranial GL261-HER2 immunocompetent mouse models, administration of the combination therapy significantly prolonged survival including complete tumor control in several animals.

#### 3.1 Selective cytotoxic activity of CAR-NK cells against HER2<sup>+</sup> cells

Since one part of the planned combinatorial approach consists of targeted CAR-NK cell therapy, the effectiveness of engineered NK cells against HER2<sup>+</sup> target cells was elucidated. First, CAR expression on the surface of CAR-NK (NK-92/5.28.z) cells was confirmed (Fig. 12A). Cytotoxic activity correlated with HER2 expression levels of the target cells, in accordance with previous work [29]. CAR-NK cells showed a high specific lytic activity towards HER2<sup>+</sup> human breast cancer cells, whereas cells lacking target antigen expression were hardly attacked by CAR-NK cells (Fig. 12B and C). Specificity of CAR-NK cell activity was further confirmed by the low lytic activity of the parental NK-92 cell line, which mediated some level of tumor cell lysis (> 20% killing efficiency), while CAR-NK cells showed significantly higher killing efficiencies (> 70% killing efficiency, Fig. 12C, left). However, regarding HER2<sup>-</sup> breast cancer cells, the killing efficiencies of CAR-NK and parental NK-92 cells were at the same low level (Fig. 12C, right).

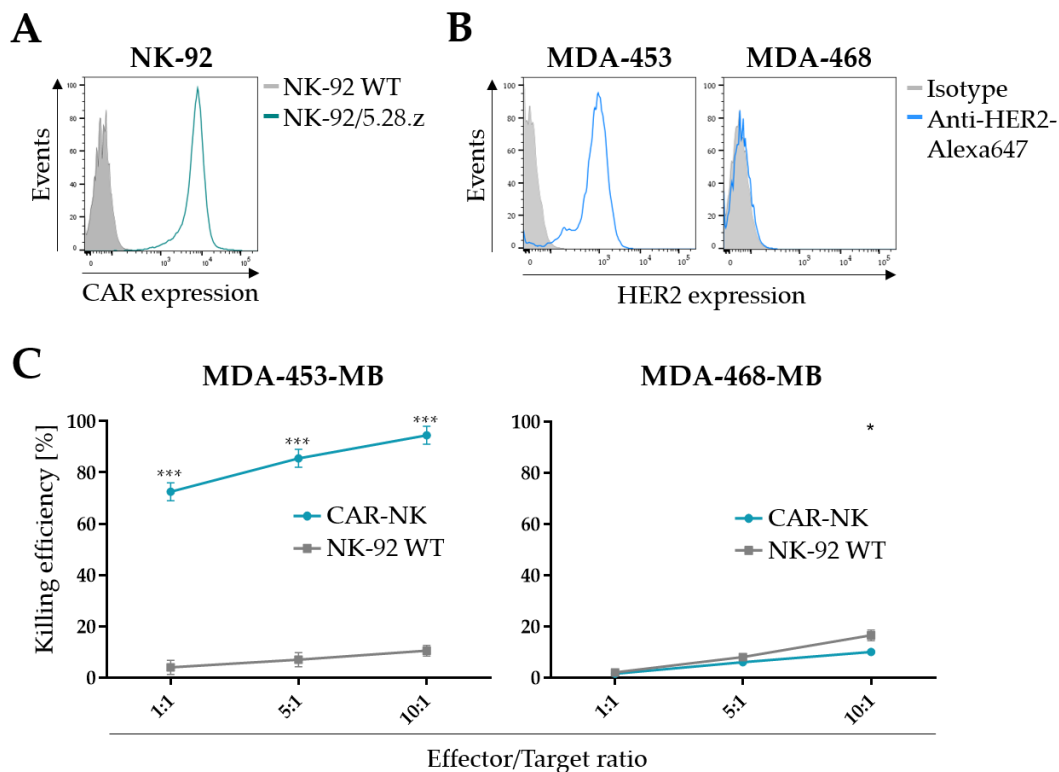


**Figure 12: HER2-targeted CAR-NK cell therapy.** (A) CAR surface expression by CAR-NK (NK-92/5.28.z cells). Parental NK-92 served as control. (B) HER2 expression of human MDA-453-MB and MDA-468-MB cells as determined via flow cytometry. (C) Cytotoxic activity of CAR-NK cells against human breast cancer cells as compared to parental NK-92 cells (Mean values  $\pm$  SD are shown;  $n=3$ , \*\*\* $p < 0.001$ ).

After target antigen specificity was evaluated in human breast cancer cells, the lytic activity of CAR-NK cells towards glioblastoma cells was investigated. Since the GL261-HER2 glioblastoma mouse model was employed for *in vivo* studies, GL261 WT cells were lentivirally transduced to express the human target antigen. As a second murine cell line, Tu9648 cells were included in the studies. Both cell lines were shown to express high levels of HER2 after lentiviral transduction (Fig. 13A). Also in this setting, CAR-NK cells showed high specificity in tumor cell lysis that depended on the expression of the target antigen on murine target cells. Killing efficiency towards GL261-HER2 and Tu9648-HER2 cells was significantly higher compared to lytic activity towards HER2<sup>-</sup> GL261 WT and Tu9648 WT cells (Fig. 13B). To take into account the complex interactions of human NK cell receptors with ligands on human GB cells, CAR-NK cell activity against the endogenously HER2<sup>+</sup> human LN-319 glioblastoma cell line was analyzed. LN-319 cells were also efficiently lysed by CAR-NK cells, with significantly higher efficiency as compared to parental NK-92 cells (Fig. 13C, bottom). This was also shown to be true for GL261-HER2 and Tu9648-HER2 cells (Fig. 13 C, top and middle).

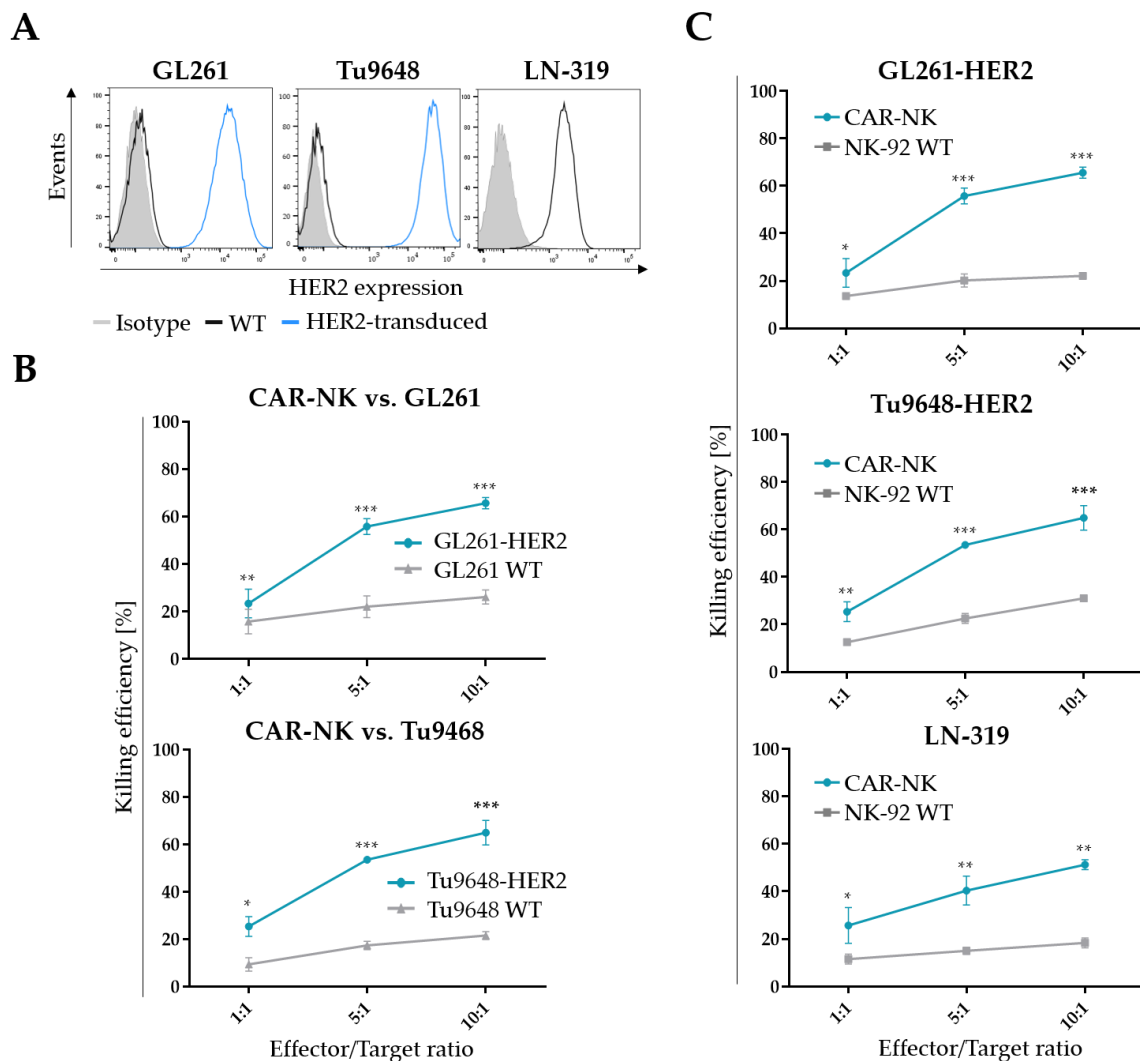


**Figure 13: CAR-NK cells efficiently lyse HER2<sup>+</sup> glioma cells.** (A) HER2 expression of murine HER2-transduced glioma cell lines (GL261, Tu9648, blue histogram) and the human glioma cell line LN-319 as determined via flow cytometry. (B) Cytotoxic activity of CAR-NK cells against human murine HER2-transduced glioma cell lines as compared to untransduced wild-type murine cell lines (Mean values  $\pm$  SD are shown;  $n=3$ , \* $p < 0.05$ , \*\* $p < 0.01$ , \*\*\* $p < 0.001$ ). (C) Cytotoxic activity of CAR-NK cells against murine as well as human HER2<sup>+</sup> glioma cells as compared to parental NK-92 cells (Mean values  $\pm$  SD are shown;  $n=3$ , \* $p < 0.05$ , \*\* $p < 0.01$ , \*\*\* $p < 0.001$ ).

As a further control for antigen-specificity, NK-92 cells transduced with a CAR targeting an unrelated antigen such as EGFRvIII (NK-92/MR1-1.28.z) on EGFRvIII-expressing LNT-229-EGFRvIII cells were used (Fig. 14A and B). EGFRvIII-specific CAR-NK cells did target LNT-229-EGFRvIII cells with significantly higher efficiency than LN-319 or GL261-HER2 cells (Fig. 14C). In direct comparison, the cytotoxic activity of HER2-specific CAR-NK towards GL261-HER2 was significantly increased as compared to NK-92/MR1-1.28.z (Fig. 14D).



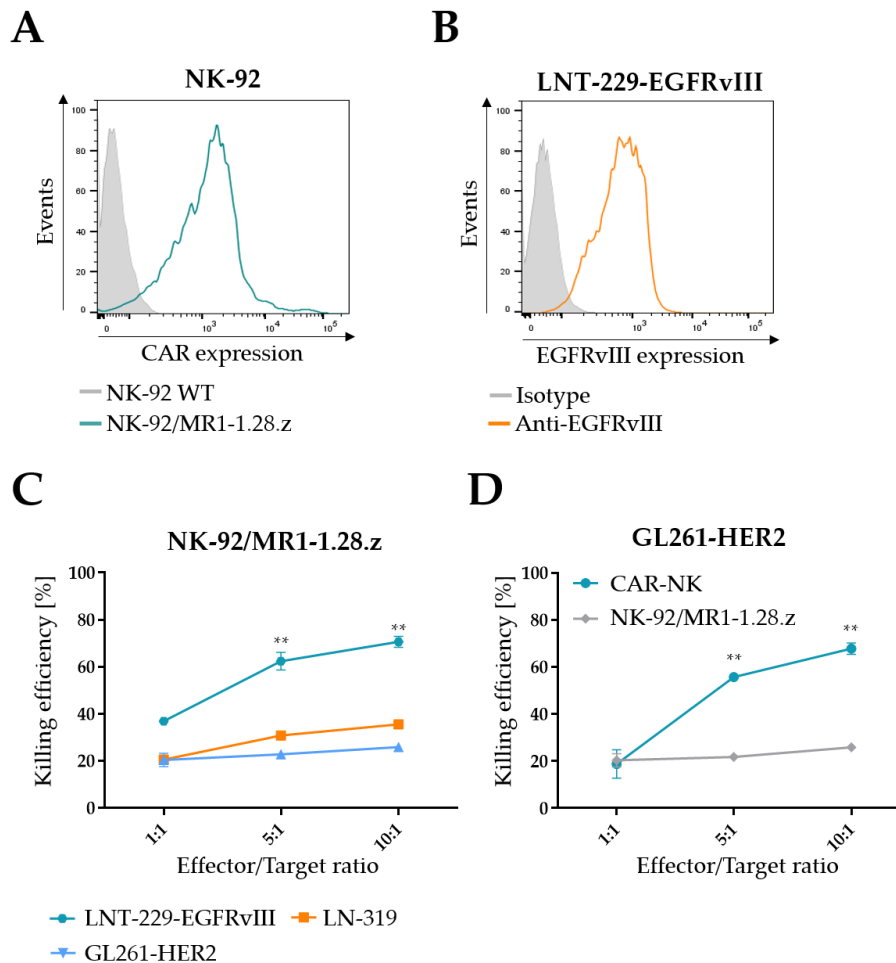


**Figure 14: Cytotoxic activity of NK-92/MR1-1.28.z cells against glioma cells. (A)** CAR surface expression by EGFRvIII-specific NK-92/MR1-1.28.z cells (green). Parental NK-92 served as a control (grey). **(B)** EGFRvIII surface expression on LNT-229-EGFRvIII cells. **(C)** Cytotoxic activity of NK-92/MR1-1.28.z against EGFRvIII-expressing LNT-229, LN-319 (human glioma cells) and GL261-HER2 (murine glioma cells),  $n=3$ ,  $**p < 0.01$ . **(D)** Differential cytotoxic activity of CAR-NK cells compared to NK-92/MR1-1.28.z cells against GL261-HER2.  $n=3$ ,  $**p < 0.01$ .

Since murine glioma cell lines express supraphysiological HER2 levels after lentiviral transduction, GL261-HER2-low cells were generated by sorting GL261-HER2 cells that express the antigen at the same level as LN-319 cells (Fig. 15A). In this way, CAR-NK cell activity on GL261-HER2-low cells that reflect the HER2 level of endogenously HER2<sup>+</sup> cells was assessed. The specificity of CAR-NK cell killing towards sorted GL261-HER2-low was confirmed in a cytotoxicity assay. GL261-HER2-low cells were lysed with significantly increased efficiency by HER2-specific CAR-NK cells as compared to parental NK-92 WT cells or NK-92/MR1-1.28.z (Fig. 15B). When directly comparing the cytotoxic activity of CAR-NK cells towards GL261-HER2 and GL261-HER2-low, no difference in killing efficiency was found (Fig. 15C).

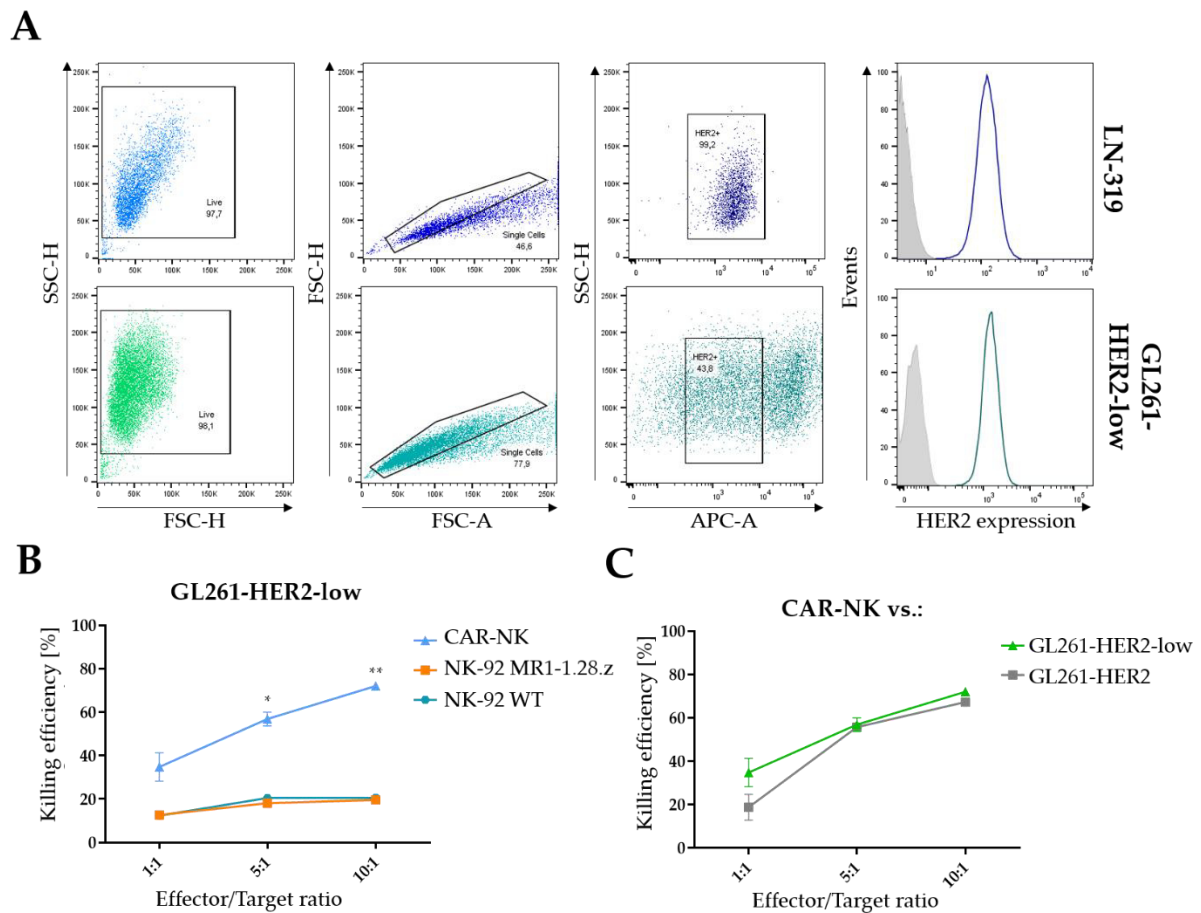


**Figure 15: Cytotoxic activity of CAR-NK cells against GL261-HER2-low cells. (A)** Gating strategy used for the generation of GL261-HER2-low cells. GL261-HER2 cells were sorted to resemble the HER2 level of endogenously HER2<sup>+</sup> human LN-319 cells. **(B)** Cytotoxic activity of NK-92 WT, NK-92/MR1-1.28.z and CAR-NK cells against GL261-HER2-low cells. Mean values  $\pm$  SD are shown;  $n=3$ , \* $p < 0.05$ , \*\* $p < 0.01$ . **(C)** Comparison of cytotoxic activity of CAR-NK cells against GL261-HER2 and GL261-HER2-low cells.

To further emphasize the translational potential of the study, the cytotoxic capacity of CAR-NK cells towards human primary glioma cells as well as tumor cells from patients enrolled in the CAR2BRAIN study was analyzed. Interestingly, in primary glioma cells, HER2 expression levels did not correlate with CAR-NK cell-mediated lysis, as killing efficiency towards MNOF-1300 cells was highest as compared to MNOF-76 and MNOF-168, while HER2 expression was lowest in MNOF-1300 (Fig. 16A). Also in patient-derived GB cells, killing efficiency appeared to not solely depend on HER2 expression levels. Although HER2 was expressed at high levels in all three cell cultures, cytotoxic activity towards CB05 was significantly increased as compared to CB013 and CB01 (Fig. 16B). Taken together, HER2-targeted CAR-NK cells exhibited selective and potent lysis of HER2<sup>+</sup> glioma cell lines as well as of patient-derived cell cultures with high specificity for the target antigen.

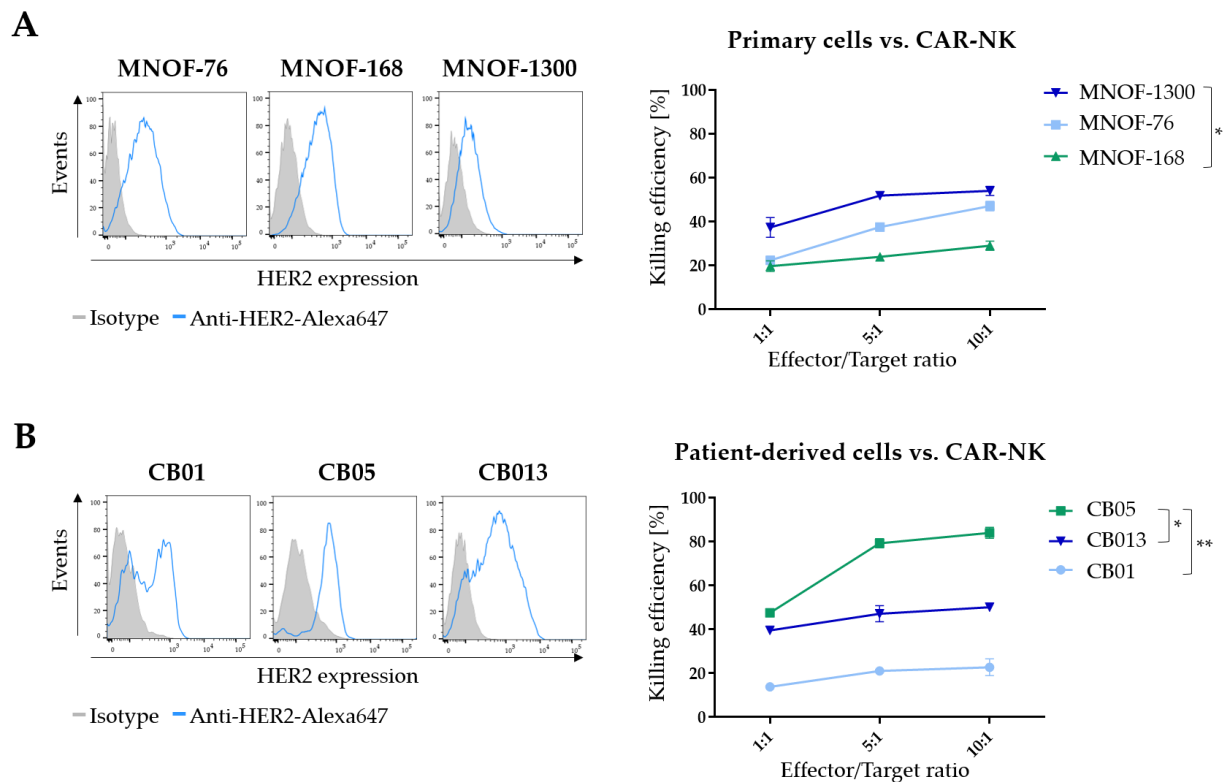


**Figure 16: CAR-NK cells efficiently lyse primary and patient-derived glioma cells. (A)** HER2 expression of human breast cancer cells (MDA-453-MB) and human primary glioma cells (MNOF-76, MNOF-168, MNOF-1300) as determined via flow cytometry (left). Cytotoxic activity of CAR-NK cells against primary human glioma cells as compared to MDA-453-MB breast cancer cells as positive control is shown on the right. Mean values  $\pm$  SD are shown;  $n=3$ ,  $**p < 0.01$ . **(B)** HER2 expression of human breast cancer cells (MDA-453-MB) and human patient-derived glioma cells (CB01, CB05, CB13) as determined via flow cytometry (left). Cytotoxic activity of CAR-NK cells against primary human glioma cells as compared to MDA-453-MB breast cancer cells as positive control is shown on the right. Mean values  $\pm$  SD are shown;  $n=3$ ,  $**p < 0.01$ .

### 3.2 The effect of CAR-NK cell-mediated tumor cell lysis on target and bystander cells

#### 3.2.1 Target antigen expression and cytokine secretion

Since target antigen downregulation is a well-known mechanism employed by tumor cells to evade CAR-specific targeting, HER2 expression levels on target cells under CAR-NK cell attack were evaluated. Neither HER2 levels on murine target cells nor human target cells were found to be decreased upon CAR-NK cell attack (Fig. 17), indicating no direct antigen downregulation in response to CAR-NK cell therapy.

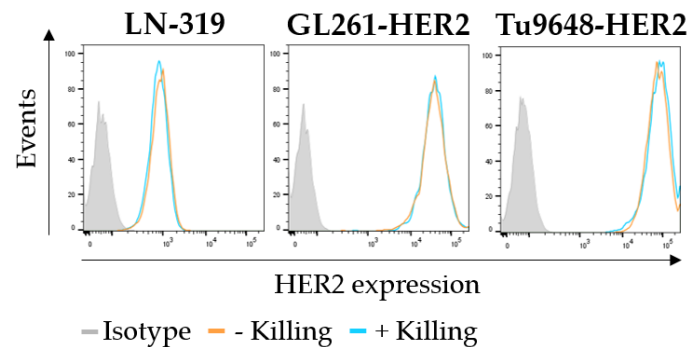


**Figure 17: HER2 expression on target cells in response to CAR-NK cell activity.** (A) HER2 expression on GL261-HER2, Tu9648 and LN-319 cells after 2 h of CAR-NK cell anti-tumor activity was determined via flow cytometry.

Since CAR-NK cell therapy is administered locally by injection into the tumor tissue within the brain, molecular alterations in cytokine milieu and surface marker expression triggered by GB cell lysis and CAR-NK cell activity will likely affect the TME. Upon CAR-NK cell attack, lysed GB cells will release tumor antigens as well as damage-associated molecular patterns (DAMPs), while activated CAR-NK cells secrete immune-modulatory cytokines, which might influence the extent and the course of the immune response. Therefore, the effect of CAR-NK cell-mediated GB cell lysis on other cell types typically present within a brain TME, like immune cells such as MG, was investigated in more detail. Cytokine secretion of various cell types of interest was assessed using a transwell assay system (Fig. 18A). In this way, it was evaluated whether activated CAR-NK cells stimulate the cytokine release of human glioma cell lines (LN-319, U138MG) as well as human MG (C20, HMC3) and non-activated bystander CAR-NK cells. Levels of several inflammatory cytokines such as IFN- $\gamma$ , TNF- $\alpha$ , MCP-1, IL-8 and IL-6 were found to be significantly increased (Fig. 18B). The glioma cell lines LN-319 and U138MG showed increased secretion of IL-8, while in MG levels of IL-6 and IL-8 were elevated. In bystander CAR-NK cells, secretion of IFN- $\gamma$ , MCP-1, IL-8 and TNF- $\alpha$  was enhanced. These data indicate a CAR-NK cell-induced pro-inflammatory effect on various cell types which comprise the TME. No significant changes in the levels of MCP-1 and IFN- $\alpha$ 2 in LN-319, U138MG or HMC3 cells were found. Levels of IL-1 $\beta$ , IL-12p70, IL-17A, IL-23, and IL-33 (for all cell types evaluated), IL-6 (LN-319, U138MG, CAR-NK), MCP-1, IFN- $\gamma$  and TNF- $\alpha$  (LN-319, U138MG, C20, HMC3) were below the detection limit of the method (data not shown). Taken together, CAR-NK cell therapy was shown to modulate the cytokine milieu of the TME by triggering the secretion of inflammatory cytokines.

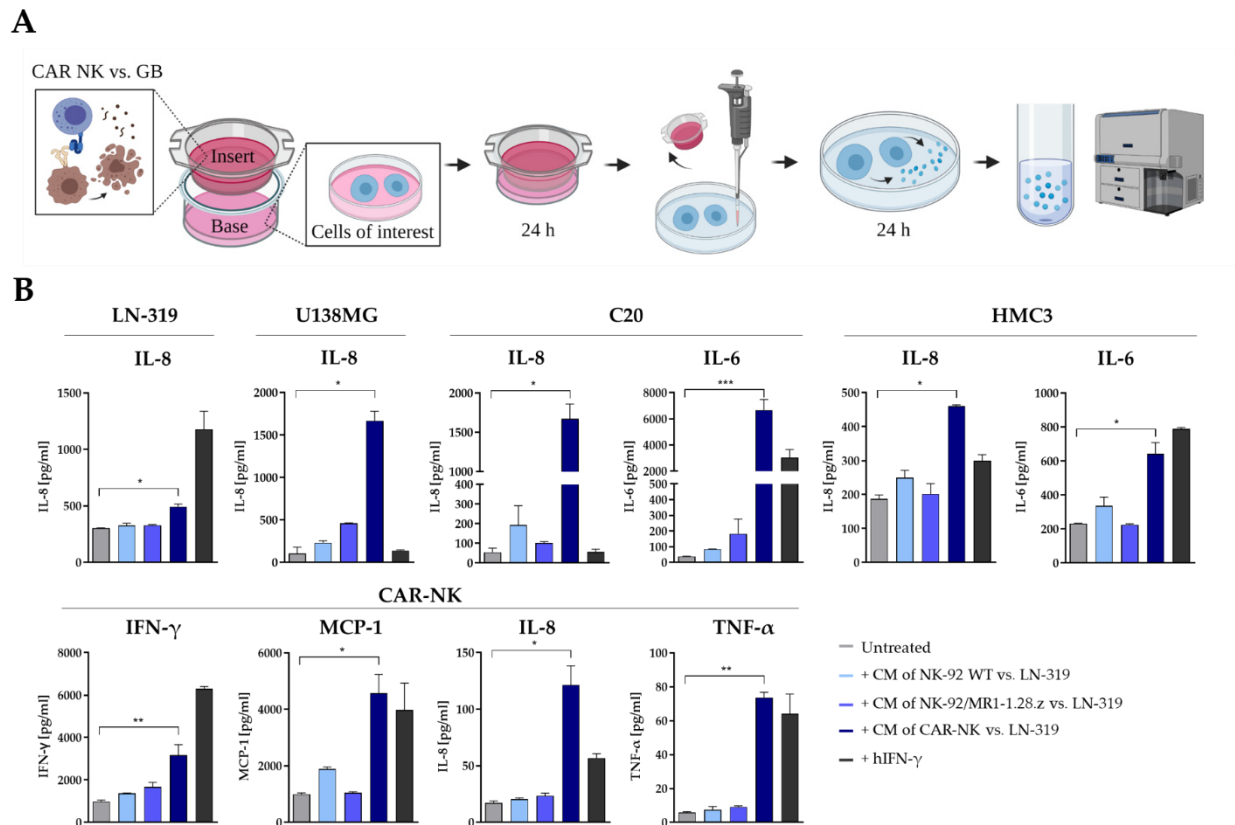


**Figure 18: Adjacent CAR-NK cell-mediated tumor cell killing leads to cytokine secretion by surrounding immune cells. (A)** Schematic representation of the cytokine secretion transwell assay design. Soluble factors secreted from CAR-NK cells stimulated by human LN-319 glioblastoma cells (GB) in the insert influence cells of interest in the base. After 24 h of co-culture, the insert is removed and fresh serum-free medium is added to the cells in the base. Stimulated cells are cultivated for a further 24 h. Cytokine levels in the conditioned medium are determined via a bead-based LEGENDplex™ assay. **(B)** Analysis of cytokine release by immune cells which had been exposed to conditioned medium (CM) from a CAR-NK cell cytotoxicity assay (assay design is depicted in (A)). Mean values  $\pm$  SD are shown;  $n=3$ . \* $p < 0.05$ , \*\* $p < 0.01$ , \*\*\* $p < 0.001$ .

### 3.2.2 Regulation of PD-L1 expression

Similar to the cytokine profile, the PD-1/PD-L1 interaction is another pivotal determinant of the immunosuppressive TME. Therefore, the PD-L1 level and its regulation on different cell lines in response to CAR-NK cell therapy were investigated. A transwell system was employed, in which soluble factors that are secreted from activated CAR-NK cells in a cell culture insert influence cells of interest in the base of a well plate (Fig. 19A). Cultivation in the presence of nearby GB cell killing by CAR-NK cells induced the upregulation of PD-L1 in human glioma cells, human MG and astrocytes (Fig. 19B). Interestingly, PD-L1 regulation was not observed in cells of murine origin, except for a slight shift in the murine MG cell line EOC2. Transwell cultivation of human cell types either with unstimulated CAR-NK cells alone or

---

with non-activated NK cells (parental NK-92 WT cells or EGFRvIII-specific NK-92/MR1-1.28.z vs. GL261-HER2 or LN-319) did not lead to differential PD-L1 expression (Fig. 19C and D).

The upregulation of PD-L1 in response to adjacent CAR-NK cell-mediated killing of GB cells is a key finding since the ensuing activation of the PD-1/PD-L1 axis can be expected to suppress further endogenous anti-glioma immunity. Especially when applying CAR-NK cell therapy, intrinsic immune stimulation has shown to be decisive for *in vivo* efficacy of CAR-NK cell therapy [29]. Since in the transwell system, CAR-NK cells in the insert and tumor cells in the base are not in direct contact with each other, the effect on PD-L1 regulation was most likely induced by soluble factors secreted by CAR-NK cells activated upon killing of tumor cells in the insert. Murine glioma cells did not show an increase in PD-L1 levels upon co-cultivation with activated human CAR-NK cells, possibly due to the species difference in the putative mediators.

To evaluate which soluble factors induce PD-L1 upregulation, the direct cytokine response of CAR-NK cells activated by target cell killing was measured. During killing of murine GB cells, a significant increase in the levels of human perforin (threefold), IFN- $\gamma$  (twofold), IL-1 $\alpha$  (twofold), TNF- $\alpha$  (twofold), IL-8 (fourfold), MCP-1 (twofold) and IL-10 (twofold) as compared to baseline cytokine levels was observed (Fig. 20A).

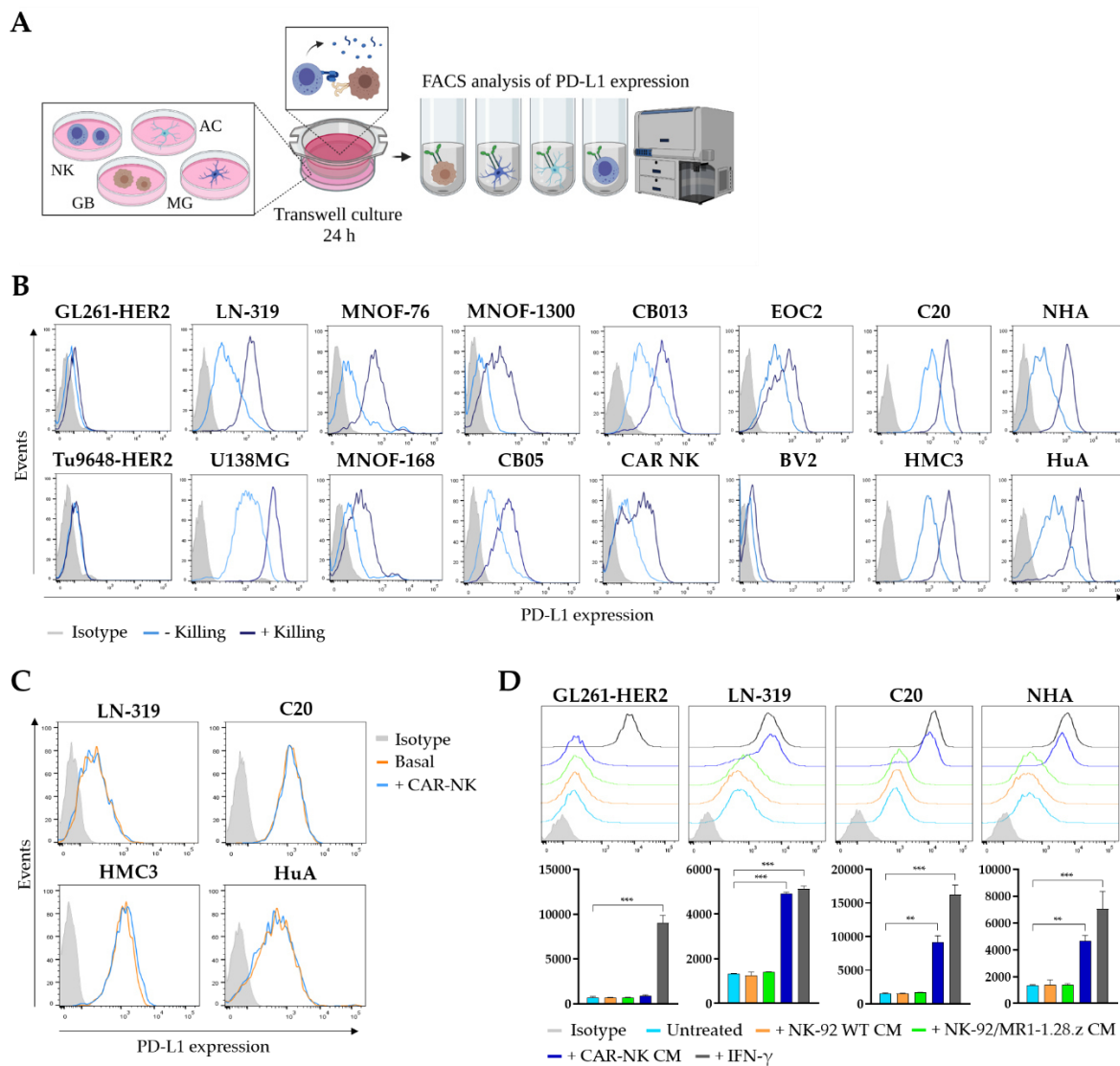


**Figure 19: CAR-NK cell-mediated tumor cell killing results in PD-L1 regulation.** (A) Schematic representation of the cytokine response transwell assay design. Soluble factors secreted from CAR-NK cells stimulated by glioblastoma cells (GB) in the insert influence cells of interest in the base (GB: glioblastoma cells, AC: astrocytes, MG: microglia). After 24 h of co-culture, the insert is removed and fresh serum-free medium is added to the cells in the base. Stimulated cells are cultivated for a further 24 h. Cytokine levels in the conditioned medium are determined via a bead-based LEGENDplex assay. (B) PD-L1 regulation in response to a transwell cytotoxicity assay was analyzed on murine (GL261, Tu9648) and human (LN-319, U87MG, MNOF-76, MNOF-168, MNOF-1300, patient-derived CB05, CB13) glioma cells as well as on immune cells such as CAR-NK cells, murine (EOC2, BV2) or human (C20, HMC3) microglia and human astrocyte (NHA, HuA) cell lines. Cells of interest were seeded in wells (base) of a 24-well plate, while a cytotoxicity assay (CAR-NK cells vs. tumor cells (species-compatible); E/T ratio 1:1) was performed in the insert. After 24 h, PD-L1 expression of cells in the base was determined via flow cytometry. (C) PD-L1 expression on LN-319, C20, HMC3 and HuA cells cultured with or without CAR-NK cells in the insert of a transwell system. (D) PD-L1 expression of various cell types cultivated in a transwell system with different NK cell/tumor cell co-cultures in the insert (E/T ratio 1:1). Co-culture in the insert consisted of NK-92 WT cells vs. LN-319 (orange), NK-92/MR1-1.28.z vs. LN-319 (green) and CAR-NK vs. LN-319 or GL261-HER2 (blue); murine (for GL261-HER2 cells), as well as human (for LN-319, C20 and NHA cells), recombinant IFN- $\gamma$  [100 ng/ml] was added to the cells as a positive control for PD-L1 upregulation (black). Cells were cultivated for 24 h, then PD-L1 expression of cells in the base was determined via flow cytometry. Mean values  $\pm$  SD are shown,  $n=3$ , \*\* $p < 0.01$ , \*\*\* $p < 0.001$ .



To determine whether one of those soluble factors might induce PD-L1 upregulation on bystander cells, PD-L1 expression on various cell types was assessed 24 h post-treatment with recombinant cytokines. Stimulation with IFN- $\gamma$  increased PD-L1 expression similar to stimulation with conditioned medium from a killing assay (Fig. 20B). Interestingly, this effect was also observed in the murine MG cell line EOC2.

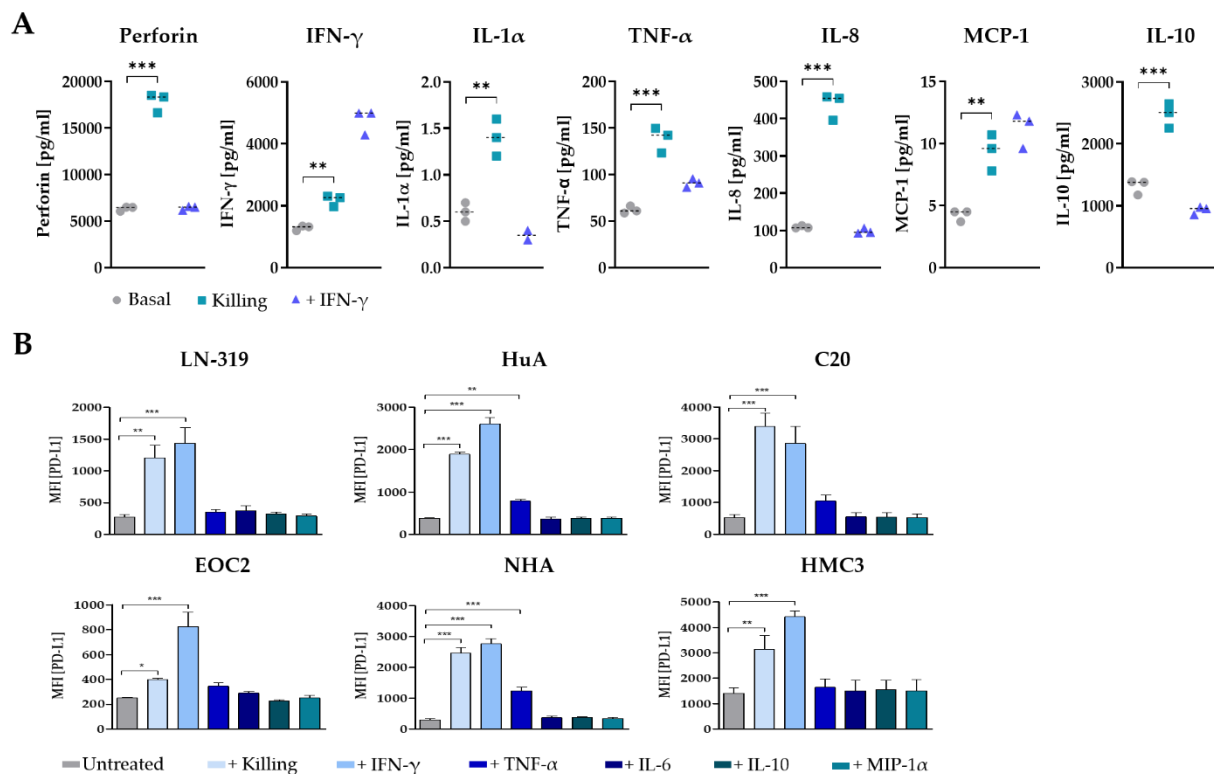


**Figure 20: Cytokine release of activated CAR-NK cells and the effect on PD-L1 regulation on surrounding cell types.** (A) Analysis of cytokine release by stimulated CAR-NK cells (CAR-NK cells vs. GL261-HER2 glioma cells). Concentrations of IFN- $\gamma$ , TNF- $\alpha$ , MCP-1, IL-1 $\alpha$ , IL-2, IL-8, IL-10 and perforin were measured in cell culture supernatants using a Luminex multiplex bead assay. Mean values  $\pm$  SD are shown; n=3. \*\*p < 0.01, \*\*\*p < 0.001. (B) PD-L1 regulation in various cell types in response to stimulation with species-compatible (human/murine) recombinant cytokines or in response to a transwell cytotoxicity assay (+ Killing, CAR-NK vs. LN-319 for human cells and CAR-NK vs. GL261-HER2 for murine cells (EOC2)) was analyzed via flow cytometry. Cells were incubated with recombinant cytokines for 24 h at a concentration of 100 ng/ml. Mean values  $\pm$  SD are shown; n=3, \*p < 0.05, \*\*p < 0.01, \*\*\*p < 0.001.

To confirm that the effect was caused by IFN- $\gamma$ , the assay setup was modified to include anti-IFN- $\gamma$ . Transwell cytotoxicity assays in the insert were either performed in the absence or presence of a human IFN- $\gamma$  antibody (Fig. 21A). The capability of anti-IFN- $\gamma$  to antagonize the effects of IFN- $\gamma$  on PD-L1 upregulation was validated in LN-319 cells (Fig. 21B). Furthermore, it was affirmed that cytotoxic activity of CAR-NK cells towards target cells was not affected in the presence of anti-IFN- $\gamma$ . Killing efficiency was not impaired; in fact, a slight yet insignificant



increase in efficiency with increasing concentrations of anti-IFN- $\gamma$  was observed (Fig. 21C). When anti-IFN- $\gamma$  was added to the experimental setup of PD-L1 regulation in response to CAR-NK cell activation, the effect of PD-L1 upregulation upon stimulation with conditioned medium was abolished (Fig. 21D). This finding defines IFN- $\gamma$  as the major driver of PD-L1 regulation upon CAR-NK cell therapy.

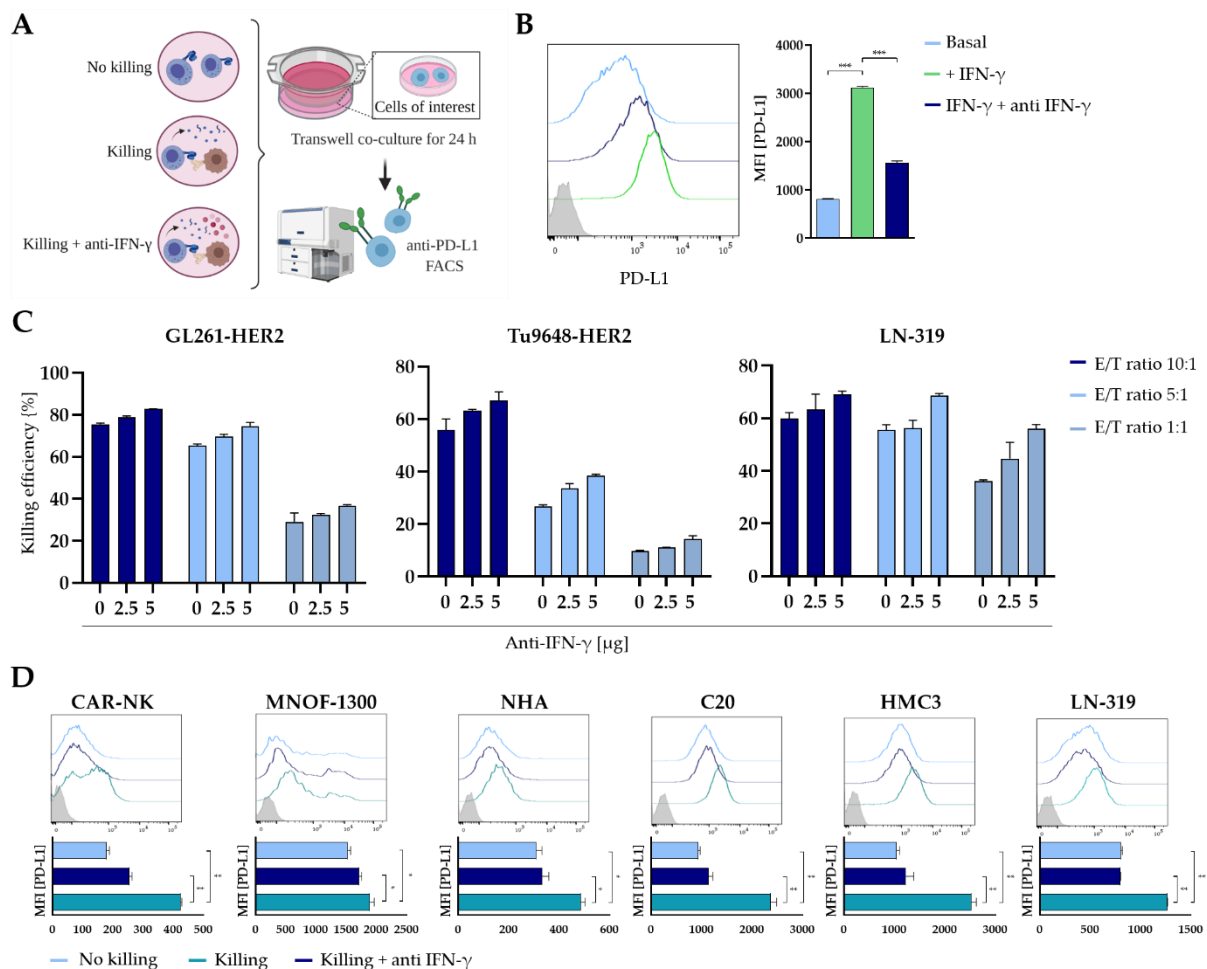


**Figure 21: IFN- $\gamma$  is the major driver for PD-L1 upregulation in surrounding cell types.** (A) PD-L1 expression in cells of interest was assessed via flow cytometry upon cultivation either in the absence (CAR-NK only) or presence of an adjacent cytotoxicity assay (CAR-NK cells vs. LN-319). Cytotoxicity assays in the insert were either performed in the absence or presence of a human IFN- $\gamma$  antibody for 24 h. (B) PD-L1 expression on LN-319 cells in the presence of recombinant human IFN- $\gamma$  (green) and an anti-human IFN- $\gamma$  antibody (dark blue). Mean values  $\pm$  SD are shown; n=3, \*\*\*p < 0.001. (C) Killing efficiency of CAR-NK cells against HER2<sup>+</sup> glioma cells in the presence of various concentrations of an anti-human IFN- $\gamma$  antibody. (D) PD-L1 expression on CAR-NK cells, MNOF-1300, NHA, C20, HMC3 and LN-319 upon cultivation either in the absence or presence of an adjacent cytotoxicity assay in the absence or presence of anti-human IFN- $\gamma$  antibody for 24 h was determined via flow cytometry (assay design depicted in (A)). Mean values  $\pm$  SD are shown; n=3. \*p < 0.05, \*\*p < 0.01.

Taken together, these data indicate that IFN- $\gamma$ -mediated upregulation of PD-L1 not only by GB cells but also by brain-resident cell types such as MG and astrocytes add to the immunosuppressive microenvironment and therefore constitute a potential mechanism of

resistance towards CAR-NK cell therapy. Consequently, selective local administration of a checkpoint inhibitor through a HER2-targeted AAV vector to specifically interfere with PD-1/PD-L1 interaction was explored in this study.

### **3.3 The effect of CAR-NK cells on brain-resident immune cells**

Since stimulation of the murine MG cell line EOC2 with conditioned medium from a killing assay resulted in upregulation of PD-L1 (Fig. 20B, bottom left), it was assessed whether other surface markers such as microglial activation markers were also differentially regulated in response to adjacent tumor cell killing. MG are among the most abundant cell types within the brain TME, and, as immune cells, they might react to alterations of their environment mediated by GB cell lysis. Therefore, markers that are associated with MG activation, such as CD68, CD86, CX3CR1, MerTK and PY2R12 [323]–[328] were analyzed either in response to adjacent CAR-NK cell-mediated GB cell lysis or in response to stimulation with recombinant cytokines that are secreted during the process of GB cell lysis.

#### **3.3.1 The effect of activated CAR-NK cells on murine microglia**

Since cell lines often lose several characteristic markers when they are maintained in culture over a long period of time, the expression of the mentioned markers on MG cell lines BV2 and EOC2 was confirmed first (Fig. 22A). In presence of tumor cell lysis, several markers were found to be significantly increased (Fig. 22B). BV2 upregulated PY2R12 and EOC2 showed increased CD68 expression, while CX3CR1 expression was increased in both cell lines.

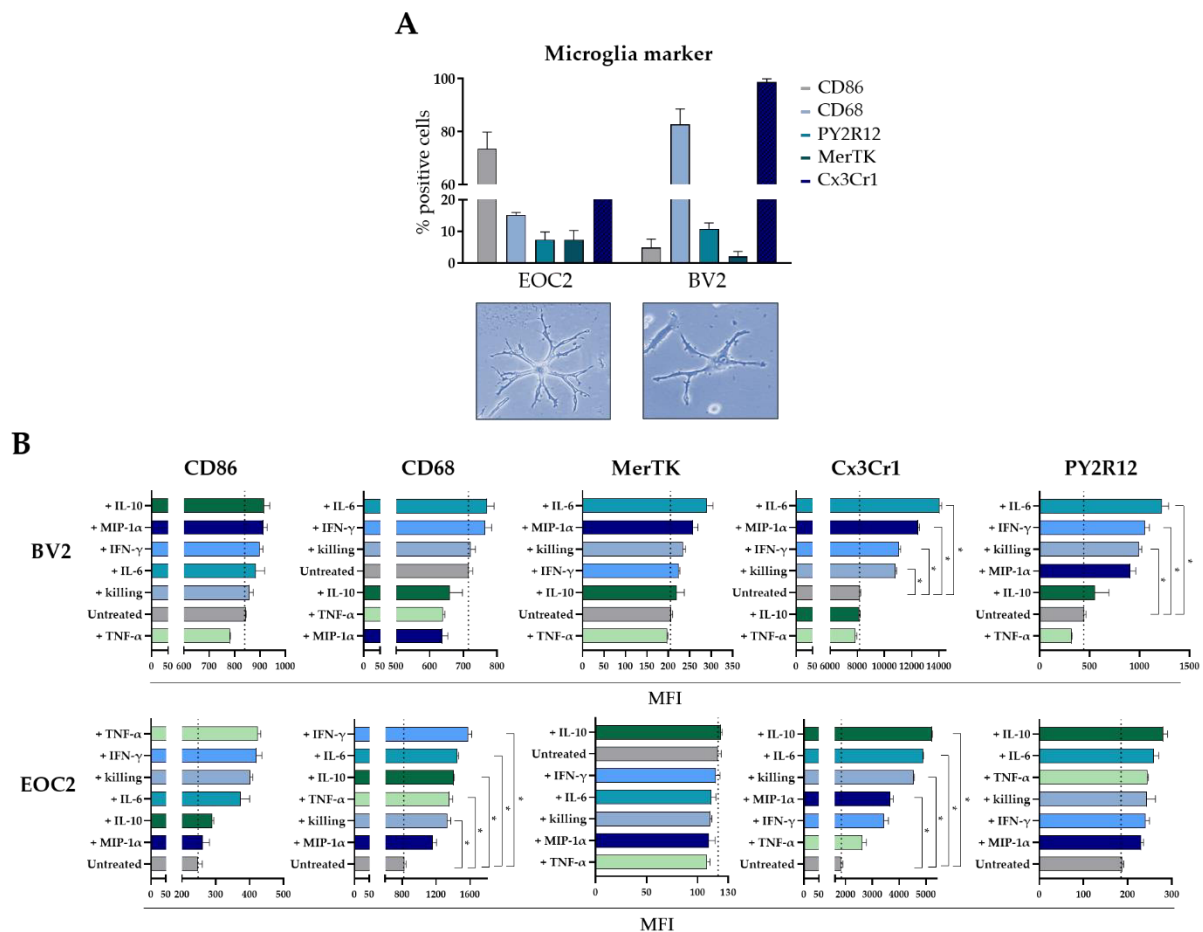


**Figure 22: Regulation of microglia markers in response to adjacent CAR-NK cell-mediated tumor cell lysis. (A)**

Analysis of MG surface marker expression as determined by flow cytometry. **(B)** Regulation of murine MG markers in response to stimulation with murine recombinant cytokines or in response to a transwell cytotoxicity assay (CAR-NK vs. GL261-HER2, E/T ratio 1:1) was analyzed via flow cytometry. Cells were incubated with recombinant cytokines for 24 h at a concentration of 100 ng/ml. Mean values  $\pm$  SD are shown;  $n=2$ . \* $p < 0.05$ .

Moreover, albeit insignificant, a trend for increased CD86 and PY2R12 expression was found in EOC2. Furthermore, PY2R12 and CX3CR1 expression were significantly increased in BV2 after stimulation with IL-6 and IFN- $\gamma$  (Fig. 22B, top), and MIP-1 $\alpha$ , whereas the addition of IFN- $\gamma$ , IL-10, TNF- $\alpha$  and IL-6 enhanced CX3CR1 and CD86 expression in EOC2 (Fig. 22B, bottom).

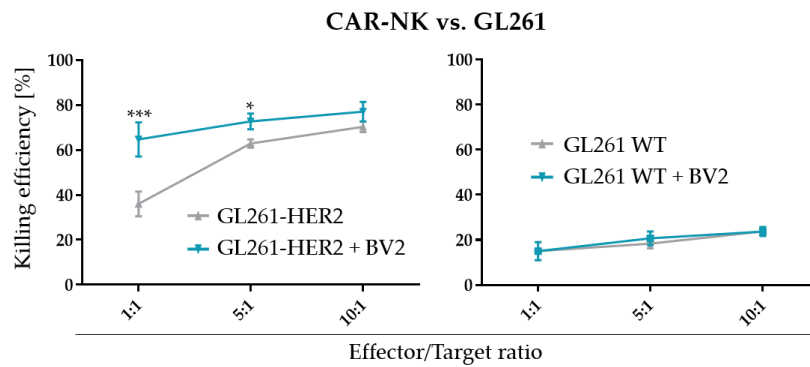


**Figure 23: Synergy between CAR-NK cells and murine microglia.** Killing efficiency of CAR-NK cells against GL261-HER2 and GL261 WT cells either in the presence or absence of murine MG (BV). Mean values  $\pm$  SD are shown;  $n=3$ . \* $p < 0.05$ , \*\*\* $p < 0.001$ .

Since MG as bystander immune cells appear to be affected by nearby GB cell lysis by CAR-NK cells, possible synergistic effects regarding CAR-NK cell killing efficiency were evaluated. When CAR-NK cells attacked GL261-HER2 cells in the presence of BV2, cytotoxic activity was significantly increased with decreased effector/target ratio of CAR-NK cells to GL261-HER2 cells (Fig. 23, left). Of note, killing efficiency towards cells lacking the target antigen was not affected by the presence of MG (Fig. 23, right).

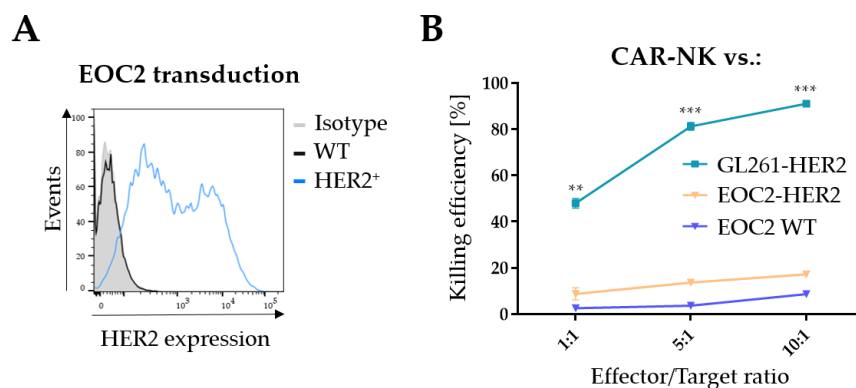


**Figure 24: Killing efficiency of CAR-NK cells towards murine microglia.** (A) HER2 expression of the murine MG cell line EOC2 before (black) and after (blue) lentiviral transduction with the antigen. (B) Cytotoxic activity of CAR-NK cells against the murine MG cell lines EOC2 before (blue) and after (orange) lentiviral transduction with the human HER2 antigen. GL261-HER2 cells served as a positive control. Mean values  $\pm$  SD are shown;  $n=3$ , \*\*\* $p < 0.001$ .

To investigate whether immune cells such as MG themselves were affected by CAR-NK cell attack to a similar extent as tumor cells, the MG cell line EOC2 was lentivirally transduced with the target antigen (Fig. 24A). As expected, EOC2 WT cells lacking HER2 expression were hardly lysed by CAR-NK cells. Surprisingly, however, almost no cytotoxic activity towards HER2-transduced MG was observed (Fig. 24B).

### 3.3.2 The effect of activated CAR-NK cells on human microglia

To investigate whether human MG cells were also less susceptible to CAR-NK cell attack, cytotoxicity assays of CAR-NK cells vs. human MG were performed. First, the expression of the target antigen by human MG was assessed. Although it has been reported that brain-resident cell types are mainly HER2<sup>-</sup>, expression is induced in response to pathophysiological conditions. In this context, surface molecule expression in cells that were maintained in cell culture over a long period of time might differ from the *in vivo* situation. Both human MG and astrocyte cell lines expressed HER2 *in vitro*, as confirmed on the mRNA as well as on the protein level (Fig. 25A and B). Nevertheless, although HER2 was shown to be expressed on the cell surface, neither human MG nor human astrocytes were efficiently lysed by CAR-NK cells, irrespective of effector/target ratio. In contrast, the killing efficiency of CAR-NK cells towards human MG was significantly lower as compared to human GB cells (Fig. 25C). To investigate whether a cytotoxicity assay of 2 h might not give CAR-NK cells enough time to mount an efficient attack towards immune cells like MG or astrocytes, a comparative cytotoxicity assay employing different time intervals was performed. MG and astrocytes were subjected to CAR-NK cell attack over either 2 h, 4 h or 8 h at different effector/target ratios. As compared to tumor cells such as the GB cell line GL261-HER2, the patient-derived glioma cell culture CB013 or the human primary glioma cell line MNOF-1300, both MG and astrocytes were less efficiently lysed by CAR-NK cells, even after 8 h of co-culture. For instance, killing efficiency towards tumor cells at an effector/target ratio of 1:1 after 8 h exceeded 70%, while efficiency towards astrocytes was only below 50% (NHA: 35,9%, HuA: 49,5%), and efficiency towards MG did not exceed 15% (HMC3: 14.5 %, C20: 13.6%; Fig. 25D). Of note, killing efficiency towards the human astrocyte cell line HuA did not exceed 50%, irrespective of time and effector/target ratio (Fig. 25D, bottom right).

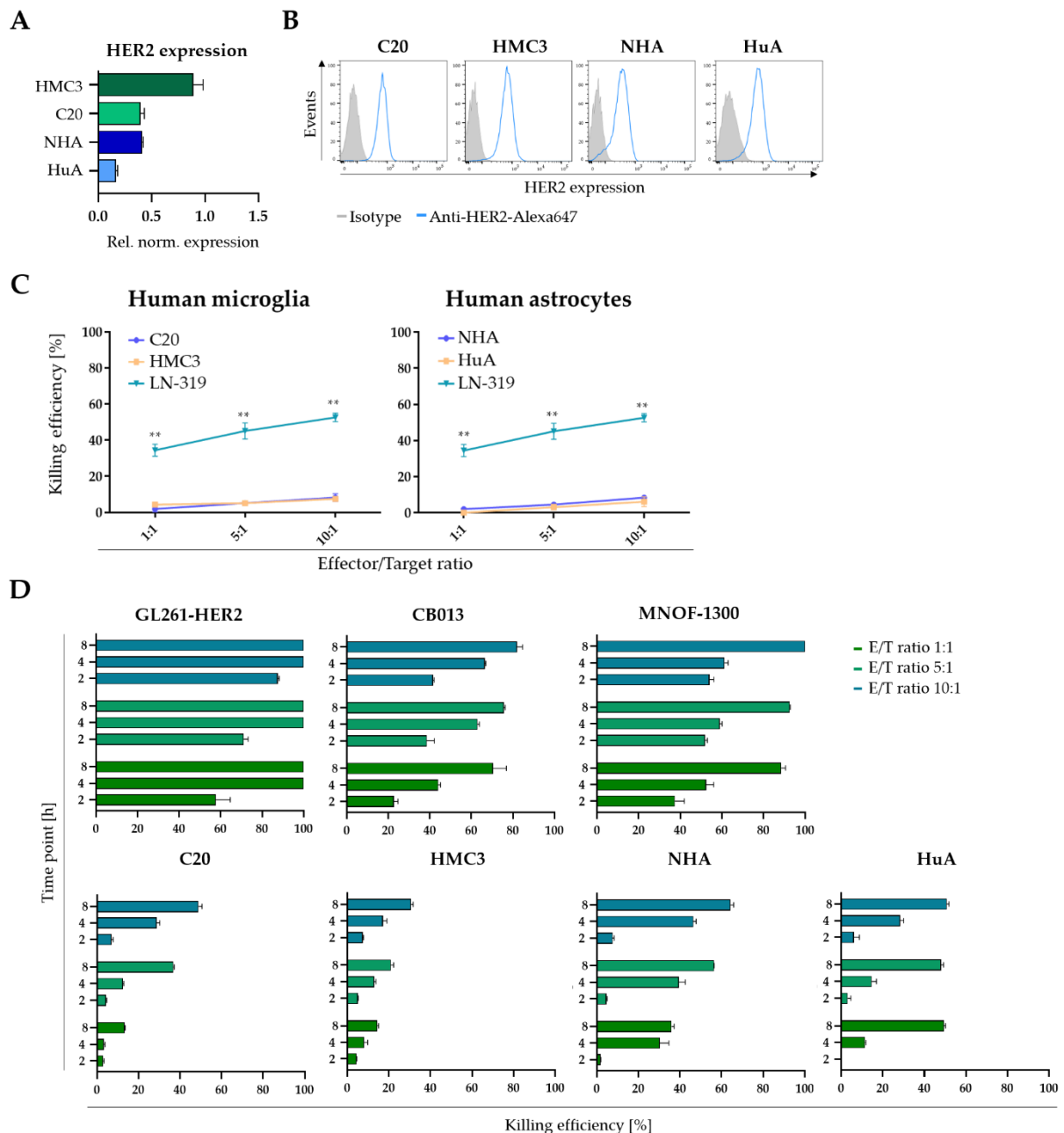


**Figure 25: Brain-resident immune cells are not susceptible to lysis by CAR-NK cells.** (A) Quantification of human HER2 expression on the mRNA level as determined by qPCR. RNA was isolated from murine HER2-transduced GL261 as well as from human MG (C20, HMC3) and human astrocytes (NHA, Hua). SDHA and 18s were used as housekeeping genes for reference. (Rel. norm. values  $\pm$  SD are shown;  $n=3$ ). (B) HER2 expression of MG (C20, HMC3) and astrocytes (NHA, HuA) of human origin as determined via flow cytometry. (C) Cytotoxic activity of CAR-NK cells against human MG as well as astrocyte cell lines as compared to the human glioblastoma cell line LN-319 as a positive control. Mean values  $\pm$  SD are shown;  $n=3$ ,  $***p < 0.001$ . (D) Quantification of CAR-NK cell killing efficiency against various cell types at different E/T ratios after 2 h, 4 h and 8 h.

Since one reason for the low killing efficiency of CAR-NK cells towards MG or astrocytes might be the inhibition of NK cell degranulation, expression of the degranulation marker CD107a upon contact of CAR-NK cells with target cells was determined. While co-culture with GL261 WT cells lacking the target antigen did not trigger CAR-NK cell degranulation, contact with GL261-HER2, but also with C20 and HMC3 MG as well as with NHA and HuA astrocytes did (Fig. 26A). These data indicate that CAR-NK cell activity was not inhibited by MG or astrocytes directly. Next, the expression of HLA-E on the surface of target cells was evaluated as a possible inhibitory mechanism. HLA-E is a ligand for the inhibitory NK cell receptor CD94/NKG2A [329]. It was found to be expressed by the MG cell line C20 as well as by the astrocyte cell line NHA, while HMC3, HuA, MNOF-1300 and CB013 were HLA-E<sup>-</sup> (Fig. 26B). Although this finding indicated that CD94/NKG2A engagement might be responsible for the low killing efficiency of CAR-NK cells towards C20 and NHA cells, HMC3 and HuA still showed decreased susceptibility regardless of HLA-E status, suggesting that this mechanism does not fully explain the observations made in Fig. 25.

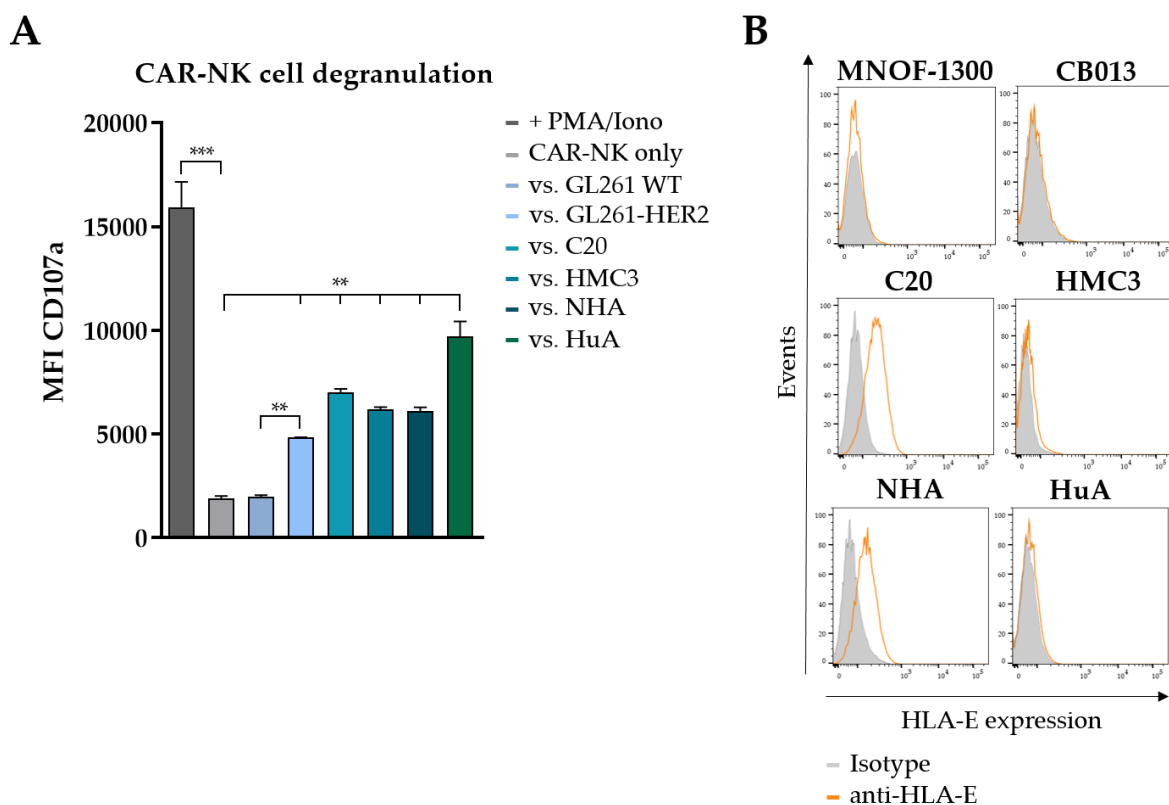


**Figure 26: Expression of HLA-E on the surface of target cells and degranulation of CAR-NK cells in response to various target cell types. (A)** Quantification of CAR-NK cell degranulation upon co-culture with target cells as determined by flow cytometric analysis of CD107a expression. Mean values  $\pm$  SD are shown;  $n=3$ ,  $**p < 0.01$ ,  $***p < 0.001$ . **(B)** Analysis of HLA-E expression on various cell types as determined by flow cytometry.

As seen in Fig. 20B, murine MG react to tumor cell lysis by CAR-NK cells in their surroundings. Therefore, it was analyzed whether CAR-NK cell-mediated tumor cell lysis also affected human MG and their activity. Interestingly, when soluble factors from a cytotoxicity assay in a transwell system influenced MG cells, their phagocytosis activity was significantly increased, similar to stimulation with IFN- $\gamma$  (Fig. 27), indicating that CAR-NK cell activity might contribute to activation of immune cells within the TME.

Taken together, CAR-NK cell therapy affects MG in terms of activation and phagocytosis, while the presence of MG appeared to enhance CAR-NK cell-mediated tumor cell lysis. Moreover, MG tolerance towards cytotoxic mediators such as perforin and GrB following CAR-NK cell degranulation was higher than that of glioma cells.

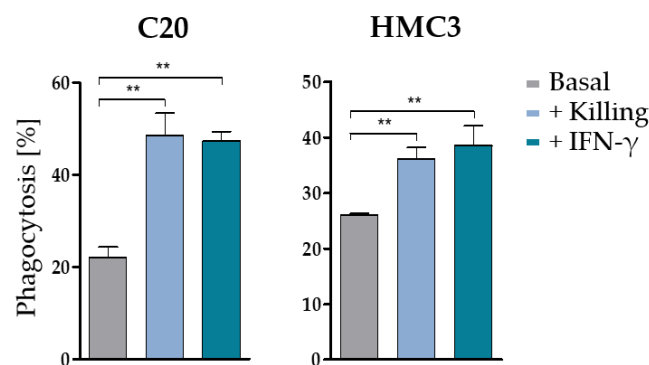


**Figure 27: Microglial phagocytosis activity is increased upon adjacent CAR-NK cell-mediated tumor cell lysis.** Phagocytosis activity of human MG in response to adjacent CAR-NK cell-mediated tumor cell lysis in a transwell system (CAR-NK vs. LN-319, E/T ratio 1:1). hIFN- $\gamma$  [100ng/ml] served as a positive control for cell stimulation. Mean values  $\pm$  SD are shown; n=3. \*\*p < 0.01.

### 3.4 aPD-1 encoding HER2-AAV vectors

The PD-1/PD-L1 axis contributes to the immunosuppressive TME of glioma to a great extent. Additionally, lysis of tumor cells by CAR-NK cells has been shown to mediate PD-L1 upregulation in surrounding cell types (Fig. 19), which further reinforces the suppression of anti-tumor immune responses. To counteract this suppression and to re-activate the immune system, HER2-AAV vectors can be applied to induce the secretion of aPD-1 after transduction of HER2<sup>+</sup> cells. Previous studies already reported a sufficient transduction efficiency of HER2-AAVs in human renal and breast cancer cells [251], [310]. The HER2-AAVs used in this study harbor a coding sequence for a fusion protein directed against murine PD-1 (HER2-AAV<sup>aPD1</sup>) (depicted in Fig. 10A-C), as the human Fc part used previously [310] was replaced by the



corresponding murine sequence. After the transduction of target cells, the production of an scFv-Fc fusion construct is induced. Two scFv-Fc molecules then dimerize via their Fc domains to form a Y-shaped antibody-like molecule, a so-called aPD-1 immunoadhesin. HER2-AAV<sup>IgG-Fc</sup> encoding only the murine Fc part of aPD-1 served as control. Detection of the recombinant aPD-1 was facilitated by an HA-tag.

### 3.4.1 *In vitro* transduction efficacy of HER2-AAV

To assess transduction efficiency on the mRNA level, RNA of target cells was isolated 24 hours post-HER2-AAV transduction and aPD-1 levels were determined via qPCR using a primer pair binding within the scFv region of aPD-1. Upon transduction of target cells with HER2-AAV<sup>aPD-1</sup>, mRNA of the aPD-1 transgene was detected only in HER2<sup>+</sup> cells (Fig. 28), indicating high specificity of the DAPRins on their capsid surface. Moreover, transduction efficiency correlated with expression levels of human HER2 on target cells. None of the murine HER2-cells incubated with HER2-AAV<sup>aPD-1</sup> produced relevant amounts of aPD-1, and neither did HER2<sup>+</sup> cells that were incubated with HER2-AAV<sup>IgG-Fc</sup> control vectors. In contrast, aPD-1 levels were higher in the supernatant of LN-319-HER2 cells modified to overexpress HER2 when compared to parental HER2<sup>+</sup> LN-319 cells. Compared to LN-319-HER2, LN-319 and Tu9648-HER2, transgene amplification was lowest in GL261-HER2 cells with 0.38-fold amplification as compared to housekeeping genes.

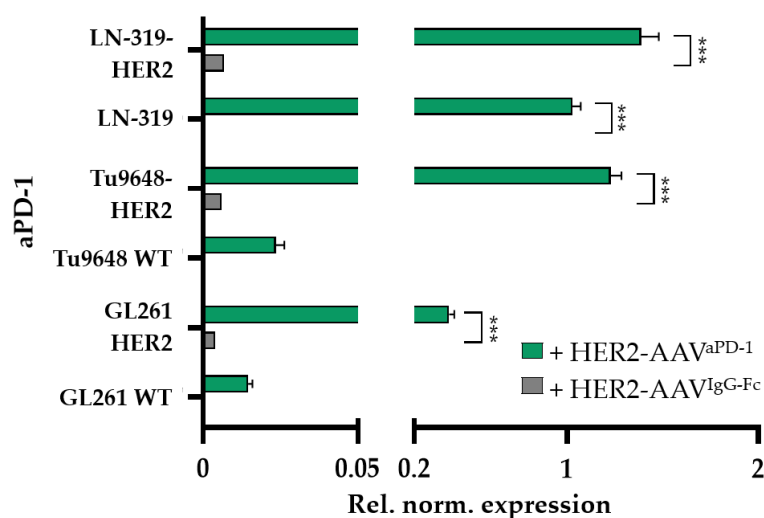


**Figure 28: Expression of HER2-AAV-encoded aPD-1 on the RNA level.** Quantification of transgene expression on the mRNA level as determined by qPCR. RNA was isolated four days post-transduction; SDHA and 18s were used as housekeeping genes for reference. (Rel. norm. values  $\pm$  SD are shown; n=3. \*p < 0.05).

Next, transduction efficiency was investigated on the protein level. Therefore, cell lysates of HER2-AAV-transduced GL261-HER2 target cells were analyzed via Western blot. It was shown that aPD-1 is present at its expected size of ~68 kDa within target cells on days 2, 6 and 10 after viral transduction (Fig. 29A).

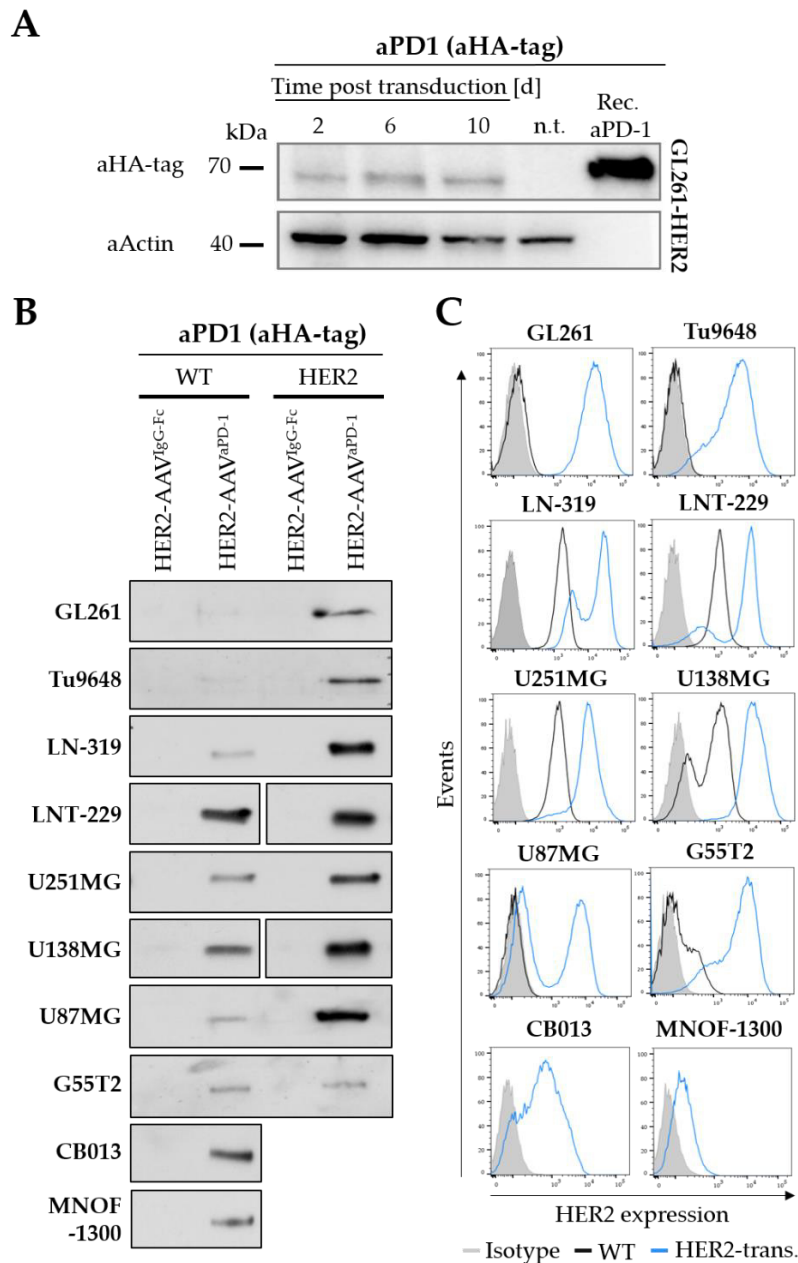


**Figure 29: Expression of HER2-AAV-encoded aPD-1 on the protein level. (A)** Cell lysates of transduced GL261-HER2 cells were prepared 2, 6 and 10 days after transduction with HER2-AAV<sup>aPD-1</sup> ( $4.5 \times 10^5$  gc/cell). Western blot analysis was performed using an HA-tag-specific antibody. Actin was used as a loading control. Lysates from untransduced cells (n.t.) and recombinant aPD-1 were used as controls. **(B)** HER2 expression of murine (GL261, Tu9648) and human (LN-319, LNT-229, U251MG, U138MG, U87MG, G55T2) glioma cell lines (wild-type cells are depicted in black, HER2-overexpressing derivatives are depicted in blue) as well as human primary (MNOF-1300) and patient-derived (CB013) cells as determined via flow cytometry. **(C)** Four days post-incubation with HER2-AAV ( $4.5 \times 10^5$  genome copies/cell), cell culture supernatants were collected and aPD-1 expression was analyzed via Western blot using an HA-specific antibody. The aPD-1 band is a size of ~68 kDa.

No decrease in aPD-1 signal intensities over time was observed, suggesting constant amounts of the immunoadhesin up to 10 days post-HER2-AAV transduction. In untransduced cells, no aPD-1 signal was detected. Since it is conceivable that transduced tumor cells produce aPD-1, but do not secrete it to a sufficient amount, it was assessed whether the immunoadhesin is present in the cell culture supernatant upon delivery of the transgene into target cells. Indeed, aPD-1 protein secretion was confirmed using Western blot analysis, as the immunoadhesin was successfully detected in the supernatant of transduced cells (Fig. 29B). Similar to transduction on the mRNA level, transduction efficiency on the protein level also correlated with the HER2 expression level on target cells. aPD-1 band intensities of samples of transduced HER2-overexpressing cells were higher than those of cells expressing HER2 at endogenous levels (Fig. 29B and C). Cells that were transduced with the HER2-AAV<sup>IgG-Fc</sup> control virus did not produce and secrete aPD-1, and neither did HER2-AAV<sup>aPD-1</sup>-transduced murine target cells lacking the antigen (GL261 WT and Tu9648 WT). Of note, also HER2<sup>+</sup> human primary glioma cells as well as patient-derived glioma cells secreted aPD-1 upon transduction with HER2-AAV<sup>aPD-1</sup>.

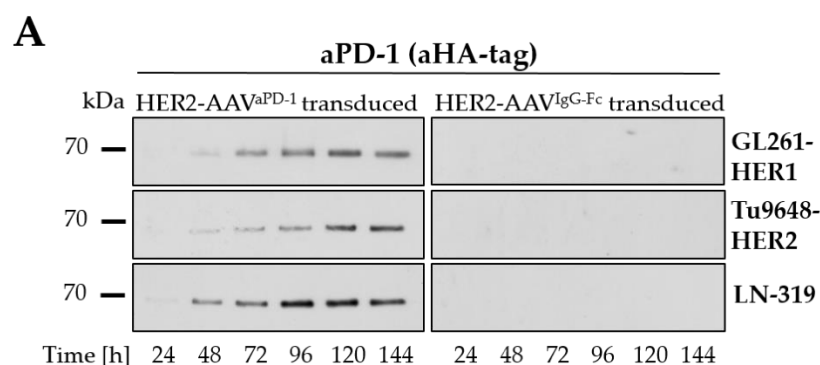


**Figure 30: Secretion of HER2-AAV-encoded aPD-1 in a time-dependent manner.** (A) aPD-1 transgene expression over time in GL261-HER2 (top), Tu9648-HER2 (middle) and LN-319 (bottom) cells monitored by Western blot analysis using an HA-specific antibody.

Furthermore, levels of aPD-1 in cell culture supernatants of GL261-HER2, Tu9648-HER2 and LN-319 accumulated over time and persisted for up to 7 days without showing signs of degradation (Fig. 30A). In summary, HER2-AAV<sup>aPD-1</sup> mediates aPD-1 gene delivery with high specificity and causes the subsequent constant production and secretion of aPD-1.

### 3.4.2 Establishment of a sandwich ELISA approach for the detection of HER2-AAV-encoded aPD-1

To quantify concentrations of secreted HA-tagged PD-1-directed immunoadhesins, an enzyme-linked immunosorbent assay (ELISA) was established. First, a protein standard for an aPD-1 standard curve was generated. Therefore, HEK293T/A cells were transiently transfected with a transfer plasmid encoding aPD-1. Over 4 days, the supernatant was harvested and purified using Protein A affinity chromatography (Fig. 31A). As transfection control, HEK293T/A cells were incubated with a GFP plasmid (Fig. 31B). Purified aPD-1 was concentrated and detected at its expected size by Western blot analysis (Fig. 31C). Its concentration was determined via microBCA. For aPD-1 quantification via ELISA, an HA-tag antibody was used as capture antibody for aPD-1 binding, which was subsequently detected via a murine IgG-specific antibody (Fig. 31D).

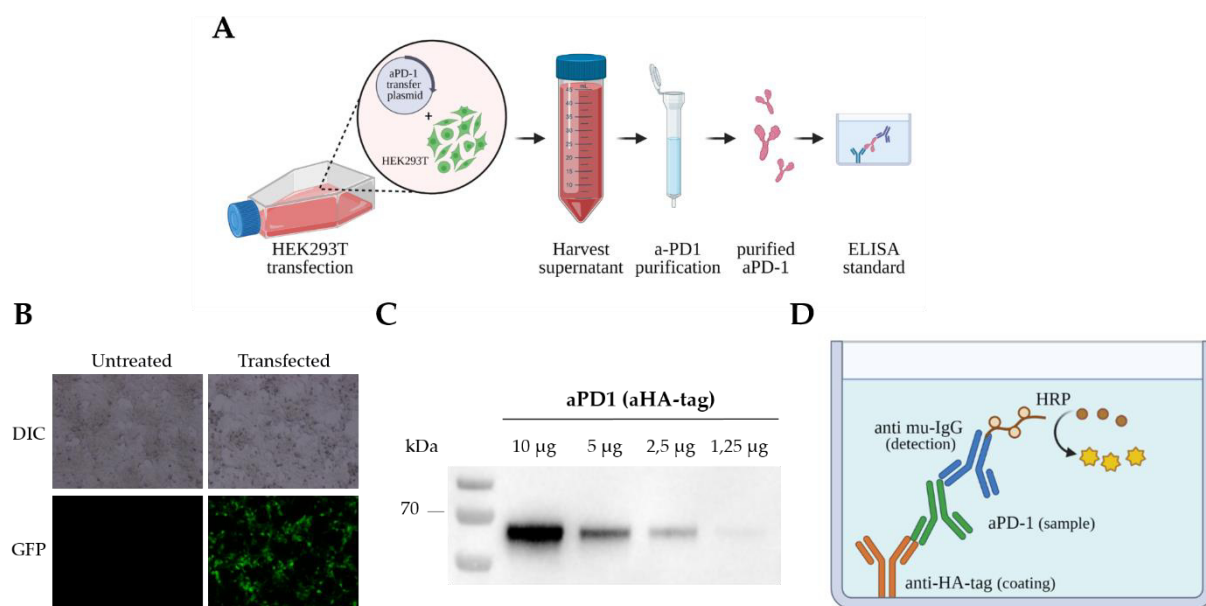


**Figure 31: Production and purification of recombinant aPD-1 for the establishment of a sandwich ELISA. (A)** HEK293T/A cells were transfected with an aPD-1 transfer plasmid. aPD-1 containing supernatants were collected and aPD-1 was purified via Protein A affinity chromatography. **(B)** As transfection control, HEK293T/A cells were transfected with a GFP plasmid. **(C)** A western blot was performed using different concentrations of the recombinant aPD-1. HA-Tag-specific antibodies were used and aPD-1 was detected at ~68 kDa. **(D)** Schematic representation of the sandwich ELISA approach. Secreted aPD-1 binds to an HA-Tag capture antibody and is detected via an HRP-coupled detection antibody directed against the murine Fc part of aPD-1.

To determine both sensitivity and detection limit of the established assay, antibody dilutions were titrated using a checkerboard titration to assess antibody as well sample concentration at the same time and the ELISA was performed with serial dilutions of the recombinant  $\alpha$ PD-1 standard. The lowest amount of aPD-1 that was detectable by the method was 25 ng (Fig. 32A).

HER2-transduced GL261 and Tu9648 cells as well as LN-319 and LN-319-HER2 cells were transduced with aPD-1 encoding HER2-AAV vectors and cell culture supernatants were analyzed by the newly established ELISA. Cell culture supernatants of either untreated or HER2-AAVaPD-1-transduced WT murine GL261 and Tu9648 cells served as a negative control. Only HER2<sup>+</sup> target cells which were transduced with HER2-AAV<sup>aPD-1</sup> produced the immunoadhesin (Fig. 32B). Similar to the data obtained in qPCR and Western blot before, aPD-1 levels were positively correlated with the HER2 expression on the target cells. For instance, endogenously HER2<sup>+</sup> LN-319 cells produced 0.64  $\mu\text{g}$  aPD-1 / 100  $\mu\text{l}$  supernatant, while HER2-overexpressing LN-319-HER2 cells produced nearly double amounts (1.13  $\mu\text{g}$  aPD-1 / 100  $\mu\text{l}$  supernatant). Only minimal amounts of aPD-1 were found after transduction of HER2<sup>-</sup> murine glioma cells with HER2-AAV<sup>aPD-1</sup> (0.09  $\mu\text{g}$  / 100  $\mu\text{l}$  supernatant (GL261 WT) and 0.04  $\mu\text{g}$  / 100  $\mu\text{l}$  supernatant (Tu9648 WT)).

Taken together, the established sandwich ELISA facilitated the precise determination of aPD-1 levels, which represented a prerequisite for the evaluation of HER2-AAV<sup>aPD-1</sup> transduction efficacy in *in vivo* models.

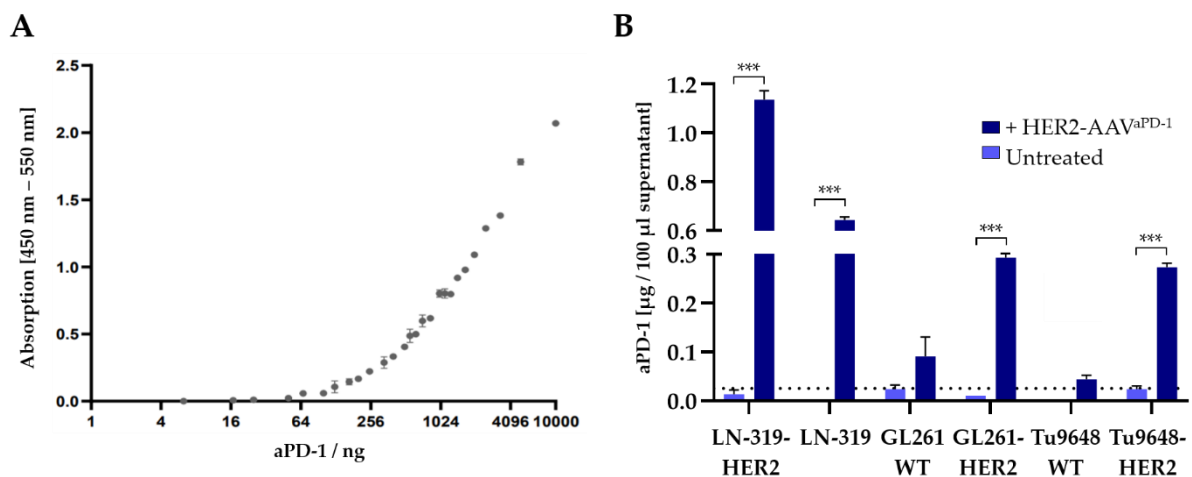


**Figure 32: Quantification of *in vitro* produced aPD-1 via sandwich ELISA. (A)** ELISA using serial dilutions of purified aPD-1. The immunoadhesin was detected via antibodies directed against the HA-tag- and the murine Fc portion of aPD-1. Mean values  $\pm$  SD are shown; n=2. **(B)** Supernatants of *in vitro* transduced glioma cells were analyzed by Sandwich-ELISA using an HA-specific antibody. Non-transduced (untreated) target cells and murine wildtype (WT) cells not expressing the target antigen were used as controls. The dotted line represents the detection limit at 0.025  $\mu\text{g}$ . Mean values  $\pm$  SD are shown; n=3. \*\*\*p < 0.001.

### 3.4.3 Functionality of HER2-AAV-encoded aPD-1

So far, it was shown that HER2-AAVs are able to efficiently mediate the production and secretion of aPD-1. However, the functionality of the immunoadhesin still needed to be demonstrated. Therefore, HER2-AAV-encoded aPD-1 was functionally characterized concerning its target binding capacity and ability to block the PD-1/PD-L1 checkpoint interaction. First, specific target binding was assessed via a binding assay employing HT1080 cells overexpressing PD-1 as depicted in Fig. 33A. Either parental HT1080 WT cells or PD-1-expressing HT1080 cells were cultivated in aPD-1-containing supernatant of transduced glioma target cells and binding of aPD-1 to PD-1 was detected via a fluorochrome-labeled antibody directed against the murine Fc-part of aPD-1. As a positive control, recombinant purified  $\alpha$ PD-1 was used, while supernatant of HER2-AAV<sup>IgG-Fc</sup> cells served as a negative control. After transduction of murine and human glioma cells with HER2-AAV<sup>aPD-1</sup>, specific binding of the secreted aPD-1 immunoadhesin, as well as the recombinant aPD-1, to PD-1 on HT1080-PD1 cells was found (Fig. 33B). In contrast, no binding was detected when supernatant of cells that were transduced with the control vector was used. It was shown before that amounts of aPD-1 in the supernatant accumulate over time post-transduction (Fig. 30A), and consequently, more aPD-1 molecules bound to PD-1 were found when supernatant was harvested after 48 h or 72 h as compared to 24 h (Fig. 33C). Since HT1080 cells do not endogenously express PD-1 but have been genetically modified to do so, freshly isolated murine splenocytes were used for target binding assays as a biological *ex vivo* system. Splenocytes comprise immune cells such as T cells, which were activated with PMA and ionomycin to induce PD-1 expression (Fig. 33D). Similar to the target binding assay before, activated splenocytes were incubated with supernatant of HER2-AAV-transduced GL261-HER2 or GL261 WT cells. In the *ex vivo* situation, recombinant as well as HER2-AAV-encoded aPD-1 secreted from GL261-HER2 cells also bound to PD-1 on activated splenocytes. Neither transduction of GL261 WT cells with HER2-AAV<sup>aPD-1</sup> nor transduction of GL261-HER2 cells with HER2-AAV<sup>IgG-Fc</sup> mediated PD-1 binding (Fig. 33D and E).

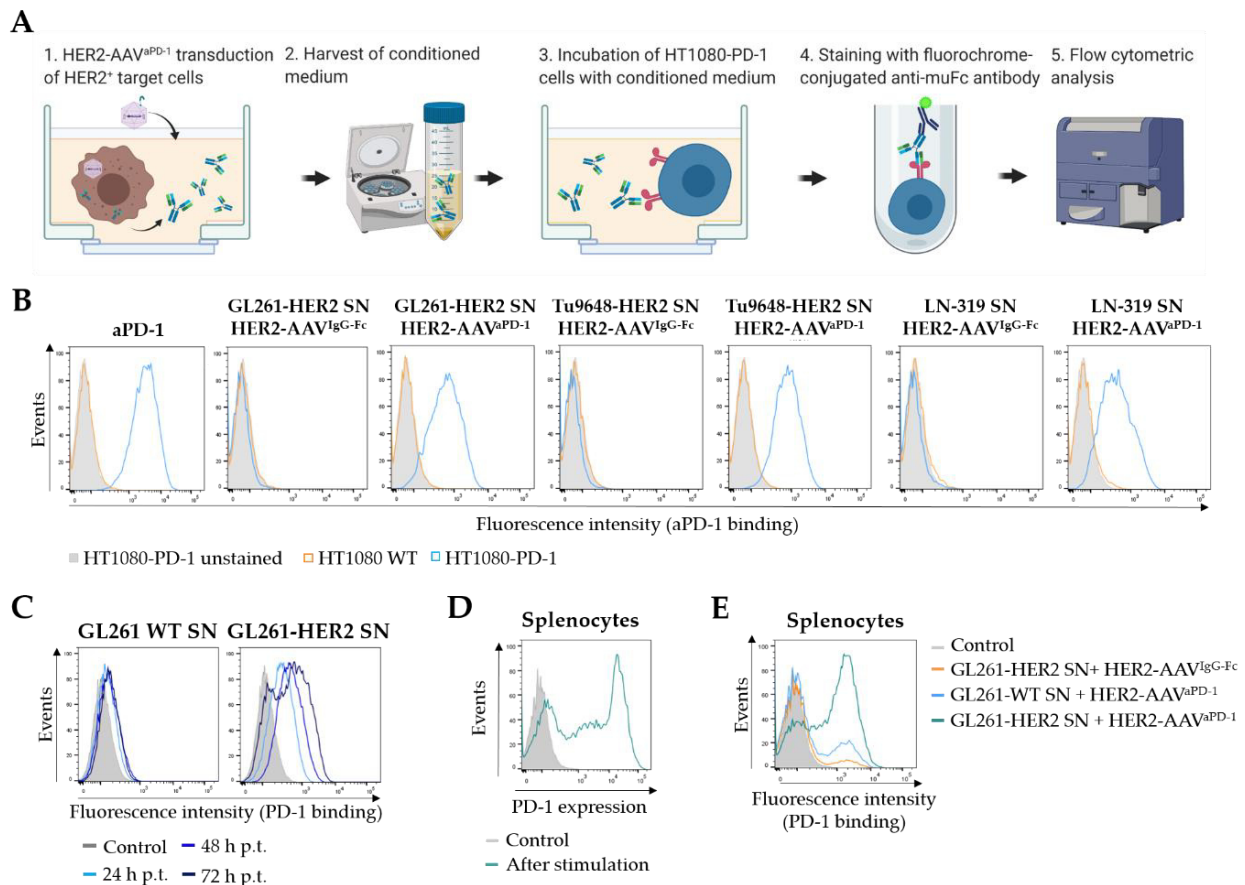


**Figure 33: Target binding of HER2-AAV-encoded aPD-1.** (A) Schematic representation of the PD-1 binding assay. PD-1-expressing cells are cultivated in aPD-1-containing supernatant of transduced glioma cells, then binding of aPD-1 to PD-1 is detected via flow cytometry using a fluorochrome-labeled antibody directed against the murine Fc part of aPD-1. (B) Specific binding of HER2-AAV-encoded aPD-1 to HT1080-PD1 (blue) and PD-1 negative HT1080 WT cells (gray). Supernatants (SN) from glioma cells that were transduced with HER2-AAV<sup>aPD-1</sup> or the control HER2-AAV<sup>IgG-Fc</sup> were tested; recombinant aPD-1 served as a positive control. (C) Analysis of aPD-1 target binding in a time-dependent manner. Cell culture supernatant of transduced GL261 cells (WT and HER2<sup>+</sup>) was harvested at different time points post-transduction and was used for an aPD-1 binding assay. (D) PD-1 expression on murine splenocytes after stimulation with DynaBeads. (E) Specific target antigen recognition of HER2-AAV-encoded aPD-1 on PD-1 expressing splenocytes. Freshly isolated murine splenocytes were stimulated with CD3/CD28 Dynabeads for 48 h to upregulate PD-1 expression before SN of transduced GL261-HER2 cells was added.

To further confirm the functionality of the aPD-1 immunoadhesin, a PD-1/PD-L1 blockade bioassay using T cells that express an NFAT-regulated reporter gene was performed. In particular, PD-1-expressing T effector cells were incubated with PD-L1-expressing aAPC cells, resulting in TCR inhibition and the subsequent suppression of NFAT-mediated luciferase expression in the absence of a checkpoint inhibitor (Fig. 34A). The supernatant of transduced glioma cells containing aPD-1-immunoadhesins blocked PD-1/PD-L1 interaction and was able to re-establish TCR activation in effector T cells (Fig. 34B). In summary, these data confirm that HER2-AAV-encoded aPD-1 specifically recognizes its target receptor after secretion from transduced target cells and is able to re-activate T cells upon PD-1 blockade *in vitro*.



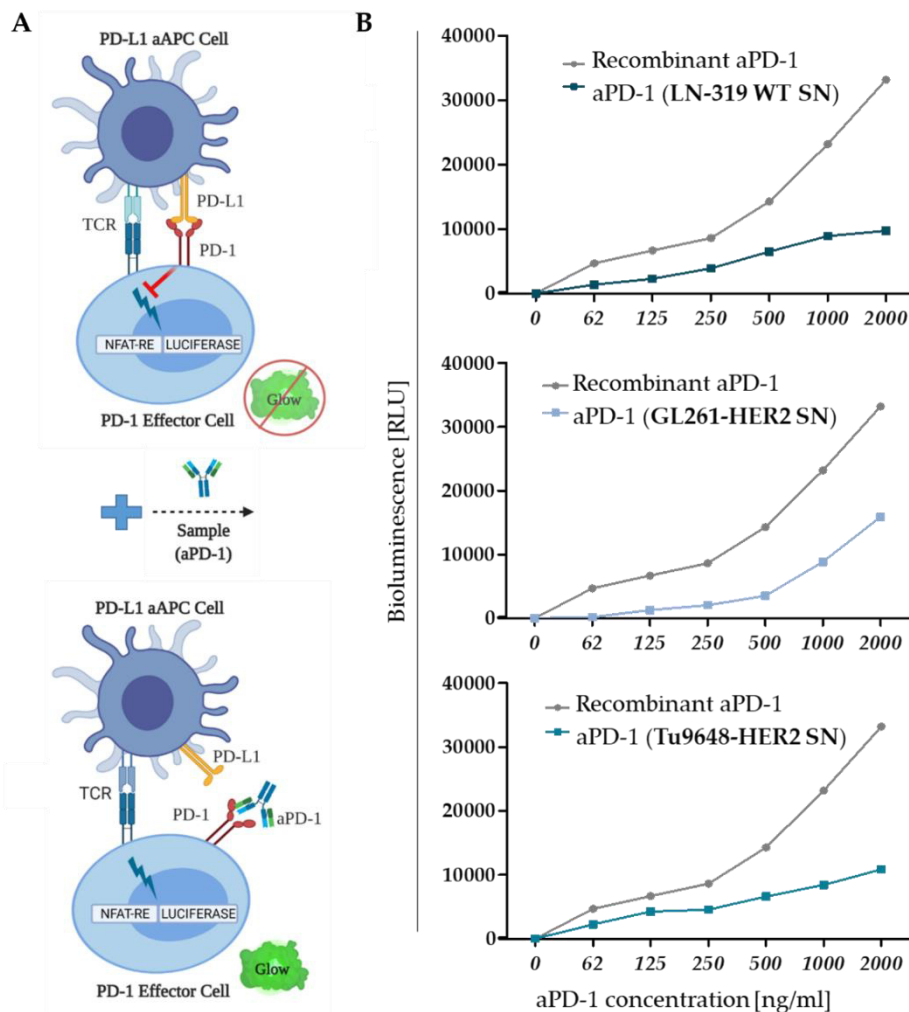


**Figure 34: PD-1/PD-L1 axis disruption of HER2-AAV-encoded aPD-1.** (A) Schematic representation of the PD-1/PD-L1 blockade bioassay. PD-L1-expressing murine aAPC/CHO-K1 target cells harbor an engineered cell surface protein mediating antigen-independent activation of T cells. The cells were incubated with murine PD-1 expressing effector T cells carrying a luciferase reporter driven by an NFAT response element. aPD-1 in the cell culture supernatant disrupts the PD-1/PD-L1 interaction between aAPC/CHO-K1 target cells and T cells. This allows activation of T cell receptors, resulting in luciferase expression via NFAT activation. (B) After the addition of aPD-1-containing cell culture supernatant, TCR activation was measured by assessing NFAT-dependent induction of luciferase expression. Bioluminescence is represented in relative light units (RLU). Recombinant aPD-1 served as a positive control.

### 3.4.4 The effect of HER2-AAV transduction on target cells

Since target cells are designated to produce and secrete the immunoadhesin, tumor cell viability should not be excessively impaired in response to viral transduction. Therefore, proliferation and cell viability of the glioma cell lines GL261, Tu9648 and LN-319 after transduction was determined. Target cell proliferation was assessed 24 h as well as 72 h after transduction with either HER2-AAV<sup>aPD-1</sup> or HER2-AAV<sup>IgG-Fc</sup>. In none of the evaluated cell lines, a significant decrease in proliferation activity was observed, irrespective of the timepoint of



the analysis (Fig. 35A). Moreover, no differences in proliferation in response to HER2-AAV<sup>aPD-1</sup> or HER2-AAV<sup>IgG-Fc</sup> were found. However, when cell viability was analyzed via PI staining 24 h after transduction, a slight, yet significant increase in cell death was observed in response to both HER2-AAV<sup>aPD-1</sup> or HER2-AAV<sup>IgG-Fc</sup> transduction (Fig. 35B). Nevertheless, the number of dead cells did not exceed 10% in either cell line, which suggests that those effects are not biologically relevant.

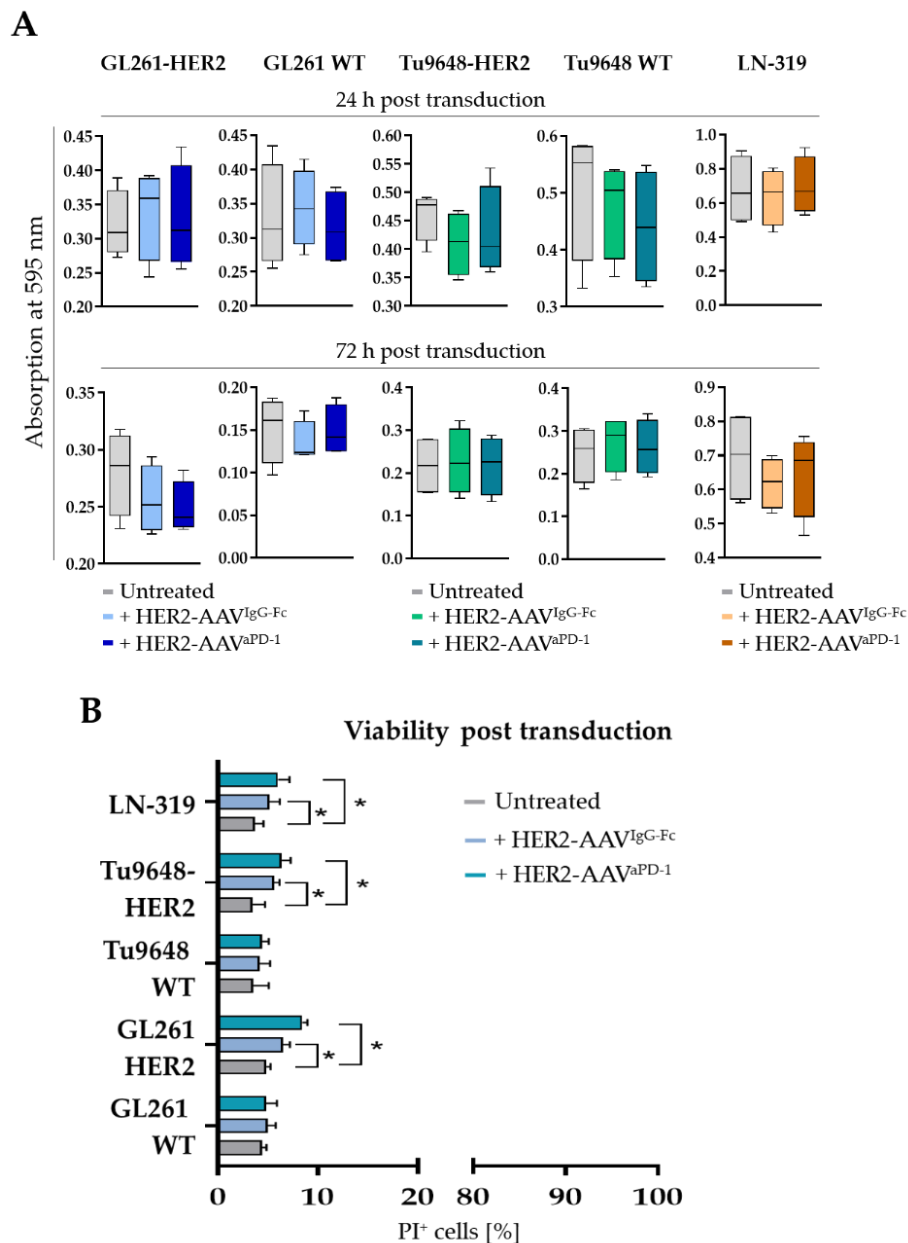


**Figure 35: The Effect of HER2-AAV transduction on proliferation and viability of glioma cells. (A)** Proliferation of glioma cells was measured by crystal violet staining 24 h and 72 h post transduction with HER2-AAV<sup>IgG-Fc</sup> or HER2-AAV<sup>aPD-1</sup>. **(B)** Viability of glioma cells 24 h post transduction with HER2-AAV<sup>IgG-Fc</sup> (light blue) or HER2-AAV<sup>aPD-1</sup> (petrol) as determined by propidium iodide (PI) FACS (mean values  $\pm$  SD are shown; n=3. \*p < 0.05).

Since for the specific combination therapy approach, the deployment of HER2 molecules as target antigens relies on their constitutive expression and presentation on the cell surface, the effect of viral transduction on HER2 expression on target cells was investigated. Via flow cytometry, it was assessed whether transduction by HER2-AAVs leads to a downregulation of HER2 on GL261-HER2, Tu9648-HER2 or LN-319. No downregulation in response to transduction in either cell line was observed (Fig. 36A). Next, it was analyzed whether viral transduction affected the expression of PD-L1, but in contrast to CAR-NK cell therapy, HER2-AAV transduction did not mediate the upregulation of PD-L1 on the tumor cell lines (Fig. 36B).

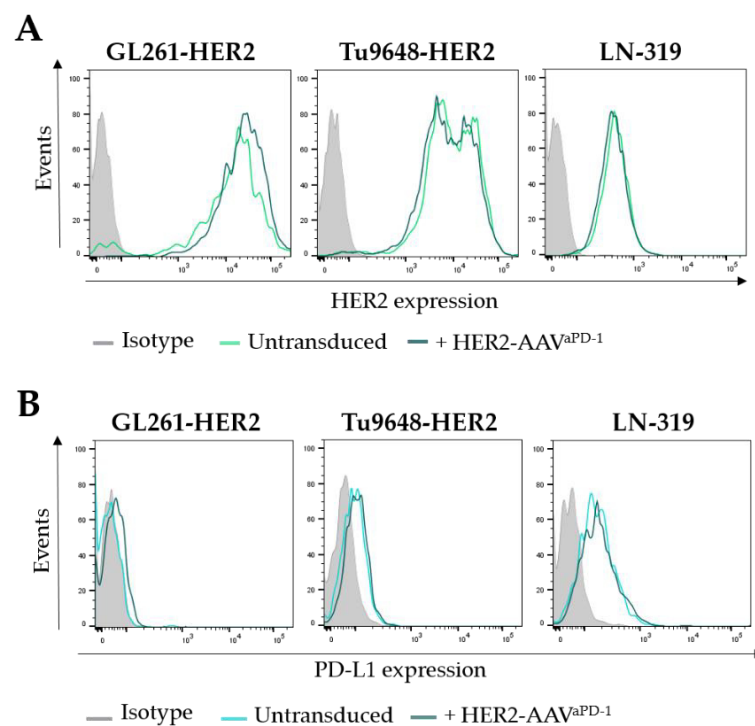


**Figure 36: The effect of HER2-AAV transduction on HER2 and PD-L1 expression on glioma cells. (A)** HER2 expression in response to HER2-AAV<sup>aPD-1</sup> transduction was determined after 24 h via flow cytometry. **(B)** PD-L1 expression on glioma cells before and after HER2-AAV<sup>aPD-1</sup> transduction.

Viral transduction could also induce increased production and secretion of soluble factors from transduced target cells. Concerning the activation of the immune system, the release of inflammatory cytokines is of crucial importance, especially in an immunosuppressed glioma TME. Therefore, the effect of HER2-AAV transduction on cytokine production of both GL261-HER2 and GL261 WT cells was investigated. First, to avoid bias in data interpretation, it was addressed whether viral transduction of murine glioma cells with the HER2 antigen itself affected cytokine secretion. Basal cytokine levels of GL261-HER2 cells in comparison with GL261 WT cells were assessed, but no differences in cytokine levels of IFN- $\gamma$ , CXCL1, TNF- $\alpha$ ,

MCP-1, IL-12p70, IL-27, IL-1 $\beta$ , GM-CSF, IL-10, IFN- $\beta$  and IFN- $\alpha$  were observed. However, IL-23 secretion was found to be significantly increased in GL261-HER2 cells (Fig. 37A). Upon transduction with HER2-AAVs, increased levels of MCP-1, IL-23 and IL-27 were detected only in GL261-HER2 target cells (Fig. 37B, top), whereas in HER2-GL261 WT cells no differences to baseline levels was observed (Fig. 37B, bottom). Levels of IFN- $\gamma$ , CXCL-1, TNF- $\alpha$ , IL-12p70, IL-1 $\beta$ , GM-CSF, IL-10, IFN- $\beta$  and IFN- $\alpha$  remained unchanged (data not shown).

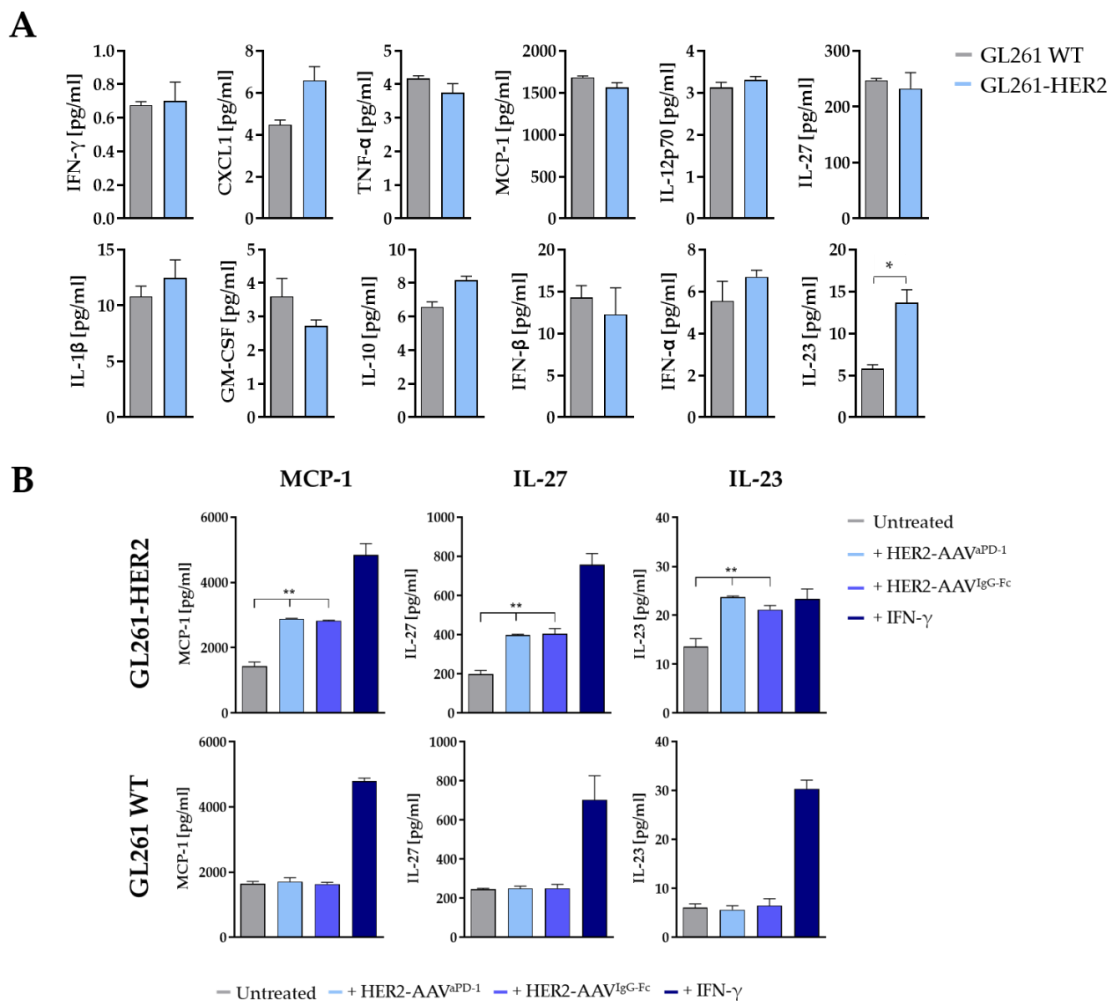


**Figure 37: The effect of HER2-AAV transduction on cytokine secretion of target tumor cells. (A)** Analysis of cytokine secretion of GL261 WT and lentivirally transduced GL261-HER2 cells. Mean values  $\pm$  SD are shown;  $n=3$ ,  $*p < 0.05$ . **(B)** Secretion of inflammatory cytokines produced by murine GL261-HER2 (top) or WT (bottom) cells in response to transduction with HER2-AAV<sup>aPD-1</sup> as compared to transduction with HER2-AAV<sup>IgG-Fc</sup> was determined using a bead-based immunoassay. As a control, cells were stimulated with recombinant murine IFN- $\gamma$  at a concentration of 100ng/ml. Mean values  $\pm$  SD are shown;  $n=3$ .  $**p < 0.01$ .

Increased levels of inflammatory cytokines were not only found in GL261-HER2 target cells, but also in cell types that constitute a relevant part of the cellular microenvironment of the brain, like MG and astrocytes. In human MG, a significant increase in levels of IL-6 (C20: 3-fold; HMC3: 2-fold) and IL-8 (C20: 1.5-fold; HMC3: 2-fold) was observed (Fig. 38, blue

quarters). In HMC3, levels of MCP-1 (2-fold), GM-CSF (2.5-fold) and IFN- $\lambda$ 1 (3-fold) were also significantly increased. In contrast, levels of cytokines secreted from HER2<sup>+</sup> murine MG that were above the detection limit, such as IFN- $\gamma$ , CXCL1 (BV2), TNF- $\alpha$  and GM-CSF (EOC2) did not increase when incubated with HER2-AAVs (Fig. 38, purple quarter). In astrocytes, levels of IFN- $\beta$  were only significantly increased (3-fold) in human cells, levels of murine astrocytes remained at baseline in response to transduction (Fig. 38, green quarter).

Taken together, transduction with HER2-AAVs modulated the cytokine release of HER2<sup>+</sup> target cells and slightly diminished their viability, whereas overall cell proliferation and target antigen expression was not affected.

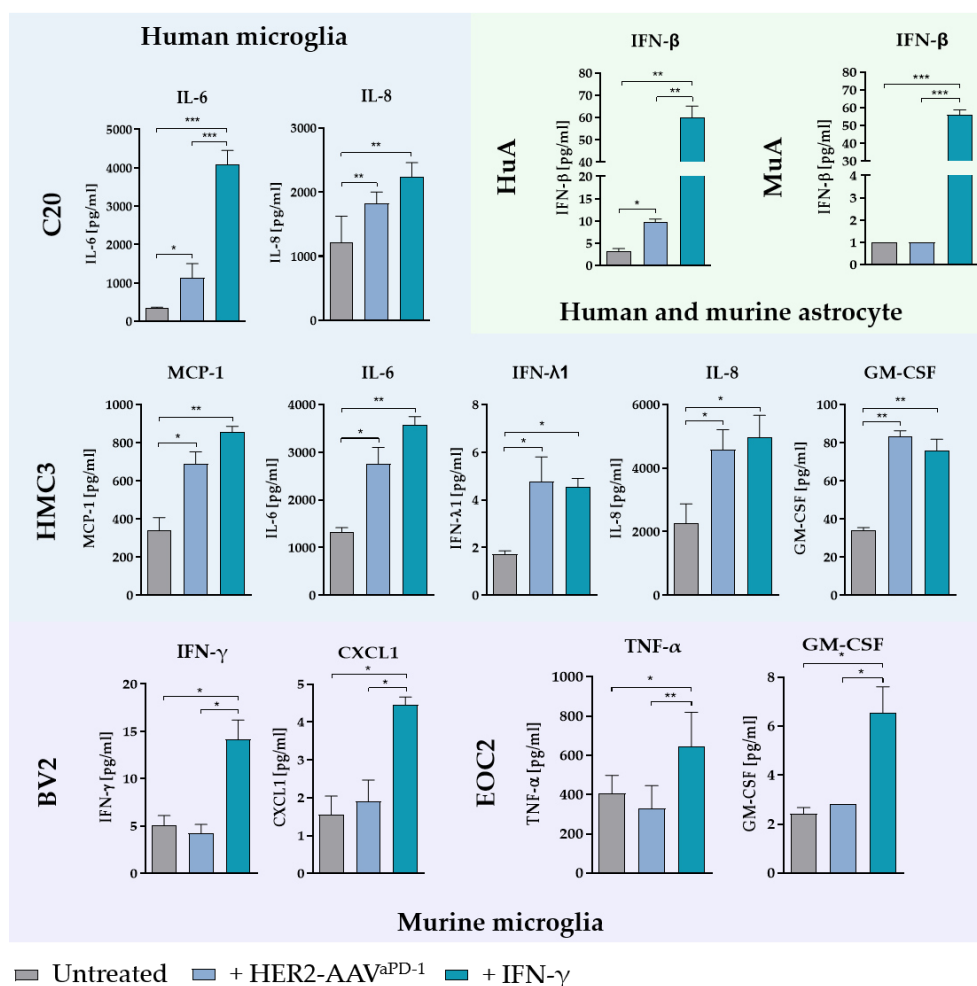


**Figure 38: The Effect of HER2-AAV on cytokine secretion of target resident brain cells.** Levels of various inflammatory cytokines produced by human microglia (blue square), murine microglia (purple square) and human and murine astrocytes (green square) in response to HER2-AAV<sup>aPD-1</sup> transduction were determined with a bead-based immunoassay. As a control, cells were stimulated with recombinant murine or human IFN- $\gamma$  at a concentration of 100 ng/ml. Mean values  $\pm$  SD are shown; n=3. \*p < 0.05, \*\*p < 0.01.

### 3.4.5 Interaction of HER2-AAV and CAR-NK cells

For the combination therapy approach, both CAR-NK cells and HER2-AAVs will exert their functions locally at the tumor site. Therefore, it is of crucial importance that HER2-AAV transduction and CAR-NK cell-mediated glioma cell lysis do not interfere with each other. In a comparative cytotoxicity assay, transduced GL261, Tu9648 and LN-319 glioma cells were subjected to CAR-NK cell attack. No difference in CAR-NK cell killing efficiency towards transduced glioma cells, irrespective of whether the vector encoded aPD-1 or not, as compared to untreated cells was found (Fig. 39A). Furthermore, CAR-NK cells lack HER2 expression and do not serve as targets for HER2-AAV (Fig. 39B and C).

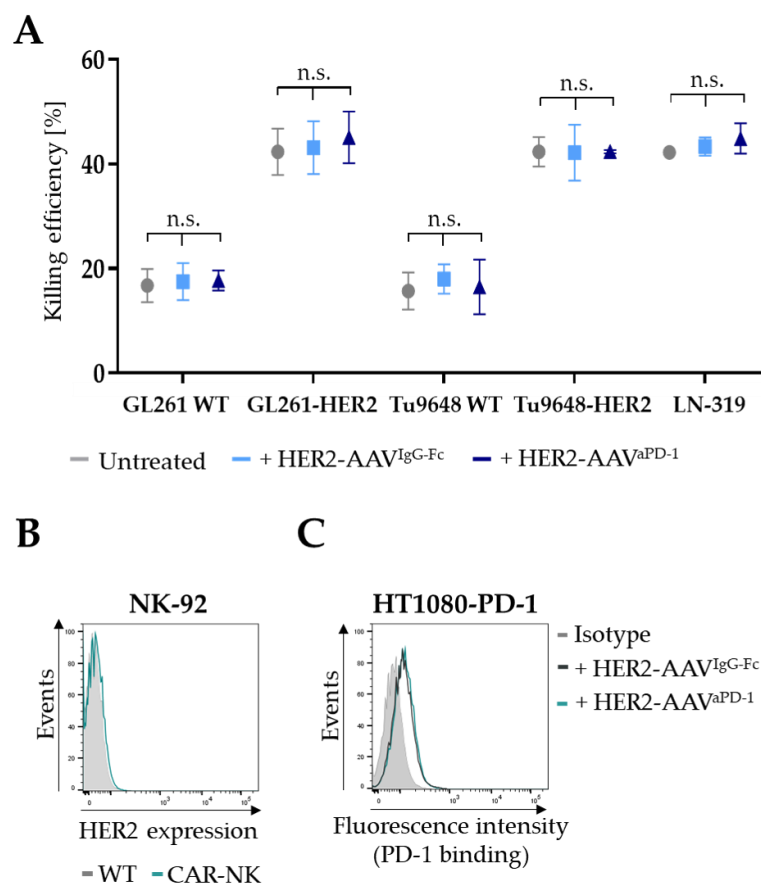


**Figure 39: The Effect of HER2-AAV transduction on killing capacity of CAR-NK cells.** (A) Killing efficiency of CAR-NK cells towards murine glioma cells was assessed 72 h post-transduction with a cytotoxicity assay (2 h co-culture, E/T ratio 5:1; mean values  $\pm$  SD are shown; n=3). (B) HER2 expression on CAR-NK cells. (C) A binding assay using cell culture supernatant from CAR-NK cells that had been incubated with HER2-AAVs for 72 h.

### 3.5 *In vivo* analyses

#### 3.5.1 Expression of HER2 and PD-L1 on glioma cells *in vivo*

For subsequent *in vivo* HER2-AAV biodistribution studies, GL261-HER2 and LN-319 cells were used. Since GL261-HER2 cells were injected in immunocompetent mice, the presence of a human surface molecule on the tumor cells might have resulted either in tumor cell clearance or HER2 loss. To confirm that GL261-HER2 tumor cells retain their HER2 expression *in vivo*, untreated tumors were explanted 8 weeks post tumor cell injection and HER2 expression was analyzed via flow cytometry. In cell culture, 93% of GL261-HER2 cells were HER2<sup>+</sup>, whereas the explanted tumor comprised of 33.2% HER2<sup>+</sup> cells (Fig. 40A, top).

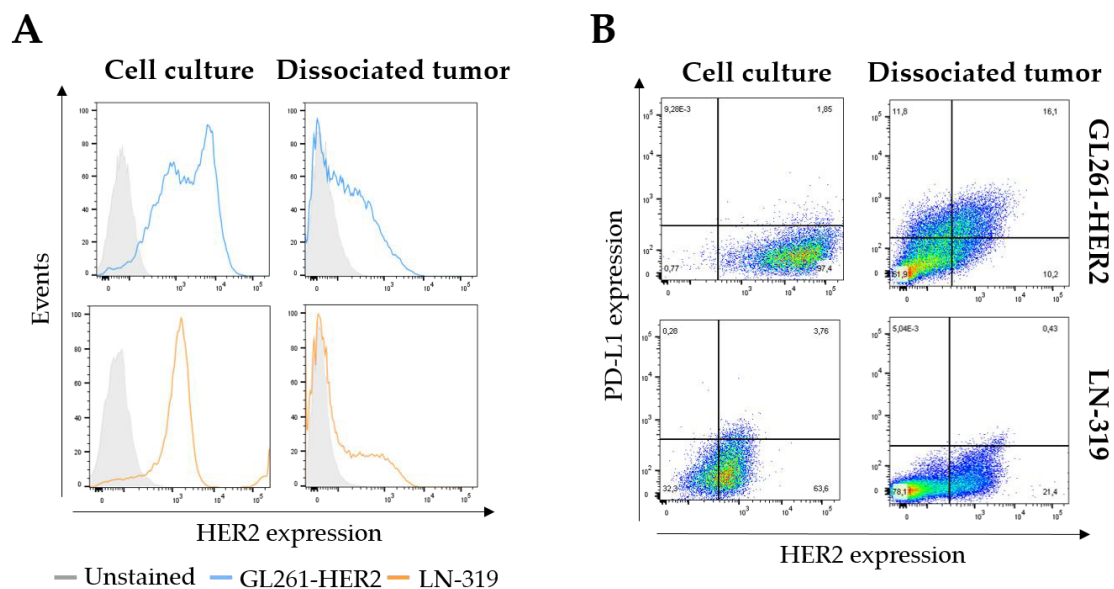


**Figure 40: HER2- and PD-L1 expression of glioma cells *in vivo*.** (A) HER2 expression of explanted subcutaneous GL261-HER2 tumors from C57BL/6 mice and LN-319 tumors from Crl:NU(NCr)-Foxn1<sup>nu</sup> mice 8 weeks post tumor cell injection, respectively. (B) PD-L1 expression on *in vitro* cultivated GL261-HER2 and LN-319 cells as compared to cells that were isolated from a 5-week old subcutaneous tumor (GL261-HER2 tumor from C57BL/6 mouse and LN-319 tumor from Crl:NU(NCr)-Foxn1<sup>nu</sup> mouse).

In this context, it should be taken into account that explanted tumors consist of various cell types other than the initially injected GL261-HER2 tumor cells, such as stromal cells, fibroblasts and immune cells. In comparison, 91.6 % of LN-319 cells in cell culture were HER2<sup>+</sup>, and explanted LN-319 tumors comprised of 34.2 % of HER2<sup>+</sup> cells (Fig. 40A, bottom). Furthermore, tumor cells are known to upregulate PD-L1 as an immune evasion mechanism *in vivo*. *In vitro*, GL261-HER2 cells do not express PD-L1, but on HER2<sup>+</sup> tumor cells explanted from tumors of immunocompetent mice, increased PD-L1 expression was found in 60% of cells (Fig. 40B, top). In LN-319 tumors that were grown in immunodeficient mice, no increase in

PD-L1 expression was observed (Fig. 40B, bottom). Taken together, continuous expression of the target antigen on GL261-HER2 cells 8 weeks post initial subcutaneous tumor cell injection was confirmed, whereas the analysis of explanted tumors of immunocompetent mice also revealed upregulation of PD-L1 by the tumor cells *in vivo*, further emphasizing the importance of checkpoint inhibition for anti-tumor immune responses.

### 3.5.2 Distribution kinetics and functionality of HER2-AAV-encoded aPD-1 *in vivo*

Gene delivery of checkpoint inhibitors using HER2-AAVs aims towards high local drug concentrations as compared to low systemic drug concentrations. Consequently, the anti-tumor immune response might locally be deblocked without the risk of systemic side effects. Previous *in vitro* studies in this project already revealed the potent transduction efficiency of HER2-AAVs in HER2<sup>+</sup> target cells as well as the subsequent production and secretion of functional aPD-1. As a next step, the characteristics of HER2-AAV biodistribution and aPD-1 production *in vivo* and the effect of transduction regarding safety, with respect to immune responses and possible toxicities was investigated in the GL261-HER2 mouse model. Furthermore, it was assessed whether neutralizing antibodies (nAbs) against the vector were generated and whether or not transduction efficacy was dependent on the route of HER2-AAV application. Therefore, the transduction efficiency achieved by HER2-AAVs was investigated and compared *in vivo* after a local injection and after systemic intravenous administration (Fig. 41A). Both the subcutaneous and the orthotopic intracranial GL261-HER2, as well as the subcutaneous LN-319 xenograft mouse model, was used to address this question. Animals were sacrificed 3, 7 and 10 days post HER2-AAV injection. Serum and tissue samples were obtained and aPD-1 concentrations, as well as the presence of nAbs, were evaluated by ELISA and neutralization assays, respectively. Furthermore, the transduction efficiency of HER2-AAVs after local injection into the tumor was compared to systemic administration via intravenous injection.

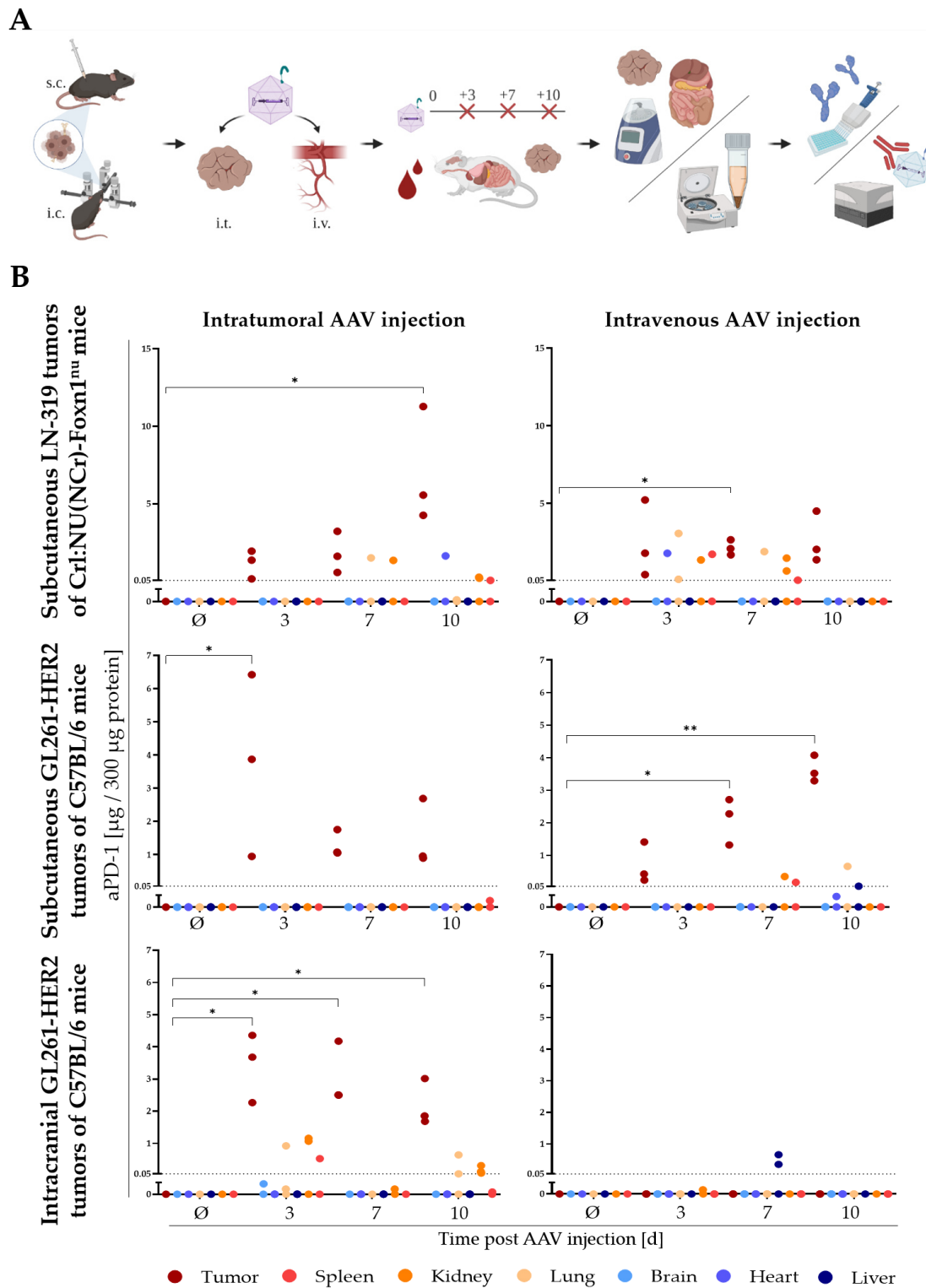


**Figure 41: Distribution kinetics of HER2-AAV-encoded aPD-1 *in vivo* and generation of neutralizing antibodies.** (A) Workflow of the kinetics study analyzing secreted aPD-1 and neutralizing antibodies (nAbs). HER2-AAV<sup>aPD1</sup> vector was injected either intravenously or intratumorally into subcutaneous or intracranial GL261-HER2 tumors in syngeneic C57BL/6 mice. Serum and tissues were obtained 3, 7 and 10 days post-HER2-AAV injection, and aPD-1 concentrations, as well as the presence of nAbs, were evaluated by ELISA and neutralization assays, respectively. (B) aPD-1 concentration in tumor tissue and organs in the subcutaneous xenograft (top), the subcutaneous syngeneic (middle) and the orthotopic intracranial (bottom) mouse model after intratumoral (left) and intravenous (right) AAV administration determined by ELISA. Organ and tumor lysates of untreated mice served as negative controls. The dotted line represents the detection limit. Negative values were set to 0 for illustration. n=3.



### 3.5.2.1 Distribution of aPD-1 in immunodeficient mice

To be able to investigate aPD-1 kinetics in human glioma cells *in vivo* without potential immune responses against the vector, immunodeficient Crl:NU(NCr)-Foxn1<sup>nu</sup> nude mice were subcutaneously injected with LN-319 cells as a xenograft model. aPD-1 was expressed in all injected tumors, irrespective of the AAV administration route (Fig. 41B, top). Interestingly, aPD-1 concentrations increased in a time-dependent manner after HER2-AAV administration, reaching a maximum at day 10 after intratumoral injection (mean value of 7.2  $\mu\text{g}$  aPD-1 per 300  $\mu\text{g}$  protein). Besides in tumor tissue, aPD-1 was found in the heart, lung, kidney and spleen ranging from 0.05  $\mu\text{g}$  to 1.63  $\mu\text{g}$  aPD-1 per 300  $\mu\text{g}$  protein. The increase in aPD-1 levels over time was not as distinct in animals that received intravenous injections. However, the amount of aPD-1 that was produced within 7 days after intravenous HER2-AAV injection (2.15  $\mu\text{g}$  aPD-1 per 300  $\mu\text{g}$  protein) was significantly higher as compared to untreated mice (Fig. 41B, top right). aPD-1 levels in organs of intravenously treated mice were higher than in intratumorally treated mice, ranging 0.06  $\mu\text{g}$  to 3.07  $\mu\text{g}$  aPD-1 per 300  $\mu\text{g}$  protein in heart, lung, kidney and spleen.

### 3.5.2.2 Distribution of aPD-1 in immunocompetent mice

Similar to the results obtained in the xenograft mouse model, aPD-1 was also detected in all tumor samples post intravenous and intratumoral AAV administration in the immunocompetent subcutaneous GL261-HER2 syngeneic glioblastoma model. Overall, aPD-1 concentrations were only slightly lower than in tumors of immunodeficient mice (mean values of 6.4  $\mu\text{g}$  (immunocompetent mice) vs. 7.2  $\mu\text{g}$  (immunodeficient mice) per 300  $\mu\text{g}$  protein, respectively) (Fig. 41B, middle). In the cohort of intratumorally treated mice, maximum aPD-1 amounts were observed at day 3 post-transduction with a mean value of 3.7  $\mu\text{g}$  aPD-1 per 300  $\mu\text{g}$  protein. Still, this concentration was 2-fold lower than the mean maximum reached in tumors of immunodeficient Crl:NU(NCr)-Foxn1<sup>nu</sup> mice. aPD-1 was produced exclusively within the tumor, while cells of other organs remained mainly untransduced (Fig. 41B, middle left). In mice that had received intravenous HER2-AAV injections, a steady and significant increase in aPD-1 concentrations in tumor tissue over time was observed, ranging from mean values of 0.7  $\mu\text{g}$  on day 3 to 2.1  $\mu\text{g}$  on day 7, and 3.6  $\mu\text{g}$  aPD-1 per 300  $\mu\text{g}$  protein on day 10. In this case, aPD-1 was detected in the spleen, kidney, liver and lung; however, in these tissues aPD-1 concentrations only ranged from 0.05  $\mu\text{g}$  to

0.66  $\mu\text{g}$  per 300  $\mu\text{g}$  protein (Fig. 41B, middle right). In general, the amount of aPD-1 in peripheral organs was lower in this model as compared to the xenograft model (mean value of 0.35  $\mu\text{g}$  vs. 1.6  $\mu\text{g}$  per 300  $\mu\text{g}$  protein, respectively).

Also in orthotopic GL261-HER2 tumors of immunocompetent C57BL/6 mice that were intratumorally injected with HER2-AAV<sup>aPD-1</sup>, aPD-1 was detectable in all tumors, ranging from 1.7  $\mu\text{g}$  to 4.4  $\mu\text{g}$  aPD-1 of 300  $\mu\text{g}$  total protein (Fig. 41B, bottom left). The maximum concentration was observed 3 days post-HER2-AAV injection with a mean value of 3.9  $\mu\text{g}$  aPD-1 in 300  $\mu\text{g}$  total protein. Small amounts of aPD-1 were also found in the lung, kidney and spleen. The aPD-1 levels in tumors slightly decreased over time. Notably, in the orthotopic tumor model no aPD-1 was detected in brain tumors after intravenous HER2-AAV administration (Fig. 41B, bottom right).

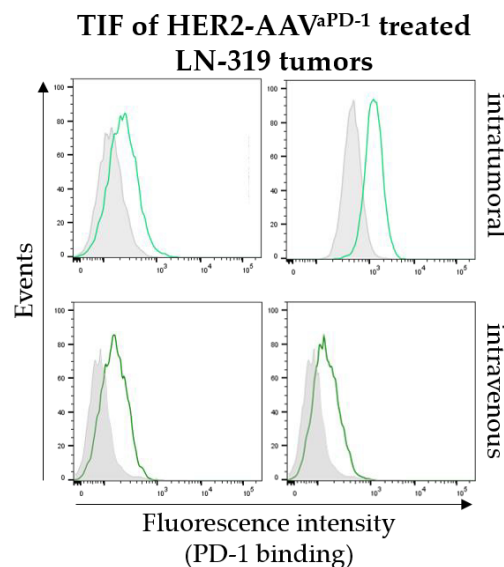


**Figure 42: Functionality of *in vivo* secreted aPD-1.** Target antigen binding of *in vivo* secreted aPD-1 in tumor interstitial fluid (TIF) of subcutaneous LN-319 tumors 7 days post intratumoral or intravenous HER2-AAV<sup>aPD-1</sup> injection.

Taken together, the transduction efficiency of HER2-AAVs *in vivo* was confirmed. Vectors mediated specific aPD-1 gene delivery to tumor lesions, resulting in high intratumoral drug concentrations and comparatively low aPD-1 levels in peripheral organs. Importantly, *in vivo* secreted aPD-1 was shown to be functional, as confirmed by the analysis of aPD-1-containing tumor interstitial fluid (TIF), which revealed aPD-1 binding to PD-1 *in vitro* (Fig. 42).

### 3.5.3 Cytokine responses after HER2-AAV transduction *in vivo*

To investigate a possible increase of inflammatory cytokines in response to HER2-AAV-mediated immune activation, cytokine profiles were determined after vector injection. Local expression of aPD-1 in the TME of brain tumors did not result in an excessive increase in serum concentrations of inflammatory cytokines. There was however a trend for increased levels of IFN- $\gamma$ , TNF- $\alpha$ , MCP-1 and IL-10 10 days after vector administration, and significantly increased levels of IL-23 (Fig. 43).

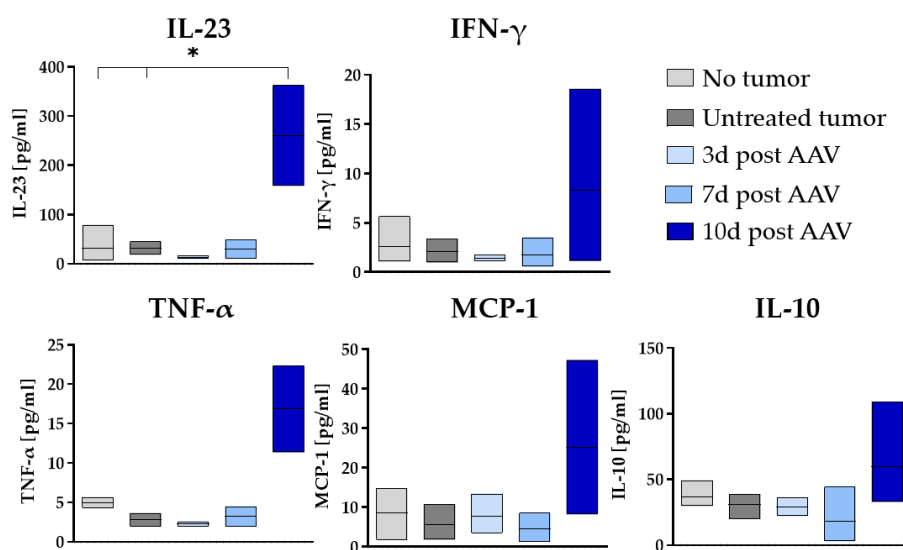


**Figure 43: Cytokine levels in the serum of HER2-AAV<sup>aPD-1</sup>-treated animals bearing an intracranial tumor.** Sera of mice bearing orthotopic intracranial tumors were collected at different time points (day 3, 7 and 10) after a single intratumoral HER2-AAV<sup>aPD-1</sup> injection. Cytokine levels were determined using a bead-based LEGENDplex assay. Sera from healthy and from tumor-bearing untreated mice were used as controls. Mean values are shown; n=3. \*p < 0.05.

### 3.5.4 Generation of neutralizing antibodies against HER2-AAV

Since AAV gene therapy is often compromised due to pre-existing or newly generated neutralizing antibodies (nAbs) against the vector, this issue was addressed using serum obtained in the HER2-AAV kinetics study. It was shown before that nAbs against AAV serotypes exist in laboratory animals including mice. Serum of HER2-AAV treated mice was collected and used for a neutralization employing HER2-Luciferase-AAVs (Fig. 44A).

Notably, the transduction activity of HER2-AAV was already inhibited by sera of untreated mice, suggesting the presence of pre-existing nAbs (Fig. 44B). Sera from injected animals reduced the gene transfer activity of HER2-AAV even more with the strongest inhibitory effect observed with sera obtained 7 and 10 days post intratumoral HER2-AAV injection.

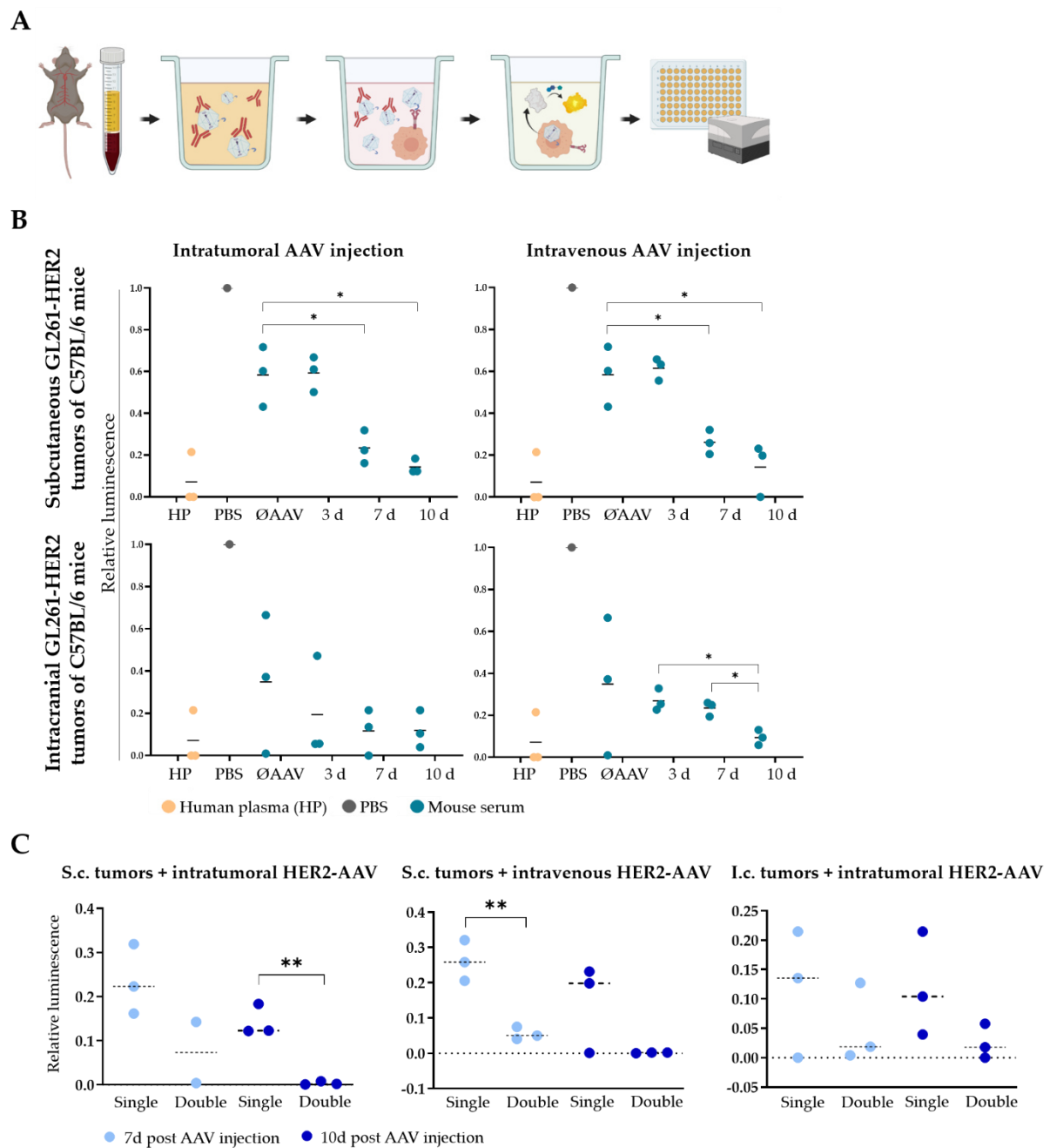


**Figure 44: Generation of neutralizing antibodies against HER2-AAV *in vivo*.** (A) Workflow of the HER2-AAV neutralization assay. HER2-Luciferase AAVs were incubated with mice sera before exposure to HER2<sup>+</sup> target cells. Luciferase expression of transduced cells was determined by the addition of the Bright Glo luciferase substrate and measuring the luminescence of the resulting product. Luminescence correlates with transduction efficiency, allowing the analysis of the presence of nAbs in serum samples. (B) The generation of nAbs in syngeneic subcutaneous (top) and orthotopic intracranial (bottom) mouse models was evaluated using a luminescence-based neutralization assay. Relative luminescence in comparison to transduction control in the absence of serum is indicated (PBS). Human plasma (HP) was used as a positive control. Sera of untreated mice (ØAAV) or mice sacrificed 3, 7 or 10 days post-HER2-AAV injection were analyzed (individual values are shown as dots, black bars represent mean values, n=3. \*p < 0.05, \*\*p < 0.01). (C) The generation of nAbs in the subcutaneous syngeneic (left, middle) and the orthotopic intracranial (right) mouse model following either single or double intratumoral (left, right) and intravenous (middle) HER2-AAV injection was evaluated using a luminescence-based neutralization assay. Sera of untreated mice (ØAAV) or mice sacrificed 7 or 10 days post-HER2-AAV injection were analyzed (individual values are shown as dots, black bars represent mean values, n=3. \*p < 0.05, \*\*p < 0.01).

Similar results were obtained after intravenous administration of the vector, indicating the generation of nAbs regardless of whether HER2-AAVs were injected locally or systemically. Also in the orthotopic intracranial model, the inhibitory activity of mouse sera on transduction increased over time, suggesting the formation of nAbs (Fig. 44B, bottom). The same time-dependent effect was observed after intravenous AAV administration. Of note, nAb levels were significantly increased in response to double HER2-AAV injections (on day 0 and day 3) in the sera of animals bearing subcutaneous GL261-HER2 tumors (Fig. 44C). In summary, these data indicate the presence of pre-existing neutralizing antibodies towards HER2-AAVs, and levels further increased over time after vector administration, irrespective of the administration route.

### **3.5.5 The effect of CAR-NK cell / HER2-AAV combination therapy on survival**

#### **3.5.5.1 Subcutaneous GL261-HER2 mouse model**

The combination of HER2-AAVs and the resulting local secretion of aPD-1-directed immunoadhesins with CAR-NK cells is intended to exploit complementary mechanisms of action and thus achieve synergistic effects. The CAR-NK cells are thought to induce an increased release of tumor-specific antigens via lysis of tumor cells and thereby promote a local anti-GB immune reaction. After modulation of the immunosuppressive TME by local production of aPD-1, the immune response triggered by CAR-NK cells could be potentiated. Based on the previously obtained data from the HER2-AAV kinetics study, a treatment scheme for survival experiments was established. The effect of HER2-AAV administration (local or systemic administration of vectors) was studied alone and in combination with CAR-NK cells in the subcutaneous as well as in the orthotopic intracranial GL261-HER2 mouse model. The impact on tumor growth and symptom-free survival of the animals was quantified.

In the subcutaneous GL261-HER2 mouse model, mice were injected with  $10^4$  GL261-HER2 cells in the area of the right flank. As therapy, intratumoral or intravenous injections of  $10^{11}$  gc HER2-AAVs and intratumoral injections of  $10^7$  CAR-NK cells were applied (Fig. 45A). Mice were treated with HER2-AAVs on day 0, 3 and 7 for tumor cells to produce aPD-1 before the start of CAR-NK cell therapy on day 7. As controls, mice received parental NK-92 cell, CAR-NK cell or HER2-AAV monotherapies. To determine whether HER2-AAV transduction alone

affected survival, mice were injected with the HER2-AAV<sup>IgG-Fc</sup> vector which does not encode aPD-1. Treatment was terminated after a maximum of 3 injections (1 per week) and tumor growth was monitored using caliper instruments. In a pilot survival study, local treatment with HER2-AAV<sup>aPD-1</sup> or HER2-AAV<sup>IgG-Fc</sup> + CAR-NK had no significant effect (median survival of 23 and 18 days, respectively), whereas administration of the combination therapy profoundly delayed tumor growth and significantly prolonged survival (median survival of 37 days, Fig. 45B and C).

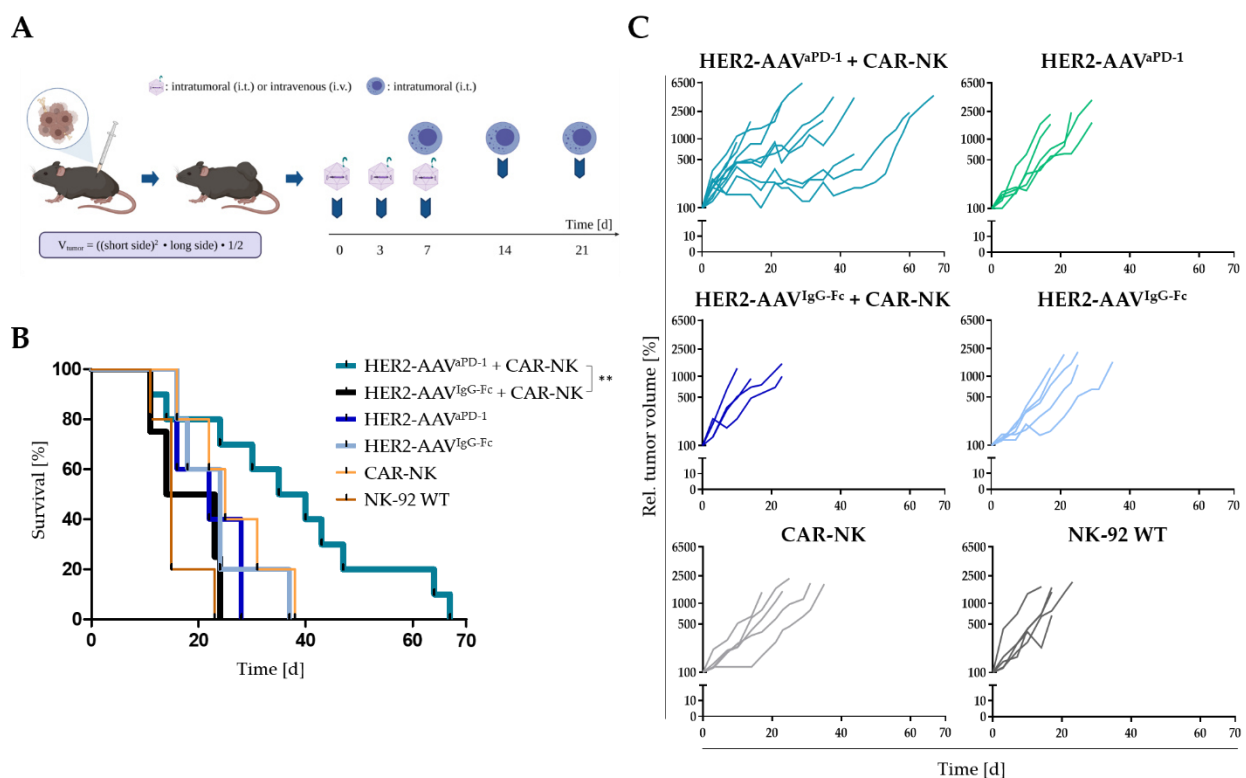


**Figure 45: Combination therapy conveys a survival benefit upon intratumoral HER2-AAV administration in the subcutaneous GL261-HER2 model. (A)** Therapy scheme for subcutaneous GL261-HER2 tumors.  $10^{11}$  gcs HER2-AAVs are either injected locally (intratumoral) or systemically (intravenous),  $10^7$  CAR-NK cells are injected locally (intratumoral). **(B)** Survival rates of different mouse cohorts after single or combined intratumoral treatment with HER2-AAV<sup>aPD-1</sup> or HER2-AAV<sup>IgG-Fc</sup> and CAR-NK cells or NK-92 WT cells, respectively. Treatment was initiated once tumors reached a size of  $80 \text{ mm}^3$ . ( $n=5-10$  per group,  $**p < 0.01$ ). **(C)** Tumor volumetrics of mice cohorts that are shown in (B).

However, tumors in these experiments were at a very advanced stage, since treatment was only initiated once tumors had reached a size of  $80 \text{ mm}^3$ . To investigate whether the synergistic effect of CAR-NK cells and HER2-AAV<sup>aPD-1</sup> would be clearer in earlier stages, tumors were injected at lower volumes ( $40 \text{ mm}^3$ ) in the next experiment. Since the administration of parental NK-92 cells only attained a median survival of 16 days in the previous study, this cohort was no longer included in the survival analysis. Animals that received the CAR-NK cell

monotherapy showed a median survival of 25 days, which is 11 days longer as compared to untreated animals. Similar survival rates were reached when mice were injected with HER2-AAV<sup>aPD-1</sup> alone, resulting in median survival of 28 days after intratumoral administration (Fig. 46A) and of 25 days after intravenous administration (Fig. 46B). In contrast, the HER2-AAV<sup>IgG-Fc</sup> monotherapy did not mediate prolonged survival, irrespective of the injection routes (median survival of 17 i.t. injection and 20 days i.v. injection). Animals receiving the combination therapy (HER2-AAV<sup>aPD-1</sup> + CAR-NK) exhibited slower tumor growth and significantly increased survival rates as compared to all other control cohorts (Fig. 46) with more than 50% complete tumor rejections. Both intratumoral and intravenous administration of HER2-AAVs was effective; however, more mice rejected the tumor after intratumoral injection (i.t.: 3/5, i.v.: 2/5). No weight loss or other signs indicating treatment-related toxicities in any of the treatment groups were observed during the study.

Taken together, these data confirm the anti-tumor effect of adoptive CAR-NK cell transfer combined with HER2-AAV<sup>aPD-1</sup> gene therapy in the subcutaneous GL261-HER mouse model.

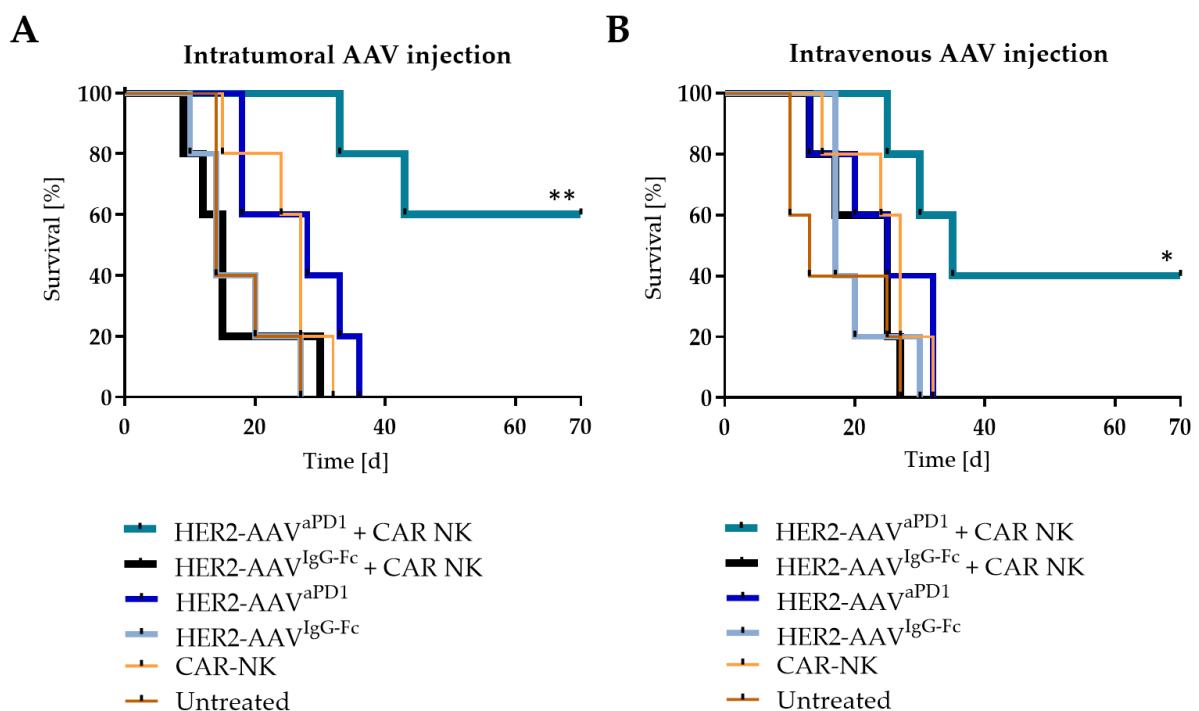


**Figure 46: Survival benefit in mice receiving intratumoral HER2-AAV in the subcutaneous GL261-HER2 model.** (A) Survival rates of different mouse cohorts after single or combined intratumoral treatment with HER2-AAV<sup>aPD-1</sup> or HER2-AAV<sup>IgG-Fc</sup> and CAR-NK cells, respectively. Treatment was initiated once tumors reached a size of 40 mm<sup>3</sup>. (n= 5 per group, \*\*p < 0.01). (B) Survival rates of different mouse cohorts after single or combined intravenous treatment with HER2-AAV<sup>aPD-1</sup> or HER2-AAV<sup>IgG-Fc</sup> and CAR-NK cells, respectively. Treatment was initiated once tumors reached a size of 40 mm<sup>3</sup>. (n= 5 per group, \*\*p < 0.01).

### 3.5.5.2 Orthotopic intracranial GL261-HER2 mouse model

Next, observations made in the subcutaneous mouse model were confirmed in the orthotopic intracranial model. On day 0,  $10^5$  GL261-HER2 cells were orthotopically implanted via stereotactic injection. Tumor cell engraftment was confirmed by small animal high field MRI measurements. From day 7,  $2 \times 10^6$  CAR-NK cells and  $3 \times 10^{10}$  gc HER2-AAVs were intracranially injected in 3  $\mu$ l medium once a week. Intratumoral AAV injection was chosen based on results obtained in the kinetics study, which revealed that no aPD-1 is delivered to the brain upon intravenous vector application (Fig. 41B, bottom right). The CAR-NK cells were also administered intratumorally because preclinical work in several mouse models has already shown that at least in these models the CAR-NK cells are not able to pass the BBB in sufficient numbers. Treatment was terminated after 3 injections, while tumor growth was monitored by continuous MRI measurements (Fig. 47A).



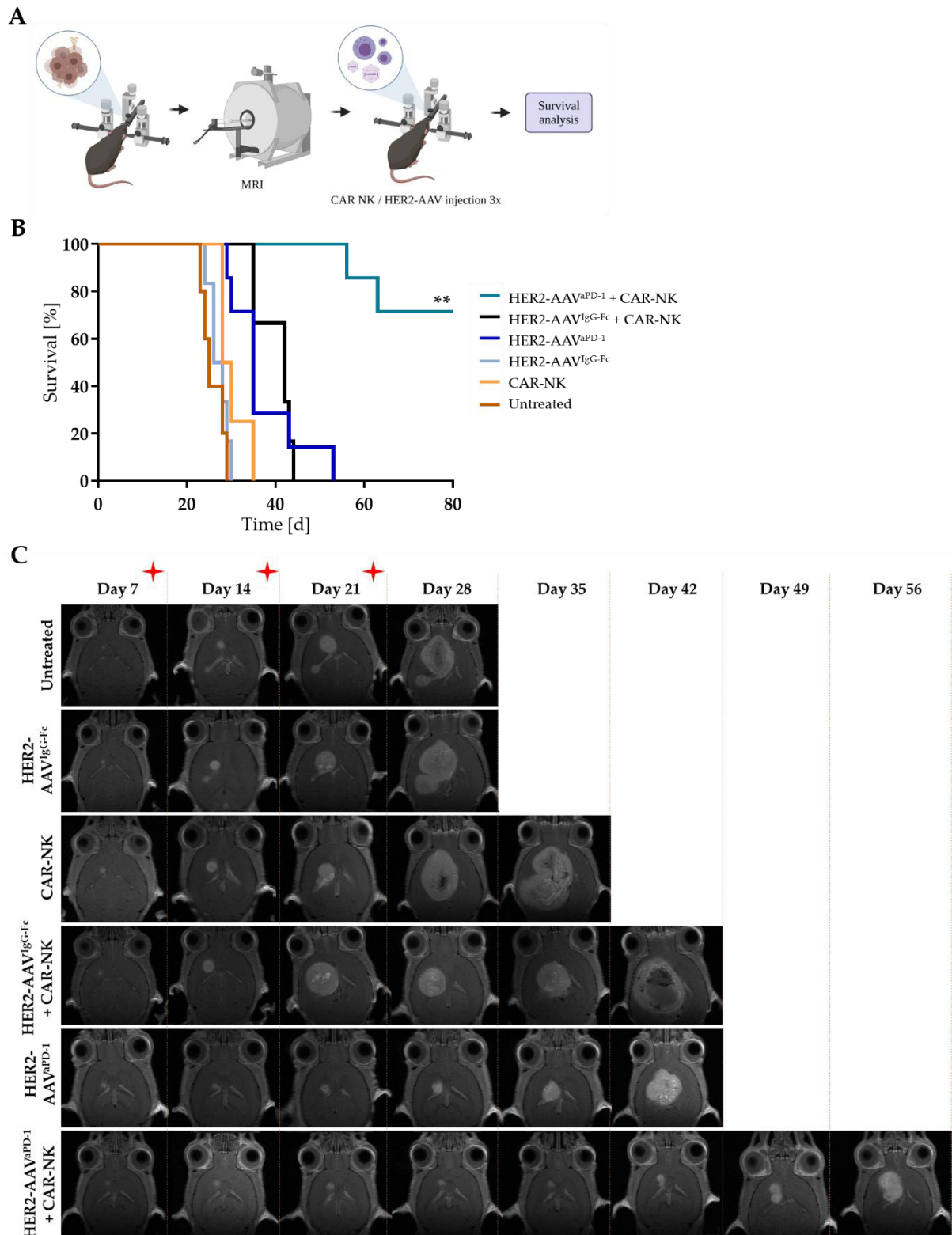


**Figure 47: Survival benefit in mice receiving HER2-AAV<sup>aPD-1</sup> + CAR-NK cells in the orthotopic intracranial GL261-HER2 model.** (A) Therapy scheme for orthotopic intracranial GL261-HER2 tumors. (B) Survival rates of different mouse cohorts after single or combined intratumoral treatment with  $3 \times 10^{10}$  HER2-AAV<sup>aPD-1</sup> or HER2-AAV<sup>IgG-Fc</sup> and  $2 \times 10^6$  CAR-NK cells, respectively ( $n = 4-7$  per group,  $**p < 0.01$ ). (C) Representative MR images of mice of different treatment cohorts in the orthotopic intracranial GL261-HER2 model. Mice were imaged weekly starting at day 7 post orthotopic intracranial GL261-HER2 injection. Red asterisks mark days of treatment application (untreated mice were sham-injected with medium).

Similar to data obtained in the subcutaneous mouse model, administration of the combination therapy of HER2-AAV<sup>aPD-1</sup> and CAR-NK cells also significantly prolonged survival in the orthotopic intracranial model as compared to all control cohorts (median survival of 74 days as compared to HER2-AAV<sup>IgG-Fc</sup>+ CAR-NK (40 days), HER2-AAV<sup>aPD-1</sup> (37 days) HER2-AAV<sup>IgG-Fc</sup> (27 days), CAR-NK (30 days) or untreated animals (25.8 days) at the time point of analysis at day 80 post initial tumor cell implantation) (Fig. 47B). All animals of the control cohorts succumbed to tumor burden within 53 days of the trial. Progression of tumor growth was considerably delayed in animals receiving the combination of HER2-AAV<sup>aPD-1</sup> and CAR-NK cells, but also in those receiving the HER2-AAV<sup>aPD-1</sup> monotherapy (Fig. 47C, Fig. 48 and Appendix Fig. 1-6). Interestingly, tumor growth in two mice of the HER2-AAV<sup>aPD-1</sup>/CAR-NK combination cohort rapidly progressed between day 7 and day 14 but was controlled during the rest of the treatment period. One mouse completely rejected the initially fast-growing tumor, while the other one showed stable disease without distinct signs of progression from day 21 onwards (Fig. 48F and Appendix Fig. 6). In general, the tumor was eventually rejected in 3/7 mice upon administration of the combination therapy. Similar to the subcutaneous model, no weight loss or other signs indicating treatment-related toxicities were observed in any of the treatment cohorts.

In summary, survival data obtained in the subcutaneous as well as in the orthotopic intracranial mouse model show a potent anti-tumor effect of the HER2-AAV<sup>aPD-1</sup>/CAR-NK combination therapy.

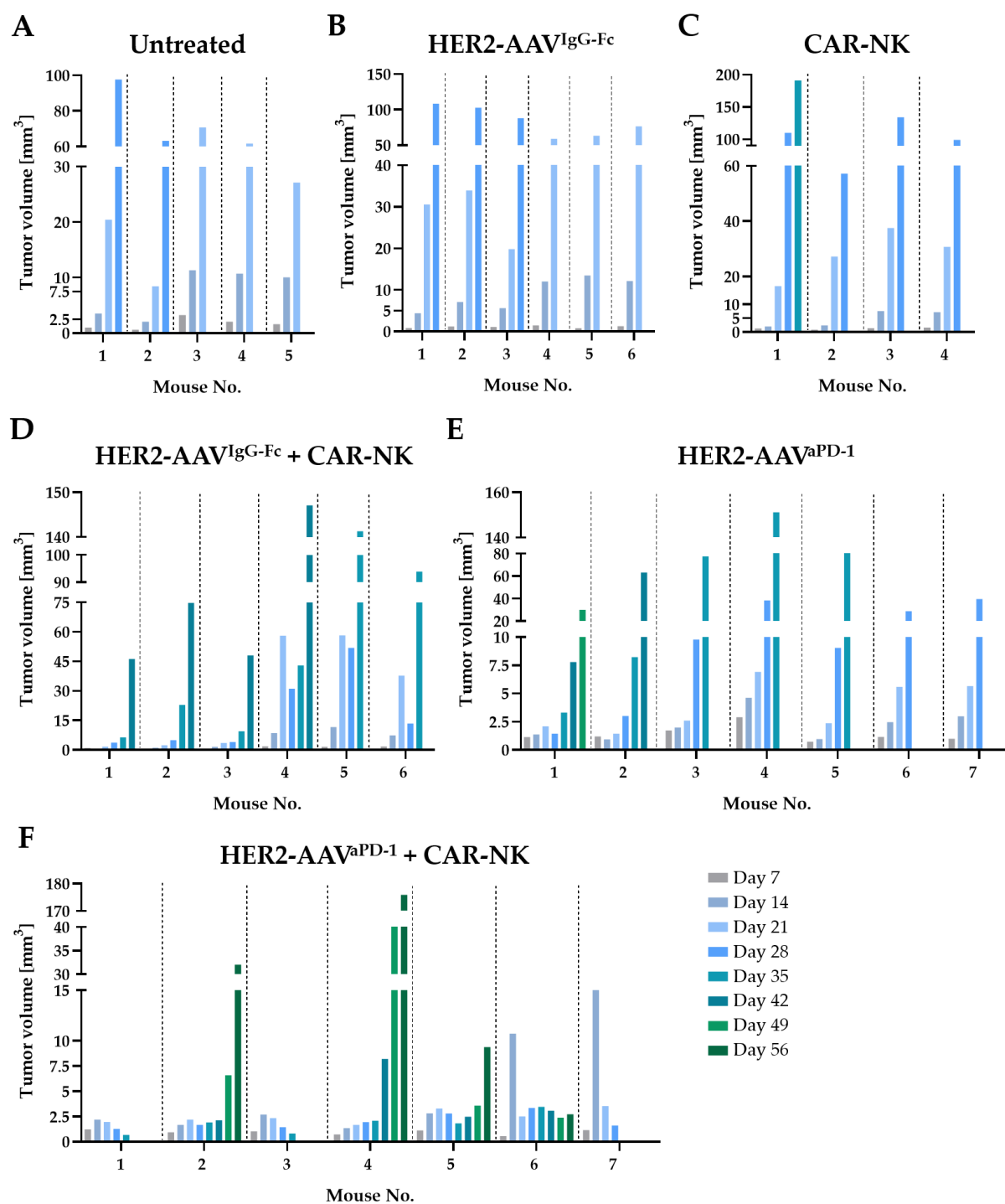


**Figure 48: Volumetries of orthotopic intracranial tumors of mice of different treatment cohorts.** Tumor volumes were determined using weekly MRI data of mice bearing orthotopic intracranial GL261-HER2 tumors (n= 4-7 per group).

## 4 Discussion

Immunotherapy is an emerging field in the clinical management of cancer, representing the shift from exclusive tumor-targeting towards the re-engagement of the patients' immune system to combat tumor growth. Since the expression of PD-L1 on GB cells has been described, immunotherapy with ICIs is a promising approach for tumor treatment. However, systemic administration of ICIs bears the risk of autoimmune-like side effects, while the intratumoral drug concentration reached may not be sufficient. Therefore, in this thesis, the delivery of an anti-PD-1 immunoadhesine through targeted AAVs as a novel approach towards local immunotherapy has been evaluated. There is mounting evidence pointing towards the effectiveness of combining multiple therapeutics rather than applying monotherapies [330], [331], wherefore the effects of checkpoint inhibition were investigated in combination with HER2-specific CAR-NK cell therapy. The prevailing immunosuppression within the TME of glioma might be disrupted via CAR-NK cell-mediated release of tumor antigens from lysed GB cells in combination with local intratumoral checkpoint inhibition through aPD-1-encoding HER2-AAV. In this project, those two components were analyzed concerning their applicability, their influence on target and bystander immune cells as well as their combined impact on anti-tumor effects *in vivo*.

### 4.1 CAR-NK cell therapy

CAR-T cell therapy has dominated the field of CAR research and development for several years now. During this time, substantial progress has been made in the treatment of recurrent refractory B cell malignant tumors by CAR-T cell therapy, resulting in the approval of two CD19-CAR-T products against acute lymphocytic leukemia (ALL) and large B cell lymphomas [332]. Nonetheless, this therapy is associated with several off-target and side effects such as cytokine release syndrome (CRS) and neurotoxicity (ICANS) or GvHD [333], [334]. In this context, CAR-NK cell therapy harbors the advantage of multiple cytotoxic mechanisms coupled with the possibility of "off-the-shelf"-manufacturing as well as a superior safety record due to the absence of CRS and GvHD [335], [336]. In the last few years, CAR-NK cell approaches have been investigated in other tumor entities as well. For instance, the clinical response of patients suffering from B cell malignancies that received CD19-specific CAR-NK cells exceeded 70 % and even led to complete remission in 7 out of 11 patients (NCT03056339,[337]).

The potent cytotoxic activity of CAR-NK cells towards HER2<sup>+</sup> glioma cells has been reported before and was confirmed in this project in several murine cell lines *in vitro* [29] (Fig. 13). However, in addition to signaling stimulated by the CAR, CAR-NK cells are able to exert their cytotoxic functions via various other mechanisms such as engagement of Fas Ligand (FasL) or TNF-related apoptosis-inducing ligand (TRAIL), and complex mechanisms of interaction of human NK cell receptors with human ligands serve to either inhibit or activate NK cell cytotoxicity [338], [339]. Therefore, to exclude xenogeneic reactivity and to model human disease more closely, CAR-NK cells were also cultured with human glioma target cell lines as well as with primary and patient-derived glioma cells in this study (Fig. 13 and 16). Besides HER2 as target antigen, CAR-NK cells that target EGFR or the constitutively active variant EGFRvIII also exert strong cytotoxicity against primary GB cells and cell lines *in vitro* [340], [341]. *In vivo*, the release of tumor neo-antigens following GB cell lysis by adoptively transferred CAR-NK cells might initiate anti-tumor immune responses upon the activation of host antigen-presenting cells (APCs) and T cells [342]. Indeed, in this study, the administration of a combination therapy of CAR-NK cells and aPD-1-encoding HER2-AAVs resulted in a significant therapeutic benefit in GL261-HER2 glioblastoma models in immunocompetent mice (Fig. 45-47). These results encourage the use of CAR-NK cells as a component of glioma immunotherapy. Also in other studies, the promotion of tumor cell death as a means to enhance immunogenicity has been proposed to have possible synergistic effects when combined with immunotherapy [163], [343]. In line with that, the NK cell-mediated recruitment of DCs to tumor lesions has been reported to enhance immunotherapy with PD-1 antibodies [344]. In turn, NK cell and CD8<sup>+</sup> T cell infiltration were increased upon anti-PD-1 therapy of GB and melanoma brain metastases, which resulted in prolonged survival of experimental animals [345], [346]. Another study employing the orthotopic intracranial GL261 glioma mouse model reported NK cell recruitment and extended survival in mice that received PD-1 antibodies conjugated with poly( $\beta$ -L-malic) acid [347]. A recent study by Lin et al. provided the first clinical evidence for the effectiveness of an NK cell/ICI combination therapy in non-small cell lung cancer (NSCLC). In this work, patients received the PD-1 antibody Pembrolizumab in combination with allogeneic NK cell therapy, which resulted in prolongation of median overall survival as compared to patients receiving the anti-PD-1 monotherapy (15.5 months vs. 13.3 months) [348].

In this project, CAR-NK cells were successfully injected intratumorally into orthotopic intracranial tumors, since previous studies have also shown that those cells are not able to cross the BBB upon intravenous administration (unpublished data). Although progressing tumor growth has been associated with destabilization and decreased integrity of the BBB via the degradation of tight junctions [349], migration of systemically administered cells into the brain parenchyma is still impaired on account of the BBB. Besides tumor burden, the administration of radiotherapy (RT) has also been reported to compromise the integrity of the BBB by increased fenestration of the endothelial barrier [64], [65], [350]. In this context, Weiss et al. were able to achieve therapeutic synergy in mice bearing orthotopic GL261-tumors after the administration of NKG2D-CAR-T cells in combination with RT. Still, they reported that intravenously injected mice were less likely to survive as compared to intratumorally injected mice, reinforcing the challenge of poor infiltration of immune cells into the brain parenchyma upon intravenous administration [351]. Although several groups reported the successful intravenous administration of autologous NK cells, patients that received NK cell therapy in those studies suffered from hematological malignancies rather than from solid tumors, for instance from acute myeloid leukemia (AML) or chronic myeloid leukemia (CML) [352], [353]. These findings support the administration route that was chosen for this study and indicate that local infusion might represent the superior injection strategy for CAR-NK cells in solid tumors [354], [355]. Furthermore, no treatment-related side effects or toxicities after local administration of HER2-specific CAR-NK cells were observed in this study. Lethal organ toxicity after infusing HER2-directed engineered cells has been a concern since a patient died of acute respiratory distress and pulmonary edema following the infusion of autologous HER2-specific CAR-T cells, possibly due to HER2 expression on healthy lung tissue [356]. However, modified vectors and protocols have shown that safe administration of HER2 CAR-T cell therapy employing the same FRP5-antibody fragment as used in this study is feasible [357]. Furthermore, HER2-specific CAR-NK cells are generally not subject to systemic administration, but rather to local infusion via intratumoral injection. In the currently active phase I clinical trial CAR2BRAIN at the University Hospital Frankfurt, the world's first CAR-NK cell study for patients with brain tumors, patients suffering from recurrent HER2<sup>+</sup> glioblastoma receive repetitive local injections of CAR-NK cells into the tumor and the resection cavity after relapse surgery (unpublished data). HER2 expression is reported to be absent in the brain under physiological conditions, and upregulation has so far only been

observed in proliferative astrocytes, as found in astrogliotic lesions [358]–[360]. In this regard, the lack of neurotoxicity observed in the dose-escalation cohort of the CAR2BRAIN-trial is further encouraging. The study has successfully completed the dose escalation without encountering dose-limiting toxicity or safety concerns. A low proportion of the CAR-NK cells injected into the brain tumor has been found to reach the systemic circulation. However, the amount of CAR-NK cells in the blood has been reported to be relatively low, and the CAR-NK cells disappeared from the blood after only several days. Study patients were closely monitored for cardiac toxicity, but no such complication was observed (unpublished data).

#### 4.2 Cytokine release upon CAR-NK cell therapy

Secretion of cytokines by CAR-NK cells has been reported to differ from the cytokine-release-syndrome (CRS)-evoking cytokines generated by CAR-T cells, such as TNF- $\alpha$ , IL-1 and IL-6 [361], [362]. In *in vitro* studies of this project, CAR-NK cells secreted increased levels of IFN- $\gamma$ , IL-1 $\alpha$ , TNF- $\alpha$ , IL-8, MCP-1 and IL-10 and perforin upon activation by target cell killing (Fig. 20), while other groups detected the secretion of IFN- $\gamma$ , GrB, sFasL, IL-8 and IL-10 [219]. Although HER2-specific CAR-NK cells secreted cytokines that are associated with CRS, no relevant toxicities were observed in experimental animals used in this thesis and previous projects [29], [222]. Moreover, with so far 15 patients treated in the CAR2BRAIN-trial, no cases of CRS or immune-effector-cell-associated-neurotoxicity-syndrome (ICANS) were observed. This is in line with a recent publication which reports a lower risk for CRS and ICANS with CAR-NK cells as compared to CAR-T cells [337]. Also other phase I/II trials did not report severe adverse events after NK cell administration [352], [353], [363].

Within the brain, CAR-NK cell-mediated tumor cell lysis most likely affects other cell types typically present within a TME, such as tumor cells themselves as well as immune cells. The surrounding TME was shown to react to nearby tumor cell lysis by CAR-NK cells via the secretion of inflammatory cytokines (Fig. 18). Especially MG secreted elevated levels of IL-6 and IL-8 in response to tumor cell lysis. IL-8 functions as a chemokine and attracts neutrophils to sites of inflammation [364]. Another important immune modulator that was found to be released in response to CAR-NK cell-mediated tumor cell killing was IL-6. It is known to be secreted by macrophages and is of importance in tumor control, as it can antagonize the effect of Tregs [365], [366]. However, it is important to consider the context-dependent activity of cytokines in cancer research and therapy. In this regard, intratumoral as well as serum levels

of cytokines in response to CAR-NK cell therapy should be closely monitored in order to be able to intervene appropriately if necessary. For instance, IL-6 has also been reported to play a role in the invasiveness of glioma [367], while elevated IL-8 serum levels have been reported to be associated with worse responses to ICIs [368].

CAR-NK cells themselves also contribute to cytokine secretion to the TME, even when not being in direct contact with target cells, as they are also affected by the release of soluble factors of other CAR-NK cells nearby which are engaged in tumor cell lysis. Levels of IFN- $\gamma$ , TNF- $\alpha$ , IL-8 and MCP-1 were found to be significantly increased (Fig. 18). Although MCP-1 has been reported to aid lymphocyte recruitment in B16F10 melanoma [369], studies in GL261 glioma mouse models revealed that MCP-1 expression was associated with increased infiltration of Tregs and myeloid-derived suppressor cells (MDSCs) [370]. TNF- $\alpha$  boosts the inflammatory response via the activation of macrophages including their subsequent release of further pro-inflammatory cytokines and mainly conveys anti-tumor effects within the TME. For instance, when immunotherapies were combined with TNF- $\alpha$  antagonists, therapy efficiency was severely diminished in murine colon carcinoma and melanoma models [371], [372]. On the other hand, chronic TNF- $\alpha$  signaling has been shown to cause activation-induced cell death of effector T cells, ultimately fueling tumor growth [373]. In addition, aPD-1-induced upregulation of TIM-3 was shown to be TNF- $\alpha$  dependent. TIM-3 as a secondary checkpoint molecule in CD8<sup>+</sup> T cells strongly triggers TIL exhaustion, suggesting the combination of aPD-1 and anti-TNF- $\alpha$  therapies [374]–[376]. IFN- $\gamma$  along with perforin and granzyme B exerts cytotoxic effects as it promotes apoptosis in tumor cells. Still, it has also been shown to trigger pro-tumorigenic effects [377]–[379]. However, studies have shown that the modulation of the TME by NK cell-mediated IFN- $\gamma$  secretion is of immense importance in GB targeting [198], [380].

### 4.3 Regulation of surface molecules in response to CAR-NK cell therapy

Glioma cells frequently misuse the PD-1/PD-L1 checkpoint to evade anti-tumor immune responses, which represents a major determinant of the immunosuppressive TME [381], [382]. Not only GB cells themselves but also lymphocytes such as Tregs as well as MG contribute to the dominant immunosuppression via the expression of PD-L1 [383]–[385], which in some cases has been shown to result from cytokine signaling of GB cells and subsequent modulation of protein expression on tumor-infiltrating MG [155]. Moreover, in breast cancer cells, PD-L1



expression is induced as a result of therapeutic interventions such as chemotherapy [386], [387]. Also, data obtained in this study revealed the impact of CAR-NK cell therapy on PD-L1 expression of surrounding cells. PD-L1 was found to be upregulated in several cell types including tumor cells and immune cells such as NK cells, MG and astrocytes (Fig. 19). Since those cell types contribute to the tumor infiltrate to a great extent, PD-L1 expression may contribute to sustained immunosuppression within the TME and subsequent inhibition of anti-tumor responses [244]. PD-L1 upregulation on surrounding cells in response to CAR-NK cell activation was mainly caused by secreted IFN- $\gamma$  (Fig. 21). NK cells, in general, have been reported to produce Th1-type cytokines including IL-1 $\beta$ , IL-2, IL-10, IL-12, TNF- $\alpha$ , and IFN- $\gamma$  upon tumor cell-related activation [192], [193], which in turn facilitates the activation of effector lymphocytes and myeloid cells [187], [195], [388]. As mentioned above, cytokine measurements upon activation of CAR-NK cells in this study indeed revealed significantly increased levels of TNF- $\alpha$  (twofold), IFN- $\gamma$  (twofold), IL-10 (twofold) (Fig. 20), which has been reported before [219]. Moreover, levels of and IL-8 (fourfold), MCP-1 (twofold), perforin (threefold) and IL-1 $\alpha$  (twofold) were found to be significantly increased. The finding of IFN- $\gamma$ -dependent upregulation of PD-L1 is consistent with the literature since, besides phosphatase and tensin homolog (PTEN) loss in GB cells, IFN- $\gamma$  was reported to be the major driver of PD-L1 expression in cells of the TME [381], [389], [390]. Furthermore, another group reported IFN- $\gamma$  induced PD-L1 expression on GL261 glioma cells, macrophages and MG *in vitro* [391]. Although unstimulated MG and astrocytes express PD-L1 on a basal level, it has been shown that inflammation leads to PD-L1 upregulation on MG *in vivo*. In a murine study of neuroinflammation, ~20% of MG from naive mice were PD-L1<sup>+</sup>, while brain infection led to an increase to over 90% [392]. In our GL261-HER2 mouse model, we also found increased PD-L1 expression on murine tumor cells 8 weeks post tumor cell inoculation (Fig. 40). This effect is likely to be intensified upon CAR-NK cell therapy, thereby promoting the suppression of potent immune reactions and hampering the effectiveness of the therapeutic intervention. Furthermore, PD-L1 has recently been associated with the induction of Tregs, since PD-L1 expression has been shown to promote the expression of FOXP3 in those cells [393]. Based on these data, the need for a combination with anti-PD-1 ICIs becomes even more eminent. Indeed, NK cell responses have been shown to be diminished when tumor cells express high levels of PD-L1, which was invertible when PD-L1 or PD-1 checkpoint inhibitors were administered [213]. Nonetheless, the combination therapy of CAR-NK cells and HER2-AAV-

mediated checkpoint inhibition was proven to be effective (Fig. 45-47), suggesting that PD-L1 upregulation on surrounding cells had no inhibiting implications for both approaches. In line with that, a synergistic effect between NK cell-mediated tumor cell lysis and checkpoint inhibition (anti-PD-L1 treatment) was recently reported by Poznanski et al. In their study, NK cells derived from lung cancer patients were expanded *ex vivo* and subsequently exhibited potent tumor cell lysis in functional cytotoxicity assays. NK cells maintained strong IFN- $\gamma$  production, which induced PD-L1 expression in tumor cells as seen in this present study as well (Fig. 21) and reinforced anti-PD-L1 response [394]. Similar results were obtained by Julia et al., where Avelumab (anti-PD-L1-antibody) treatment augmented NK cell-mediated lysis of triple-negative breast cancer cells. PD-L1 levels were positively correlated with the susceptibility towards Avelumab-mediated ADCC [395].

Not only PD-L1 upregulation is an issue when assessing targeted CAR-NK cells therapies, but also target antigen downregulation. Since this is a common mechanism that tumor cells employ to evade CAR-specific targeting, the second part of the proposed combination therapy, namely the viral transduction and intratumoral aPD-1 expression, would be affected as well. In this study, however, evaluation of HER2 expression stability in response to CAR-NK cell attack as well as in response to HER2-AAV transduction *in vitro* did not reveal downregulation of the antigen on a short-term basis (Fig. 17 and 36). In previous work from our group, HER2 expression in response to CAR-NK cell therapy was evaluated in several glioblastoma mouse models on a long-term basis as well, and no downregulation of HER2 after repetitive intratumoral CAR-NK cell injections was observed [29]. The same study also confirmed that HER2 expression is relatively stable in patients suffering from a glioblastoma relapse as compared to the initial tumor. In this context, antigen loss which has been reported i.e. for EGFRvIII was not observed for HER2. In this context, it is also important to consider that mechanisms of CAR-NK cell-mediated tumor cell lysis can be both CAR-dependent and NK receptor-dependent, which implies that also cells lacking the target antigen might become subject to attack. Therefore, not only antigen specificity accounts for CAR-NK cell activity, but also the interplay of stimulatory and inhibitory signals recognized via NK cell receptors themselves [396], [397].

#### 4.4 Possible mechanisms to augment CAR-NK cell function in the TME

Similar to the cytotoxicity data obtained in the present study, Yilmaz et al., also observed considerable killing efficiencies *in vitro* [355]. However, cytotoxic activity was diminished upon *in vivo* injection due to the secretion of immunosuppressive cues such as TGF- $\beta$  or IL-10 by cells like macrophages or Tregs [355]. As a pro-tumor cytokine, TGF- $\beta$  has been shown to downregulate both the activating NK cell receptors and their ligands on tumor cells in the brain [398]–[402]. Therefore, the application of TGF- $\beta$  kinase inhibitors might prevent the decrease in NK cell cytotoxic capacity and engage the activation of NK receptors NKG2D and CD16 [403]. In fact, in glioma or medulloblastoma patients the neutralization of TGF- $\beta$  in the TME restored the anti-tumor function of NK cells [404]–[406]. Besides the suppression of NK cell activation, brain tumor cells employ mechanisms such as HLA-E or Lectin-like transcript-1 (LLT1) expression to foster NK cell inhibition [406]–[410]. Two studies reported the stimulation of NK cell activity against GB cells via siRNA-mediated HLA-E or LLT1 blockade [406], [411], [412].

As mentioned above, CAR-NK cells produced and secreted IFN- $\gamma$  upon target cell recognition (Fig. 20), which has been shown to promote the differentiation of GB stem cells [413]. However, another effect of IFN- $\gamma$ -induced stem cell differentiation was increased sensitivity to chemotherapy, implying that synergy of combined therapies could further be promoted via the application of multiple therapeutic strategies [414], [415]. In this regard, the immunosuppressive TME is generally characterized by the interaction of multiple immunosuppressive mechanisms and may potentially be disrupted by combination therapy with a cocktail of optimized HER2-AAVs encoding two or more immunoadhesins with different targets. While systemic administration of combination ICI therapy has been shown to increase immune-related adverse effects and is therefore limited, local combination therapy enabled by the combinatorial intratumoral application of HER2-AAVs may become feasible. For instance, in murine glioma models, the inhibition of immunosuppressive lymphocytes such as Tregs, which are abundant in glioma patients' blood samples [132], via the administration of neutralizing antibodies against CD25 increased the anti-tumor response of cytotoxic T cells and even led to 100% glioma cell rejection in combination with DC vaccination [58], [416]. Additionally, direct activation of T cells utilizing an agonistic OX40 antibody, which enhances the function of activated T cells, has been shown to improve the efficacy of vaccines

in preclinical glioma models [417], and might therefore serve as an additional "payload" for the HER2-AAV system to create synergy with CAR-NK cell and aPD-1 therapy.

Apart from that, CTLA-4 represents another promising target for ICI therapy, as administration of the CTLA-4 antibodies, Ipilimumab or Tremelimumab, has been shown to result in prolonged survival in melanoma patients [418], [419]. Furthermore, there is evidence that Ipilimumab treatment profoundly boosted cytotoxic activity and the subsequent secretion of IL-2 and IFN- $\gamma$  in NK cells [420]. NK cell-mediated tumor cell lysis has also been shown to be enhanced by blockade of T cell immunoreceptor with Ig and ITIM domains (TIGIT) in an *in vivo* lung adenocarcinoma model [421], [422]. In line with that, a study by Woroniecka et al. on T cell exhaustion signatures reported that the most dysfunctional T cells in GB patients expressed multiple immune checkpoints [232]. Accordingly, the combination of CAR-NK cell therapy with inhibitors of various checkpoint proteins at once, facilitated via the administration of AAVs encoding inhibitors of CTLA-4 and TIGIT or OX40 agonists might augment preferable outcomes in cancer therapy [423]. In addition, the in-depth immunomonitoring program of the CAR2BRAIN study can be employed to reverse-translate therapy-induced alteration in tumor tissue obtained from patients of the CAR2BRAIN-CHECK cohort (CAR-NK cells + anti-PD-1) after CAR-NK cell monotherapy or combination therapy with CAR-NK cells and anti-PD-1 checkpoint inhibition to identify additional promising targets. In this context, CAR-based cell therapy in combination with AAV-mediated multimodal targeted treatment might enable more personalized therapeutic options for the clinical management of GB in the future.

#### **4.5 Tolerance of microglia and astrocytes towards CAR-NK cell lysis**

Gliomas are known to be frequently infiltrated by immune cells such as MG and astrocytes [93], [113], [424]. As bystander immune cells, both cell types appeared to be affected by nearby CAR-NK cell-mediated tumor cell lysis in terms of cytokine production (Fig. 18). However, they were not affected by CAR-NK cell attack themselves (Fig. 25), not even when expressing high amounts of the HER2 target antigen (Fig. 24), suggesting that they tolerate cytotoxic cues to a greater extent than other cell types such as tumor cells. Successful degranulation of CAR-NK cells upon contact with MG and astrocytes proved that CAR-NK cell activity was not actively inhibited by the target cells (Fig. 26). Furthermore, not all unaffected target cell types expressed the non-classical MHC-I molecule HLA-E (Fig. 26), which is known to engage with

the inhibitory NK cell receptor NKG2A [329], [425], indicating that those cells employ a different strategy to countenance the attack. As regulators of immune responses in the central nervous system, those cells might require the ability to remain resistant to cytotoxic attack facilitated by perforin-mediated cell lysis or the induction of apoptosis by other immune effector cells such as CD8<sup>+</sup> T cells or NK cells during an ongoing immune response. There is evidence that immune cells are able to engage mechanisms that shield themselves from granule-mediated cell death. As stated in a review by Osińska et al., CD8<sup>+</sup> T cells and NK cells have been reported to inhibit perforin-mediated pore formation in their cell membrane via the impediment of perforin binding [426]–[428]. Another mechanism of resistance to perforin has been linked to cathepsin B, which has been associated with the proteolytic inactivation of perforin by tumor cells [429], [430]. Tumor cell resistance to NK cell-mediated lysis was also reported by Lehmann et al., who found that similar to the findings of this present study, NK cells become activated but target cells remained unaffected. In their study, Lehmann et al. also found the insufficient binding capacity of perforin to the target cell membrane to be the reason for resistance to NK cell attack [431]. But not only the effects of perforin can be undermined, also the activity of the apoptosis-initiator GrB has been shown to be inhibited in several cell types. This is facilitated by the serpin proteinase inhibitor-9 (PI-9) [432], [433], which does not only protect CD8<sup>+</sup> T cells or NK cells from misdirected cell lysis but also bystander cells such as B cells, monocytes and DCs [433]–[438]. The determination of PI-9 expression levels in MG and astrocytes might help identify the reason for their tolerance towards CAR-NK cell-mediated cytotoxicity. In this context, PI-9 upregulation in response to exposure to inflammatory cytokines such as TNF- $\alpha$  and IFN- $\gamma$  has been described [439], [440], which were also shown to be secreted by activated CAR-NK cells in this study (Fig. 20).

Apart from that, MG, in general, are of enormous interest in brain tumor research, since they are able to display ambivalent characteristics due to their vast heterogeneity and plasticity. Tumor cells frequently render them incapable of T cell activation, while their innate functions are exploited with respect to the secretion of MG-derived growth factors or pro-tumorigenic cytokines, which eventually leads to recruitment and stimulation of Tregs and the promotion of immune evasion and subsequent tumor cell survival [99], [118], [119], [441]. However, data obtained in the present study suggest that CAR-NK cell-mediated tumor cell lysis might have an activating effect on MG, since the secretion of inflammatory cytokines, the expression of

activation markers as well as phagocytic activity was shown to be increased upon adjacent tumor cell death (Fig. 18, 22 and 27). But in the glioma TME, direct contact between tumor cells and MG has been shown to result in their re-programming to an M2-like pro-tumor phenotype [442]. In this context, one study revealed MG activation and increased phagocytic activity similar to the results obtained in the present study, but only in the first 3 h of co-cultivation with GB cells. After 6 h, this effect was no longer evident [443], underlining the dominant crosstalk between tumor cells and MG towards prominent immunosuppression. But not only MG are commissioned as tumor promoters, also astrocytes are rendered reactive and pro-tumorigenic [444]–[446], wherefore targeting of the MG/astrocyte–GB cell crosstalk harbors the auspicious potential for the development of anti-glioma therapies [447], [448]. For instance, GB cells exploit the SIRP $\alpha$ -CD47 axis by expression of the anti-phagocytic protein CD47 on their surface, which inhibits cytotoxic effector function and enables immune evasion [449]–[451]. Gholamin et al. showed that blockade of the SIRP $\alpha$ -CD47 axis via a CD47 antibody abolished pro-tumorigenic effects in MG and prolonged animal survival in patient-derived xenograft models of pediatric brain tumors [450]. In line with that, anti-tumor effects of MG were also restored upon intracranial injection of IL-12-encoding AAVs, resulting in delayed tumor progression and increased survival [451], [452]. Of note, IL-12 has also been shown to enhance the cytotoxicity of NK cells towards solid tumors [453]. Taken together, with respect to its immense versatility, the AAV system proposed in the present study might also be employed for the targeting and re-programming of formerly pro-tumorigenic immune cells such as MG and astrocytes or the augmentation of cytotoxic effector cells.

#### **4.6 Refinement of targeted CAR-NK cell therapies for the treatment of glioblastoma**

Although CAR-NK cells used in this study exhibited superior killing efficiencies as compared to parental NK cells and were able to mediate prolonged survival and tumor clearance upon the combination with HER2-AAV-encoded aPD-1 (Fig 13 and 45-47), this sort of adoptive cell therapy can still be adjusted to increase efficiency even further. This comprises the selection and modification of the CAR construct or the choice of effector cell in general. For instance, the use of primary NK cells would make sublethal irradiation of NK cells superfluous and enable expansion *in vivo*. For safety reasons, the currently used NK-92 cell line has to be irradiated before administration to the patient due to its origin from a lymphoma patient. Recently, research focused on the employment of primary NK cells for therapeutic

intervention; however, there are still various obstacles to overcome. For instance, efficient expansion under good manufacturing practice (GMP) conditions, as well as reliable viral transduction, needs to be improved substantially [454].

Furthermore, another mechanism to enhance CAR-NK cell activity engages the silencing of NK inhibitory receptors. Modified CAR constructs have been shown to promote CAR-T cell proliferation, while the cells were also less susceptible to the inhibitory effects of IL-4 in the TME, wherefore the modification of CAR-NK cell constructs might represent a valuable strategy as well [397], [455]. Besides the modification of the CAR construct, dual targeting approaches are also currently under evaluation for creating synergy with CAR-NK cell therapies. For instance, the bi-specific antibody NKAB-ErbB2 synergized with CAR-NK cells due to the crosslinking lymphocytes and tumor cells, resulting in improved cytotoxicity and enhanced anti-tumor activity towards HER2<sup>+</sup> target cells and tumor clearance in the majority of animals [456].

#### **4.7 Intratumoral delivery of immune checkpoint inhibitors**

Immunotherapy via intravenous administration of ICIs has revolutionized the treatment of various malignancies [226]. In GB, both tumor cells and monocytes/macrophages express PD-L1, which hinders CD8<sup>+</sup> and CD4<sup>+</sup> T cell activation [155], [244]. Therefore, immunotherapy with ICIs directed against the PD-1/PD-L1 axis is a promising approach for GB treatment. In a study involving 35 patients, Pembrolizumab (anti-PD-1) increased survival in the neoadjuvant setting [457], however, several randomized trials in recurrent or adjuvant settings exploring ICI monotherapy failed to meet their primary endpoint [56]. Besides disadvantages such as the limited response in cancer patients (between 15 % up to 40 %), prevalent grade 3 - 4 immune-related adverse events (5 % up to 16 % of cases) and tremendous costs due to the high amount of inhibitors that are needed for treatment, only 5 -10 % of the administered amount of monoclonal ICI antibodies reach the target tissue upon systemic application [458]–[461]. However, the amount of ICI that has to reach the tumor to fully exert its function in conveying potent PD-1/PD-L1 blockade still has to be determined. Although response rates of patients to ICI treatment have been shown to be improved after combined administration of e.g. aPD-1 and aCTLA-4, the combination of multiple ICIs also potentiates the risk of severe toxicities. For instance, in the Checkmate-067 study, patients suffering from advanced melanoma received either Nivolumab, Ipilimumab or a combination of both. The occurrence of serious

immune-related adverse events (irAEs) resulted in the discontinuation of 42% of patients that received the combination therapy as compared to 13% and 15% that received Nivolumab or Ipilimumab monotherapies, respectively [462]–[464]. Consequently, also the combination of inhibitors of immune checkpoints such as TIM-3 or LAG-3 with other ICIs might result in more frequent and more severe adverse events [465], [466].

In line with that, cargo gene expression limited to the tumor area will result in high intratumoral and low systemic drug concentrations, enhancing the efficacy and simultaneously limiting toxicities in the form of irAEs [467]. In the past few years, several groups investigated the local delivery of ICIs via strategies such as antibody-loaded montanide emulsions, polymeric microparticles or cell lines that are genetically engineered to continuously express and secrete the desired ICI [468]–[470]. In this context, by local or systemic injection of AAVs, local expression and secretion of ICIs after the transduction of tumor cells becomes feasible.

#### **4.8 Local expression of aPD-1 via HER2-AAV-mediated transgene delivery**

Currently, AAVs are the most effective tool for *in vivo* gene delivery and subsequent expression in target cells [471]. To avoid gene transfer into non-relevant cells, receptor-targeted AAVs that allow for selective genetic modification of target cells have been established [251], [297]. The use of HER2-targeted AAVs as vectors enables the specific gene transfer of a-PD1 in HER2<sup>+</sup> glioma cells. Since maximum packaging capacity is not recommended to exceed 3.3 kb [472], incorporation of the genetic information of a full-length IgG is not achievable. In this context, Johnson et al. generated simian immunodeficiency virus (SIV)-specific immunoadhesins, which are smaller, antibody-like molecules comprising of the Fc region of an IgG and the ligand-binding portion of a receptor molecule [473] and enabled long-lasting expression within experimental animals upon delivery via AAV vectors [474]. Similar to this strategy, the HER2-AAVs used in the present study harbor a coding sequence for an aPD-1 fusion protein that is ~2.6 kb in size [310], [311]. The selective transfer of ICIs by engineered HER2-AAV vectors has been shown before in human breast and ovarian cancer cell lines as well as in a murine renal carcinoma cell line [251], [310].

*In vitro* data obtained in this study demonstrated the potent transduction efficacy in GB cells of both murine and human origin as confirmed on the transcriptional as well as on the



translational level (Fig. 28-30). Also, the transduction of human primary glioma cells with the vector was achieved (Fig. 29). Constant aPD-1 protein levels could be found within transduced cells 10 days after initial transduction, indicating stable gene expression upon vector entrance without signs of degradation (Fig. 30), which is a general advantage as opposed to the short half-life of systemically administered antibodies in mice [475]. After target cell transduction by AAVs, the viral genome persists in the host cell as an episome and transgene expression is maintained for the lifetime of the cell [476], [477]. Of note, gene expression has been reported to be maintained for years in post-mitotic cells such as muscle cells after a single AAV injection [478]. Knowledge about sustained transgene expression is particularly relevant when designing treatment schemes using HER2-AAVs as therapeutic gene transfer vectors. Continuous transgene expression especially in the brain has been described due to the slow turnover rate of brain-resident cell types [479] but has also been reported upon transduction of post-mitotic tissue such as liver and muscle [480], [481].

The release of HER2-AAV-encoded aPD-1 has also been confirmed after transduction of various murine and human cell lines (Fig. 29B). In general, transduction efficacy was highly HER2-dependent and the amount of secreted aPD-1 was increased in LN-319 glioma cells which overexpressed HER2 (Fig. 29B and C). These data underscore the compelling specificity of this targeted approach. Moreover, the ability of HER2-AAV-encoded aPD-1 to bind to its natural target receptor PD-1 was confirmed *in vitro* as well as *in vivo*, indicating correct folding and dimerization of the immunoadhesin following its secretion by glioma cells (Fig. 33B). However, the binding assay using HT1080 cells that have been genetically modified to express murine aPD-1 represents a rather engineered system, therefore data based on a biological *ex vivo* system where freshly isolated murine splenocytes were used for target binding assays have also been generated (Fig. 33E). Furthermore, the disruption of the PD-1/PD-L1 axis was shown via the re-activation of T cell activity, suggesting that secreted aPD-1 is also able to restore T cell immunity *in vivo* (Fig. 34). Finally, aPD-1 functionality was confirmed with interstitial fluid generated *in vivo* from HER2-AAV<sup>aPD-1</sup>-treated s.c. tumors (Fig. 42).

For glioma cells to produce and secrete aPD-1, cell viability must not be impaired. On the contrary, the death of some tumor cells might evoke desired anti-tumor immune responses. Although slightly decreased cell viability was observed 24 h after transduction, ~90% of transduced cells remained unaffected (Fig. 35). It has been reported that AAV transduction

only affects the viability of undifferentiated cells to a greater extent [482]. Another group found no decrease in cell viability and proliferation rate either 3, 6 or 9 days after AAV transduction [483]. Also, innate immune responses to AAV vectors have been reported to be rare [484]. Still, significant upregulation of MCP-1 (twofold), IL-23 (2.5-fold) and IL-27 (2.5-fold) were found in glioma target cells in response to HER2-AAV transduction (Fig. 37). Transduction has also been reported to cause TLR9-dependent production of type I IFNs by human plasmacytoid dendritic cells (pDCs) *in vitro* [485]. However, AAV vectors are incapable of activating the inflammasome, suggesting that interaction between the immune system and the administered AAVs is unlikely to interfere with gene therapy success [486]. Exuberant immune activation in response to immunotherapy, which in some cases resulted in multi-organ failure and death, has been reported multiple times [487], [488]. In this context, AAV therapy is generally considered safe, and also no cytokine storms or other immune-related adverse events that are known to occur after systemic administration of conventional ICIs have been observed [289]. In line with that, also no evidence for excessive cytokine production in response to HER2-AAV treatment *in vivo* was found (Fig. 43). HER2-AAV transduction did not result in downregulation of the target antigen, so CAR-NK cells were still able to lyse glioma cells (Fig. 36A and 39A). Even though following ligand binding HER2 is internalized via receptor-mediated endocytosis [489], it is recycled and brought back to the cell membrane rather than to be degraded in the lysosome [490]. Consistent with those data, interference of both therapy approaches can be excluded based on data obtained in the present study.

#### **4.9 Distribution kinetics of HER2-AAV-encoded aPD-1 *in vivo***

Since knowledge about the characteristics of the *in vivo* secretion of HER2-AAV-encoded aPD-1 is crucial for the implementation of a combination therapy with CAR-NK cells, aPD-1 biodistribution kinetics was evaluated in several mouse models. Being a prerequisite regarding both HER2-targeted therapies, stable HER2 expression *in vivo* was confirmed in the syngeneic as well as in the xenograft mouse model (Fig. 40). In both models, high transduction efficacies and accordingly high levels of aPD-1 in subcutaneous tumors that had been treated with HER2-AAVs either intravenously or intratumorally were reached (Fig. 41B). In orthotopic intracranial tumors, aPD-1 was only found upon intratumoral HER2-AAV administration, indicating that the vectors are not able to cross the BBB and reach the tumor (Fig. 41B). The AAV9 serotype may be more suitable as a vector to achieve gene transfer to the

brain since it possesses a natural tropism towards CNS tissue [491]. For instance, AAV9 vectors encoding IFN- $\beta$  have successfully been used to treat GB in orthotopic mouse models after intravenous administration [492] and efforts to re-target AAV9 vectors to GB cells are ongoing in the Buchholz laboratory.

Of paramount importance for the proposed strategy, after injection of the vector, aPD-1 was produced almost exclusively within the tumor, while cells of other organs remained mainly untransduced (Fig. 41B). Minimal concentrations of aPD-1 were found only in lung, spleen, liver and kidney tissue. It is conceivable that either HER2-AAVs entered the bloodstream and transduced the other organs or aPD-1 produced by tumor cells was transported to the periphery via vasculature as well. Minimal off-target effects following HER2-AAV administration have been reported before [310]. To confirm off-target transduction of the organs, aPD-1 RNA levels would need to be determined and serum of experimental animals should be analyzed for aPD-1 abundance. However, aPD-1 levels in organs were ~20-fold lower than in tumor tissue, indicating a high transduction selectivity and specificity. In contrast, other groups reported severe liver toxicities following transduction of liver cells after intravenous WT AAV2 injection [297], which we did not observe after HER2-AAV administration.

Checkpoint inhibitors that are currently used for the treatment of cancer patients are full-length IgGs such as Pembrolizumab (anti-PD-L1) or Nivolumab (anti-PD-1). For HER2-AAV-mediated ICI delivery in a clinical setting, sequences of already approved ICIs should be incorporated in the vectors. Reul et al. were able to show that transduction of target cells with HER2-AAVs encoding the sequence of the approved antibody Nivolumab (human anti-PD-1) resulted in successful secretion of functionally active Nivolumab. However, significantly lower amounts of the transgene product have been determined as compared to the murine  $\alpha$ PD-1 antibody (0.153 ng per mg total protein vs. 1.9 ng per mg total protein, probably due to mitigated transduction efficacy in the context of increased packaging capacity [310]. Nevertheless, targeted delivery of a full-length IgG has still been proven to be achievable in an *in vivo* setting.

A major challenge in AAV-mediated gene therapy is the generation of nAbs against the vector capsid. Natural exposure to wild-type AAV triggers humoral immunity early in life, and

antibodies directed against serotype 2 are among the most prevalent in humans, ranging up to 70% [493], [494]. It has also been reported before that sera of lab animals contain pre-existing antibodies against AAV serotypes such as AAV1, AAV2, AAV6 and AAV9 [495]. Also in the present study, evidence for pre-existing nAbs against AAV2 in serum of experimental animals was found (Fig. 44B). In animals that received treatment, nAb titers increased over time after a single injection, which is why double injections of the vector did not result in higher aPD-1 concentrations. In fact, double injections rather led to increased nAb titers, regardless of the administration route (Fig. 44C). However, given the pre-existence and further generation of nAbs, still high aPD-1 concentrations in tumor tissue were observed (Fig. 41B). To avoid recognition by pre-existing antibodies, further modifications that aim to shield neutralizing epitopes on the capsid surface have been evaluated. For instance, crosslinking synthetic polymers such as polyethylene glycol to the capsid surface has already been performed by several groups and resulted in reduced neutralization activity [496], [497]. As mentioned before, AAV9 represents a promising tool for the transduction of brain tissue following intravenous administration, and the prevalence of nAbs directed against this serotype is also lower in humans [498], [499]. A group of researchers has been able to target the brain after a single intravenous injection of AAV9 which had been packaged into extracellular vesicles to avoid nAb-mediated neutralization [500].

In summary, it was shown that the transduction of HER2<sup>+</sup> cells *in vivo* leads to high aPD-1 levels in tumors after intratumoral AAV administration and for subcutaneous tumor models even after intravenous AAV administration, while only low systemic concentrations were reached. Furthermore, the release of inflammatory cytokines was observed in response to AAV administration. Taken together with the functionality of aPD-1 to restore T cell activity demonstrated *in vitro*, the use of targeted HER2-AAVs mediating the production of aPD-1 immunoadhesin can modify the immunosuppressive TME and holds promise for GB therapy.

#### 4.10 The effect of combined HER2-AAV/CAR-NK cell therapy on survival

In this study, immune checkpoint blockade in combination with CAR-NK cell therapy was shown to have a beneficial effect on survival in an immunocompetent glioblastoma mouse model. A dominant synergistic effect of CAR-NK cells and HER2-AAV<sup>aPD-1</sup> was observed in the subcutaneous as well as in the orthotopic intracranial mouse model. Tumors of animals receiving the combination therapy grew slower, and their survival was significantly prolonged as compared to all control cohorts (Fig. 46) with a (median survival of 74 days as compared to HER2-AAV<sup>IgG-Fc</sup> + CAR-NK (40 days), HER2-AAV<sup>aPD-1</sup> (37 days) HER2-AAV<sup>IgG-Fc</sup> (27 days), CAR-NK (30 days) or untreated animals (25.8 days)). Complete tumor rejection was observed in 3/7 mice in the orthotopic intracranial model and 3/5 mice in the subcutaneous model upon intratumoral administration of the combination therapy. Intravenous administration was impractical on account of the BBB, as neither CAR-NK cells nor HER2-AAV-encoded aPD-1 was able to reach the brain after intravenous administration (Fig. 41B and unpublished data). Nonetheless, intratumoral immunotherapy is recently considered a promising opportunity for the conversion of “cold” tumors into “hot” tumors. As reviewed by Marabelle et al., intratumoral immunotherapy harbors many advantages over systemic administration [501]. As mentioned before, not all patients benefit from systemically injected immunotherapies, which might depend on the limited bioavailability within tumor lesions. Studies have shown that higher doses of ICIs correlate with enhanced efficacy of the drug [502], [503], but higher ICI doses also result in more severe irAEs [502], [504]. It was also discussed before that the combination of multiple ICIs further increases the risk for treatment-related toxicities. Another study reported tumor relapse in mice that have been systemically injected with ICIs, most likely due to the absence of the specific epitope that was targeted by the intervention. However, the addition of intratumoral immunotherapy prevented cancer relapse by stimulation and subsequent anti-tumor effects of CD8<sup>+</sup> T cells [505].

Mounting of a sustained adaptive immune response requires both priming and anti-tumor activity of T cells. The release of neo-antigens or tumor-associated antigens upon the lysis of tumor cells by CAR-NK cells is likely to induce a potent stimulation of the immune system by both local priming of T cells and their dissemination into the periphery to ensure systemic activation of the immune system. Once this anti-tumor response is triggered, intratumoral delivery of aPD-1 by HER2-AAVs will likely facilitate the continuing immune activation by

preventing the immunosuppressive traits of the TME to prevail. Recruitment of peripheral immune cells by a therapy-induced release of tumor antigens is especially relevant in “cold” tumors such as GB. In fact, tumor growth in animals that received the combination therapy in this study was effectively controlled in the majority of mice (Appendix Fig. 6). 2/7 animals showed no signs of tumor progression for weeks after initial treatment stopped, while 3/7 mice completely rejected the tumor. 2/7 mice eventually succumbed to tumor burden, but the onset of tumor progression was delayed until 4 weeks after the last treatment administration, while tumor volumes of control animals began to escalate during or within 1 week after treatment had stopped (Appendix Fig. 1-6). These data suggest that the combination therapy triggered a long-lasting immune response that was able to control tumor growth. Also, the well-known off-target toxicities that are associated with systemic immunotherapy administration were not observed in animals receiving intratumoral immunotherapy.

Although the evidence of anti-tumor effects that are triggered by the combination therapy in mice is encouraging, there are limitations regarding the transferability to the situation in humans. The methylcholanthrene-induced GL261 model, one of the most frequently used orthotopically implanted immunocompetent mouse models, was chosen for the present study [506], [507]. The highly mutated GL261 cell line has been shown to be sensitive towards immune checkpoint blockade in a study reporting complete tumor clearance in over 50% of GL261 bearing mice [508]. Survival benefit and macrophage re-polarization upon anti-PD-1 administration in immunocompetent mice bearing intracranial tumors has also been reported [509]. Still, it has to be considered that murine cell lines are not able to fully model the precise TME of human GB. Several limitations of the GL261 model have been reviewed by Haddad et al. [510]. As mentioned above, this model was chemically induced and therefore carries a high mutational burden [511], as opposed to the low mutational burden of human GB [151], [512]. For instance, high MHC-I expression as well as numerous non-synonymous exome mutations and neoepitopes have been reported for GL261 [506]. In this context, it is of great importance to ensure that the successful immunotherapy implemented in this study is not biased by the high tumor mutational load of GL261 cells. With the divergence in success rates between preclinical immunotherapy experiments and actual clinical trials [510], [513], [514], Genoud et al. propose the use of models that display the mutational load and microenvironment in

scenarios more closely related to human GB, such as the SB28 model, which was not induced chemically but genetically [508].

Furthermore, the feasibility of intratumoral immunotherapy is of course dependent on the accessibility of tumor lesions, which has been particularly difficult in brain malignancies. Still, even tumors of the CNS have been shown to be a possible subject to local injection, as patients in the CAR2BRAIN trial receive intratumoral CAR-NK cells injections via a so-called rickham catheter. However, there are still some issues that need to be explored before the implementation of the CAR-NK/AAV combination therapy in a clinical setting. For instance, the number, as well as frequency, of injections has to be determined, and also the dose and volume of intratumoral injections had to be carefully chosen. These questions have already been addressed in the CAR2BRAIN trial for CAR-NK cells so far, but still, they need to be elucidated for AAVs. Also, the treatment schedule could be optimized, with respect to repeated treatments and the timing (separate vs. combined injection) of CAR-NK and AAV administration.

Taken together, this study revealed synergistic anti-tumor effects of CAR-NK cell therapy in combination with HER2-AAV-mediated intratumoral immunotherapy. To further stimulate immune effector cells a combination of immunostimulatory drugs or ICIs might be feasible via the intratumoral administration of AAV. CAR-NK cell therapy might be compatible with co-injection of a variety of AAVs that are able to mediate the local release of immune modulators, especially in patients that do not respond to classical ICI therapy. Based on the evidence gathered in this study, further exploration of the proposed treatment approach might pave the way for more personalized immunotherapy in GB patients.

#### **4.11 Conclusions and outlook**

Data obtained in this study reveal that target-activated CAR-NK cells can induce upregulation of checkpoint molecules on neighboring tumor and immune cells, emphasizing the potential benefit of a combination therapy with an ICI-encoding HER2-AAV. Hence, HER2-AAV<sup>aPD-1</sup> induce local secretion of the aPD-1 immunoadhesin by transduced tumor cells, which can modulate the immunosuppressive TME, support re-activation of T cells and thereby mediate synergistic effects when combined with adoptive transfer of CAR-NK cells (Fig. 11). Moreover,

the option to combine AAVs with different payloads may provide an advantage over the traditional systemic application of anti-PD1 antibodies. Taken together, evidence gathered in this study reveals that intratumoral as well as intravenous injection of HER2-AAV<sup>aPD-1</sup> in combination with CAR-NK cell-mediated tumor cell lysis resulted in a significant therapeutic benefit without treatment-related side effects, representing a promising novel strategy for GB immunotherapy.

These results encourage the next step to evaluate the impact of combined therapy on the composition and signaling pathways within the TME. The mechanisms underlying the cooperation of CAR-NK cells and HER2-AAV-mediated aPD-1 therapy will need to be investigated via detailed analyses of local and systemic changes of the immune reaction via exploration of the immune infiltrate, transcriptome analyses of immune cells and T cell receptor (TCR) sequencing for the determination of immunogenic antigens [515], [516]. In particular, the different lymphocyte subpopulations, as well as their activity, will be determined by RNA sequencing as well as multipanel FACS analysis. The aim is to achieve a better understanding of the immune response which are triggered by the combination therapy and the recognition of new targets for HER2-AAV mediated immunomodulation. Additionally, multispectral high-throughput histology will be employed to histologically characterize the various immune cell populations and their interactions not only with each other but also with stroma cells, tumor cells and the vasculature. In tumor tissue, the infiltration and the activation of T cells will be assessed, while the number and polarization of microglial cells and macrophages will be determined in the TME. To address the risk of neurotoxicity and systemic toxicity of the combination therapy, organs of experimental animals will be examined for lymphocyte and macrophage/microglial infiltration, neuronal loss and signs of astrogliosis.

Furthermore, TCR sequencing will reveal tumor-reactive T cell signatures by combined scVDJ/RNA-seq from sorted tumor-infiltrating lymphocytes as described previously [517]. TCR sequences will be used to track back T cell clonotypes and for comparison between the treatment cohorts. As a mechanistic control for preclinical efficacy experiments, CD8<sup>+</sup> T cell depletion experiments are planned in the subcutaneous and orthotopic intracranial GL261/HER2 mouse models.



Since especially HER2-targeted AAV vector particles are a highly important innovative tool for immunotherapy of GB, research currently focuses on improving the gene delivery activity mediated by HER2-AAV. In particular, insertion of the HER2-specific DARPin into alternative capsid insertion sites, such as the GH2/GH3 loop in VP1, is currently being investigated. This strategy has recently been published to accommodate the functional surface display of nanobodies [518] and could be implemented for a delivery system employing AAV9 to improve the targeting of specific cell types within the brain.

Moreover, the choice of the target antigen might need to be reconsidered due to HER2-AAV and CAR-NK cells targeting the same antigen. Since HER2<sup>+</sup> target cells will only produce the transgene product throughout their lifetime, target cell lysis by CAR-NK cells will likely hamper the accumulation of sufficient aPD-1 levels in the TME. However, due to the high flexibility in AAV and CAR-NK cell target selection as well as for AAV payload, the system has the potential to customize immunotherapy to the malignant cells and the microenvironment of a specific tumor. Still, it remains to be investigated what threshold needs to be reached for HER2-AAV-encoded aPD-1 to be therapeutically effective. Data obtained in this study do not provide sufficient evidence whether systemic effects of immune checkpoint blockade, e.g. in peripheral lymphoid organs such as lymph nodes or the spleen are crucial for therapeutic success. Once these questions have been addressed, the AAV vector dose that needs to be applied can be adjusted accordingly. Additional data on the aPD-1 levels required to evoke an immune response in combination with other treatment modalities such as CAR-NK cells are required. Moreover, upon administration of AAV therapy in a clinical setting, serum levels of checkpoint inhibitors should be closely monitored to avoid side effects similar to those observed after systemic ICI injection.

Finally, the combination of local administration of CAR-NK cells with an anti-PD1 antibody will likely be tested in patients suffering from HER2<sup>+</sup> recurrent GB in the upcoming cohort of the CAR2BRAIN trial. The scientific translational program of the study will help to address many of the questions regarding the mechanism of synergy between anti-PD1-strategies and CAR-NK cells and will allow refinement and further development of the therapeutic approach using AAVs as a delivery system in future studies.

## 5 References

- [1] A. Brodbelt *et al.*, "Glioblastoma in England: 2007–2011," *Eur. J. Cancer*, vol. 51, no. 4, pp. 533–542, Mar. 2015, doi: 10.1016/J.EJCA.2014.12.014.
- [2] J. Ferlay *et al.*, "Cancer incidence and mortality worldwide: Sources, methods and major patterns in GLOBOCAN 2012," *Int. J. Cancer*, vol. 136, no. 5, pp. E359–E386, Mar. 2015, doi: 10.1002/IJC.29210.
- [3] H. Ohgaki *et al.*, "Genetic pathways to glioblastoma: a population-based study," *Cancer Res.*, vol. 64, no. 19, pp. 6892–6899, Oct. 2004, doi: 10.1158/0008-5472.CAN-04-1337.
- [4] R. G. Verhaak *et al.*, "Integrated genomic analysis identifies clinically relevant subtypes of glioblastoma characterized by abnormalities in PDGFRA, IDH1, EGFR, and NF1," *Cancer Cell*, vol. 17, no. 1, pp. 98–110, Jan. 2010, doi: 10.1016/J.CCR.2009.12.020.
- [5] D. Gramatzki *et al.*, "Glioblastoma in the Canton of Zurich, Switzerland revisited: 2005 to 2009," *Cancer*, vol. 122, no. 14, pp. 2206–2215, Jul. 2016, doi: 10.1002/CNCR.30023.
- [6] M. Preusser *et al.*, "Current concepts and management of glioblastoma," *Ann. Neurol.*, vol. 70, no. 1, pp. 9–21, Jul. 2011, doi: 10.1002/ANA.22425.
- [7] M. Ijzerman-Korevaar *et al.*, "Prevalence of symptoms in glioma patients throughout the disease trajectory: a systematic review," *J. Neurooncol.*, vol. 140, pp. 485–496, 2018, doi: 10.1007/s11060-018-03015-9.
- [8] C. McKinnon *et al.*, "Glioblastoma: clinical presentation, diagnosis, and management," *BMJ*, vol. 374, Jul. 2021, doi: 10.1136/BMJ.N1560.
- [9] G. P. Dunn *et al.*, "Emerging insights into the molecular and cellular basis of glioblastoma," *Genes Dev.*, vol. 26, no. 8, pp. 756–784, Apr. 2012, doi: 10.1101/GAD.187922.112.
- [10] H.J. Hoffman *et al.*, "Extraneural metastases of central nervous system tumors.," *Cancer*, vol. 56, no. 7 Suppl, pp. 1778–1782, Oct. 1985, doi: 10.1002/1097-0142(19851001)56:7+<1778::aid-cnrcr2820561309>3.0.co;2-i.
- [11] V. A. Cuddapah *et al.*, "A neurocentric perspective on glioma invasion," *Nat. Rev. Neurosci.* 2014 157, vol. 15, no. 7, pp. 455–465, Jun. 2014, doi: 10.1038/nrn3765.
- [12] C. W. Brennan *et al.*, "The somatic genomic landscape of glioblastoma," *Cell*, vol. 155, no. 2, p. 462, Oct. 2013, doi: 10.1016/J.CELL.2013.09.034.
- [13] M. Ceccarelli *et al.*, "Molecular Profiling Reveals Biologically Discrete Subsets and Pathways of Progression in Diffuse Glioma," *Cell*, vol. 164, no. 3, pp. 550–563, Jan. 2016, doi: 10.1016/J.CELL.2015.12.028.
- [14] M. Yao *et al.*, "Cellular origin of glioblastoma and its implication in precision therapy," *Cell. Mol. Immunol.* 2017 158, vol. 15, no. 8, pp. 737–739, Mar. 2018, doi: 10.1038/cmi.2017.159.
- [15] H. J. Kim *et al.*, "Genetic Architectures and Cell-of-Origin in Glioblastoma," *Front. Oncol.*, vol. 10, p. 3097, Jan. 2021, doi: 10.3389/FONC.2020.615400/BIBTEX.
- [16] D. N. Louis *et al.*, "The 2016 World Health Organization Classification of Tumors of the Central Nervous System: a summary," *Acta Neuropathol.*, vol. 131, no. 6, pp. 803–820, 2016, doi: 10.1007/s00401-016-1545-1 PM - 27157931 M4 - Citavi.
- [17] C. Brennan *et al.*, "Glioblastoma subclasses can be defined by activity among signal transduction pathways and associated genomic alterations," *PLoS One*, vol. 4, no. 11, Nov. 2009, doi: 10.1371/JOURNAL.PONE.0007752.
- [18] W. Szopa *et al.*, "Diagnostic and Therapeutic Biomarkers in Glioblastoma: Current Status and Future

- Perspectives," *Biomed Res. Int.*, vol. 2017, 2017, doi: 10.1155/2017/8013575.
- [19] E. Lee *et al.*, "Comparison of glioblastoma (GBM) molecular classification methods," *Semin. Cancer Biol.*, vol. 53, pp. 201–211, Dec. 2018, doi: 10.1016/J.SEMCANCER.2018.07.006.
- [20] D. Ghosh *et al.*, "Combination therapy to checkmate Glioblastoma: clinical challenges and advances," *Clin. Transl. Med.*, vol. 7, no. 1, Dec. 2018, doi: 10.1186/S40169-018-0211-8.
- [21] A. Shergalis *et al.*, "Current Challenges and Opportunities in Treating Glioblastoma," *Pharmacol. Rev.*, vol. 70, no. 3, pp. 412–445, Jul. 2018, doi: 10.1124/PR.117.014944.
- [22] M. Paoillo *et al.*, "Glioblastoma under Siege: An Overview of Current Therapeutic Strategies," *Brain Sci.*, vol. 8, no. 1, Jan. 2018, doi: 10.3390/BRAINSCI8010015.
- [23] F. E. Bleeker *et al.*, "Recent advances in the molecular understanding of glioblastoma," *J. Neurooncol.*, vol. 108, no. 1, p. 11, May 2012, doi: 10.1007/S11060-011-0793-0.
- [24] D. N. Louis *et al.*, "The 2021 WHO Classification of Tumors of the Central Nervous System: a summary," *Neuro. Oncol.*, vol. 23, no. 8, pp. 1231–1251, Aug. 2021, doi: 10.1093/NEUONC/NOAB106.
- [25] H. Ohgaki and P. Kleihues, "The definition of primary and secondary glioblastoma," *Clin. Cancer Res.*, vol. 19, no. 4, pp. 764–772, Feb. 2013, doi: 10.1158/1078-0432.CCR-12-3002.
- [26] G. Carrabba *et al.*, "Aberrant signalling complexes in GBMs: Prognostic and therapeutic implications," *Glioblastoma Mol. Mech. Pathog. Curr. Ther. Strateg.*, pp. 95–129, 2010, doi: 10.1007/978-1-4419-0410-2\_5.
- [27] N. Ahmed *et al.*, "HER2-Specific T Cells Target Primary Glioblastoma Stem Cells and Induce Regression of Autologous Experimental Tumors," *Clin. Cancer Res.*, vol. 16, no. 2, pp. 474–485, Jan. 2010, doi: 10.1158/1078-0432.CCR-09-1322.
- [28] G. Liu *et al.*, "HER-2, gp100, and MAGE-1 are expressed in human glioblastoma and recognized by cytotoxic T cells," *Cancer Res.*, vol. 64, no. 14, pp. 4980–4986, Jul. 2004, doi: 10.1158/0008-5472.CAN-03-3504.
- [29] C. Zhang *et al.*, "ErbB2/HER2-Specific NK Cells for Targeted Therapy of Glioblastoma," 2015, doi: 10.1093/jnci/djv375.
- [30] D. J. Riese and D. F. Stern, "Specificity within the EGF family/ErbB receptor family signaling network," *Bioessays*, vol. 20, no. 1, pp. 41–8, Jan. 1998, doi: 10.1002/(SICI)1521-1878(199801)20:1<41::AID-BIES7>3.0.CO;2-V.
- [31] P. W. Brandt-Rauf *et al.*, "The c-erbB-2 protein in oncogenesis: molecular structure to molecular epidemiology," *Crit. Rev. Oncog.*, vol. 5, no. 2–3, pp. 313–29, 1994, doi: 10.1615/critrevoncog.v5.i2-3.100.
- [32] P. P. Di Fiore *et al.*, "ErbB-2 is a potent oncogene when overexpressed in NIH/3T3 cells," *Science (80-. )*, vol. 237, no. 4811, pp. 178–182, Jul. 1987, doi: 10.1126/science.2885917.
- [33] W. J. Muller *et al.*, "Single-step induction of mammary adenocarcinoma in transgenic mice bearing the activated c-neu oncogene," *Cell*, vol. 54, no. 1, pp. 105–115, Jul. 1988, doi: 10.1016/0092-8674(88)90184-5.
- [34] M. F. Press *et al.*, "Expression of the HER-2/neu proto-oncogene in normal human adult and fetal tissues," *Oncogene*, vol. 5, no. 7, pp. 953–962, 1990.
- [35] N. Ahmed *et al.*, "HER2-specific T cells target primary glioblastoma stem cells and induce regression of autologous experimental tumors," *Clin. Cancer Res.*, vol. 16, no. 2, pp. 474–485, Jan. 2010, doi: 10.1158/1078-0432.CCR-09-1322.
- [36] H. Colman *et al.*, "A multigene predictor of outcome in glioblastoma," *Neuro. Oncol.*, vol. 12, no. 1, pp. 49–57, Jan. 2010, doi: 10.1093/NEUONC/NOP007.
- [37] R. Stupp *et al.*, "Radiotherapy plus Concomitant and Adjuvant Temozolomide for Glioblastoma," *N. Engl.*

- J. Med.*, vol. 352, no. 10, pp. 987–996, Mar. 2005, doi: 10.1056/NEJMoa043330.
- [38] R. Stupp *et al.*, “NovoTTF-100A versus physician’s choice chemotherapy in recurrent glioblastoma: A randomised phase III trial of a novel treatment modality,” *Eur. J. Cancer*, vol. 48, no. 14, pp. 2192–2202, Sep. 2012, doi: 10.1016/j.ejca.2012.04.011.
- [39] M. Weller *et al.*, “EANO guidelines on the diagnosis and treatment of diffuse gliomas of adulthood,” *Nat. Rev. Clin. Oncol.* 2020 183, vol. 18, no. 3, pp. 170–186, Dec. 2020, doi: 10.1038/s41571-020-00447-z.
- [40] A. M. Molinaro *et al.*, “Association of Maximal Extent of Resection of Contrast-Enhanced and Non-Contrast-Enhanced Tumor With Survival Within Molecular Subgroups of Patients With Newly Diagnosed Glioblastoma,” *JAMA Oncol.*, vol. 6, no. 4, pp. 495–503, Apr. 2020, doi: 10.1001/JAMAONCOL.2019.6143.
- [41] T. S. Armstrong, “Head’s up on the treatment of malignant glioma patients,” *Oncol. Nurs. Forum*, vol. 36, no. 5, Sep. 2009, doi: 10.1188/09.ONF.E232-E240.
- [42] W. Stummer *et al.*, “Fluorescence-guided surgery with 5-aminolevulinic acid for resection of malignant glioma: a randomised controlled multicentre phase III trial,” *Lancet Oncol.*, vol. 7, no. 5, pp. 392–401, May 2006, doi: 10.1016/S1470-2045(06)70665-9.
- [43] R. H. Press *et al.*, “Optimal timing of chemoradiotherapy after surgical resection of glioblastoma: Stratification by validated prognostic classification,” *Cancer*, vol. 126, no. 14, pp. 3255–3264, Jul. 2020, doi: 10.1002/CNCR.32797.
- [44] R. Stupp *et al.*, “Effects of radiotherapy with concomitant and adjuvant temozolomide versus radiotherapy alone on survival in glioblastoma in a randomised phase III study: 5-year analysis of the EORTC-NCIC trial,” *Lancet Oncol.*, vol. 10, no. 5, pp. 459–466, May 2009, doi: 10.1016/S1470-2045(09)70025-7.
- [45] J. R. Perry *et al.*, “Short-Course Radiation plus Temozolomide in Elderly Patients with Glioblastoma,” <http://dx.doi.org/10.1056/NEJMoa1611977>, vol. 376, no. 11, pp. 1027–1037, Mar. 2017, doi: 10.1056/NEJMOA1611977.
- [46] M. E. Hegi *et al.*, “MGMT Gene Silencing and Benefit from Temozolomide in Glioblastoma,” <http://dx.doi.org/10.1056/NEJMoa043331>, vol. 352, no. 10, pp. 997–1003, Oct. 2009, doi: 10.1056/NEJMOA043331.
- [47] M. Preusser *et al.*, “Prospects of immune checkpoint modulators in the treatment of glioblastoma,” *Nat. Rev. Neurol.*, vol. 11, no. 9, pp. 504–514, 2015, doi: 10.1038/nrneurol.2015.139 PM - 26260659 M4 - Citavi.
- [48] M. A. Patel *et al.*, “The future of glioblastoma therapy: synergism of standard of care and immunotherapy,” *Cancers (Basel)*, vol. 6, no. 4, pp. 1953–1985, Dec. 2014, doi: 10.3390/CANCERS6041953.
- [49] R. Li *et al.*, “Comprehensive portrait of recurrent glioblastoma multiforme in molecular and clinical characteristics,” *Oncotarget*, vol. 6, no. 31, pp. 30968–30974, 2015, doi: 10.18632/ONCOTARGET.5038.
- [50] M. J van den Bent *et al.*, “Changes in the EGFR amplification and EGFRvIII expression between paired primary and recurrent glioblastomas,” *Neuro. Oncol.*, vol. 17, no. 7, pp. 935–941, Jul. 2015, doi: 10.1093/NEUONC/NOV013.
- [51] B. K. Neilsen *et al.*, “Comprehensive genetic alteration profiling in primary and recurrent glioblastoma,” *J. Neurooncol.*, vol. 142, no. 1, pp. 111–118, Mar. 2019, doi: 10.1007/S11060-018-03070-2.
- [52] N. Schäfer *et al.*, “Longitudinal heterogeneity in glioblastoma: moving targets in recurrent versus primary tumors,” *J. Transl. Med.*, vol. 17, no. 1, Mar. 2019, doi: 10.1186/S12967-019-1846-Y.
- [53] G. Lombardi *et al.*, “Regorafenib compared with lomustine in patients with relapsed glioblastoma (REGOMA): a multicentre, open-label, randomised, controlled, phase 2 trial,” *Lancet Oncol.*, vol. 20, no. 1,

- pp. 110–119, Jan. 2019, doi: 10.1016/S1470-2045(18)30675-2.
- [54] W. Wick *et al.*, “Lomustine and Bevacizumab in Progressive Glioblastoma,” <http://dx.doi.org/10.1056/NEJMoa1707358>, vol. 377, no. 20, pp. 1954–1963, Nov. 2017, doi: 10.1056/NEJMoa1707358.
- [55] T. N. Kreisl *et al.*, “Phase II trial of single-agent bevacizumab followed by bevacizumab plus irinotecan at tumor progression in recurrent glioblastoma,” *J. Clin. Oncol.*, vol. 27, no. 5, pp. 740–745, Feb. 2009, doi: 10.1200/JCO.2008.16.3055.
- [56] D. A. Reardon *et al.*, “Effect of Nivolumab vs Bevacizumab in Patients With Recurrent Glioblastoma: The CheckMate 143 Phase 3 Randomized Clinical Trial,” *JAMA Oncol.*, vol. 6, no. 7, pp. 1003–1010, Jul. 2020, doi: 10.1001/JAMAONCOL.2020.1024.
- [57] A. Pace *et al.*, “Determining medical decision-making capacity in brain tumor patients: Why and how?,” *Neuro-Oncology Pract.*, vol. 7, no. 6, pp. 599–612, Dec. 2020, doi: 10.1093/NOP/NPAA040.
- [58] D. F. Quail and J. A. Joyce, “The Microenvironmental Landscape of Brain Tumors,” *Cancer Cell*, vol. 31, no. 3, pp. 326–341, Mar. 2017, doi: 10.1016/J.CCELL.2017.02.009.
- [59] H. A. Goubran *et al.*, “Regulation of Tumor Growth and Metastasis: The Role of Tumor Microenvironment,” *Cancer Growth Metastasis*, vol. 7, p. CGM.S11285, Jan. 2014, doi: 10.4137/CGM.S11285.
- [60] T. D. Tlsty and L. M. Coussens, “Tumor stroma and regulation of cancer development,” *Annu. Rev. Pathol.*, vol. 1, pp. 119–150, 2006, doi: 10.1146/ANNUREV.PATHOL.1.110304.100224.
- [61] Q. Klopfenstein *et al.*, “Cell lines and immune classification of glioblastoma define patient’s prognosis,” *Br. J. Cancer*, vol. 120, no. 8, pp. 806–814, Apr. 2019, doi: 10.1038/S41416-019-0404-Y.
- [62] A. Louveau *et al.*, “Structural and functional features of central nervous system lymphatic vessels,” *Nature*, vol. 523, no. 7560, pp. 337–341, 2015, doi: 10.1038/nature14432 PM - 26030524 M4 - Citavi.
- [63] A. Louveau *et al.*, “Revisiting the Mechanisms of CNS Immune Privilege,” *Trends Immunol.*, vol. 36, no. 10, pp. 569–577, 2015, doi: 10.1016/j.it.2015.08.006 PM - 26431936 M4 - Citavi.
- [64] M. van Vulpen *et al.*, “Changes in blood-brain barrier permeability induced by radiotherapy: Implications for timing of chemotherapy? (Review).”
- [65] W. Fauquette *et al.*, “Radiation-induced blood-brain barrier damages: an in vitro study,” *Brain Res.*, vol. 1433, pp. 114–126, Jan. 2012, doi: 10.1016/J.BRAINRES.2011.11.022.
- [66] A. S. Berghoff *et al.*, “Density of tumor-infiltrating lymphocytes correlates with extent of brain edema and overall survival time in patients with brain metastases,” *Oncoimmunology*, vol. 5, no. 1, 2015, doi: 10.1080/2162402X.2015.1057388.
- [67] R. D. Schreiber *et al.*, “Cancer immunoediting: Integrating immunity’s roles in cancer suppression and promotion,” *Science*, vol. 331, no. 6024. American Association for the Advancement of Science, pp. 1565–1570, Mar. 25, 2011, doi: 10.1126/science.1203486.
- [68] I. F. Parney *et al.*, “Glioma immunology and immunotherapy,” *Neurosurgery*, vol. 46, no. 4, pp. 778–792, Apr. 2000, doi: 10.1097/00006123-200004000-00002.
- [69] G. Fossati *et al.*, “Neutrophil infiltration into human gliomas,” *Acta Neuropathol.*, vol. 98, no. 4, pp. 349–354, 1999.
- [70] K. Gabrusiewicz, “Glioblastoma-infiltrated innate immune cells resemble M0 macrophage phenotype,” *JCI insight*, vol. 1, no. 2, Feb. 2016, doi: 10.1172/JCI.INSIGHT.85841.
- [71] J. Liang *et al.*, “Neutrophils promote the malignant glioma phenotype through S100A4,” *Clin. Cancer Res.*, vol. 20, no. 1, pp. 187–198, 2014, doi: 10.1158/1078-0432.CCR-13-1279 PM - 24240114 M4 - Citavi.

- [72] D. N. Hart *et al.*, "Demonstration and characterization of Ia-positive dendritic cells in the interstitial connective tissues of rat heart and other tissues, but not brain," *J. Exp. Med.*, vol. 154, no. 2, pp. 347–361, Aug. 1981, doi: 10.1084/JEM.154.2.347.
- [73] W. F. Hickey and H. Kimura, "Perivascular microglial cells of the CNS are bone marrow-derived and present antigen in vivo," *Science*, vol. 239, no. 4837, pp. 290–292, 1988, doi: 10.1126/SCIENCE.3276004.
- [74] J. Lowe *et al.*, "Microglial cells in human brain have phenotypic characteristics related to possible function as dendritic antigen presenting cells," *J. Pathol.*, vol. 159, no. 2, pp. 143–149, 1989, doi: 10.1002/PATH.1711590209.
- [75] E. Ulvestad *et al.*, "Human microglial cells have phenotypic and functional characteristics in common with both macrophages and dendritic antigen-presenting cells," *J. Leukoc. Biol.*, vol. 56, no. 6, pp. 732–740, 1994, doi: 10.1002/JLB.56.6.732.
- [76] S. Anguille *et al.*, "Clinical use of dendritic cells for cancer therapy," *Lancet. Oncol.*, vol. 15, no. 7, pp. e257–67, 2014, doi: 10.1016/S1470-2045(13)70585-0 PM - 24872109 M4 - Citavi.
- [77] K. Palucka and J. Banchereau, "Cancer immunotherapy via dendritic cells," *Nat. Rev. Cancer*, vol. 12, no. 4, pp. 265–277, Apr. 2012, doi: 10.1038/NRC3258.
- [78] R. M Prins *et al.*, "Gene expression profile correlates with T-cell infiltration and relative survival in glioblastoma patients vaccinated with dendritic cell immunotherapy," *Clin. Cancer Res.*, vol. 17, no. 6, pp. 1603–1615, Mar. 2011, doi: 10.1158/1078-0432.CCR-10-2563.
- [79] M. V. Sofroniew, "Reactive astrocytes in neural repair and protection," *Neuroscientist*, vol. 11, no. 5, pp. 400–407, Oct. 2005, doi: 10.1177/1073858405278321.
- [80] N. J. Abbott *et al.*, "Astrocyte-endothelial interactions at the blood-brain barrier," *Nat. Rev. Neurosci.*, vol. 7, no. 1, pp. 41–53, Jan. 2006, doi: 10.1038/NRN1824.
- [81] H. Kettenmann and B. R. Ransom, "The Concept of Neuroglia: A Historical Perspective," *Neuroglia*, Sep. 2004, doi: 10.1093/ACPROF:OSO/9780195152227.003.0001.
- [82] H. K. Kimelberg, "Functions of mature mammalian astrocytes: A current view," *Neuroscientist*, vol. 16, no. 1, pp. 79–106, Feb. 2010, doi: 10.1177/1073858409342593.
- [83] E. Jang *et al.*, "Phenotypic polarization of activated astrocytes: the critical role of lipocalin-2 in the classical inflammatory activation of astrocytes," *J. Immunol.*, vol. 191, no. 10, pp. 5204–5219, Nov. 2013, doi: 10.4049/JIMMUNOL.1301637.
- [84] F. Adhami *et al.*, "Deleterious Effects of Plasminogen Activators in Neonatal Cerebral Hypoxia-Ischemia," *Am. J. Pathol.*, vol. 172, no. 6, p. 1704, 2008, doi: 10.2353/AJPATH.2008.070979.
- [85] M. Yepes *et al.*, "Neuroserpin reduces cerebral infarct volume and protects neurons from ischemia-induced apoptosis," *Blood*, vol. 96, no. 2, pp. 569–576, Jul. 2000, doi: 10.1182/BLOOD.V96.2.569.
- [86] M. V. Sofroniew, "Astrocyte barriers to neurotoxic inflammation," *Nat. Rev. Neurosci.*, vol. 16, no. 5, pp. 249–263, Apr. 2015, doi: 10.1038/NRN3898.
- [87] A. Sierra *et al.*, "Astrocyte-derived cytokines contribute to the metastatic brain specificity of breast cancer cells.," *undefined*, 1997.
- [88] T. Seike *et al.*, "Interaction between lung cancer cells and astrocytes via specific inflammatory cytokines in the microenvironment of brain metastasis," *Clin. Exp. Metastasis*, vol. 28, no. 1, pp. 13–25, Jan. 2011, doi: 10.1007/S10585-010-9354-8.
- [89] R. R. Langley and I. J. Fidler, "The biology of brain metastasis," *Clin. Chem.*, vol. 59, no. 1, pp. 180–189, Jan. 2013, doi: 10.1373/CLINCHEM.2012.193342.

- [90] M. Lorger, "Tumor microenvironment in the brain," *Cancers (Basel)*, vol. 4, no. 1, pp. 218–243, Mar. 2012, doi: 10.3390/CANCERS4010218.
- [91] N. A. Charles *et al.*, "The brain tumor microenvironment," *Glia*, vol. 59, no. 8, pp. 1169–1180, Aug. 2011, doi: 10.1002/GLIA.21136.
- [92] I. Bechmann *et al.*, "Astrocyte-induced T cell elimination is CD95 ligand dependent," *J. Neuroimmunol.*, vol. 132, no. 1–2, pp. 60–65, Nov. 2002, doi: 10.1016/S0165-5728(02)00311-9.
- [93] Y. Zhang *et al.*, "Purification and Characterization of Progenitor and Mature Human Astrocytes Reveals Transcriptional and Functional Differences with Mouse," *Neuron*, vol. 89, no. 1, pp. 37–53, Jan. 2016, doi: 10.1016/J.NEURON.2015.11.013.
- [94] Q. Chen *et al.*, "Carcinoma-astrocyte gap junctions promote brain metastasis by cGAMP transfer," *Nature*, vol. 533, no. 7604, pp. 493–498, May 2016, doi: 10.1038/NATURE18268.
- [95] L. J. Lawson *et al.*, "Heterogeneity in the distribution and morphology of microglia in the normal adult mouse brain," *Neuroscience*, vol. 39, no. 1, pp. 151–170, 1990, doi: 10.1016/0306-4522(90)90229-W.
- [96] I. Yang *et al.*, "The role of microglia in central nervous system immunity and glioma immunology," *J. Clin. Neurosci.*, vol. 17, no. 1, pp. 6–10, Jan. 2010, doi: 10.1016/J.JOCN.2009.05.006.
- [97] K. Saijo and C. K. Glass, "Microglial cell origin and phenotypes in health and disease," *Nat. Rev. Immunol.*, vol. 11, no. 11, pp. 775–787, Nov. 2011, doi: 10.1038/NRI3086.
- [98] K. Helmut *et al.*, "Physiology of microglia," *Physiol. Rev.*, vol. 91, no. 2, pp. 461–553, Apr. 2011, doi: 10.1152/PHYSREV.00011.2010.
- [99] A. S. Berghoff and M. Preusser, "The inflammatory microenvironment in brain metastases: potential treatment target?," *Chinese Clin. Oncol.*, vol. 4, no. 2, 2015, doi: 10.3978/J.ISSN.2304-3865.2015.06.03.
- [100] M. Prinz and J. Priller, "Microglia and brain macrophages in the molecular age: from origin to neuropsychiatric disease," *Nat. Rev. Neurosci.* 2014 155, vol. 15, no. 5, pp. 300–312, Apr. 2014, doi: 10.1038/nrn3722.
- [101] A. R. Patel *et al.*, "Microglia and ischemic stroke: a double-edged sword," *Int. J. Physiol. Pathophysiol. Pharmacol.*, vol. 5, no. 2, p. 73, 2013, Accessed: Aug. 29, 2021. [Online]. Available: /pmc/articles/PMC3669736/.
- [102] H. Grégoire *et al.*, "Targeting Tumor Associated Macrophages to Overcome Conventional Treatment Resistance in Glioblastoma," *Front. Pharmacol.*, vol. 0, p. 368, Apr. 2020, doi: 10.3389/FPHAR.2020.00368.
- [103] A. S. Berghoff *et al.*, "Programmed death ligand 1 expression and tumor-infiltrating lymphocytes in glioblastoma," *Neuro. Oncol.*, vol. 17, no. 8, pp. 1064–1075, Aug. 2015, doi: 10.1093/NEUONC/NOU307.
- [104] C. Anfray *et al.*, "Current Strategies to Target Tumor-Associated-Macrophages to Improve Anti-Tumor Immune Responses," *Cells 2020, Vol. 9, Page 46*, vol. 9, no. 1, p. 46, Dec. 2019, doi: 10.3390/CELLS9010046.
- [105] J. D. Cherry *et al.*, "Neuroinflammation and M2 microglia: the good, the bad, and the inflamed," *J. Neuroinflammation 2014 111*, vol. 11, no. 1, pp. 1–15, Jun. 2014, doi: 10.1186/1742-2094-11-98.
- [106] B. Badie and J. Schartner, "Role of microglia in glioma biology," *Microsc. Res. Tech.*, vol. 54, no. 2, pp. 106–113, Jul. 2001, doi: 10.1002/JEMT.1125.
- [107] K. Gabrusiewicz *et al.*, "Characteristics of the alternative phenotype of microglia/macrophages and its modulation in experimental gliomas," *PLoS One*, vol. 6, no. 8, Aug. 2011, doi: 10.1371/JOURNAL.PONE.0023902.
- [108] R. A. Morantz *et al.*, "Macrophages in experimental and human brain tumors. Part 2: studies of the macrophage content of human brain tumors," *J. Neurosurg.*, vol. 50, no. 3, pp. 305–311, 1979, doi:

- 10.3171/JNS.1979.50.3.0305.
- [109] L. Sevenich *et al.*, "Analysis of tumor- and stroma-supplied proteolytic networks reveals a brain metastasis-promoting role for cathepsin S," *Nat. Cell Biol.*, vol. 16, no. 9, p. 876, 2014, doi: 10.1038/NCB3011.
- [110] R. L. Bowman *et al.*, "Macrophage Ontogeny Underlies Differences in Tumor-Specific Education in Brain Malignancies," *Cell Rep.*, vol. 17, no. 9, pp. 2445–2459, Nov. 2016, doi: 10.1016/J.CELREP.2016.10.052.
- [111] W. Li and M. B. Graeber, "The molecular profile of microglia under the influence of glioma," *Neuro. Oncol.*, vol. 14, no. 8, pp. 958–978, Aug. 2012, doi: 10.1093/NEUONC/NOS116.
- [112] S. Brandenburg *et al.*, "Resident microglia rather than peripheral macrophages promote vascularization in brain tumors and are source of alternative pro-angiogenic factors," *Acta Neuropathol.*, vol. 131, no. 3, pp. 365–378, Mar. 2016, doi: 10.1007/S00401-015-1529-6.
- [113] P. S. Zeiner *et al.*, "Distribution and prognostic impact of microglia/macrophage subpopulations in gliomas," *Brain Pathol.*, vol. 29, no. 4, pp. 513–529, Jul. 2019, doi: 10.1111/BPA.12690.
- [114] M. D. Sørensen *et al.*, "Tumour-associated microglia/macrophages predict poor prognosis in high-grade gliomas and correlate with an aggressive tumour subtype," *Neuropathol. Appl. Neurobiol.*, vol. 44, no. 2, pp. 185–206, Feb. 2018, doi: 10.1111/NAN.12428.
- [115] M. D. Caponegro *et al.*, "Expression of neuropilin-1 is linked to glioma associated microglia and macrophages and correlates with unfavorable prognosis in high grade gliomas," *Oncotarget*, vol. 9, no. 86, pp. 35655–35665, Nov. 2018, doi: 10.18632/ONCOTARGET.26273.
- [116] J. Zhou *et al.*, "MR Imaging Characteristics Associate with Tumor-Associated Macrophages in Glioblastoma and Provide an Improved Signature for Survival Prognostication," *AJNR. Am. J. Neuroradiol.*, vol. 39, no. 2, pp. 252–259, Feb. 2018, doi: 10.3174/AJNR.A5441.
- [117] M. C. Takenaka *et al.*, "Control of tumor-associated macrophages and T cells in glioblastoma via AHR and CD39," *Nat. Neurosci.*, vol. 22, no. 5, pp. 729–740, May 2019, doi: 10.1038/s41593-019-0370-y.
- [118] R. B. Rock *et al.*, "Role of Microglia in Central Nervous System Infections," *Clin. Microbiol. Rev.*, vol. 17, no. 4, p. 942, Oct. 2004, doi: 10.1128/CMR.17.4.942-964.2004.
- [119] D. Laoui *et al.*, "Functional Relationship between Tumor-Associated Macrophages and Macrophage Colony-Stimulating Factor as Contributors to Cancer Progression," *Front. Immunol.*, vol. 5, no. OCT, 2014, doi: 10.3389/FIMMU.2014.00489.
- [120] A. S. Berghoff *et al.*, "Programmed death ligand 1 expression and tumor-infiltrating lymphocytes in glioblastoma," *Neuro. Oncol.*, vol. 17, no. 8, pp. 1064–1075, Aug. 2015, doi: 10.1093/neuonc/nou307.
- [121] S. F. Hussain *et al.*, "The role of human glioma-infiltrating microglia/macrophages in mediating antitumor immune responses," *Neuro. Oncol.*, vol. 8, no. 3, pp. 261–279, 2006, doi: 10.1215/15228517-2006-008 PM - 16775224 M4 - Citavi.
- [122] A. Mantovani *et al.*, "Tumour-associated macrophages as treatment targets in oncology," *Nature Reviews Clinical Oncology*, vol. 14, no. 7. Nature Publishing Group, pp. 399–416, Jul. 01, 2017, doi: 10.1038/nrclinonc.2016.217.
- [123] A. S. Berghoff *et al.*, "Characterization of the inflammatory response to solid cancer metastases in the human brain," *Clin. Exp. Metastasis*, vol. 30, no. 1, pp. 69–81, Jan. 2013, doi: 10.1007/S10585-012-9510-4.
- [124] M. Platten *et al.*, "Microenvironmental clues for glioma immunotherapy," *Curr. Neurol. Neurosci. Rep.*, vol. 14, no. 4, 2014, doi: 10.1007/S11910-014-0440-1.
- [125] F. Masson *et al.*, "Brain microenvironment promotes the final functional maturation of tumor-specific effector CD8+ T cells," *J. Immunol.*, vol. 179, no. 2, pp. 845–853, 2007.



- [126] O. Fornara *et al.*, "Poor survival in glioblastoma patients is associated with early signs of immunosenescence in the CD4 T-cell compartment after surgery," <https://doi.org/10.1080/2162402X.2015.1036211>, vol. 4, no. 9, pp. 1–14, Jan. 2015, doi: 10.1080/2162402X.2015.1036211.
- [127] D. Focosi *et al.*, "CD57+ T lymphocytes and functional immune deficiency," *J. Leukoc. Biol.*, vol. 87, no. 1, pp. 107–116, Jan. 2010, doi: 10.1189/JLB.0809566.
- [128] M. Strioga *et al.*, "CD8+ CD28- and CD8+ CD57+ T cells and their role in health and disease," *Immunology*, vol. 134, no. 1, pp. 17–32, Sep. 2011, doi: 10.1111/J.1365-2567.2011.03470.X.
- [129] M. Hahne *et al.*, "Melanoma Cell Expression of Fas(Apo-1/CD95) Ligand: Implications for Tumor Immune Escape," *Science (80- )*, vol. 274, no. 5291, pp. 1363–1366, Nov. 1996, doi: 10.1126/SCIENCE.274.5291.1363.
- [130] S. Strand *et al.*, "Lymphocyte apoptosis induced by CD95 (APO-1/Fas) ligand-expressing tumor cells--a mechanism of immune evasion?," *Nat. Med.*, vol. 2, no. 12, pp. 1361–1366, Dec. 1996, doi: 10.1038/NM1296-1361.
- [131] V. V Didenko *et al.*, "Apoptosis of T lymphocytes invading glioblastomas multiforme: a possible tumor defense mechanism," *J. Neurosurg.*, vol. 96, no. 3, pp. 580–584, 2002, doi: 10.3171/jns.2002.96.3.0580 U6 - <https://www.ncbi.nlm.nih.gov/pubmed/11883844> M4 - Citavi.
- [132] P. E. Fecci *et al.*, "Increased regulatory T-cell fraction amidst a diminished CD4 compartment explains cellular immune defects in patients with malignant glioma," *Cancer Res.*, vol. 66, no. 6, pp. 3294–3302, Mar. 2006, doi: 10.1158/0008-5472.CAN-05-3773.
- [133] A. El Andaloussi and M. S. Lesniak, "An increase in CD4+CD25+FOXP3+ regulatory T cells in tumor-infiltrating lymphocytes of human glioblastoma multiforme," *Neuro. Oncol.*, vol. 8, no. 3, pp. 234–243, Jul. 2006, doi: 10.1215/15228517-2006-006.
- [134] S. Hori *et al.*, "Control of Regulatory T Cell Development by the Transcription Factor Foxp3," *Science (80- )*, vol. 299, no. 5609, pp. 1057–1061, Feb. 2003, doi: 10.1126/SCIENCE.1079490.
- [135] K. J. Maloy *et al.*, "Intralymphatic immunization enhances DNA vaccination," *Proc. Natl. Acad. Sci.*, vol. 98, no. 6, pp. 3299–3303, Mar. 2001, doi: 10.1073/PNAS.051630798.
- [136] D. Dieckmann *et al.*, "Ex Vivo Isolation and Characterization of Cd4+Cd25+ T Cells with Regulatory Properties from Human Blood," *J. Exp. Med.*, vol. 193, no. 11, pp. 1303–1310, Jun. 2001, doi: 10.1084/JEM.193.11.1303.
- [137] M. Abou-Ghazal *et al.*, "The Incidence, Correlation with Tumor-Infiltrating Inflammation, and Prognosis of Phosphorylated STAT3 Expression in Human Gliomas," *Clin. Cancer Res.*, vol. 14, no. 24, pp. 8228–8235, Dec. 2008, doi: 10.1158/1078-0432.CCR-08-1329.
- [138] M. Kortylewski *et al.*, "Inhibiting Stat3 signaling in the hematopoietic system elicits multicomponent antitumor immunity," *Nat. Med.*, vol. 11, no. 12, pp. 1314–1321, Dec. 2005, doi: 10.1038/NM1325.
- [139] H. Yu *et al.*, "STATs in cancer inflammation and immunity: a leading role for STAT3," *Nat. Rev. Cancer*, vol. 9, no. 11, pp. 798–809, Nov. 2009, doi: 10.1038/NRC2734.
- [140] M. Buggert *et al.*, "T-bet and Eomes are differentially linked to the exhausted phenotype of CD8+ T cells in HIV infection," *PLoS Pathog.*, vol. 10, no. 7, 2014, doi: 10.1371/JOURNAL.PPAT.1004251.
- [141] P. P. Lee *et al.*, "Characterization of circulating T cells specific for tumor-associated antigens in melanoma patients," *Nat. Med.*, vol. 5, no. 6, pp. 677–685, Jun. 1999, doi: 10.1038/9525.
- [142] K. Woroniecka *et al.*, "T-cell exhaustion signatures vary with tumor type and are severe in glioblastoma," *Clin. Cancer Res.*, vol. 24, no. 17, pp. 4175–4186, Sep. 2018, doi: 10.1158/1078-0432.CCR-17-1846.
- [143] K. I. Woroniecka *et al.*, "T-cell Dysfunction in Glioblastoma: Applying a New Framework," *Clin. Cancer*

- Res.*, vol. 24, no. 16, pp. 3792–3802, Aug. 2018, doi: 10.1158/1078-0432.CCR-18-0047.
- [144] I. Galea *et al.*, “What is immune privilege (not)?,” *Trends Immunol.*, vol. 28, no. 1, pp. 12–18, Jan. 2007, doi: 10.1016/J.IT.2006.11.004.
- [145] F. Dyrna *et al.*, “The blood-brain barrier,” *J. Neuroimmune Pharmacol.*, vol. 8, no. 4, pp. 763–773, Sep. 2013, doi: 10.1007/S11481-013-9473-5.
- [146] F. L. Cardoso *et al.*, “Looking at the blood-brain barrier: molecular anatomy and possible investigation approaches,” *Brain Res. Rev.*, vol. 64, no. 2, pp. 328–363, Sep. 2010, doi: 10.1016/J.BRAINRESREV.2010.05.003.
- [147] H. J. Stemmler *et al.*, “Ratio of trastuzumab levels in serum and cerebrospinal fluid is altered in HER2-positive breast cancer patients with brain metastases and impairment of blood-brain barrier,” *Anticancer. Drugs*, vol. 18, no. 1, pp. 23–28, Jan. 2007, doi: 10.1097/01.CAD.0000236313.50833.EE.
- [148] P. R. Lockman *et al.*, “Heterogeneous blood-tumor barrier permeability determines drug efficacy in experimental brain metastases of breast cancer,” *Clin. Cancer Res.*, vol. 16, no. 23, pp. 5664–5678, Dec. 2010, doi: 10.1158/1078-0432.CCR-10-1564.
- [149] A. P. Patel *et al.*, “Single-cell RNA-seq highlights intratumoral heterogeneity in primary glioblastoma,” *Science (80-. )*, vol. 344, no. 6190, pp. 1396–1401, Jun. 2014, doi: 10.1126/science.1254257.
- [150] C. M. Jackson *et al.*, “Mechanisms of immunotherapy resistance: lessons from glioblastoma,” *Nature Immunology*, vol. 20, no. 9. Nature Publishing Group, pp. 1100–1109, Sep. 01, 2019, doi: 10.1038/s41590-019-0433-y.
- [151] T. R. Hodges *et al.*, “Mutational burden, immune checkpoint expression, and mismatch repair in glioma: Implications for immune checkpoint immunotherapy,” *Neuro. Oncol.*, vol. 19, no. 8, pp. 1047–1057, Aug. 2017, doi: 10.1093/neuonc/nox026.
- [152] M. M. Gubin *et al.*, “Tumor neoantigens: Building a framework for personalized cancer immunotherapy,” *Journal of Clinical Investigation*, vol. 125, no. 9. American Society for Clinical Investigation, pp. 3413–3421, Sep. 01, 2015, doi: 10.1172/JCI80008.
- [153] A. M. Goodman *et al.*, “Tumor mutational burden as an independent predictor of response to immunotherapy in diverse cancers,” *Mol. Cancer Ther.*, vol. 16, no. 11, pp. 2598–2608, Nov. 2017, doi: 10.1158/1535-7163.MCT-17-0386.
- [154] P. N. Harter *et al.*, “Distribution and prognostic relevance of tumor-infiltrating lymphocytes (TILs) and PD-1/PD-L1 immune checkpoints in human brain metastases,” *Oncotarget*, vol. 6, no. 38, pp. 40836–40849, 2015, doi: 10.18632/ONCOTARGET.5696.
- [155] O. Bloch *et al.*, “Gliomas Promote Immunosuppression through Induction of B7-H1 Expression in Tumor-Associated Macrophages,” *Clin. Cancer Res.*, vol. 19, no. 12, pp. 3165–3175, Jun. 2013, doi: 10.1158/1078-0432.CCR-12-3314.
- [156] M. Chae *et al.*, “Increasing glioma-associated monocytes leads to increased intratumoral and systemic myeloid-derived suppressor cells in a murine model,” *Neuro. Oncol.*, vol. 17, no. 7, pp. 978–991, Jul. 2015, doi: 10.1093/neuonc/nou343.
- [157] A. Q. Sugihara *et al.*, “Regulatory T cells actively infiltrate metastatic brain tumors,” *Int. J. Oncol.*, vol. 34, no. 6, pp. 1533–1540, Jun. 2009, doi: 10.3892/ijo\_00000282.
- [158] B. C. Kennedy *et al.*, “Dynamics of central and peripheral immunomodulation in a murine glioma model,” *BMC Immunol.*, vol. 10, no. 1, pp. 1–8, Feb. 2009, doi: 10.1186/1471-2172-10-11.
- [159] R. Ueda *et al.*, “Systemic inhibition of transforming growth factor- $\beta$  in glioma-bearing mice improves the therapeutic efficacy of glioma-associated antigen peptide vaccines,” *Clin. Cancer Res.*, vol. 15, no. 21, pp.

- 6551–6559, Nov. 2009, doi: 10.1158/1078-0432.CCR-09-1067.
- [160] B. Kaminska *et al.*, “TGF beta signaling and its role in glioma pathogenesis,” *Adv. Exp. Med. Biol.*, vol. 986, pp. 171–187, 2013, doi: 10.1007/978-94-007-4719-7\_9.
- [161] D. A. Wainwright *et al.*, “IDO expression in brain tumors increases the recruitment of regulatory T cells and negatively impacts survival,” *Clin. Cancer Res.*, vol. 18, no. 22, pp. 6110–6121, Nov. 2012, doi: 10.1158/1078-0432.CCR-12-2130.
- [162] P. Chongsathidkiet *et al.*, “Sequestration of T cells in bone marrow in the setting of glioblastoma and other intracranial tumors,” *Nat. Med.*, vol. 24, no. 9, pp. 1459–1468, 2018, doi: 10.1038/s41591-018-0135-2 PM - 30104766 M4 - Citavi.
- [163] W. H. Meisen and B. Kaur, “How can we trick the immune system into overcoming the detrimental effects of oncolytic viral therapy to treat glioblastoma?,” *Expert Rev. Neurother.*, vol. 13, no. 4, pp. 341–343, Apr. 2013, doi: 10.1586/ERN.13.25.
- [164] I. Langers *et al.*, “Natural killer cells: role in local tumor growth and metastasis,” *Biologics*, vol. 6, p. 73, Apr. 2012, doi: 10.2147/BTT.S23976.
- [165] H. G. Ljunggren and K. Kärre, “Host resistance directed selectively against H-2-deficient lymphoma variants. Analysis of the mechanism,” *J. Exp. Med.*, vol. 162, no. 6, pp. 1745–1759, Dec. 1985, doi: 10.1084/JEM.162.6.1745.
- [166] K. S. Campbell *et al.*, “Natural killer cell biology: an update and future directions,” *J. Allergy Clin. Immunol.*, vol. 132, no. 3, pp. 536–544, Sep. 2013, doi: 10.1016/J.JACI.2013.07.006.
- [167] K. Imai *et al.*, “Natural cytotoxic activity of peripheral-blood lymphocytes and cancer incidence: an 11-year follow-up study of a general population,” *Lancet*, vol. 356, no. 9244, pp. 1795–1799, Nov. 2000, doi: 10.1016/S0140-6736(00)03231-1.
- [168] S. Coca *et al.*, “The prognostic significance of intratumoral natural killer cells in patients with colorectal carcinoma,” *Cancer*, vol. 79, no. 12, pp. 2320–2328, Jun. 1997, doi: 10.1002/(sici)1097-0142(19970615)79:12<2320::aid-cnrcr5>3.0.co;2-p.
- [169] S. Ishigami *et al.*, “Prognostic Value of Intratumoral Natural Killer Cells in Gastric Carcinoma,” 2000, doi: 10.1002/(SICI)1097-0142(20000201)88:3.
- [170] F. R. Villegas *et al.*, “Prognostic significance of tumor infiltrating natural killer cells subset CD57 in patients with squamous cell lung cancer,” *Lung Cancer*, vol. 35, no. 1, pp. 23–28, 2002, doi: 10.1016/S0169-5002(01)00292-6.
- [171] L. L. Lanier *et al.*, “Natural killer cells: definition of a cell type rather than a function,” *J. Immunol.*, vol. 137, no. 9, 1986.
- [172] L. L. Lanier *et al.*, “Identity of Leu-19 (CD56) leukocyte differentiation antigen and neural cell adhesion molecule,” *J. Exp. Med.*, vol. 169, no. 6, pp. 2233–2238, Jun. 1989, doi: 10.1084/JEM.169.6.2233.
- [173] T. Walzer *et al.*, “Identification, activation, and selective in vivo ablation of mouse NK cells via NKp46,” *Proc. Natl. Acad. Sci.*, vol. 104, no. 9, pp. 3384–3389, Feb. 2007, doi: 10.1073/PNAS.0609692104.
- [174] R. Kiessling *et al.*, “„Natural” killer cells in the mouse. I. Cytotoxic cells with specificity for mouse Moloney leukemia cells. Specificity and distribution according to genotype,” *Eur. J. Immunol.*, vol. 5, no. 2, pp. 112–117, Feb. 1975, doi: 10.1002/EJL.1830050208.
- [175] L. L. Lanier, “Up on the tightrope: natural killer cell activation and inhibition,” *Nat. Immunol.* 2008 95, vol. 9, no. 5, pp. 495–502, Apr. 2008, doi: 10.1038/ni1581.
- [176] J. A. Lopez *et al.*, “Perforin forms transient pores on the target cell plasma membrane to facilitate rapid access of granzymes during killer cell attack,” *Blood*, vol. 121, no. 14, pp. 2659–2668, Apr. 2013, doi:

- 10.1182/BLOOD-2012-07-446146.
- [177] R. H. P. Law *et al.*, "The structural basis for membrane binding and pore formation by lymphocyte perforin," *Nat.* 2010 4687322, vol. 468, no. 7322, pp. 447–451, Oct. 2010, doi: 10.1038/nature09518.
- [178] L. T. Quan *et al.*, "Proteolytic activation of the cell death protease Yama/CPP32 by granzyme B," *Proc. Natl. Acad. Sci.*, vol. 93, no. 5, pp. 1972–1976, Mar. 1996, doi: 10.1073/PNAS.93.5.1972.
- [179] F. Andrade *et al.*, "Granzyme B Directly and Efficiently Cleaves Several Downstream Caspase Substrates: Implications for CTL-Induced Apoptosis," *Immunity*, vol. 8, no. 4, pp. 451–460, Apr. 1998, doi: 10.1016/S1074-7613(00)80550-6.
- [180] M. Barry *et al.*, "Granzyme B Short-Circuits the Need for Caspase 8 Activity during Granule-Mediated Cytotoxic T-Lymphocyte Killing by Directly Cleaving Bid," *Mol. Cell. Biol.*, vol. 20, no. 11, pp. 3781–3794, Jun. 2000, doi: 10.1128/MCB.20.11.3781-3794.2000.
- [181] V. R. Sutton *et al.*, "Initiation of Apoptosis by Granzyme B Requires Direct Cleavage of Bid, but Not Direct Granzyme B-Mediated Caspase Activation," *J. Exp. Med.*, vol. 192, no. 10, pp. 1403–1414, Nov. 2000, doi: 10.1084/JEM.192.10.1403.
- [182] M. J. Smyth *et al.*, "Activation of NK cell cytotoxicity," *Mol. Immunol.*, vol. 42, no. 4, pp. 501–510, Feb. 2005, doi: 10.1016/J.MOLIMM.2004.07.034.
- [183] H. Stabile *et al.*, "Role of Distinct Natural Killer Cell Subsets in Anticancer Response," *Front. Immunol.*, vol. 0, no. MAR, p. 293, Mar. 2017, doi: 10.3389/FIMMU.2017.00293.
- [184] E. Rouvier *et al.*, "Fas involvement in Ca(2+)-independent T cell-mediated cytotoxicity," *J. Exp. Med.*, vol. 177, no. 1, pp. 195–200, Jan. 1993, doi: 10.1084/JEM.177.1.195.
- [185] D. Kagi *et al.*, "Fas and perforin pathways as major mechanisms of T cell-mediated cytotoxicity," *Science (80- )*, vol. 265, no. 5171, pp. 528–530, Jul. 1994, doi: 10.1126/SCIENCE.7518614.
- [186] A. Strasser *et al.*, "The Many Roles of FAS Receptor Signaling in the Immune System," *Immunity*, vol. 30, no. 2, pp. 180–192, Feb. 2009, doi: 10.1016/J.IMMUNI.2009.01.001.
- [187] T. Walzer *et al.*, "Natural-killer cells and dendritic cells: 'l'union fait la force,'" *Blood*, vol. 106, no. 7, pp. 2252–2258, Oct. 2005, doi: 10.1182/BLOOD-2005-03-1154.
- [188] K. Rajasekaran *et al.*, "Signaling in Effector Lymphocytes: Insights toward Safer Immunotherapy," *Front. Immunol.*, vol. 0, no. MAY, p. 176, 2016, doi: 10.3389/FIMMU.2016.00176.
- [189] C. Fauriat *et al.*, "Regulation of human NK-cell cytokine and chemokine production by target cell recognition," *Blood*, vol. 115, no. 11, pp. 2167–2176, Mar. 2010, doi: 10.1182/blood-2009-08-238469.
- [190] B. E. Freeman *et al.*, "Cytokine-Mediated Activation of NK Cells during Viral Infection," *J. Virol.*, vol. 89, no. 15, pp. 7922–7931, Aug. 2015, doi: 10.1128/JVI.00199-15.
- [191] Y. Zhang and B. Huang, "The Development and Diversity of ILCs, NK Cells and Their Relevance in Health and Diseases," *Adv. Exp. Med. Biol.*, vol. 1024, pp. 225–244, 2017, doi: 10.1007/978-981-10-5987-2\_11.
- [192] E. Vivier *et al.*, "Innate or Adaptive Immunity? The Example of Natural Killer Cells," *Science (80- )*, vol. 331, no. 6013, pp. 44–49, Jan. 2011, doi: 10.1126/SCIENCE.1198687.
- [193] K. D. Cook *et al.*, "NK Cells and Their Ability to Modulate T Cells during Virus Infections," *Crit. Rev. Immunol.*, vol. 34, no. 5, pp. 359–388, 2014, doi: 10.1615/CRITREVIMMUNOL.2014010604.
- [194] D. K. Blanchard *et al.*, "Production of granulocyte-macrophage colony-stimulating factor (GM-CSF) by monocyte and large granular lymphocytes stimulated with Mycobacterium avium-M. intracellulare: Activation of bactericidal activity by GM-CSF," *Infect. Immun.*, vol. 59, no. 7, pp. 2396–2402, 1991, doi: 10.1128/IAI.59.7.2396-2402.1991.

- [195] G. van den Bosch *et al.*, "Granulocyte-macrophage colony-stimulating factor (GM-CSF) counteracts the inhibiting effect of monocytes on natural killer (NK) cells," *Clin. Exp. Immunol.*, vol. 101, no. 3, pp. 515–520, Sep. 1995, doi: 10.1111/J.1365-2249.1995.TB03143.X.
- [196] Q. Liu *et al.*, "Neural stem cells sustain natural killer cells that dictate recovery from brain inflammation," *Nat. Neurosci.*, vol. 19, no. 2, pp. 243–252, Jan. 2016, doi: 10.1038/NN.4211.
- [197] I. Yang *et al.*, "Immune cell infiltrate differences in pilocytic astrocytoma and glioblastoma: evidence of distinct immunological microenvironments that reflect tumor biology," *J. Neurosurg.*, vol. 115, no. 3, pp. 505–511, Sep. 2011, doi: 10.3171/2011.4.JNS101172.
- [198] J. Kmiecik *et al.*, "Natural killer cells in intracranial neoplasms: presence and therapeutic efficacy against brain tumours," *J. Neurooncol.*, vol. 116, no. 1, p. 1, Jan. 2014, doi: 10.1007/S11060-013-1265-5.
- [199] J. Kmiecik *et al.*, "Elevated CD3+ and CD8+ tumor-infiltrating immune cells correlate with prolonged survival in glioblastoma patients despite integrated immunosuppressive mechanisms in the tumor microenvironment and at the systemic level," *J. Neuroimmunol.*, vol. 264, no. 1–2, pp. 71–83, 2013, doi: 10.1016/j.jneuroim.2013.08.013.
- [200] C. E. Fadul *et al.*, "Immune modulation effects of concomitant temozolomide and radiation therapy on peripheral blood mononuclear cells in patients with glioblastoma multiforme," *Neuro. Oncol.*, vol. 13, no. 4, pp. 393–400, Apr. 2011, doi: 10.1093/NEUONC/NOQ204.
- [201] R. D. Jachimowicz *et al.*, "Induction of in vitro and in vivo NK cell cytotoxicity using high-avidity immunoligands targeting prostate-specific membrane antigen in prostate carcinoma," *Mol. Cancer Ther.*, vol. 10, no. 6, pp. 1036–1045, Jun. 2011, doi: 10.1158/1535-7163.MCT-10-1093.
- [202] F. Ren *et al.*, "The R132H mutation in IDH1 promotes the recruitment of NK cells through CX3CL1/CX3CR1 chemotaxis and is correlated with a better prognosis in gliomas," *Immunol. Cell Biol.*, vol. 97, no. 5, pp. 457–469, May 2019, doi: 10.1111/IMCB.12225.
- [203] A. B. Barrow *et al.*, "Natural Killer Cells Control Tumor Growth by Sensing a Growth Factor," *Cell*, vol. 172, no. 3, pp. 534–548.e19, Jan. 2018, doi: 10.1016/J.CELL.2017.11.037.
- [204] A. D. Barrow and M. Colonna, "Exploiting NK Cell Surveillance Pathways for Cancer Therapy," *Cancers (Basel)*, vol. 11, no. 1, Jan. 2019, doi: 10.3390/CANCERS11010055.
- [205] E. Vauleon *et al.*, "Immune genes are associated with human glioblastoma pathology and patient survival," *BMC Med. Genomics*, vol. 5, 2012, doi: 10.1186/1755-8794-5-41.
- [206] M. Bockmayr *et al.*, "Immunologic Profiling of Mutational and Transcriptional Subgroups in Pediatric and Adult High-Grade Gliomas," *Cancer Immunol. Res.*, vol. 7, no. 9, pp. 1401–1411, 2019, doi: 10.1158/2326-6066.CIR-18-0939.
- [207] C. Zhu *et al.*, "Development and validation of an interferon signature predicting prognosis and treatment response for glioblastoma," *Oncoimmunology*, vol. 8, no. 9, Sep. 2019, doi: 10.1080/2162402X.2019.1621677.
- [208] S. J. Lee *et al.*, "Natural killer (NK) cells inhibit systemic metastasis of glioblastoma cells and have therapeutic effects against glioblastomas in the brain," *BMC Cancer*, vol. 15, no. 1, Dec. 2015, doi: 10.1186/S12885-015-2034-Y.
- [209] G. J. Baker *et al.*, "Natural killer cells require monocytic Gr-1(+)/CD11b(+) myeloid cells to eradicate orthotopically engrafted glioma cells," *Oncoimmunology*, vol. 5, no. 6, Jun. 2016, doi: 10.1080/2162402X.2016.1163461.
- [210] H. Mostafa *et al.*, "Immune phenotypes predict survival in patients with glioblastoma multiforme," *J. Hematol. Oncol.*, vol. 9, no. 1, Sep. 2016, doi: 10.1186/S13045-016-0272-3.
- [211] J. Fares *et al.*, "Immune checkpoint inhibitors: Advances and impact in neuro-oncology," *Surg. Neurol. Int.*,

- vol. 10, no. 1, Jan. 2019, doi: 10.4103/SNI.SNI\_366\_18.
- [212] H. Ogbomo *et al.*, “Immunotherapy in gliomas: limitations and potential of natural killer (NK) cell therapy,” *Trends Mol. Med.*, vol. 17, no. 8, pp. 433–441, Aug. 2011, doi: 10.1016/J.MOLMED.2011.03.004.
- [213] J. Hsu *et al.*, “Contribution of NK cells to immunotherapy mediated by PD-1/PD-L1 blockade,” *J. Clin. Invest.*, vol. 128, no. 10, pp. 4654–4668, Oct. 2018, doi: 10.1172/JCI99317.
- [214] K. Rezvani *et al.*, “Engineering Natural Killer Cells for Cancer Immunotherapy,” *Mol. Ther.*, vol. 25, no. 8, pp. 1769–1781, Aug. 2017, doi: 10.1016/J.YMTHE.2017.06.012.
- [215] T. Tonn *et al.*, “Treatment of patients with advanced cancer with the natural killer cell line NK-92,” *Cytotherapy*, vol. 15, no. 12, pp. 1563–1570, Dec. 2013, doi: 10.1016/J.JCYT.2013.06.017.
- [216] M. C. Burger *et al.*, “P04.05 The CAR2BRAIN study: a monocentric phase I trial with ErbB2-specific NK-92/5.28.z cells in recurrent glioblastoma,” *Neuro. Oncol.*, vol. 18, no. Suppl 4, p. iv24, Oct. 2016, doi: 10.1093/NEUONC/NOW188.083.
- [217] M. C. Burger *et al.*, “CAR-Engineered NK Cells for the Treatment of Glioblastoma: Turning Innate Effectors Into Precision Tools for Cancer Immunotherapy,” *Frontiers in Immunology*, vol. 10, Frontiers Media S.A., Nov. 14, 2019, doi: 10.3389/fimmu.2019.02683.
- [218] K. Schönfeld *et al.*, “Selective inhibition of tumor growth by clonal NK cells expressing an ErbB2/HER2-specific chimeric antigen receptor,” *Mol. Ther.*, vol. 23, no. 2, pp. 330–338, Feb. 2015, doi: 10.1038/mt.2014.219.
- [219] P. Nowakowska *et al.*, “Clinical grade manufacturing of genetically modified, CAR-expressing NK-92 cells for the treatment of ErbB2-positive malignancies,” *Cancer Immunol. Immunother.*, vol. 67, no. 1, pp. 25–38, Jan. 2018, doi: 10.1007/S00262-017-2055-2.
- [220] H. Klingemann *et al.*, “Natural Killer Cells for Immunotherapy – Advantages of the NK-92 Cell Line over Blood NK Cells,” *Front. Immunol.*, vol. 0, no. MAR, p. 91, Mar. 2016, doi: 10.3389/FIMMU.2016.00091.
- [221] C. Zhang *et al.*, “Chimeric Antigen Receptor-Engineered NK-92 Cells: An Off-the-Shelf Cellular Therapeutic for Targeted Elimination of Cancer Cells and Induction of Protective Antitumor Immunity,” *Front. Immunol.*, vol. 0, no. MAY, p. 533, May 2017, doi: 10.3389/FIMMU.2017.00533.
- [222] S. Genßler *et al.*, “Dual targeting of glioblastoma with chimeric antigen receptor-engineered natural killer cells overcomes heterogeneity of target antigen expression and enhances antitumor activity and survival,” *Oncoimmunology*, vol. 5, no. 4, Apr. 2015, doi: 10.1080/2162402X.2015.1119354.
- [223] F. Strassheimer *et al.*, “P04.21 Combination therapy of CAR-NK cells and anti-PD-1 antibody displays potent efficacy against late-stage Glioblastoma and induces protective antitumor immunity,” *Neuro. Oncol.*, vol. 20, no. Suppl 3, p. iii283, Sep. 2018, doi: 10.1093/NEUONC/NOY139.255.
- [224] W. Alexander, “The Checkpoint Immunotherapy Revolution: What Started as a Trickle Has Become a Flood, Despite Some Daunting Adverse Effects; New Drugs, Indications, and Combinations Continue to Emerge,” *Pharm. Ther.*, vol. 41, no. 3, p. 185, Mar. 2016, Accessed: Sep. 01, 2021. [Online]. Available: /pmc/articles/PMC4771089/.
- [225] C. Robert, “A decade of immune-checkpoint inhibitors in cancer therapy,” *Nat. Commun.* 2020 111, vol. 11, no. 1, pp. 1–3, Jul. 2020, doi: 10.1038/s41467-020-17670-y.
- [226] F. S. Hodi *et al.*, “Improved survival with ipilimumab in patients with metastatic melanoma,” *N. Engl. J. Med.*, vol. 363, no. 8, pp. 711–723, Aug. 2010, doi: 10.1056/NEJMOA1003466.
- [227] J. Larkin *et al.*, “Overall Survival in Patients With Advanced Melanoma Who Received Nivolumab Versus Investigator’s Choice Chemotherapy in CheckMate 037: A Randomized, Controlled, Open-Label Phase III Trial,” <https://doi.org/10.1200/JCO.2016.71.8023>, vol. 36, no. 4, pp. 383–390, Jul. 2017, doi:

- 10.1200/JCO.2016.71.8023.
- [228] S. McGettigan *et al.*, "Harnessing the Immune System in the Treatment of Melanoma," *J. Adv. Pract. Oncol.*, vol. 9, no. 7, Dec. 2018, doi: 10.6004/JADPRO.2018.9.7.11.
- [229] H. Mostafa *et al.*, "Immune phenotypes predict survival in patients with glioblastoma multiforme," *J. Hematol. Oncol.*, vol. 9, no. 1, Sep. 2016, doi: 10.1186/S13045-016-0272-3.
- [230] Z. Liu *et al.*, "Expression of the galectin-9-Tim-3 pathway in glioma tissues is associated with the clinical manifestations of glioma," *Oncol. Lett.*, vol. 11, no. 3, pp. 1829–1834, Mar. 2016, doi: 10.3892/OL.2016.4142.
- [231] C. Camisaschi *et al.*, "LAG-3 expression defines a subset of CD4(+)CD25(high)Foxp3(+) regulatory T cells that are expanded at tumor sites," *J. Immunol.*, vol. 184, no. 11, pp. 6545–6551, Jun. 2010, doi: 10.4049/JIMMUNOL.0903879.
- [232] K. Woroniecka *et al.*, "T-Cell Exhaustion Signatures Vary with Tumor Type and Are Severe in Glioblastoma," *Clin. Cancer Res.*, vol. 24, no. 17, pp. 4175–4186, Sep. 2018, doi: 10.1158/1078-0432.CCR-17-1846.
- [233] M. Vareki *et al.*, "Biomarkers of response to PD-1/PD-L1 inhibition," *Crit. Rev. Oncol. Hematol.*, vol. 116, pp. 116–124, Aug. 2017, doi: 10.1016/J.CRITREVNOC.2017.06.001.
- [234] A. Snyder *et al.*, "Genetic basis for clinical response to CTLA-4 blockade in melanoma," *N. Engl. J. Med.*, vol. 371, no. 23, pp. 2189–2199, Dec. 2014, doi: 10.1056/NEJMOA1406498.
- [235] N. A. Rizvi *et al.*, "Cancer immunology. Mutational landscape determines sensitivity to PD-1 blockade in non-small cell lung cancer," *Science*, vol. 348, no. 6230, pp. 124–128, Apr. 2015, doi: 10.1126/SCIENCE.AAA1348.
- [236] E. M. Van Allen *et al.*, "Genomic correlates of response to CTLA-4 blockade in metastatic melanoma," *Science*, vol. 350, no. 6257, pp. 207–211, Oct. 2015, doi: 10.1126/SCIENCE.AAD0095.
- [237] W. Hugo *et al.*, "Genomic and Transcriptomic Features of Response to Anti-PD-1 Therapy in Metastatic Melanoma," *Cell*, vol. 165, no. 1, pp. 35–44, Mar. 2016, doi: 10.1016/J.CELL.2016.02.065.
- [238] T. Jiang *et al.*, "Tumor neoantigens: from basic research to clinical applications," *J. Hematol. Oncol.* 2019 121, vol. 12, no. 1, pp. 1–13, Sep. 2019, doi: 10.1186/S13045-019-0787-5.
- [239] R. Zappasodi *et al.*, "Emerging Concepts for Immune Checkpoint Blockade-Based Combination Therapies," *Cancer Cell*, vol. 33, no. 4, pp. 581–598, Apr. 2018, doi: 10.1016/J.CCELL.2018.03.005.
- [240] T. F. Gajewski, "The Next Hurdle in Cancer Immunotherapy: Overcoming the Non-T-Cell-Inflamed Tumor Microenvironment," *Semin. Oncol.*, vol. 42, no. 4, pp. 663–671, Aug. 2015, doi: 10.1053/J.SEMINONCOL.2015.05.011.
- [241] R. M. Zemek *et al.*, "Sensitization to immune checkpoint blockade through activation of a STAT1/NK axis in the tumor microenvironment," *Sci. Transl. Med.*, vol. 11, no. 501, p. 7816, Jul. 2019, doi: 10.1126/SCITRANSLMED.AAV7816.
- [242] L. Wang *et al.*, "Tumor mutational burden is associated with poor outcomes in diffuse glioma," *BMC Cancer* 2020 201, vol. 20, no. 1, pp. 1–12, Mar. 2020, doi: 10.1186/S12885-020-6658-1.
- [243] E. K. Nduom *et al.*, "Immunosuppressive mechanisms in glioblastoma," *Neuro. Oncol.*, vol. 17 Suppl 7, pp. vii9–vii14, 2015, doi: 10.1093/neuonc/nov151 PM - 26516226 M4 - Citavi.
- [244] S. Wintterle *et al.*, "Expression of the B7-related molecule B7-H1 by glioma cells: a potential mechanism of immune paralysis," *undefined*, 2003.
- [245] P. E. Fecci *et al.*, "Systemic CTLA-4 blockade ameliorates glioma-induced changes to the CD4+ T cell compartment without affecting regulatory T-cell function," *Clin. Cancer Res.*, vol. 13, no. 7, pp. 2158–2167,

- 2007, doi: 10.1158/1078-0432.CCR-06-2070 PM - 17404100 M4 - Citavi.
- [246] J. V. Cohen and H. M. Kluger, "Systemic Immunotherapy for the Treatment of Brain Metastases," *Front. Oncol.*, vol. 6, no. MAR, 2016, doi: 10.3389/FONC.2016.00049.
- [247] P. E. Fecci *et al.*, "Immunotherapy for primary brain tumors: no longer a matter of privilege," *Clin. Cancer Res.*, vol. 20, no. 22, pp. 5620–5629, Nov. 2014, doi: 10.1158/1078-0432.CCR-14-0832.
- [248] J. S. Weber *et al.*, "Management of immune-related adverse events and kinetics of response with ipilimumab," *J. Clin. Oncol.*, vol. 30, no. 21, pp. 2691–2697, Jul. 2012, doi: 10.1200/JCO.2012.41.6750.
- [249] J. H. Sampson *et al.*, "Preliminary safety and activity of nivolumab and its combination with ipilimumab in recurrent glioblastoma (GBM): CHECKMATE-143.," *J. Clin. Oncol.*, vol. 33, no. 15\_suppl, pp. 3010–3010, May 2015, doi: 10.1200/jco.2015.33.15\_suppl.3010.
- [250] A. Omuro *et al.*, "Nivolumab with or without ipilimumab in patients with recurrent glioblastoma: Results from exploratory phase i cohorts of CheckMate 143," *Neuro. Oncol.*, vol. 20, no. 5, pp. 674–686, Apr. 2018, doi: 10.1093/neuonc/nox208.
- [251] R. C. Münch *et al.*, "Off-target-free gene delivery by affinity-purified receptor-targeted viral vectors," *Nat. Commun.*, vol. 6, no. 1, p. 6246, Dec. 2015, doi: 10.1038/ncomms7246.
- [252] C. E. Dunbar *et al.*, "Gene therapy comes of age," *Science*, vol. 359, no. 6372, Jan. 2018, doi: 10.1126/SCIENCE.AAN4672.
- [253] M. A. Kotterman *et al.*, "Viral Vectors for Gene Therapy: Translational and Clinical Outlook," *Annu. Rev. Biomed. Eng.*, vol. 17, pp. 63–89, Dec. 2015, doi: 10.1146/ANNUREV-BIOENG-071813-104938.
- [254] K. Lundstrom, "Gene Therapy Applications of Viral Vectors;," <http://dx.doi.org/10.1177/153303460400300508>, vol. 3, no. 5, pp. 467–477, Jun. 2016, doi: 10.1177/153303460400300508.
- [255] M. A. Kay, "State-of-the-art gene-based therapies: the road ahead," *Nat. Rev. Genet.*, vol. 12, no. 5, pp. 316–328, May 2011, doi: 10.1038/NRG2971.
- [256] M. Cavazzana-Calvo *et al.*, "Gene therapy of human severe combined immunodeficiency (SCID)-X1 disease," *Science*, vol. 288, no. 5466, pp. 669–672, Apr. 2000, doi: 10.1126/SCIENCE.288.5466.669.
- [257] A. Aiuti and M. G. Roncarolo, "Ten years of gene therapy for primary immune deficiencies," *Hematology*, vol. 2009, no. 1, pp. 682–689, Jan. 2009, doi: 10.1182/ASHEDUCATION-2009.1.682.
- [258] S. Hacein-Bey-Abina *et al.*, "LMO2-associated clonal T cell proliferation in two patients after gene therapy for SCID-X1," *Science*, vol. 302, no. 5644, pp. 415–419, Oct. 2003, doi: 10.1126/SCIENCE.1088547.
- [259] S. Stein *et al.*, "Genomic instability and myelodysplasia with monosomy 7 consequent to EVI1 activation after gene therapy for chronic granulomatous disease," *Nat. Med.*, vol. 16, no. 2, pp. 198–204, Feb. 2010, doi: 10.1038/NM.2088.
- [260] S. J. Howe *et al.*, "Insertional mutagenesis combined with acquired somatic mutations causes leukemogenesis following gene therapy of SCID-X1 patients," *J. Clin. Invest.*, vol. 118, no. 9, pp. 3143–3150, Sep. 2008, doi: 10.1172/JCI35798.
- [261] H. Büning *et al.*, "Recent developments in adeno-associated virus vector technology," *Journal of Gene Medicine*, vol. 10, no. 7, pp. 717–733, Jul. 2008, doi: 10.1002/jgm.1205.
- [262] F. Mingozzi and K. A. High, "Therapeutic in vivo gene transfer for genetic disease using AAV: Progress and challenges," *Nature Reviews Genetics*, vol. 12, no. 5, pp. 341–355, May 2011, doi: 10.1038/nrg2988.
- [263] Z. Wu *et al.*, "Adeno-associated virus serotypes: vector toolkit for human gene therapy," *Mol. Ther.*, vol. 14, no. 3, pp. 316–327, Sep. 2006, doi: 10.1016/J.YMTHE.2006.05.009.



- [264] E. Hastie and R. J. Samulski, "Adeno-associated virus at 50: a golden anniversary of discovery, research, and gene therapy success--a personal perspective," *Hum. Gene Ther.*, vol. 26, no. 5, pp. 257–265, May 2015, doi: 10.1089/HUM.2015.025.
- [265] C. Li and R. J. Samulski, "Engineering adeno-associated virus vectors for gene therapy," *Nat. Rev. Genet.* 2020 214, vol. 21, no. 4, pp. 255–272, Feb. 2020, doi: 10.1038/s41576-019-0205-4.
- [266] R. W. Atchison *et al.*, "Adenovirus-associated defective virus particles," *Science (80-. )*, vol. 149, no. 3685, pp. 754–756, 1965, doi: 10.1126/SCIENCE.149.3685.754.
- [267] T. Gaj *et al.*, "Genome engineering using Adeno-associated virus: Basic and clinical research applications," *Mol. Ther.*, vol. 24, no. 3, pp. 458–464, Mar. 2016, doi: 10.1038/MT.2015.151.
- [268] "Atomic structure of Adeno-Associated Virus (PDB 1LP3), a vector for Stock Photo - Alamy." <https://www.alamy.com/stock-photo-atomic-structure-of-adeno-associated-virus-pdb-1lp3-a-vector-for-human-52098472.html> (accessed Sep. 01, 2021).
- [269] H. Büning, "Gene therapy enters the pharma market: the short story of a long journey," *EMBO Mol. Med.*, vol. 5, no. 1, pp. 1–3, Jan. 2013, doi: 10.1002/EMMM.201202291.
- [270] S. Ylä-Herttuala, "Endgame: Glybera Finally Recommended for Approval as the First Gene Therapy Drug in the European Union," *Mol. Ther.*, vol. 20, no. 10, p. 1831, Oct. 2012, doi: 10.1038/MT.2012.194.
- [271] E. Smalley, "First AAV gene therapy poised for landmark approval," *Nat. Biotechnol.*, vol. 35, no. 11, pp. 998–999, Nov. 2017, doi: 10.1038/NBT1117-998.
- [272] A. M. Keeler and T. R. Flotte, "Recombinant Adeno-Associated Virus Gene Therapy in Light of Luxturna (and Zolgensma and Glybera): Where Are We, and How Did We Get Here?," *Annu. Rev. Virol.*, vol. 6, no. 1, p. 601, Sep. 2019, doi: 10.1146/ANNUREV-VIROLOGY-092818-015530.
- [273] "Statement from FDA Commissioner Scott Gottlieb, M.D. and Peter Marks, M.D., Ph.D., Director of the Center for Biologics Evaluation and Research on new policies to advance development of safe and effective cell and gene therapies | FDA." <https://www.fda.gov/news-events/press-announcements/statement-fda-commissioner-scott-gottlieb-md-and-peter-marks-md-phd-director-center-biologics> (accessed Sep. 01, 2021).
- [274] B. Dong *et al.*, "Characterization of genome integrity for oversized recombinant AAV vector," *Mol. Ther.*, vol. 18, no. 1, pp. 87–92, Jan. 2010, doi: 10.1038/MT.2009.258.
- [275] S. K. Powell *et al.*, "Viral expression cassette elements to enhance transgene target specificity and expression in gene therapy," *Discov. Med.*, vol. 19, no. 102, pp. 49–57, 2015, Accessed: Sep. 01, 2021. [Online]. Available: <https://pubmed.ncbi.nlm.nih.gov/25636961/>.
- [276] R. Waehler *et al.*, "Engineering targeted viral vectors for gene therapy," *Nature Reviews Genetics*, vol. 8, no. 8, pp. 573–587, Aug. 03, 2007, doi: 10.1038/nrg2141.
- [277] G. Gao *et al.*, "Clades of Adeno-associated viruses are widely disseminated in human tissues," *J. Virol.*, vol. 78, no. 12, pp. 6381–8, Jun. 2004, doi: 10.1128/JVI.78.12.6381-6388.2004.
- [278] A. C. Nathwani *et al.*, "Long-term safety and efficacy following systemic administration of a self-complementary AAV vector encoding human FIX pseudotyped with serotype 5 and 8 capsid proteins," *Mol. Ther.*, vol. 19, no. 5, pp. 876–885, May 2011, doi: 10.1038/mt.2010.274.
- [279] A. Toromanoff *et al.*, "Safety and efficacy of regional intravenous (RI) versus intramuscular (IM) delivery of rAAV1 and rAAV8 to nonhuman primate skeletal muscle," *Mol. Ther.*, vol. 16, no. 7, pp. 1291–1299, Jul. 2008, doi: 10.1038/mt.2008.87.
- [280] K. B. Kaufmann *et al.*, "Gene therapy on the move," *EMBO Mol. Med.*, vol. 5, no. 11, pp. 1642–1661, Nov. 2013, doi: 10.1002/emmm.201202287.

- [281] M. Izmirli *et al.*, "The war against cancer: Suicide gene therapy," *Adv. Mod. Oncol. Res.*, vol. 2, no. 3, pp. 139–149, Jun. 2016, doi: 10.18282/AMOR.V2.I3.103.
- [282] A. M. Rossor *et al.*, "Antisense oligonucleotides and other genetic therapies made simple," *Pract. Neurol.*, vol. 18, no. 2, pp. 126–131, Apr. 2018, doi: 10.1136/PRACTNEUROL-2017-001764.
- [283] J. Y. Shin *et al.*, "Aerosol delivery of beclin1 enhanced the anti-tumor effect of radiation in the lungs of K-rasLA1 mice," *J. Radiat. Res.*, vol. 53, no. 4, pp. 506–515, 2012, doi: 10.1093/JRR/RRS005.
- [284] Y. Liu *et al.*, "Efficacy of adenovirally expressed soluble TRAIL in human glioma organotypic slice culture and glioma xenografts," *Cell Death Dis.*, vol. 2, no. 2, Feb. 2011, doi: 10.1038/CDDIS.2010.95.
- [285] J. Wojas-Turek *et al.*, "Antitumor effect of murine dendritic and tumor cells transduced with IL-2 gene," *Folia Histochem. Cytobiol.*, vol. 50, no. 3, pp. 414–419, Oct. 2012, doi: 10.5603/19750.
- [286] S. Hallaj-Nezhadi *et al.*, "Nanoparticle-mediated interleukin-12 cancer gene therapy," *J. Pharm. Pharm. Sci.*, vol. 13, no. 3, pp. 472–485, 2010, doi: 10.18433/J3630V.
- [287] P. Zarogoulidis *et al.*, "Suicide Gene Therapy for Cancer – Current Strategies," *J. Genet. Syndr. Gene Ther.*, vol. 4, no. 04, 2013, doi: 10.4172/2157-7412.1000139.
- [288] J. A. Hossain *et al.*, "Suicide gene therapy for the treatment of high-grade glioma: past lessons, present trends, and future prospects," *Neuro-Oncology Adv.*, vol. 2, no. 1, pp. 1–12, Jan. 2020, doi: 10.1093/NOAJNL/VDAA013.
- [289] H. C. Verdara *et al.*, "AAV Vector Immunogenicity in Humans: A Long Journey to Successful Gene Transfer," *Mol. Ther.*, vol. 28, no. 3, pp. 723–746, Mar. 2020, doi: 10.1016/J.YMTHE.2019.12.010.
- [290] H. Büning *et al.*, "Engineering the AAV capsid to optimize vector-host-interactions," *Curr. Opin. Pharmacol.*, vol. 24, pp. 94–104, Oct. 2015, doi: 10.1016/J.COPH.2015.08.002.
- [291] T. Gjetting *et al.*, "In vitro and in vivo effects of polyethylene glycol (PEG)-modified lipid in DOTAP/cholesterol-mediated gene transfection," *Int. J. Nanomedicine*, vol. 5, no. 1, pp. 371–383, 2010, doi: 10.2147/IJN.S10462.
- [292] C. Tros de Ilarduya *et al.*, "Gene delivery by lipoplexes and polyplexes," *Eur. J. Pharm. Sci.*, vol. 40, no. 3, pp. 159–170, Jun. 2010, doi: 10.1016/J.EJPS.2010.03.019.
- [293] L. Liu *et al.*, "Advances in viral-vector systemic cytokine gene therapy against cancer," *Vaccine*, vol. 28, no. 23, pp. 3883–3887, May 2010, doi: 10.1016/J.VACCINE.2010.03.041.
- [294] D. Chen *et al.*, "Insulin-like growth factor-binding protein-7 (IGFBP7): a promising gene therapeutic for hepatocellular carcinoma (HCC)," *Mol. Ther.*, vol. 21, no. 4, pp. 758–766, 2013, doi: 10.1038/MT.2012.282.
- [295] X. Zeng *et al.*, "Recombinant adenovirus carrying the hepatocyte nuclear factor-1alpha gene inhibits hepatocellular carcinoma xenograft growth in mice," *Hepatology*, vol. 54, no. 6, pp. 2036–2047, Dec. 2011, doi: 10.1002/HEP.24647.
- [296] L. Zhao *et al.*, "Local gene delivery for cancer therapy," *Curr. Gene Ther.*, vol. 11, no. 5, pp. 423–432, Nov. 2011, doi: 10.2174/156652311797415854.
- [297] R. C. Münch *et al.*, "Displaying high-affinity ligands on adeno-associated viral vectors enables tumor cell-specific and safe gene transfer," *Mol. Ther.*, vol. 21, no. 1, pp. 109–118, Jan. 2013, doi: 10.1038/mt.2012.186.
- [298] C. J. Buchholz *et al.*, "Surface-Engineered Viral Vectors for Selective and Cell Type-Specific Gene Delivery," *Trends Biotechnol.*, vol. 33, no. 12, pp. 777–790, Dec. 2015, doi: 10.1016/J.TIBTECH.2015.09.008.
- [299] J. Boucas *et al.*, "Engineering adeno-associated virus serotype 2-based targeting vectors using a new insertion site-position 453-and single point mutations," *J. Gene Med.*, vol. 11, no. 12, pp. 1103–1113, Dec. 2009, doi: 10.1002/jgm.1392.

- [300] A. Kern *et al.*, "Identification of a Heparin-Binding Motif on Adeno-Associated Virus Type 2 Capsids," *J. Virol.*, vol. 77, no. 20, pp. 11072–11081, Oct. 2003, doi: 10.1128/jvi.77.20.11072-11081.2003.
- [301] S. R. Opie *et al.*, "Identification of Amino Acid Residues in the Capsid Proteins of Adeno-Associated Virus Type 2 That Contribute to Heparan Sulfate Proteoglycan Binding," *J. Virol.*, vol. 77, no. 12, pp. 6995–7006, Jun. 2003, doi: 10.1128/jvi.77.12.6995-7006.2003.
- [302] K. Lux *et al.*, "Green Fluorescent Protein-Tagged Adeno-Associated Virus Particles Allow the Study of Cytosolic and Nuclear Trafficking," *J. Virol.*, vol. 79, no. 18, pp. 11776–11787, Sep. 2005, doi: 10.1128/jvi.79.18.11776-11787.2005.
- [303] V. Mitropoulos *et al.*, "The interfacial behavior of designed ankyrin repeat proteins," doi: 10.1039/c1sm05256j.
- [304] M. T. Stumpp *et al.*, "DARPin: A new generation of protein therapeutics," *Drug Discov. Today*, vol. 13, no. 15–16, pp. 695–701, Aug. 2008, doi: 10.1016/J.DRUDIS.2008.04.013.
- [305] H. K. Binz *et al.*, "High-affinity binders selected from designed ankyrin repeat protein libraries," *Nat. Biotechnol.*, vol. 22, no. 5, pp. 575–582, May 2004, doi: 10.1038/nbt962.
- [306] M. T. Stumpp *et al.*, "DARPin: A new generation of protein therapeutics," *Drug Discovery Today*, vol. 13, no. 15–16, pp. 695–701, Aug. 2008, doi: 10.1016/j.drudis.2008.04.013.
- [307] J. Hartmann *et al.*, "A Library-Based Screening Strategy for the Identification of DARPins as Ligands for Receptor-Targeted AAV and Lentiviral Vectors," *Mol. Ther. - Methods Clin. Dev.*, vol. 10, pp. 128–143, Sep. 2018, doi: 10.1016/j.omtm.2018.07.001.
- [308] A. Plückthun, "Designed ankyrin repeat proteins (DARPins): binding proteins for research, diagnostics, and therapy," *Annu. Rev. Pharmacol. Toxicol.*, vol. 55, pp. 489–511, Jan. 2015, doi: 10.1146/ANNUREV-PHARMTOX-010611-134654.
- [309] D. Steiner *et al.*, "Efficient Selection of DARPins with Sub-nanomolar Affinities using SRP Phage Display," *J. Mol. Biol.*, vol. 382, no. 5, pp. 1211–1227, Oct. 2008, doi: 10.1016/j.jmb.2008.07.085.
- [310] J. Reul *et al.*, "Tumor-Specific Delivery of Immune Checkpoint Inhibitors by Engineered AAV Vectors," *Front. Oncol.*, vol. 9, p. 52, Feb. 2019, doi: 10.3389/fonc.2019.00052.
- [311] J. Reul, "Viral gene transfer systems for cancer immunotherapy: semireplication-competent VSV and receptor-targeted AAV for the delivery of immunomodulatory proteins," 2019.
- [312] E. Blasi *et al.*, "Immortalization of murine microglial cells by a v-raf/v-myc carrying retrovirus," *J. Neuroimmunol.*, vol. 27, no. 2–3, pp. 229–237, 1990, doi: 10.1016/0165-5728(90)90073-V.
- [313] Y. Garcia-Mesa *et al.*, "Immortalization of primary microglia: a new platform to study HIV regulation in the central nervous system," *J. Neurovirol.*, vol. 23, no. 1, pp. 47–66, Feb. 2017, doi: 10.1007/S13365-016-0499-3.
- [314] W. S. Walker *et al.*, "Mouse microglial cell lines differing in constitutive and interferon- $\gamma$ -inducible antigen-presenting activities for naive and memory CD4+ and CD8+ T cells," *J. Neuroimmunol.*, vol. 63, no. 2, pp. 163–174, Dec. 1995, doi: 10.1016/0165-5728(95)00146-8.
- [315] Y. M. Li *et al.*, "Upregulation of CXCR4 is essential for HER2-mediated tumor metastasis," *Cancer Cell*, vol. 6, no. 5, pp. 459–469, 2004, doi: 10.1016/J.CCR.2004.09.027.
- [316] N. Janabi *et al.*, "Establishment of human microglial cell lines after transfection of primary cultures of embryonic microglial cells with the SV40 large T antigen," *Neurosci. Lett.*, vol. 195, no. 2, pp. 105–108, Aug. 1995, doi: 10.1016/0304-3940(94)11792-H.
- [317] J. P. Steinbach *et al.*, "Inhibition of epidermal growth factor receptor signaling protects human malignant glioma cells from hypoxia-induced cell death," *Cancer Res.*, vol. 64, no. 5, pp. 1575–1578, Mar. 2004, doi:

- 10.1158/0008-5472.CAN-03-3775.
- [318] Y. Sonoda *et al.*, "Formation of intracranial tumors by genetically modified human astrocytes defines four pathways critical in the development of human anaplastic astrocytoma," *Cancer Res.*, vol. 61, no. 13, pp. 4956–4960, Jul. 2001.
- [319] J. E. Grady *et al.*, "An Improved Tissue Culture Assay III. Alternate Methods for Measuring Cell Growth," *Cancer Res.*, vol. 20, no. 7, 1960.
- [320] J. P. Steinbach *et al.*, "Hypoxia-induced cell death in human malignant glioma cells: energy deprivation promotes decoupling of mitochondrial cytochrome c release from caspase processing and necrotic cell death," *Cell Death Differ.* 2003 107, vol. 10, no. 7, pp. 823–832, Jun. 2003, doi: 10.1038/sj.cdd.4401252.
- [321] C. Sahm *et al.*, "Expression of IL-15 in NK cells results in rapid enrichment and selective cytotoxicity of gene-modified effectors that carry a tumor-specific antigen receptor," *Cancer Immunol. Immunother.*, vol. 61, no. 9, pp. 1451–1461, Sep. 2012, doi: 10.1007/S00262-012-1212-X.
- [322] W. H. Chae *et al.*, "Evaluating Magnetic Resonance Spectroscopy as a Tool for Monitoring Therapeutic Response of Whole Brain Radiotherapy in a Mouse Model for Breast-to-Brain Metastasis," *Front. Oncol.*, vol. 9, Nov. 2019, doi: 10.3389/FONC.2019.01324.
- [323] C. Böttcher *et al.*, "Human microglia regional heterogeneity and phenotypes determined by multiplexed single-cell mass cytometry," *Nat. Neurosci.*, vol. 22, no. 1, pp. 78–90, Jan. 2019, doi: 10.1038/S41593-018-0290-2.
- [324] B. A. Jones *et al.*, "Fractalkine/CX3CL1: a potential new target for inflammatory diseases," *Mol. Interv.*, vol. 10, no. 5, pp. 263–270, Oct. 2010, doi: 10.1124/MI.10.5.3.
- [325] J. Marschallinger *et al.*, "Lipid-droplet-accumulating microglia represent a dysfunctional and proinflammatory state in the aging brain," *Nat. Neurosci.*, vol. 23, no. 2, pp. 194–208, Feb. 2020, doi: 10.1038/S41593-019-0566-1.
- [326] T. Zrzavy *et al.*, "Pro-inflammatory activation of microglia in the brain of patients with sepsis," *Neuropathol. Appl. Neurobiol.*, vol. 45, no. 3, pp. 278–290, Apr. 2019, doi: 10.1111/NAN.12502.
- [327] M. Prinz *et al.*, "Ontogeny and homeostasis of CNS myeloid cells," *Nat. Immunol.*, vol. 18, no. 4, pp. 385–392, Mar. 2017, doi: 10.1038/NI.3703.
- [328] M. Greter *et al.*, "Microglia Versus Myeloid Cell Nomenclature during Brain Inflammation," *Front. Immunol.*, vol. 6, no. MAY, 2015, doi: 10.3389/FIMMU.2015.00249.
- [329] V. M. Braud *et al.*, "HLA-E binds to natural killer cell receptors CD94/NKG2A, B and C," *Nature*, vol. 391, no. 6669, pp. 795–799, Feb. 1998, doi: 10.1038/35869.
- [330] D. Ghosh *et al.*, "Combination therapy to checkmate Glioblastoma: clinical challenges and advances," *Clin. Transl. Med.*, vol. 7, no. 1, p. 33, Dec. 2018, doi: 10.1186/S40169-018-0211-8.
- [331] R. B. Mokhtari *et al.*, "Combination therapy in combating cancer," *Oncotarget*, vol. 8, no. 23, pp. 38022–38043, 2017, doi: 10.18632/ONCOTARGET.16723.
- [332] "Novartis receives first ever FDA approval for a CAR-T cell therapy, Kymriah(TM) (CTL019), for children and young adults with B-cell ALL that is refractory or has relapsed at least twice | Novartis." <https://www.novartis.com/news/media-releases/novartis-receives-first-ever-fda-approval-car-t-cell-therapy-kymriah-tm-ctl019-children-and-young-adults-b-cell-all-refractory-or-has-relapsed-least-twice> (accessed Dec. 05, 2021).
- [333] J. Hartmann *et al.*, "Clinical development of CAR T cells-challenges and opportunities in translating innovative treatment concepts," *EMBO Mol. Med.*, vol. 9, no. 9, pp. 1183–1197, Sep. 2017, doi: 10.15252/EMMM.201607485.

- [334] V. A. Chow *et al.*, "Outcomes of patients with large B-cell lymphomas and progressive disease following CD19-specific CAR T-cell therapy," *Am. J. Hematol.*, vol. 94, no. 8, p. E209, Aug. 2019, doi: 10.1002/AJH.25505.
- [335] F. Marofi *et al.*, "CAR-NK Cell: A New Paradigm in Tumor Immunotherapy," *Front. Oncol.*, vol. 11, Jun. 2021, doi: 10.3389/FONC.2021.673276.
- [336] P. S. A. Becker *et al.*, "Selection and expansion of natural killer cells for NK cell-based immunotherapy," *Cancer Immunol. Immunother.*, vol. 65, no. 4, pp. 477–484, Apr. 2016, doi: 10.1007/S00262-016-1792-Y.
- [337] E. Liu *et al.*, "Use of CAR-Transduced Natural Killer Cells in CD19-Positive Lymphoid Tumors," *N. Engl. J. Med.*, vol. 382, no. 6, pp. 545–553, Feb. 2020, doi: 10.1056/NEJM0A1910607.
- [338] T. Bald *et al.*, "The NK cell–cancer cycle: advances and new challenges in NK cell-based immunotherapies," *Nat. Immunol. 2020 218*, vol. 21, no. 8, pp. 835–847, Jul. 2020, doi: 10.1038/s41590-020-0728-z.
- [339] W. Widowati *et al.*, "Effect of interleukins (IL-2, il-15, il-18) on receptors activation and cytotoxic activity of natural killer cells in breast cancer cell," *Afr. Health Sci.*, vol. 20, no. 2, pp. 822–832, Jun. 2020, doi: 10.4314/AHS.V20I2.36.
- [340] J. Han *et al.*, "CAR-Engineered NK Cells Targeting Wild-Type EGFR and EGFRvIII Enhance Killing of Glioblastoma and Patient-Derived Glioblastoma Stem Cells," *Sci. Rep.*, vol. 5, Jul. 2015, doi: 10.1038/SREP11483.
- [341] N. Müller *et al.*, "Engineering NK cells modified with an EGFRvIII-specific chimeric antigen receptor to overexpress CXCR4 improves immunotherapy of CXCL12/SDF-1 $\alpha$ -secreting glioblastoma," *J. Immunother.*, vol. 38, no. 5, p. 197, May 2015, doi: 10.1097/CJI.0000000000000082.
- [342] J. A. Myers and J. S. Miller, "Exploring the NK cell platform for cancer immunotherapy," *Nat. Rev. Clin. Oncol.*, vol. 18, no. 2, pp. 85–100, Feb. 2021, doi: 10.1038/S41571-020-0426-7.
- [343] C. M. Suryadevara *et al.*, "Immunotherapy Gone Viral: Bortezomib and oHSV Enhance Antitumor NK-Cell Activity," *Clin. Cancer Res.*, vol. 22, no. 21, pp. 5164–5166, Nov. 2016, doi: 10.1158/1078-0432.CCR-16-1666.
- [344] K. C. Barry *et al.*, "A natural killer–dendritic cell axis defines checkpoint therapy–responsive tumor microenvironments," *Nat. Med. 2018 248*, vol. 24, no. 8, pp. 1178–1191, Jun. 2018, doi: 10.1038/s41591-018-0085-8.
- [345] D. A. Reardon *et al.*, "Glioblastoma Eradication Following Immune Checkpoint Blockade in an Orthotopic, Immunocompetent Model," *Cancer Immunol. Res.*, vol. 4, no. 2, pp. 124–135, Feb. 2016, doi: 10.1158/2326-6066.CIR-15-0151.
- [346] H. Ding *et al.*, "Distinct mechanisms of membrane permeation induced by two polymeric acid copolymers," *Biomaterials*, vol. 34, no. 1, pp. 217–225, Jan. 2013, doi: 10.1016/J.BIOMATERIALS.2012.08.016.
- [347] A. Galstyan *et al.*, "Blood-brain barrier permeable nano immunoconjugates induce local immune responses for glioma therapy," *Nat. Commun.*, vol. 10, no. 1, Dec. 2019, doi: 10.1038/S41467-019-11719-3.
- [348] M. Lin *et al.*, "Pembrolizumab plus allogeneic NK cells in advanced non–small cell lung cancer patients," *J. Clin. Invest.*, vol. 130, no. 5, pp. 2560–2569, May 2020, doi: 10.1172/JCI132712.
- [349] R. D. Zhang *et al.*, "Differential permeability of the blood-brain barrier in experimental brain metastases produced by human neoplasms implanted into nude mice.," *Am. J. Pathol.*, vol. 141, no. 5, p. 1115, 1992, Accessed: Dec. 08, 2021. [Online]. Available: /pmc/articles/PMC1886664/?report=abstract.
- [350] Y. Li *et al.*, "Endothelial apoptosis initiates acute blood-brain barrier disruption after ionizing radiation.,"

- undefined*, 2003.
- [351] T. Weiss *et al.*, “NKG2D-Based CAR T Cells and Radiotherapy Exert Synergistic Efficacy in Glioblastoma,” *Cancer Res.*, vol. 78, no. 4, pp. 1031–1043, Feb. 2018, doi: 10.1158/0008-5472.CAN-17-1788.
- [352] S. O. Ciurea *et al.*, “Phase 1 clinical trial using mbIL21 ex vivo-expanded donor-derived NK cells after haploidentical transplantation,” *Blood*, vol. 130, no. 16, p. 1857, Oct. 2017, doi: 10.1182/BLOOD-2017-05-785659.
- [353] F. Concha-Benavente *et al.*, “PD-L1 Mediates Dysfunction in Activated PD-1 + NK Cells in Head and Neck Cancer Patients,” *Cancer Immunol. Res.*, vol. 6, no. 12, pp. 1548–1560, Dec. 2018, doi: 10.1158/2326-6066.CIR-18-0062.
- [354] O. Melaiu *et al.*, “Influence of the Tumor Microenvironment on NK Cell Function in Solid Tumors,” *Front. Immunol.*, vol. 10, Jan. 2020, doi: 10.3389/FIMMU.2019.03038.
- [355] A. Yilmaz *et al.*, “Chimeric antigen receptor-engineered natural killer cells for cancer immunotherapy,” *J. Hematol. Oncol.*, vol. 13, no. 1, Dec. 2020, doi: 10.1186/S13045-020-00998-9.
- [356] R. A. Morgan *et al.*, “Case report of a serious adverse event following the administration of T cells transduced with a chimeric antigen receptor recognizing ERBB2,” *Mol. Ther.*, vol. 18, no. 4, pp. 843–851, Apr. 2010, doi: 10.1038/MT.2010.24.
- [357] N. Ahmed *et al.*, “Human Epidermal Growth Factor Receptor 2 (HER2) -Specific Chimeric Antigen Receptor-Modified T Cells for the Immunotherapy of HER2-Positive Sarcoma,” *J. Clin. Oncol.*, vol. 33, no. 15, pp. 1688–1696, May 2015, doi: 10.1200/JCO.2014.58.0225.
- [358] J. G. Zhang *et al.*, “Antigenic Profiling of Glioma Cells to Generate Allogeneic Vaccines or Dendritic Cell-Based Therapeutics,” *Clin. Cancer Res.*, vol. 13, no. 2, pp. 566–575, Jan. 2007, doi: 10.1158/1078-0432.CCR-06-1576.
- [359] J. Chen *et al.*, “A role for erbb signaling in the induction of reactive astrogliosis,” *Cell Discov.*, vol. 3, no. 1, 2017, doi: 10.1038/CELLDISC.2017.44.
- [360] “Tissue expression of ERBB2 - Summary - The Human Protein Atlas.” <https://www.proteinatlas.org/ENSG00000141736-ERBB2/tissue> (accessed Nov. 13, 2021).
- [361] G. Dranoff, “GM-CSF-based cancer vaccines,” *Immunol. Rev.*, vol. 188, pp. 147–154, Oct. 2002, doi: 10.1034/J.1600-065X.2002.18813.X.
- [362] C. Harrison, “Calming the cytokine storm,” *Nat. Rev. Drug Discov.* 2010 95, vol. 9, no. 5, pp. 360–361, May 2010, doi: 10.1038/nrd3162.
- [363] N. Sakamoto *et al.*, “Phase I clinical trial of autologous NK cell therapy using novel expansion method in patients with advanced digestive cancer,” *J. Transl. Med.*, vol. 13, no. 1, Aug. 2015, doi: 10.1186/S12967-015-0632-8.
- [364] H. U. Zellhofer “Role of interleukin-8 in neutrophil signaling,” *Curr. Opin. Hematol.*, vol. 7, no. 3, pp. 178–182, 2000, doi: 10.1097/00062752-200005000-00009.
- [365] G. Lin *et al.*, “Interleukin-6 inhibits regulatory T cells and improves the proliferation and cytotoxic activity of cytokine-induced killer cells,” *J. Immunother.*, vol. 35, no. 4, pp. 337–343, May 2012, doi: 10.1097/CJI.0B013E318255ADA3.
- [366] A. Kimura and T. Kimura, “IL-6: regulator of Treg/Th17 balance,” *Eur. J. Immunol.*, vol. 40, no. 7, pp. 1830–1835, Jul. 2010, doi: 10.1002/EJI.201040391.
- [367] Y. Shan *et al.*, “Role of IL-6 in the invasiveness and prognosis of glioma,” *undefined*, 2015.
- [368] K. A. Schalper *et al.*, “Elevated serum interleukin-8 is associated with enhanced intratumor neutrophils

- and reduced clinical benefit of immune-checkpoint inhibitors," *Nat. Med.* 2020 265, vol. 26, no. 5, pp. 688–692, May 2020, doi: 10.1038/s41591-020-0856-x.
- [369] Y. Nakasone *et al.*, "Host-derived MCP-1 and MIP-1 $\alpha$  regulate protective anti-tumor immunity to localized and metastatic B16 melanoma," *Am. J. Pathol.*, vol. 180, no. 1, pp. 365–374, Jan. 2012, doi: 10.1016/J.AJPATH.2011.09.005.
- [370] A. L. Chang *et al.*, "CCL2 produced by the glioma microenvironment is essential for the recruitment of regulatory T cells and myeloid-derived suppressor cells," *Cancer Res.*, vol. 76, no. 19, p. 5671, Oct. 2016, doi: 10.1158/0008-5472.CAN-16-0144.
- [371] L. Zhao *et al.*, "The antitumour activity of 5,6-dimethylxanthenone-4-acetic acid (DMXAA) in TNF receptor-1 knockout mice," *Br. J. Cancer*, vol. 87, no. 4, p. 465, Aug. 2002, doi: 10.1038/SJ.BJC.6600479.
- [372] R. van Horssen *et al.*, "TNF-alpha in cancer treatment: molecular insights, antitumor effects, and clinical utility," *Oncologist*, vol. 11, no. 4, pp. 397–408, Apr. 2006, doi: 10.1634/THEONCOLOGIST.11-4-397.
- [373] L. Zheng *et al.*, "Induction of apoptosis in mature T cells by tumour necrosis factor," *Nat.* 1995 3776547, vol. 377, no. 6547, pp. 348–351, Sep. 1995, doi: 10.1038/377348a0.
- [374] F. Bertrand *et al.*, "TNF $\alpha$  blockade overcomes resistance to anti-PD-1 in experimental melanoma," *Nat. Commun.* 2017 81, vol. 8, no. 1, pp. 1–13, Dec. 2017, doi: 10.1038/s41467-017-02358-7.
- [375] K. Sakuishi *et al.*, "Targeting Tim-3 and PD-1 pathways to reverse T cell exhaustion and restore anti-tumor immunity," *J. Exp. Med.*, vol. 207, no. 10, pp. 2187–2194, Sep. 2010, doi: 10.1084/JEM.20100643.
- [376] S. Koyama *et al.*, "Adaptive resistance to therapeutic PD-1 blockade is associated with upregulation of alternative immune checkpoints," *Nat. Commun.*, vol. 7, Feb. 2016, doi: 10.1038/NCOMMS10501.
- [377] J. L. Mendoza *et al.*, "Structure of the IFN $\gamma$  receptor complex guides design of biased agonists," *Nat.* 2019 5677746, vol. 567, no. 7746, pp. 56–60, Feb. 2019, doi: 10.1038/s41586-019-0988-7.
- [378] G. Z. Tau *et al.*, "Regulation of IFN- $\gamma$  Signaling Is Essential for the Cytotoxic Activity of CD8+ T Cells," *J. Immunol.*, vol. 167, no. 10, pp. 5574–5582, Nov. 2001, doi: 10.4049/JIMMUNOL.167.10.5574.
- [379] N. R. Maimela *et al.*, "Fates of CD8+ T cells in Tumor Microenvironment," *Comput. Struct. Biotechnol. J.*, vol. 17, p. 1, Jan. 2019, doi: 10.1016/J.CSBJ.2018.11.004.
- [380] A. Poli *et al.*, "Targeting glioblastoma with NK cells and mAb against NG2/CSPG4 prolongs animal survival," *Oncotarget*, vol. 4, no. 9, p. 1527, 2013, doi: 10.18632/ONCOTARGET.1291.
- [381] M. L. Broekman *et al.*, "Multidimensional communication in the microenvirons of glioblastoma," *Nat. Rev. Neurol.*, vol. 14, no. 8, pp. 1–14, Jul. 2018, doi: 10.1038/S41582-018-0025-8.
- [382] M. E. Keir *et al.*, "PD-1 and its ligands in tolerance and immunity," *Annu. Rev. Immunol.*, vol. 26, pp. 677–704, 2008, doi: 10.1146/ANNUREV.IMMUNOL.26.021607.090331.
- [383] L. Wang *et al.*, "Programmed death 1 ligand signaling regulates the generation of adaptive Foxp3+CD4+ regulatory T cells," *Proc. Natl. Acad. Sci. U. S. A.*, vol. 105, no. 27, pp. 9331–9336, Jul. 2008, doi: 10.1073/PNAS.0710441105.
- [384] E. Gianchecchi and A. Fierabracci, "Inhibitory Receptors and Pathways of Lymphocytes: The Role of PD-1 in Treg Development and Their Involvement in Autoimmunity Onset and Cancer Progression," *Front. Immunol.*, vol. 9, no. OCT, Oct. 2018, doi: 10.3389/FIMMU.2018.02374.
- [385] J. Cai *et al.*, "The role of PD-1/PD-L1 axis and macrophage in the progression and treatment of cancer," *J. Cancer Res. Clin. Oncol.*, vol. 145, no. 6, pp. 1377–1385, Jun. 2019, doi: 10.1007/S00432-019-02879-2.
- [386] D. Samanta *et al.*, "Chemotherapy induces enrichment of CD47 +/CD73 +/PDL1 + immune evasive triple-negative breast cancer cells," *Proc. Natl. Acad. Sci. U. S. A.*, vol. 115, no. 6, pp. E1239–E1248, Feb. 2018, doi:

- 10.1073/PNAS.1718197115.
- [387] P. Zhang *et al.*, "Chemopreventive agents induce programmed death-1-ligand 1 (PD-L1) surface expression in breast cancer cells and promote PD-L1-mediated T cell apoptosis," *Mol. Immunol.*, vol. 45, no. 5, pp. 1470–1476, Mar. 2008, doi: 10.1016/J.MOLIMM.2007.08.013.
- [388] D. Blanchard *et al.*, "Production of granulocyte-macrophage colony-stimulating factor by large granular lymphocytes stimulated with *Candida albicans*: role in activation of human neutrophil function," *Blood*, vol. 77, no. 10, pp. 2259–2265, May 1991, doi: 10.1182/BLOOD.V77.10.2259.2259.
- [389] L. M. Francisco *et al.*, "The PD-1 pathway in tolerance and autoimmunity," *Immunol. Rev.*, vol. 236, no. 1, pp. 219–242, Jul. 2010, doi: 10.1111/J.1600-065X.2010.00923.X.
- [390] A. T. Parsa *et al.*, "Loss of tumor suppressor PTEN function increases B7-H1 expression and immunoresistance in glioma," *Nat. Med.*, vol. 13, no. 1, pp. 84–88, 2007, doi: 10.1038/nm1517 PM - 17159987 M4 - Citavi.
- [391] J. Qian *et al.*, "The IFN- $\gamma$ /PD-L1 axis between T cells and tumor microenvironment: hints for glioma anti-PD-1/PD-L1 therapy," *J. Neuroinflammation* 2018 151, vol. 15, no. 1, pp. 1–13, Oct. 2018, doi: 10.1186/S12974-018-1330-2.
- [392] S. J. Schachtele *et al.*, "Glial cells suppress postencephalitic CD8+ T lymphocytes through PD-L1," *Glia*, vol. 62, no. 10, pp. 1582–1594, 2014, doi: 10.1002/GLIA.22701.
- [393] L. M. Francisco *et al.*, "PD-L1 regulates the development, maintenance, and function of induced regulatory T cells," *J. Exp. Med.*, vol. 206, no. 13, pp. 3015–3029, Dec. 2009, doi: 10.1084/JEM.20090847.
- [394] S. M. Poznanski *et al.*, "Expanded human NK cells from lung cancer patients sensitize patients' PDL1-negative tumors to PD1-blockade therapy," *J. Immunother. Cancer*, vol. 9, no. 1, p. e001933, Jan. 2021, doi: 10.1136/JITC-2020-001933.
- [395] E. P. Juliá *et al.*, "Avelumab, an IgG1 anti-PD-L1 immune checkpoint inhibitor, triggers NK cell-mediated cytotoxicity and cytokine production against triple negative breast cancer cells," *Front. Immunol.*, vol. 9, no. SEP, p. 2140, Sep. 2018, doi: 10.3389/FIMMU.2018.02140/BIBTEX.
- [396] J. O. J. Davies *et al.*, "Opportunities and limitations of natural killer cells as adoptive therapy for malignant disease," *Cytotherapy*, vol. 16, no. 11, pp. 1453–1466, Nov. 2014, doi: 10.1016/J.JCYT.2014.03.009.
- [397] W. Wang *et al.*, "CAR-NK for tumor immunotherapy: Clinical transformation and future prospects," *Cancer Lett.*, vol. 472, pp. 175–180, Mar. 2020, doi: 10.1016/J.CANLET.2019.11.033.
- [398] L. O. Roy *et al.*, "Transforming growth factor-beta and its implication in the malignancy of gliomas," *Target. Oncol.*, vol. 10, no. 1, Mar. 2015, doi: 10.1007/S11523-014-0308-Y.
- [399] C. A. Crane *et al.*, "TGF-beta downregulates the activating receptor NKG2D on NK cells and CD8+ T cells in glioma patients," *Neuro. Oncol.*, vol. 12, no. 1, pp. 7–13, Jan. 2010, doi: 10.1093/NEUONC/NOP009.
- [400] C. P. Beier *et al.*, "The cancer stem cell subtype determines immune infiltration of glioblastoma," *Stem Cells Dev.*, vol. 21, no. 15, pp. 2753–2761, Oct. 2012, doi: 10.1089/SCD.2011.0660.
- [401] H. J. Close *et al.*, "Expression profiling of single cells and patient cohorts identifies multiple immunosuppressive pathways and an altered NK cell phenotype in glioblastoma," *Clin. Exp. Immunol.*, vol. 200, no. 1, pp. 33–44, Apr. 2020, doi: 10.1111/CEI.13403.
- [402] G. Eisele *et al.*, "TGF-beta and metalloproteinases differentially suppress NKG2D ligand surface expression on malignant glioma cells," *Brain*, vol. 129, no. Pt 9, pp. 2416–2425, 2006, doi: 10.1093/BRAIN/AWL205.
- [403] F. Otegbeye *et al.*, "Inhibiting TGF-beta signaling preserves the function of highly activated, in vitro expanded natural killer cells in AML and colon cancer models," *PLoS One*, vol. 13, no. 1, p. e0191358, Jan.



- 2018, doi: 10.1371/JOURNAL.PONE.0191358.
- [404] M. A. Friese *et al.*, "RNA interference targeting transforming growth factor-beta enhances NKG2D-mediated antiglioma immune response, inhibits glioma cell migration and invasiveness, and abrogates tumorigenicity in vivo," *Cancer Res.*, vol. 64, no. 20, pp. 7596–7603, Oct. 2004, doi: 10.1158/0008-5472.CAN-04-1627.
- [405] A. B. Powell *et al.*, "Medulloblastoma rendered susceptible to NK-cell attack by TGF $\beta$  neutralization," *J. Transl. Med.*, vol. 17, no. 1, Sep. 2019, doi: 10.1186/S12967-019-2055-4.
- [406] A. J. Sedgwick *et al.*, "The Role of NK Cells and Innate Lymphoid Cells in Brain Cancer," *Front. Immunol.*, vol. 11, p. 1549, Jul. 2020, doi: 10.3389/FIMMU.2020.01549/BIBTEX.
- [407] D. B. Rosen *et al.*, "Cutting edge: lectin-like transcript-1 is a ligand for the inhibitory human NKR-P1A receptor," *J. Immunol.*, vol. 175, no. 12, pp. 7796–7799, Dec. 2005, doi: 10.4049/JIMMUNOL.175.12.7796.
- [408] V. M. Braud *et al.*, "HLA-E binds to natural killer cell receptors CD94/NKG2A, B and C," *Nature*, vol. 391, no. 6669, pp. 795–799, Feb. 1998, doi: 10.1038/35869.
- [409] N. Lee *et al.*, "HLA-E is a major ligand for the natural killer inhibitory receptor CD94/NKG2A," *Proc. Natl. Acad. Sci. U. S. A.*, vol. 95, no. 9, pp. 5199–5204, Apr. 1998, doi: 10.1073/PNAS.95.9.5199.
- [410] H. Aldemir *et al.*, "Cutting edge: lectin-like transcript 1 is a ligand for the CD161 receptor," *J. Immunol.*, vol. 175, no. 12, pp. 7791–7795, Dec. 2005, doi: 10.4049/JIMMUNOL.175.12.7791.
- [411] P. Roth *et al.*, "Malignant glioma cells counteract antitumor immune responses through expression of lectin-like transcript-1," *Cancer Res.*, vol. 67, no. 8, pp. 3540–3544, Apr. 2007, doi: 10.1158/0008-5472.CAN-06-4783.
- [412] M. Weller *et al.*, "HLA-E Protects Glioma Cells from NKG2D-Mediated Immune Responses In Vitro: Implications for Immune Escape In Vivo," *J. Neuropathol. Exp. Neurol.*, vol. 64, no. 6, pp. 523–528, 2005, doi: 10.1093/jnen/64.6.523 U6 - <https://dx.doi.org/10.1093/jnen/64.6.523> M4 - Citavi.
- [413] A. K. Kozłowska *et al.*, "Resistance to cytotoxicity and sustained release of interleukin-6 and interleukin-8 in the presence of decreased interferon- $\gamma$  after differentiation of glioblastoma by human natural killer cells," *Cancer Immunol. Immunother.*, vol. 65, no. 9, pp. 1085–1097, Sep. 2016, doi: 10.1007/S00262-016-1866-X.
- [414] A. K. Kozłowska *et al.*, "Differentiation by NK cells is a prerequisite for effective targeting of cancer stem cells/poorly differentiated tumors by chemopreventive and chemotherapeutic drugs," *J. Cancer*, vol. 8, no. 4, pp. 537–554, 2017, doi: 10.7150/JCA.15989.
- [415] M. Ruscetti *et al.*, "NK cell-mediated cytotoxicity contributes to tumor control by a cytostatic drug combination," *Science*, vol. 362, no. 6421, pp. 1416–1422, Dec. 2018, doi: 10.1126/SCIENCE.AAS9090.
- [416] P. E. Fecci *et al.*, "Systemic anti-CD25 monoclonal antibody administration safely enhances immunity in murine glioma without eliminating regulatory T cells," *Clin. Cancer Res.*, vol. 12, no. 14 Pt 1, pp. 4294–4305, 2006, doi: 10.1158/1078-0432.CCR-06-0053 PM - 16857805 M4 - Citavi.
- [417] N. Jahan *et al.*, "Agonist OX40 immunotherapy improves survival in glioma-bearing mice and is complementary with vaccination with irradiated GM-CSF-expressing tumor cells," *Neuro. Oncol.*, vol. 20, no. 1, pp. 44–54, Jan. 2018, doi: 10.1093/NEUONC/NOX125.
- [418] A. Ribas *et al.*, "Phase III randomized clinical trial comparing tremelimumab with standard-of-care chemotherapy in patients with advanced melanoma," *J. Clin. Oncol.*, vol. 31, no. 5, pp. 616–622, Feb. 2013, doi: 10.1200/JCO.2012.44.6112.
- [419] C. Robert *et al.*, "Ipilimumab plus Dacarbazine for Previously Untreated Metastatic Melanoma," *N. Engl. J. Med.*, vol. 364, no. 26, pp. 2517–2526, Jun. 2011, doi:

- 10.1056/NEJMOA1104621/SUPPL\_FILE/NEJMOA1104621\_DISCLOSURES.PDF.
- [420] M. Passariello *et al.*, "Ipilimumab and Its Derived EGFR Aptamer-Based Conjugate Induce Efficient NK Cell Activation against Cancer Cells," *Cancers* 2020, Vol. 12, Page 331, vol. 12, no. 2, p. 331, Feb. 2020, doi: 10.3390/CANCERS12020331.
- [421] D. Han *et al.*, "A novel human anti-TIGIT monoclonal antibody with excellent function in eliciting NK cell-mediated antitumor immunity," *Biochem. Biophys. Res. Commun.*, vol. 534, pp. 134–140, Jan. 2021, doi: 10.1016/j.bbrc.2020.12.013.
- [422] W. Ng *et al.*, "Targeting CD155 by radiocide-A overcomes tumour immuno-resistance to natural killer cells," <https://doi.org/10.1080/13880209.2020.1865410>, vol. 59, no. 1, pp. 47–53, 2021, doi: 10.1080/13880209.2020.1865410.
- [423] A. Rakita *et al.*, "Re-epithelialization and immune cell behaviour in an ex vivo human skin model," *Sci. Rep.*, vol. 10, no. 1, 2020, doi: 10.1038/S41598-019-56847-4.
- [424] D. Henrik Heiland *et al.*, "Tumor-associated reactive astrocytes aid the evolution of immunosuppressive environment in glioblastoma," *Nat. Commun.* 2019 101, vol. 10, no. 1, pp. 1–12, Jun. 2019, doi: 10.1038/s41467-019-10493-6.
- [425] F. Borrego *et al.*, "Recognition of human histocompatibility leukocyte antigen (HLA)-E complexed with HLA class I signal sequence-derived peptides by CD94/NKG2 confers protection from natural killer cell-mediated lysis," *J. Exp. Med.*, vol. 187, no. 5, pp. 813–818, Mar. 1998, doi: 10.1084/JEM.187.5.813.
- [426] S. Jiang *et al.*, "Perforin binding to cells and lipid membranes determined by a simple competition assay," *J. Immunol. Methods*, vol. 126, no. 1, pp. 29–37, Jan. 1990, doi: 10.1016/0022-1759(90)90008-J.
- [427] C. C. Liu *et al.*, "Resistance of cytolytic lymphocytes to perforin-mediated killing. Induction of resistance correlates with increase in cytotoxicity," *J. Exp. Med.*, vol. 169, no. 6, pp. 2211–2225, 1989, doi: 10.1084/JEM.169.6.2211.
- [428] I. Osińska *et al.*, "Perforin: an important player in immune response," *undefined*, vol. 39, no. 1, pp. 109–115, 2014, doi: 10.5114/CEJI.2014.42135.
- [429] K. N. Balaji *et al.*, "Surface cathepsin B protects cytotoxic lymphocytes from self-destruction after degranulation," *J. Exp. Med.*, vol. 196, no. 4, pp. 493–503, Aug. 2002, doi: 10.1084/JEM.20011836.
- [430] J. A. Lopez *et al.*, "Protecting a serial killer: pathways for perforin trafficking and self-defence ensure sequential target cell death," *Trends Immunol.*, vol. 33, no. 8, pp. 406–412, Aug. 2012, doi: 10.1016/j.it.2012.04.001.
- [431] C. Lehmann *et al.*, "Impaired binding of perforin on the surface of tumor cells is a cause of target cell resistance against cytotoxic effector cells," *Blood*, vol. 96, no. 2, pp. 594–600, Jul. 2000, doi: 10.1182/BLOOD.V96.2.594.
- [432] C. A. Sprecher *et al.*, "Molecular cloning, expression, and partial characterization of two novel members of the ovalbumin family of serine proteinase inhibitors," *J. Biol. Chem.*, vol. 270, no. 50, pp. 29854–29861, Dec. 1995, doi: 10.1074/JBC.270.50.29854.
- [433] J. Sun *et al.*, "A cytosolic granzyme B inhibitor related to the viral apoptotic regulator cytokine response modifier A is present in cytotoxic lymphocytes," *J. Biol. Chem.*, vol. 271, no. 44, pp. 27802–27809, 1996, doi: 10.1074/JBC.271.44.27802.
- [434] C. H. Bird *et al.*, "Selective Regulation of Apoptosis: the Cytotoxic Lymphocyte Serpin Proteinase Inhibitor 9 Protects against Granzyme B-Mediated Apoptosis without Perturbing the Fas Cell Death Pathway," *Mol. Cell. Biol.*, vol. 18, no. 11, p. 6387, Nov. 1998, doi: 10.1128/MCB.18.11.6387.
- [435] C. E. Hirst *et al.*, "The intracellular granzyme B inhibitor, proteinase inhibitor 9, is up-regulated during

- accessory cell maturation and effector cell degranulation, and its overexpression enhances CTL potency," *J. Immunol.*, vol. 170, no. 2, pp. 805–815, Jan. 2003, doi: 10.4049/JIMMUNOL.170.2.805.
- [436] H. Ida *et al.*, "Granzyme B leakage-induced cell death: a new type of activation-induced natural killer cell death," *Eur. J. Immunol.*, vol. 33, no. 12, pp. 3284–3292, Dec. 2003, doi: 10.1002/EJL.200324376.
- [437] C. F. Classen *et al.*, "Modulation of the granzyme B inhibitor proteinase inhibitor 9 (PI-9) by activation of lymphocytes and monocytes in vitro and by Epstein–Barr virus and bacterial infection," *Clin. Exp. Immunol.*, vol. 143, no. 3, p. 534, Mar. 2006, doi: 10.1111/J.1365-2249.2006.03006.X.
- [438] M. Bots *et al.*, "Proteinase inhibitor-9 expression is induced by maturation in dendritic cells via p38 MAP kinase," *Hum. Immunol.*, vol. 68, no. 12, pp. 959–964, Dec. 2007, doi: 10.1016/J.HUMIMM.2007.10.011.
- [439] M. S. Buzza *et al.*, "The granzyme B inhibitor, PI-9, is present in endothelial and mesothelial cells, suggesting that it protects bystander cells during immune responses," *Cell. Immunol.*, vol. 210, no. 1, pp. 21–29, May 2001, doi: 10.1006/CIMM.2001.1806.
- [440] P. Kannan-Thulasiraman and D. J. Shapiro, "Modulators of inflammation use nuclear factor-kappa B and activator protein-1 sites to induce the caspase-1 and granzyme B inhibitor, proteinase inhibitor 9," *J. Biol. Chem.*, vol. 277, no. 43, pp. 41230–41239, Oct. 2002, doi: 10.1074/JBC.M200379200.
- [441] A. R. Hussain *et al.*, "Curcumin induces apoptosis via inhibition of PI3'-kinase/AKT pathway in acute T cell leukemias," *Apoptosis*, vol. 11, no. 2, pp. 245–254, Feb. 2006, doi: 10.1007/S10495-006-3392-3.
- [442] W. Li and M. B. Graeber, "The molecular profile of microglia under the influence of glioma," *Neuro. Oncol.*, vol. 14, no. 8, pp. 958–978, Aug. 2012, doi: 10.1093/NEUONC/NOS116.
- [443] P. Voisin *et al.*, "Microglia in close vicinity of glioma cells: correlation between phenotype and metabolic alterations," *Front. Neuroenergetics*, vol. 2, 2010, doi: 10.3389/FNENE.2010.00131.
- [444] K. Roessler *et al.*, "Detection of tumor necrosis factor- $\alpha$  protein and messenger RNA in human glial brain tumors: comparison of immunohistochemistry with in situ hybridization using molecular probes," *J. Neurosurg.*, vol. 83, no. 2, pp. 291–297, Aug. 1995, doi: 10.3171/JNS.1995.83.2.0291.
- [445] X. Guan *et al.*, "Reactive Astrocytes in Glioblastoma Multiforme," *Mol. Neurobiol.* 2018 558, vol. 55, no. 8, pp. 6927–6938, Jan. 2018, doi: 10.1007/S12035-018-0880-8.
- [446] D. Matias *et al.*, "Microglia/astrocytes–glioblastoma crosstalk: Crucial molecular mechanisms and microenvironmental factors," *Front. Cell. Neurosci.*, vol. 12, p. 235, Aug. 2018, doi: 10.3389/FNCEL.2018.00235/BIBTEX.
- [447] X. Ye *et al.*, "Tumor-associated microglia/macrophages enhance the invasion of glioma stem-like cells via TGF- $\beta$ 1 signaling pathway," *J. Immunol.*, vol. 189, no. 1, pp. 444–453, Jul. 2012, doi: 10.4049/JIMMUNOL.1103248.
- [448] A. C. C. Da Fonseca *et al.*, "Microglia in Cancer: For Good or for Bad?," *Adv. Exp. Med. Biol.*, vol. 949, pp. 245–261, Oct. 2016, doi: 10.1007/978-3-319-40764-7\_12.
- [449] T. Deuse *et al.*, "The SIRP $\alpha$ -CD47 immune checkpoint in NK cells," *J. Exp. Med.*, vol. 218, no. 3, Mar. 2021, doi: 10.1084/JEM.20200839/211668.
- [450] S. Gholamin *et al.*, "Disrupting the CD47-SIRP $\alpha$  anti-phagocytic axis by a humanized anti-CD47 antibody is an efficacious treatment for malignant pediatric brain tumors," *Sci. Transl. Med.*, vol. 9, no. 381, Mar. 2017, doi: 10.1126/SCITRANSLMED.AAF2968/SUPPL\_FILE/AAF2968\_SM.PDF.
- [451] N. Geribaldi-Doldán *et al.*, "The Role of Microglia in Glioblastoma," *Front. Oncol.*, vol. 10, Jan. 2020, doi: 10.3389/FONC.2020.603495.
- [452] H. Grégoire *et al.*, "Targeting Tumor Associated Macrophages to Overcome Conventional Treatment Resistance in Glioblastoma," *Front. Pharmacol.*, vol. 11, p. 368, Apr. 2020, doi:

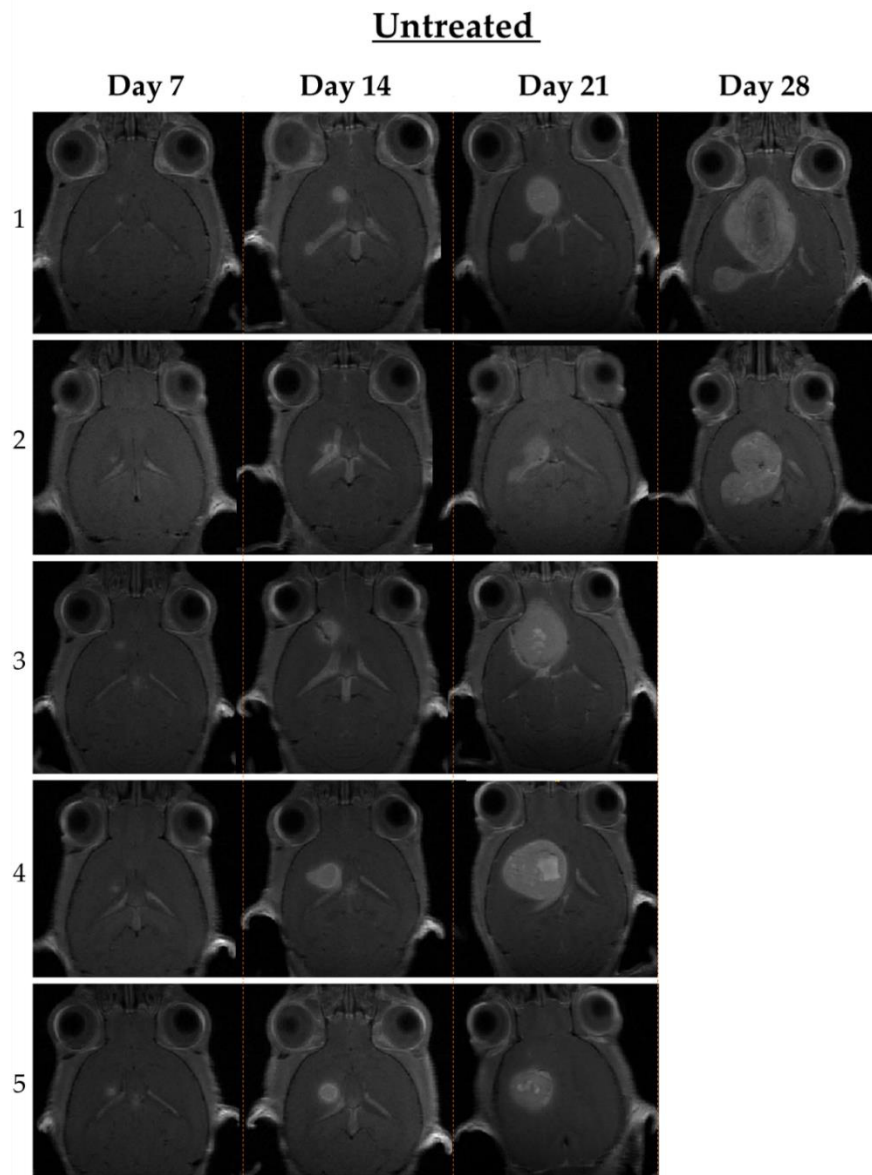
- 10.3389/FPHAR.2020.00368/BIBTEX.
- [453] C. Zhang *et al.*, "Interleukin-12 improves cytotoxicity of natural killer cells via upregulated expression of NKG2D," *Hum. Immunol.*, vol. 69, no. 8, pp. 490–500, Aug. 2008, doi: 10.1016/J.HUMIMM.2008.06.004.
- [454] N. Albinger *et al.*, "Current status and perspective of CAR-T and CAR-NK cell therapy trials in Germany," *Gene Ther.* 2021 289, vol. 28, no. 9, pp. 513–527, Mar. 2021, doi: 10.1038/s41434-021-00246-w.
- [455] S. Mohammed *et al.*, "Improving Chimeric Antigen Receptor-Modified T Cell Function by Reversing the Immunosuppressive Tumor Microenvironment of Pancreatic Cancer," *Mol. Ther.*, vol. 25, no. 1, pp. 249–258, Jan. 2017, doi: 10.1016/J.YMTHE.2016.10.016.
- [456] C. Zhang *et al.*, "Original research: Bispecific antibody-mediated redirection of NKG2D-CAR natural killer cells facilitates dual targeting and enhances antitumor activity," *J. Immunother. Cancer*, vol. 9, no. 10, Oct. 2021, doi: 10.1136/JITC-2021-002980.
- [457] T. F. Cloughesy *et al.*, "Neoadjuvant anti-PD-1 immunotherapy promotes a survival benefit with intratumoral and systemic immune responses in recurrent glioblastoma," *Nat. Med.*, vol. 25, no. 3, pp. 477–486, Mar. 2019, doi: 10.1038/S41591-018-0337-7.
- [458] A. Natarajan *et al.*, "Novel Radiotracer for ImmunoPET Imaging of PD-1 Checkpoint Expression on Tumor Infiltrating Lymphocytes," *Bioconjug. Chem.*, vol. 26, no. 10, pp. 2062–2069, Oct. 2015, doi: 10.1021/ACS.BIOCONJCHEM.5B00318.
- [459] J. S. Weber *et al.*, "Nivolumab versus chemotherapy in patients with advanced melanoma who progressed after anti-CTLA-4 treatment (CheckMate 037): a randomised, controlled, open-label, phase 3 trial," *Lancet Oncol.*, vol. 16, no. 4, pp. 375–384, 2015, doi: 10.1016/S1470-2045(15)70076-8.
- [460] C. Robert *et al.*, "Anti-programmed-death-receptor-1 treatment with pembrolizumab in ipilimumab-refractory advanced melanoma: a randomised dose-comparison cohort of a phase 1 trial," *Lancet (London, England)*, vol. 384, no. 9948, pp. 1109–1117, Sep. 2014, doi: 10.1016/S0140-6736(14)60958-2.
- [461] S. L. Topalian *et al.*, "Survival, durable tumor remission, and long-term safety in patients with advanced melanoma receiving nivolumab," *J. Clin. Oncol.*, vol. 32, no. 10, pp. 1020–1030, Apr. 2014, doi: 10.1200/JCO.2013.53.0105.
- [462] L. Gu *et al.*, "The safety and tolerability of combined immune checkpoint inhibitors (anti-PD-1/PD-L1 plus anti-CTLA-4): a systematic review and meta-analysis," *BMC Cancer*, vol. 19, no. 1, Jun. 2019, doi: 10.1186/S12885-019-5785-Z.
- [463] J. Larkin *et al.*, "Five-Year Survival with Combined Nivolumab and Ipilimumab in Advanced Melanoma," *N. Engl. J. Med.*, vol. 381, no. 16, pp. 1535–1546, Oct. 2019, doi: 10.1056/NEJM0A1910836.
- [464] Z. N. Willmore *et al.*, "Combined anti-PD-1 and anti-CTLA-4 checkpoint blockade: Treatment of melanoma and immune mechanisms of action," *Eur. J. Immunol.*, vol. 51, no. 3, pp. 544–556, Mar. 2021, doi: 10.1002/EJI.202048747.
- [465] D. M. Pardoll, "The blockade of immune checkpoints in cancer immunotherapy," *Nat. Rev. Cancer* 2012 124, vol. 12, no. 4, pp. 252–264, Mar. 2012, doi: 10.1038/nrc3239.
- [466] J. A. Marin-Acevedo *et al.*, "Next generation of immune checkpoint inhibitors and beyond," *J. Hematol. Oncol.* 2021 141, vol. 14, no. 1, pp. 1–29, Mar. 2021, doi: 10.1186/S13045-021-01056-8.
- [467] M. A. Aznar *et al.*, "Intratumoral Delivery of Immunotherapy-Act Locally, Think Globally," *J. Immunol.*, vol. 198, no. 1, pp. 31–39, Jan. 2017, doi: 10.4049/JIMMUNOL.1601145.
- [468] A. D. Simmons *et al.*, "Local secretion of anti-CTLA-4 enhances the therapeutic efficacy of a cancer immunotherapy with reduced evidence of systemic autoimmunity," *Cancer Immunol. Immunother.*, vol. 57, no. 8, pp. 1263–1270, Aug. 2008, doi: 10.1007/S00262-008-0451-3.

- [469] S. Rahimian *et al.*, "Polymeric microparticles for sustained and local delivery of antiCD40 and antiCTLA-4 in immunotherapy of cancer," *Biomaterials*, vol. 61, pp. 33–40, Aug. 2015, doi: 10.1016/J.BIOMATERIALS.2015.04.043.
- [470] M. F. Fransen *et al.*, "Controlled local delivery of CTLA-4 blocking antibody induces CD8+ T-cell-dependent tumor eradication and decreases risk of toxic side effects," *Clin. Cancer Res.*, vol. 19, no. 19, pp. 5381–5389, Oct. 2013, doi: 10.1158/1078-0432.CCR-12-0781.
- [471] B. C. Schnepf and P. R. Johnson, "Adeno-associated virus delivery of broadly neutralizing antibodies," *Curr. Opin. HIV AIDS*, vol. 9, no. 3, pp. 250–256, 2014, doi: 10.1097/COH.000000000000056.
- [472] J. Wu *et al.*, "Self-complementary recombinant adeno-associated viral vectors: packaging capacity and the role of rep proteins in vector purity," *Hum. Gene Ther.*, vol. 18, no. 2, pp. 171–182, Feb. 2007, doi: 10.1089/HUM.2006.088.
- [473] S. M. Chamow and A. Ashkenazi, "Immunoadhesins: principles and applications," *Trends Biotechnol.*, vol. 14, no. 2, pp. 52–60, 1996, doi: 10.1016/0167-7799(96)80921-8.
- [474] P. R. Johnson *et al.*, "Vector-mediated gene transfer engenders long-lived neutralizing activity and protection against SIV infection in monkeys," *Nat. Med.*, vol. 15, no. 8, pp. 901–906, Aug. 2009, doi: 10.1038/NM.1967.
- [475] C. E. Deal and A. B. Balazs, "Vectored antibody gene delivery for the prevention or treatment of HIV infection," *Curr. Opin. HIV AIDS*, vol. 10, no. 3, pp. 190–197, May 2015, doi: 10.1097/COH.0000000000000145.
- [476] R. H. Smith, "Adeno-associated virus integration: virus versus vector," *Gene Ther.*, vol. 15, no. 11, pp. 817–822, Jun. 2008, doi: 10.1038/GT.2008.55.
- [477] S. P. Fuchs and R. C. Desrosiers, "Promise and problems associated with the use of recombinant AAV for the delivery of anti-HIV antibodies," *Mol. Ther. - Methods Clin. Dev.*, vol. 3, p. 16068, Jan. 2016, doi: 10.1038/MTM.2016.68.
- [478] B. C. Schnepf *et al.*, "Recombinant Adeno-Associated Virus Vector Genomes Take the Form of Long-Lived, Transcriptionally Competent Episomes in Human Muscle," *Hum. Gene Ther.*, vol. 27, no. 1, pp. 32–42, Jan. 2016, doi: 10.1089/HUM.2015.136.
- [479] J. Körbelin *et al.*, "A brain microvasculature endothelial cell-specific viral vector with the potential to treat neurovascular and neurological diseases," *EMBO Mol. Med.*, vol. 8, no. 6, p. 609, Jun. 2016, doi: 10.15252/EMMM.201506078.
- [480] H. Nakai *et al.*, "Adeno-Associated Viral Vector-Mediated Gene Transfer of Human Blood Coagulation Factor IX Into Mouse Liver," *Blood*, vol. 91, no. 12, pp. 4600–4607, Jun. 1998, doi: 10.1182/BLOOD.V91.12.4600.
- [481] S. P. Fuchs *et al.*, "AAV-Delivered Antibody Mediates Significant Protective Effects against SIVmac239 Challenge in the Absence of Neutralizing Activity," *PLOS Pathog.*, vol. 11, no. 8, p. e1005090, Aug. 2015, doi: 10.1371/JOURNAL.PPAT.1005090.
- [482] K. Rapti *et al.*, "Effectiveness of gene delivery systems for pluripotent and differentiated cells," *Mol. Ther. - Methods Clin. Dev.*, vol. 2, p. 14067, Jan. 2015, doi: 10.1038/MTM.2014.67.
- [483] J. Zhang *et al.*, "Establishment of a HEK293T cell line able to site-specifically integrate and stably express GDNF by rAAV-2 vector," *Electron. J. Biotechnol.*, vol. 22, pp. 75–80, Jul. 2016, doi: 10.1016/J.EJBT.2016.05.001.
- [484] A. K. Zaiss *et al.*, "Differential activation of innate immune responses by adenovirus and adeno-associated virus vectors," *J. Virol.*, vol. 76, no. 9, pp. 4580–4590, May 2002, doi: 10.1128/JVI.76.9.4580-4590.2002.

- [485] J. Zhu *et al.*, "The TLR9-MyD88 pathway is critical for adaptive immune responses to adeno-associated virus gene therapy vectors in mice," *J. Clin. Invest.*, vol. 119, no. 8, pp. 2388–2398, Aug. 2009, doi: 10.1172/JCI37607.
- [486] A. T. Martino *et al.*, "The genome of self-complementary adeno-associated viral vectors increases Toll-like receptor 9-dependent innate immune responses in the liver," *Blood*, vol. 117, no. 24, pp. 6459–6468, Jun. 2011, doi: 10.1182/BLOOD-2010-10-314518.
- [487] F. Kroschinsky *et al.*, "New drugs, new toxicities: severe side effects of modern targeted and immunotherapy of cancer and their management," *Crit. Care*, vol. 21, no. 1, Apr. 2017, doi: 10.1186/S13054-017-1678-1.
- [488] D. C. Fajgenbaum and C. H. June, "Cytokine Storm," <https://doi.org/10.1056/NEJMra2026131>, vol. 383, no. 23, pp. 2255–2273, Dec. 2020, doi: 10.1056/NEJMRA2026131.
- [489] A. Sorkin *et al.*, "Endocytosis and intracellular trafficking of ErbBs," *Exp. Cell Res.*, vol. 315, no. 4, pp. 683–696, Feb. 2009, doi: 10.1016/J.YEXCR.2008.07.029.
- [490] O. N. Shilova *et al.*, "Internalization and Recycling of the HER2 Receptor on Human Breast Adenocarcinoma Cells Treated with Targeted Phototoxic Protein DARPiniSOG," *Acta Naturae*, vol. 7, no. 3, p. 126, 2015, Accessed: Jul. 15, 2021. [Online]. Available: /pmc/articles/PMC4610174/.
- [491] K. D. Foust *et al.*, "Intravascular AAV9 preferentially targets neonatal neurons and adult astrocytes," *Nat. Biotechnol.*, vol. 27, no. 1, pp. 59–65, Jan. 2009, doi: 10.1038/NBT.1515.
- [492] D. GuhaSarkar *et al.*, "Systemic AAV9-IFN $\beta$  gene delivery treats highly invasive glioblastoma," *Neuro. Oncol.*, vol. 18, no. 11, pp. 1508–1518, Nov. 2016, doi: 10.1093/NEUONC/NOW097.
- [493] R. Calcedo *et al.*, "Adeno-associated virus antibody profiles in newborns, children, and adolescents," *Clin. Vaccine Immunol.*, vol. 18, no. 9, pp. 1586–1588, Sep. 2011, doi: 10.1128/CVI.05107-11.
- [494] C. Li *et al.*, "Neutralizing antibodies against adeno-associated virus examined prospectively in pediatric patients with hemophilia," *Gene Ther.*, vol. 19, no. 3, pp. 288–294, Mar. 2012, doi: 10.1038/GT.2011.90.
- [495] K. Rapti *et al.*, "Neutralizing antibodies against AAV serotypes 1, 2, 6, and 9 in sera of commonly used animal models," *Mol. Ther.*, vol. 20, no. 1, pp. 73–83, Jan. 2012, doi: 10.1038/mt.2011.177.
- [496] S. E. Hofherr *et al.*, "Polyethylene glycol modification of adenovirus reduces platelet activation, endothelial cell activation, and thrombocytopenia," *Hum. Gene Ther.*, vol. 18, no. 9, pp. 837–848, Sep. 2007, doi: 10.1089/HUM.2007.0051.
- [497] M. Bartel *et al.*, "Enhancing the clinical potential of aav vectors by capsid engineering to evade pre-existing immunity," *Frontiers in Microbiology*, vol. 2, no. OCT. Frontiers Research Foundation, 2011, doi: 10.3389/fmicb.2011.00204.
- [498] A. Asokan *et al.*, "The AAV Vector Toolkit: Poised at the Clinical Crossroads," *Mol. Ther.*, vol. 20, no. 4, pp. 699–708, Apr. 2012, doi: 10.1038/MT.2011.287.
- [499] J. Xu *et al.*, "Prevalence of neutralizing antibodies against AAV8, AAV9, and AAV843 in a Chinese population," *Int J Clin Exp Med*, vol. 12, no. 8, pp. 10253–10261, 2019, Accessed: Jul. 16, 2021. [Online]. Available: [www.ijcem.com/](http://www.ijcem.com/).
- [500] B. György *et al.*, "Naturally enveloped AAV vectors for shielding neutralizing antibodies and robust gene delivery in vivo," *Biomaterials*, vol. 35, no. 26, pp. 7598–7609, 2014, doi: 10.1016/J.BIOMATERIALS.2014.05.032.
- [501] A. Marabelle *et al.*, "Intratumoral immunotherapy: using the tumor as the remedy," *Ann. Oncol.*, vol. 28, pp. xii33–xii43, Dec. 2017, doi: 10.1093/ANNONC/MDX683.
- [502] P. A. Ascierto *et al.*, "Ipilimumab 10 mg/kg versus ipilimumab 3 mg/kg in patients with unresectable or

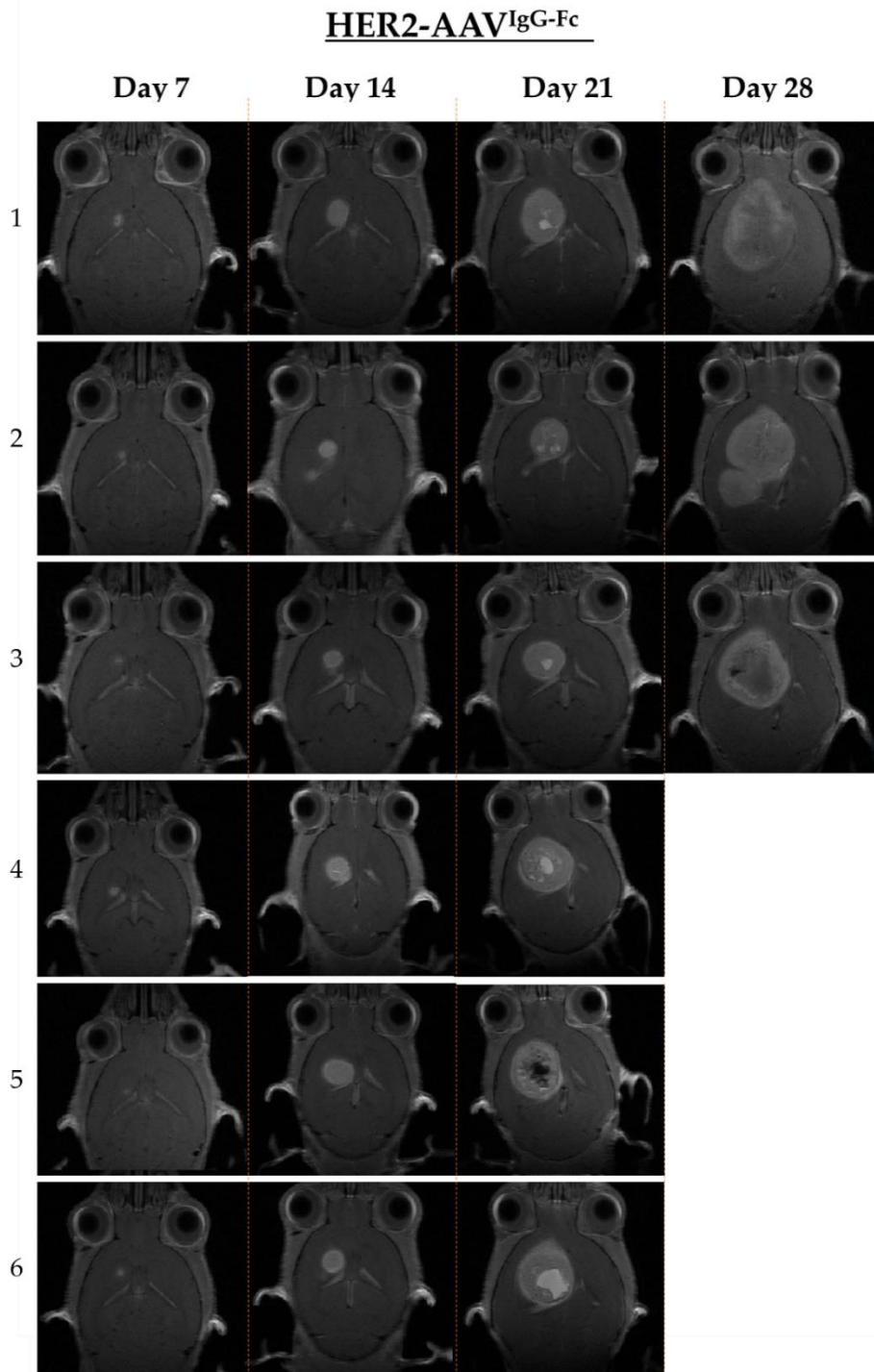
- metastatic melanoma: a randomised, double-blind, multicentre, phase 3 trial," *Lancet Oncol.*, vol. 18, no. 5, pp. 611–622, May 2017, doi: 10.1016/S1470-2045(17)30231-0.
- [503] E. Wang *et al.*, "Population pharmacokinetic and pharmacodynamic analysis of tremelimumab in patients with metastatic melanoma," *J. Clin. Pharmacol.*, vol. 54, no. 10, pp. 1108–1116, Oct. 2014, doi: 10.1002/JCPH.309.
- [504] A. M. M. Eggermont *et al.*, "Prolonged Survival in Stage III Melanoma with Ipilimumab Adjuvant Therapy," *N. Engl. J. Med.*, vol. 375, no. 19, pp. 1845–1855, Nov. 2016, doi: 10.1056/NEJMOA1611299.
- [505] B. Varghese *et al.*, "Generation of CD8+ T cell-mediated immunity against idiotype-negative lymphoma escapees," *Blood*, vol. 114, no. 20, pp. 4477–4485, Nov. 2009, doi: 10.1182/BLOOD-2009-05-223263.
- [506] T. M. Johanns *et al.*, "Endogenous Neoantigen-Specific CD8 T Cells Identified in Two Glioblastoma Models Using a Cancer Immunogenomics Approach," *Cancer Immunol. Res.*, vol. 4, no. 12, pp. 1007–1015, Dec. 2016, doi: 10.1158/2326-6066.CIR-16-0156.
- [507] J. I. Ausman *et al.*, "Studies on the Chemotherapy of Experimental Brain Tumors: Development of an Experimental Model," *Cancer Res.*, vol. 30, no. 9, 1970.
- [508] V. Genoud *et al.*, "Responsiveness to anti-PD-1 and anti-CTLA-4 immune checkpoint blockade in SB28 and GL261 mouse glioma models," *Oncoimmunology*, vol. 7, no. 12, Dec. 2018, doi: 10.1080/2162402X.2018.1501137.
- [509] G. Rao *et al.*, "Anti-PD-1 Induces M1 Polarization in the Glioma Microenvironment and Exerts Therapeutic Efficacy in the Absence of CD8 Cytotoxic T Cells," *Clin. Cancer Res.*, vol. 26, no. 17, pp. 4699–4712, Sep. 2020, doi: 10.1158/1078-0432.CCR-19-4110.
- [510] A. F. Haddad *et al.*, "Mouse models of glioblastoma for the evaluation of novel therapeutic strategies," *Neuro-Oncology Adv.*, vol. 3, no. 1, pp. 1–16, Jan. 2021, doi: 10.1093/NOAJNL/VDAB100.
- [511] W. Maes and S. W. Van Gool, "Experimental immunotherapy for malignant glioma: lessons from two decades of research in the GL261 model," *Cancer Immunol. Immunother.*, vol. 60, no. 2, pp. 153–160, Feb. 2011, doi: 10.1007/S00262-010-0946-6.
- [512] R. M. Samstein *et al.*, "Tumor mutational load predicts survival after immunotherapy across multiple cancer types," *Nat. Genet.*, vol. 51, no. 2, pp. 202–206, Feb. 2019, doi: 10.1038/S41588-018-0312-8.
- [513] A. C. Filley *et al.*, "Recurrent glioma clinical trial, CheckMate-143: the game is not over yet," *Oncotarget*, vol. 8, no. 53, pp. 91779–91794, 2017, doi: 10.18632/ONCOTARGET.21586.
- [514] D. A. Wainwright *et al.*, "Durable therapeutic efficacy utilizing combinatorial blockade against IDO, CTLA-4, and PD-L1 in mice with brain tumors," *Clin. Cancer Res.*, vol. 20, no. 20, pp. 5290–5301, 2014, doi: 10.1158/1078-0432.CCR-14-0514 PM - 24691018 M4 - Citavi.
- [515] M. De Simone *et al.*, "Single cell T cell receptor sequencing: Techniques and future challenges," *Front. Immunol.*, vol. 9, no. JUL, p. 1638, Jul. 2018, doi: 10.3389/FIMMU.2018.01638/BIBTEX.
- [516] M. J. T. Stubbington *et al.*, "Single-cell transcriptomics to explore the immune system in health and disease," *Science (80-. )*, vol. 358, no. 6359, pp. 58–63, Oct. 2017, doi: 10.1126/SCIENCE.AAN6828/ASSET/F50CA522-9704-48C5-83E4-B0AF091F304C/ASSETS/GRAPHIC/358\_58\_F4.JPEG.
- [517] M. Platten *et al.*, "A vaccine targeting mutant IDH1 in newly diagnosed glioma," *Nat.* 2021 5927854, vol. 592, no. 7854, pp. 463–468, Mar. 2021, doi: 10.1038/s41586-021-03363-z.
- [518] A. M. Eichhoff *et al.*, "Nanobody-Enhanced Targeting of AAV Gene Therapy Vectors," *Mol. Ther. Methods Clin. Dev.*, vol. 15, pp. 211–220, Dec. 2019, doi: 10.1016/J.OMTM.2019.09.003.

## 6 Appendix

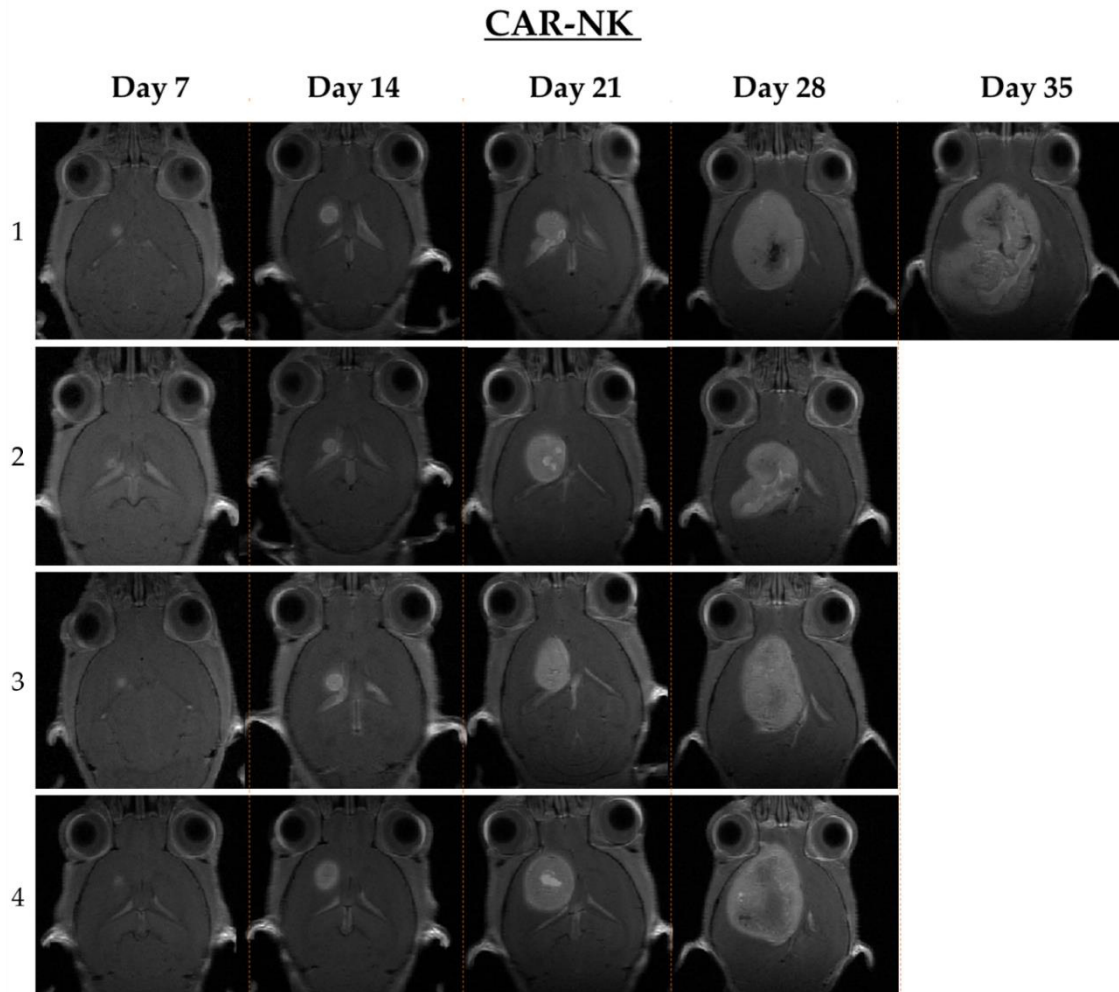


Appendix figure 1: MR images of animals receiving intratumoral sham-injections (medium).

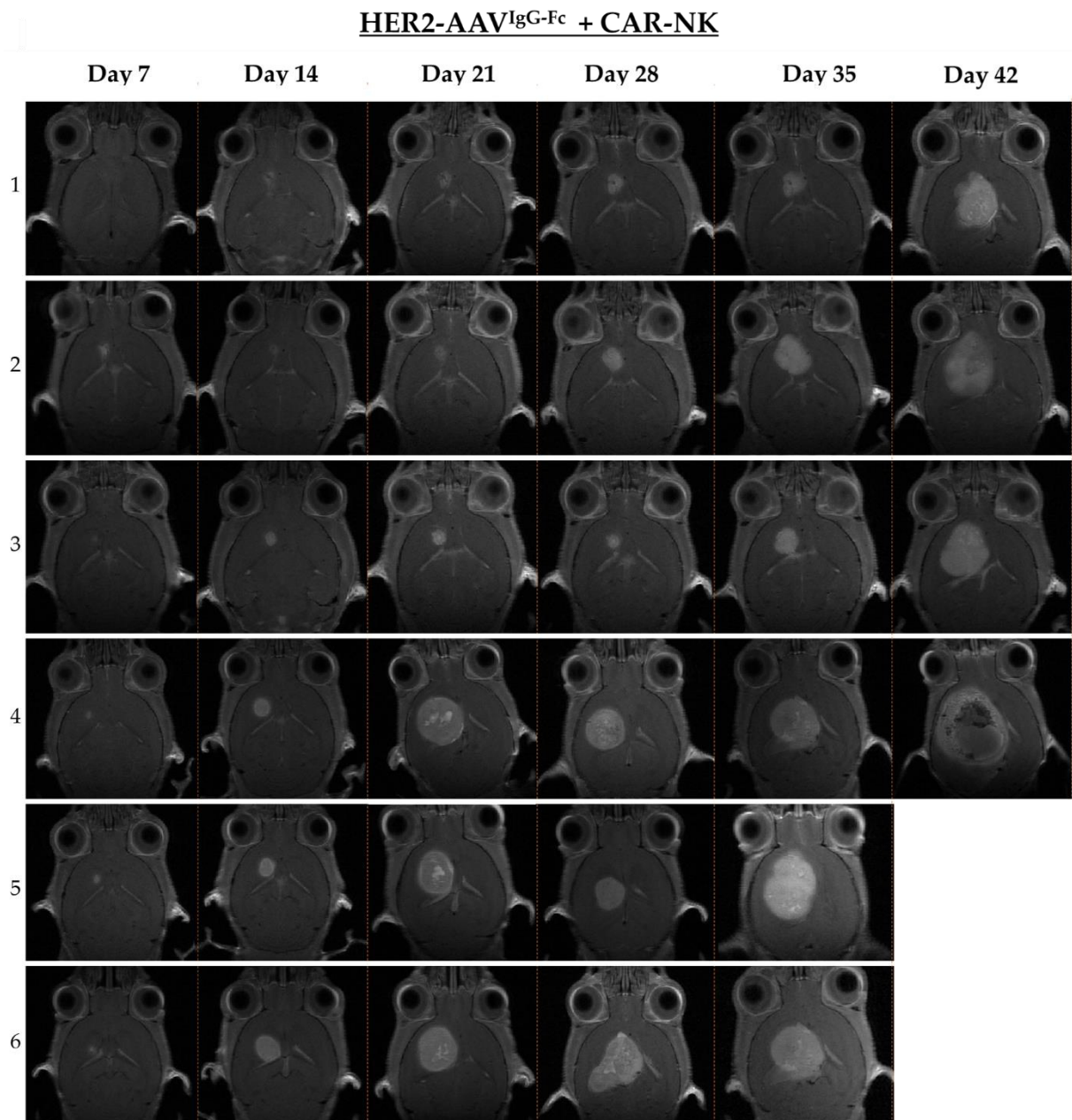




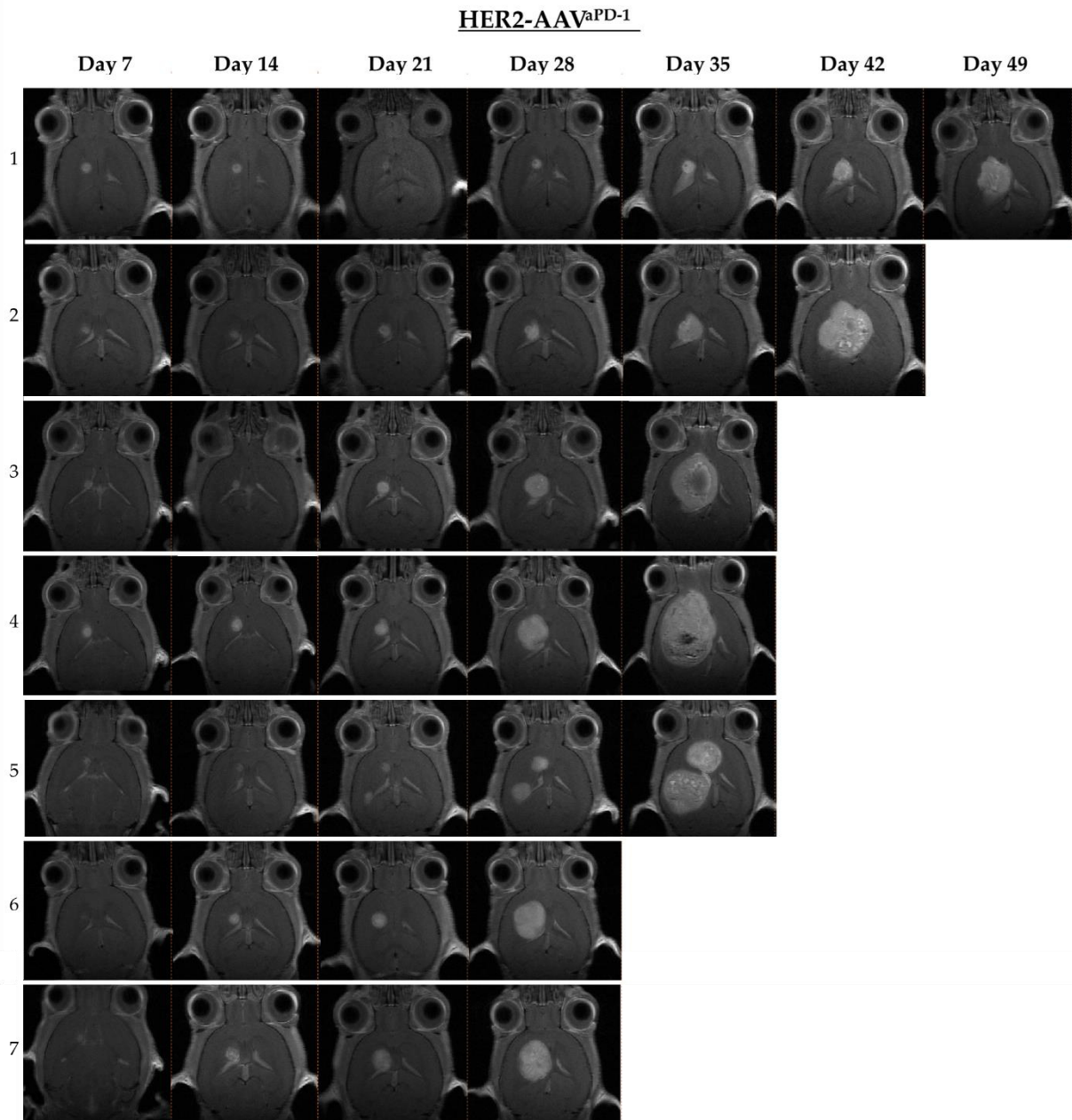
Appendix figure 2: MR images of animals receiving intratumoral injections of HER2-AAV<sup>IgG-Fc</sup>.



Appendix figure 3: MR images of animals receiving intratumoral injections of CAR-NK cells.

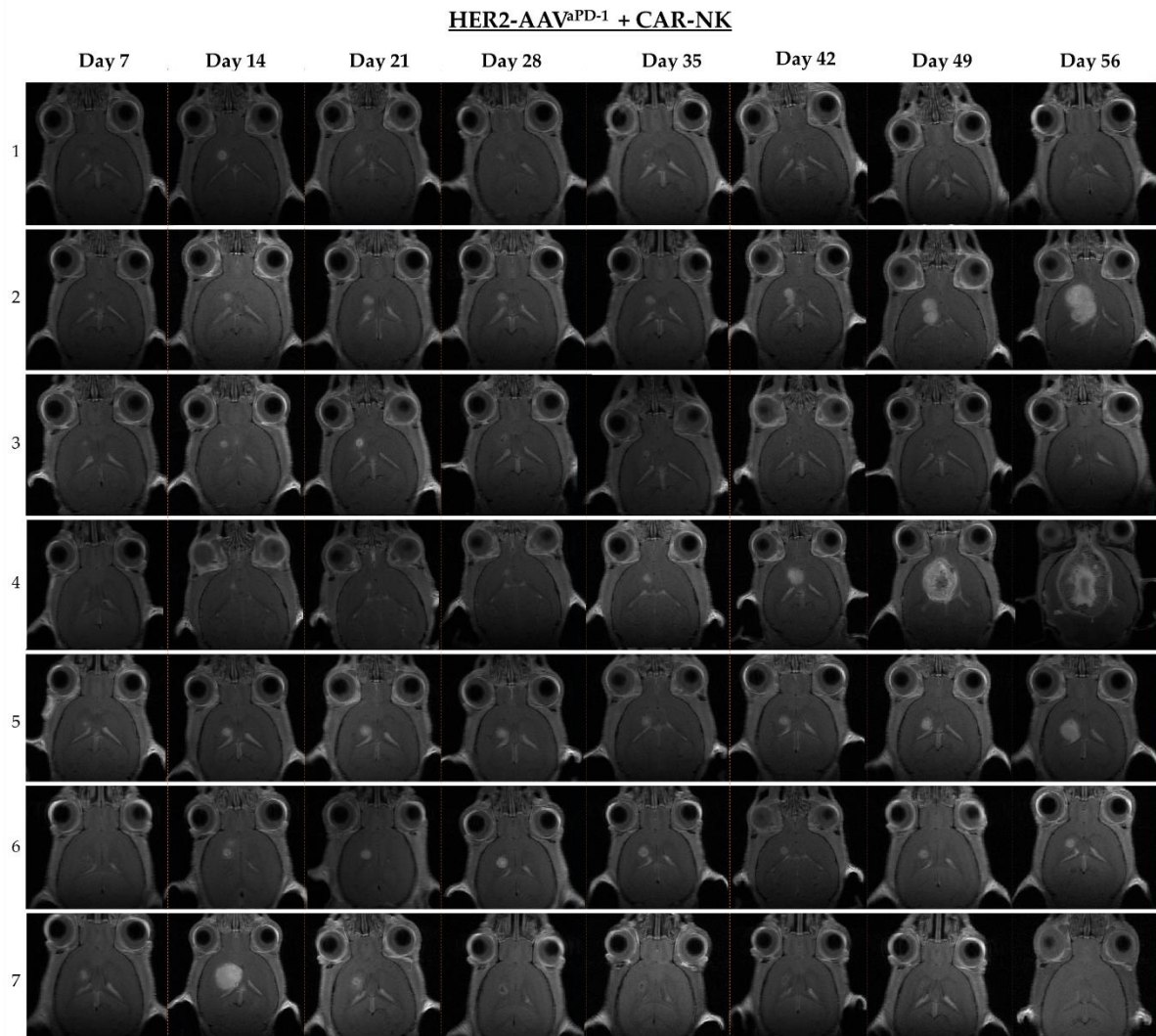


Appendix figure 4: MR images of animals receiving intratumoral injections of HER2-AAV<sup>IgG-Fc</sup> and CAR-NK cells.



Appendix figure 5: MR images of animals receiving intratumoral injections of HER2-AAV<sup>aPD-1</sup>.





Appendix figure 6: MR images of animals receiving intratumoral injections of HER2-AAV<sup>aPD-1</sup> and CAR-NK cells.

## 7 Curriculum vitae

### Personal information

Name	Maja Isabelle Strecker
Date of birth	09.05.1992
Place of birth	Marburg/Lahn

### Academic qualifications

since 02/2019	PhD student at Dr. Senckenbergisches Institute for Neurooncology (Goethe University Frankfurt)
10/2015 – 10/2018	M.Sc. Molecular Medicine (Goethe University Frankfurt, main focus: cardio-vascular research, immunology, oncology, molecular pharmacology)
10/2014 – 09/2015	Research assistant at Philipps University Marburg (Parasitology)
10/2011 – 10/2014	B.Sc. Biology (Philipps University Marburg, main focus: immunology, parasitology)

## 8 Publications

Barialai L, **Strecker MI**, Luger AL, Jäger M, Bruns I, Sittig ACM, Mildenerger IC, Heller SM, Delaidelli A, Lorenz NI, Voss M, Ronellenfisch MW, Steinbach JP, Burger MC (2020). AMPK activation protects astrocytes from hypoxia-induced cell death. *Int J Mol Med.* 45(5):1385-1396

Duecker R, Baer P, Eickmeier O, **Strecker M**, Kurz J, Schaible A, Henrich D, Zielen S, Schubert R (2018). Oxidative stress-driven pulmonary inflammation and fibrosis in a mouse model of human ataxia-telangiectasia. *Redox Biol.* 14:645-655

Rhiel M, Bittl V, Tribensky A, Charnaud SC, **Strecker M**, Müller S, Lanzer M, Sanchez C, Schaeffer-Reiss C, Westermann B, Crabb BS, Gilson PR, Külzer S, Przyborski JM (2016). Trafficking of the exported *P. falciparum* chaperone PfHsp70x. *Sci Rep.* 6:36174

### Presentations at scientific conferences

**Maja I. Strecker**, Karolin Wlotzka, Florian Strassheimer, Jasmin Röder, Claudia Opitz, Tijna Alekseeva, Johanna Reul, Lisa Sevenich, Thorsten Tonn, Winfried S. Wels, Joachim P. Steinbach, Christian J. Buchholz, Michael C. Burger. *AAV/DARPin-mediated local combination immunotherapy for glioma.* (Talk & poster presentation)

3rd Rhein-Main Cancer Retreat, October 28-28, 2021 in Königstein im Taunus, Germany

**Maja I. Strecker**, Karolin Wlotzka, Florian Strassheimer, Jasmin Röder, Claudia Opitz, Tijna Alekseeva, Johanna Reul, Lisa Sevenich, Thorsten Tonn, Winfried S. Wels, Joachim P. Steinbach, Christian J. Buchholz, Michael C. Burger. *Local immunotherapy of glioblastoma via AAV-mediated gene transfer of checkpoint inhibitors in combination with CAR-NK cells.* (Talk & poster presentation)

23. NOA Annual Meeting, October 7-8, 2021 in Frankfurt am Main, Germany

**Maja I. Strecker**, Florian Strassheimer, Johanna Reul, Patrick N. Harter, Thorsten Tonn, Joachim P. Steinbach, Winfried S. Wels, Christian J. Buchholz, Michael C. Burger. *A novel local treatment approach? Targeted immunotherapy of glioblastoma via AAV-mediated gene transfer of checkpoint inhibitors through locally administered HER2-AAVs in combination with CAR-NK cells.* (Poster presentation)

9th UCT Science Day, September 4, 2019 in Frankfurt am Main, Germany

**Maja I. Strecker**, Florian Strassheimer, Johanna Reul, Patrick N. Harter, Thorsten Tonn, Joachim P. Steinbach, Winfried S. Wels, Christian J. Buchholz, Michael C. Burger. *Targeted local combination therapy with checkpoint inhibitors and CAR-NK cells in glioblastoma using DARPin-linked AAV vectors.* (Poster presentation)

14th EANO Meeting, September 19-22, 2019 in Lyon, France

**Maja I. Strecker**, Florian Strassheimer, Johanna Reul, Patrick N. Harter, Thorsten Tonn, Joachim P. Steinbach, Winfried S. Wels, Christian J. Buchholz, Michael C. Burger. *Targeted local combination therapy with checkpoint inhibitors and CAR-NK cells in glioblastoma using DARPIn-linked AAV vectors*. (Poster presentation)

11th DGfi Autumn School – Current Concepts in Immunology, October 14-19, 2019 in Merseburg, Germany



## 9 Danksagung

Da eine wissenschaftliche Arbeit nie das Werk einer einzelnen Person ist, möchte ich die Gelegenheit nutzen und mich bei all denjenigen bedanken, die es mir ermöglicht haben, diese Phase meiner akademischen Laufbahn zu absolvieren.

Besonderer Dank gilt an dieser Stelle Herrn Prof. Dr. Joachim Steinbach, welcher mir die Möglichkeit gegeben hat, innerhalb seines Instituts an diesem spannenden sowie relevanten Projekt zu forschen. Die stetige konstruktive Diskussionsbereitschaft und seine wertvollen Anregungen haben diese Arbeit maßgeblich geprägt. Gleichmaßen bedanke ich mich bei PD Dr. Michael Burger für die Betreuung in seiner Arbeitsgruppe und die Unterstützung während dieser gesamten Promotion. Frau Prof. Dr. Amparo Acker-Palmer möchte ich für die professionelle und unkomplizierte Betreuung dieses Projekts seitens des Fachbereichs Biowissenschaften der Goethe-Universität danken.

Meinen wissenschaftlichen Kollegen am Dr. Senckenbergischen Institut für Neuroonkologie; dies sind Nadja Lorenz, Benedikt Sauer, Karolin Wlotzka und Florian Straßheimer, danke ich ebenfalls von ganzem Herzen für ihre tatkräftige, verbale und auch mentale Unterstützung während dieser herausfordernden Zeit. Ihr alle habt maßgeblich zu unserer produktiven Arbeitsatmosphäre beigetragen und ich hatte stets Spaß daran, mit Euch zusammenzuarbeiten. PD Dr. Dr. Michael Ronellenfisch danke ich für sein stetig offenes Ohr und seine fachlichen Ratschläge.

Ganz herzlich bedanke ich mich auch bei Jasmin Röder, welche mir fachkundig mit Rat und Tat zur Seite stand, sowie bei Prof. Dr. Christian Buchholz, Gundula Braun und Dr. Tijna Aleekseeva für die herzliche und unkomplizierte Zusammenarbeit.

Eine herausragende Stellung nehmen an dieser Stelle meine Freunde ein, welche mir in den vergangenen Jahren ein erhebliches Maß an Geduld und Zuversicht entgegengebracht haben. Insbesondere meinem Vater danke ich für die kontinuierliche Unterstützung aus der Ferne. Ebenfalls sehr herzlich bedanken möchte ich mich bei Maximilian, welcher sich trotz eines eigenen vollen Terminkalenders die Zeit genommen hat, diese Arbeit Korrektur zu lesen (t.hanks mus).

## 10 Ehrenwörtliche Erklärung

Ich versichere hiermit, dass ich die vorliegende Arbeit selbständig und ohne Benutzung anderer als der angegebenen Quellen und Hilfsmittel verfasst habe. Wörtlich übernommene Sätze oder Satzteile sind als Zitat belegt, andere Anlehnungen, hinsichtlich Aussage und Umfang, unter Quellenangabe kenntlich gemacht.

Die Arbeit hat in gleicher oder ähnlicher Form noch keiner Prüfungsbehörde vorgelegen und ist nicht veröffentlicht. Sie wurde nicht, auch nicht auszugsweise, für eine andere Prüfungs- oder Studienleistung verwendet.

Frankfurt, den

.....

(Maja Isabelle Strecker)